# Sustainability Matters: Polylactic acid, a natural origin polyester for the rapid prototyping of microfluidic devices. From point-of-care to Organ-on-chip applications

Alfredo Edoardo Ongaro

Submitted for the degree of Doctor of Philosophy

Heriot-Watt University

School of Engineering and Physical Sciences

Institute of Biological Chemistry, Biophysics and Bioengineering

October 2019

# ABSTRACT

The nature of the material to be employed is one of the first factors manufacturers must take into account when embarking upon the design and production of a new microfluidic device. Silicon and glass have traditionally been used for manufacturing micro-features but polymeric materials, including thermoplastics, have recently been explored. The required microfluidic functions, degree of integration and application are the principal issues that must be considered when choosing a material. However, environmental sustainability is another concern that is of increasing importance due to the dramatic rise in the amount of medical plastic waste produced globally, largely driven by the use of single-use, disposable medical equipment. The advent of point-of-care diagnostics, in lab-on-chip format, is likely to add further to the amount of healthcare waste generated and, therefore, embedding sustainability at the research stage is essential. This thesis describes the possibility of making research prototypes and future products more sustainable across their entire lifecycle, from raw material to the finished article, by proposing the use of chemically recycled and natural origin polymers. First, a safe and cost effective protocol to bond conventional polymethyl metacrylate, PMMA, based microfluidic devices is investigated and the possibility to use chemically recycled PMMA taken into consideration. Polylactic acid, PLA, is introduced as environmentally sustainable solution and the $CO_2$ laser cut workability improved to microstructure microfluidic devices. PLA material properties are investigated to assess material suitability for point-of-care and microfluidic cell culture applications.

## DEDICATION

*When I started the PhD I did not know I was starting one of the most intense journey and adventure of my life. It was full of up and downs and plenty of surprises. I would define it as a personal "odyssey" through science and life. Everything started when Prof Vincenzo La Carrubba, my Master supervisor back in Palermo (Italy), pointed out to me an available PhD position at Heriot Watt Univeristy to investigate the use of a plant derived polymer for the production of environmentally sustainable microfluidic devices. Well, it was a match at first sight. I could have merged my Bachelor background in environmental engineering with the most recents Master studies in Material Science and Engineering. It was a very appealing project and I had nothing to hold me back to start a new journey. To him go my sincere thanks.*

*With the backpack on my shoulder and the conviction that the Scottish weather was not too cold, I arrived in Edinburgh in a rainy and cold day. Not too rainy but definitely too cold for me. To warm me up, there was one of the best improvised welcome by Antonio Liga, a PhD student first, Research associate then in my same group. Knowing that I was new in the city and that I did not know anyone he invited me to my first of a long series of Party in Scotland. To him go my thanks to have been a bridge between my previous life and the new one and between being a master and a PhD student.*

*Better skip the hangover of that night and going directly to Monday, when I firstly met my PhD supervisor Maïwenn Kersaudy-Kerhoas. What to say, it is well know that the student-supervisor relationship is controvertial, endig up with the student "hating" the supervisor because of urgently assigned deadline to the day before. Or for apparently new urgently game changing assigned task that will be forget at the next one-to-one meeting. My case was different, she has been for me like a coach. A science coach. I felt free and*

*encouraged to be creative in my project, in finding solutions and things to do. She has been able to recognise when I was demotivated or lost and promptly she had that task to assign, that game changer for my own curiosity and motivation. She taught me to celebrate when a task was achieved and to never give up. To Her my thanks for all of my achievements.*

*When I started, we were a small group, three PhD student and one supervisor. In no time we became 11. And to all the MKK Clinical Microfluidic group go my thanks. But expecially to Ieva Keraite, that she has been for me a collegue, a closed friend, a sister and she helped me feeling at home. Another acknowledgment goes to Alvaro Conde, a big brother for me and a very priceless teacher.*

*I have met many other person that have been of unvaluable help for me. Nicola Howarth my second supervisor, ready to help when needed and one of the first to congratulate me for each achievement. Virginia Pensabene that open to me the door of Organ on Chip, an important chapter of this PhD journey. Davide Di Giuseppe a PhD Student as me with which we share the same nerdy passion for science and technology. Valeria Arrighi and Filipe VIlella to have hosted me in their lab and supported me. Luca Pellegrino, who was ready to tell me how I did not know chemistry, but there to help. Vincenzo Bruno who was always there.*

*And to myself that I did really enjoy it a lot.*

# Research Thesis Submission

Please note this form should be bound into the submitted thesis.

| | | | |
|---|---|---|---|
| Name: | Alfredo Edoardo Ongaro | | |
| School: | School of Engineering and Physical Sciences, Institute of Biological Chemistry, Biophysics and Bioengineering | | |
| Version: *(i.e. First, Resubmission, Final)* | Final | Degree Sought: | Doctor of Philosophy |

## Declaration

In accordance with the appropriate regulations I hereby submit my thesis and I declare that:

1. The thesis embodies the results of my own work and has been composed by myself
2. Where appropriate, I have made acknowledgement of the work of others
3. The thesis is the correct version for submission and is the same version as any electronic versions submitted*.
4. My thesis for the award referred to, deposited in the Heriot-Watt University Library, should be made available for loan or photocopying and be available via the Institutional Repository, subject to such conditions as the Librarian may require
5. I understand that as a student of the University I am required to abide by the Regulations of the University and to conform to its discipline.
6. I confirm that the thesis has been verified against plagiarism via an approved plagiarism detection application e.g. Turnitin.

## ONLY for submissions including published works

Please note you are only required to complete the Inclusion of Published Works Form (page 2) if your thesis contains published works)

7. Where the thesis contains published outputs under Regulation 6 (9.1.2) or Regulation 43 (9) these are accompanied by a critical review which accurately describes my contribution to the research and, for multi-author outputs, a signed declaration indicating the contribution of each author (complete)
8. Inclusion of published outputs under Regulation 6 (9.1.2) or Regulation 43 (9) shall not constitute plagiarism.

* *Please note that it is the responsibility of the candidate to ensure that the correct version of the thesis is submitted.*

| | | | |
|---|---|---|---|
| Signature of Candidate: | 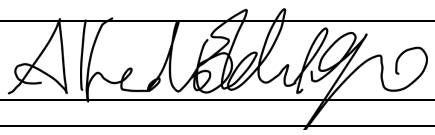 | Date: | 19/05/2020 |

## Submission

| | |
|---|---|
| Submitted By *(name in capitals):* | ALFREDO EDOARDO ONGARO |
| Signature of Individual Submitting: | 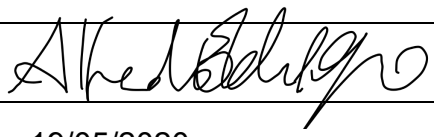 |
| Date Submitted: | 19/05/2020 |

## For Completion in the Student Service Centre (SSC)

| | | | | | | | | | | |
|---|---|---|---|---|---|---|---|---|---|---|
| Limited Access | Requested | Yes | | No | | Approved | Yes | | No | |
| *E-thesis Submitted (**mandatory for final theses**)* | | | | | | | | | | |
| Received in the SSC by *(name in capitals):* | | | | | | Date: | | | | |

# Inclusion of Published Works

Please note you are only required to complete the Inclusion of Published Works Form if your thesis contains published works under Regulation 6 (9.1.2)

## Declaration

This thesis contains one or more multi-author published works. In accordance with Regulation 6 (9.1.2) I hereby declare that the contributions of each author to these publications is as follows:

| | |
|---|---|
| Citation details | Ongaro, AE, Conoscenti, G, Liga, A, Brucato, V, Desmulliez, MPY, Howarth, N, La Carrubba, V & Kersaudy-Kerhoas, M 2017, Ultra-fast-prototyping of PMMA structures for micro-engineering applications: Choosing the right material. in J Gao, M El Souri & S Keates (eds), Advances in Manufacturing Technology XXXI - Proceedings of the 15th International Conference on Manufacturing Research, ICMR 2017: Incorporating the 32nd National Conference on Manufacturing Research. vol. 6, Advances in Transdisciplinary Engineering, IOS Press, pp. 181-186, 15th International Conference on Manufacturing Research, London, United Kingdom, 5/09/17. https://doi.org/10.3233/978-1-61499-792-4-181 |
| Ongaro, Alfredo E. | Performed all the experiments but the DSC analysis, experimental conception and design, writing |
| Conoscenti, Gioacchino | Performed DSC Analysis, contribution to the analysis of the results |
| Liga, Antonio | contribution to the analysis of the results |
| Brucato, Valerio B. | Proof read the article, contribution to the analysis of the results |
| Desmulliez, Marc P. Y. | Proof read the article, contribution to the analysis of the results |
| Howarth, Nicola | Proof read the article, contribution to the analysis of the results |
| La Carrubba, Vincenzo | Proof read the article, contribution to the analysis of the results |
| Kersaudy-Kerhoas, Maiwenn | experimental conception and design, writing |
| Signature: | 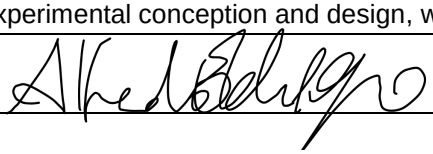 |
| Date: | 19/05/2020 |

| | |
|---|---|
| Citation details | Ongaro, AE, Keraite, I, Liga, A, Conoscenti, G, Coles, S, Schulze, H, Bachmann, TT, Parvez, K, Casiraghi, C, Howarth, N, La Carubba, V & Kersaudy-Kerhoas, M 2018, 'Laser Ablation of Poly(lactic acid) Sheets for the Rapid Prototyping of Sustainable, Single-Use, Disposable Medical Microcomponents', ACS Sustainable Chemistry and Engineering, vol. 6, no. 4, pp. 4899–4908. https://doi.org/10.1021/acssuschemeng.7b04348 |
| Ongaro, Alfredo E. | experimental conception and design, writing, experimental part but biological characterization, the electrode printing, electrochemical measurements. Analysis of the results |
| Keraite, Ieva | experimental part about biological experiments and analysis of the results |
| Liga, Antonio | Analysis of the results |
| Conoscenti, Gioacchino | Analysis of the results |
| Coles, Stuart | contribution to the literature on lifecycle analysis of PLA |
| Schulze, Holger | Experimental part about the electrochemical measurement |
| Bachmann, Till T. | contribution to the reagents and materials and the analysis of the electrochemical measurement results |
| Parvez, Khaled | Experimental part about electrode printing |
| Casiraghi, Cinzia | contribution to the reagents and materials and the conception and analysis of the electrode printing results |

| | |
|---|---|
| Howarth, Nicola | Analysis of the results, writing |
| La Carubba, Vincenzo | Analysis of the results |
| Kersaudy-Kerhoas Maiwenn | experimental conception and design, writing, Analysis of the results |
| Signature: | 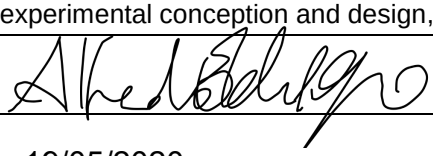 |
| Date: | 19/05/2020 |

| | |
|---|---|
| Citation details | Ongaro, A. E., Howarth, N., La Carrubba, V., & Kersaudy-Kerhoas, M. (2018). Rapid prototyping for micro-engineering and microfluidic applications: Recycled pmma, a sustainable substrate material. In P. Thorvald, & K. Case (Eds.), Advances in Manufacturing Technology XXXII (pp. 107-112). (Advances in Transdisciplinary Engineering; Vol. 8). IOS Press. https://doi.org/10.3233/978-1-61499-902-7-107 |
| Ongaro, Alfredo E. | Experimental part, experimental conception and design, writing, analysis of the results |
| Howarth, Nicola | analysis of the results |
| La Carrubba, Vincenzo | analysis of the results |
| Kersaudy-Kerhoas, Maiwenn | experimental conception and design, analysis of the results , writing |
| Signature: | 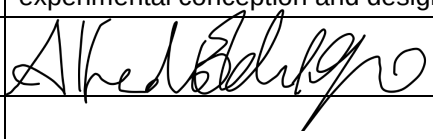 |
| Date: | 19/05/2020 |

| | |
|---|---|
| Citation details | Alfredo E. Ongaro, Davide Di Giuseppe, Ali Kermanizadeh, Allende Miguelez Crespo, Arianna Mencatti, Lina Ghibelli, Vanessa Mancini, Krystian L. Wlodarczyk, Duncan P. Hand, Eugenio Martinelli, Vicki Stone, Nicola Howarth, Vincenzo La Carrubba, Virginia Pensabene, Maïwenn Kersaudy-Kerhoas, Polylactic is a Sustainable, Low Absorption, Low Autofluorescence Alternative to Other Plastics for Microfluidic and Organ-on-Chip Applications, Analytical Chemistry,ASAP, 2020 https://doi.org/10.1021/acs.analchem.0c00651 |
| Alfredo E. Ongaro | experimental conception and design, experimental part but the cell culture and tracking experiments. Device manufacturing numerical simulation, analysis of the results, writing |
| Davide Di Giuseppe | Cell tracking, analysis of the results about cell tracking |
| Ali Kermanizadeh | Biocompatibility experiment, analysis of the results |
| Allende Miguelez Crespo, | analysis of the optical properties |
| Arianna Mencatti | analysis of the results about cell tracking |
| Lina Ghibelli | analysis of the results about cell tracking |
| Vanessa Mancini | Biocompatibility on chip, analysis of the results |
| Krystian L. Wlodarczyk | PLA microstructuring, SI |
| Duncan P. Hand | analysis of the results about PLA microstructuring, SI |
| Eugenio Martinelli | Cell tracking design and analysis of the results |
| Vicki Stone | Analysis of the results about biocompatibility study |
| Nicola Howarth | Proof read the article, analysis of the results |
| Vincenzo La Carrubba | analysis of the results |
| Virginia Pensabene | experimental conception and design, analysis of the results |
| Maïwenn Kersaudy-Kerhoas | experimental conception and design, analysis of the results, writing |

| | |
|---|---|
| Signature: | 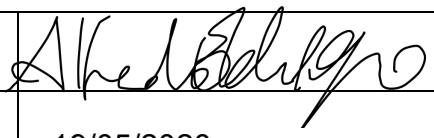 |
| Date: | 19/05/2020 |

# TABLE OF CONTENTS

# LIST OF PUBLICATIONS BY THE CANDIDATE

## Peer-reviewed journal articles

**A. E. Ongaro**, I. Keraite, A. Liga, G. Conoscenti, S. Coles, H. Schulze, T. Bachmann, K. Parvez, C. Casiraghi, N. Howarth, V. La Carrubba, M. Kersaudy-Kerhoas, *Laser Ablation of Poly(lactic acid) Sheets for the Rapid Prototyping of Sustainable, Single-Use, Disposable Medical Microcomponents*, ACS Sustainable Chem. Eng, 2018, 6,4, 4899-4908, doi:10.1021/acssuschemeng.7b04348. pp 68-78

Conoscenti G, Carfì Pavia F, **A.E. Ongaro**, et al., *Human nasoseptal chondrocytes maintain their differentiated phenotype on PLLA scaffolds produced by thermally induced phase separation and supplemented with bioactive glass* 1393, Connect Tissue Res. 2018.

A. Conde, I. Keraite, **A. E. Ongaro**, M. Kersaudy-Kerhoas, *Versatile hybrid acoustic micromixer with demonstration of circulating cell-free DNA extraction from sub-ml plasma samples, 17 Jan 2020 In: Lab on a Chip, 20(4), 741-748*

**A.E. Ongaro**, D. Di Giuseppe, A. Kermanizadeh, A. Crespo, A. Mencatti, L. Ghibelli, V. Mancini, K. L. Wlodarczyk, D. P. Hand, E. Martinelli, V. Stone, N. Howarth, V. La Carrubba, V. Pensabene, M. Kersaudy-Kerhoas, *Polylactic is a Sustainable, Low Absorption, Low Autofluorescence Alternative to Other Plastics for Microfluidic and Organ-on-Chip Applicat*ions, Analytical Chemistry, ASAP, 2020 https://doi.org/10.1021/acs.analchem.0c00651

## Peer-reviewed conference articles

**A. E. Ongaro**, G. Conoscenti, A. Liga, V. Brucato, M. P. Y. Desmulliez, N. Howarth, V. La Carrubba, and M. Kersauy-Kerhoas, *Ultra-fast-prototyping of PMMA structures for micro-engineering applications: Choosing the right material*, Adv TRansdicipl Eng. 2017

**A. E. Ongaro**, La Carrubba V, N. Howarth, M. Kersaudy-Kerhoas, *Rapid Prototyping for Micro-Engineering and Microfluidic Applications: Recycled PMMA, a Sustainable Substrate Material*. Adv Transdiscipl Eng. 2018;8(XXXII):107-112.

**A. E. Ongaro**, N. Howarth, La Carrubba V, M. Kersaudy-Kerhoas, *Fast and Green: Sustainable Rapid-Prototypung of microfluidic chips on Polylactic acid Substrates*, MicroTAS conference proceeding, Taiwann, 2018

## In Submission journal articles

F. Lopresti, **A. E. Ongaro**, I. Keraite, N. Howarth, V. Brucato, V. La Carrubba, M. Kersaudy-Kerhoas, *Engineered memrbanes for residual cell trapping on microfluidic blood plasma separation systems. A comparison between porous and nanofibrous membranes*, 2020, (in subsmission to Advanced Healthcare Materials)

## Selected peer-reviewed conference abstracts

**A.E. Ongaro**,N. D'Anna, A. Liga, G. Conoscenti, N. Howarth, V. La Carrubba and M. Kersaudy-Kerhoas, *Experimental investigations of $CO_2$ laser cut quality in poly(lactic acid) for microfluidic rapid-prototyping of sustainable devices*, European Advanced Materials Congress, 2017. DOI: 10.5185/eamc.2017

**A. E. Ongaro**, N. Howarth, V. La Carrubba, M. Kersaudy-Kerhoas, *Materials Matter: Polylactic acid, a natural origin polyester for the rapid prototyping of microfluidic devices*, EMBL, Heidelberg, Germany, 2018

**A. E. Ongaro,** D. Di Giuseppe, A. Kermanizadeh, E. Martinelli, S. Maucci, M. Skolimowski, H. Becker, V. Pensabene and M. Kersaudy-Kerhoas, *Next-Generation Material for high-volume production of Sustainable, Biocompatible Organ-On-Chip devices,* BioMedEng 2019, Imperial College, London, Organ on a chip technology network, 2019 (invited)

# Chapter 1- INTRODUCTION

The daily waste of a typical western world hospital was estimated to be 1,267 kg/day in 2015, with 3.5 million of tonnes of medical waste produced only in USA. Thirty to forty percent of all combustible waste is estimated to be plastic, consisting of syringes, and various disposable plastic items made up of non-degradable polymers [1]–[3]. About 92% of clinical waste is treated by incineration which removes contamination issues and reduces waste volume by about 90%. On the other hand, poorly controlled incineration procedures and waste stream can generate the release of a significant quantity of pollutants[4]. The advent of disposable medical consumable items, which annihilate cross-contamination, and alleviate the need for disinfection, has participated in the recent increase of medical plastic waste [5] [6]. With the development of personalised medicine technologies, namely new point-of care diagnostic tests often made of disposable polymeric plastic cartridges, it can be anticipated that the volume of plastic waste might increase dramatically in the coming years. This additional waste could bear an increased financial burden for communities, linked to the control of pollution emission.
Plastic waste has become a global challenge, and considering the entire life cycle of a product, from the raw material production, processing, manufacturing, use and end of life is the key to develop environmentally sustainable plastic devices. Even though the contribution of microfluidic devices to the actual plastic pollution from hospital and medical wastes at the moment of writing is negligible with respect to the one from syringes, plates, packaging and medical kit in general, it is never too early to start thinking to embed sustainable solution at the design stage of emerging technologies. The development of environmentally sustainable solutions for the rapid prototyping of microfluidic device for point-of-care, cell culture and organ-on-a-chip applications has been the motivation for, and the overarching goal of, this thesis investigation.

This PhD thesis provides a practical guide to microfluidic researcher and manufacturers to embed sustainability solution at the design stage. For the first time a clear and fast prototyping maskless technique to manufacture complex microfluidic devices has been developed by choosing PLA as sustainable substrate material and a $CO_2$ based layer by layer approach as manufacturing technique. An in depth characterization of manufacturability, transparency, absorption and adsorption and compatibility with

biological protocol for point-of-care and advanced cell culture applications is herein provided.

Chapter 2 covers an overview of the material and rapid fabrication methods used to prototype microfluidic devices and introduce the need of a sustainable solution for the production of next generation microfluidic devices. The state-of-the-art is illustrated and the existing sustainable solutions are reported.

Chapter 3 introduces the non-sustainable rapid prototyping technique developed in our laboratory. The solvent assisted method is capable of bonding microfluidic devices made of laser cut Poly methyl methacrylate (PMMA) in less than 15 minutes from design to test. A small guide on the choice on the right solvent is given by using the Hildebrandt parameters and an investigation on the suitability of the method on different PMMA materials available worldwide is reported. The work described has been published in 2017 Advances in Manufacturing Technology XXXI.

Chapter 4 reports on the first attempt to introduce Design for Sustainability in the rapid-prototyping protocol introduced in Chapter 3, with the use of chemically recycled PMMA. The work described has been published in 2018 Advances in Manufacturing Technology XXXII. An introduction on thermoplastic polymer recycling is presented.

In Chapter 5 the replacement of petrochemical-derived material with biodegradable polymer from non-fossil resources is investigated as possible solution to address the growing issue of medical plastic waste environmental impact. The use of biodegradable and bioderived polymers bring different end-of-life scenarios with respect to recycled PMMA [2], [3], [5]–[11].

The first and most common application of biodegradable polymers are found in healthcare (e.g. re-absorbable surgical sutures, tissue engineering, drug delivery). In more recent years new application fields have included food containers, agriculture films and packaging in general [12]. Their capability to degrade in biological environment (e.g. soil, sees, river) make them attractive not only for biomedical application but also like ecological polymers [13]. Additionally, due to their heterogeneity in the chemical and physical behaviours and the possibility to tune final properties as required by the designers and engineers, more applications can be foreseen in the near future [14].

The use of Polylactic acid (PLA) as bioderived material is introduced in context of a sustainable production of microfluidic devices in conjunction with the protocol described in chapter 3 and 4. The chapter describes a method developed during this PhD to microstructure PLA using a $CO_2$ laser cutter. This work has been published in 2018 in ACS Sustainable Chemistry and Engineering and includes a general introduction on the current method to laser microstructure thermoplastic materials and on the state of art of laser microstructuring PLA.

Chapter 6 describes the characterization of PLA for microfluidic cell culture and organ-on-a-chip applications. This work has been published in 2019 as preprint on Biorxiv. The article introduces the drawbacks that can been encountered while using conventional OOC and microfluidic cell culture materials. The suitability and superiority of PLA with respect to other common thermoplastic materials available in the market is shown.

Chapter 7 draws conclusions and final remarks and suggest future work.

The work of this thesis has received considerably attention from the microfluidic community, at the research scale and from major European microfluidic manufacturing companies such as Microfluidic ChipShop and Micronit. Results from this thesis has been presented at MicroTAS 2018, Kaioshiung, Taiwann, a selective and competitive microfluidic conference, for which the work on using PLA as sustainable material for manufacturing the next generation microfluidic devices has been awarded the Micromachines (MDPI) – Travel Awards ($ 1,000) (https://cbmsociety.org/awards/). The in depth characterization of optical and functional properties of PLA has led to the production of 300 parts of the very first mass manufactured environmentally sustainable PLA microfluidic device of a total value of £ 8,000 donated to the project and showcased from Microfluidic ChipShop to several conferences such as SelectBio 2019.

# Chapter 2-STATE OF THE ART: MATERIAL AND FABRICATION METHODS IN MICROFLUIDIC

## 2.1 Material and fabrication methods in Microfluidic

Microfluidic is a multidisciplinary field of science that studies the manipulation of fluids at the microscopic level. Microfluidic deals with the transport of small amount of fluids (e.g. from micro to picoliters) inside channels that have at least one dimension smaller than 1 millimeter. At this scale, fluids behave differently than at the macroscale. For instance, the chaotic, turbulent and stochastic flows that one can observe in daily-life, do not manifest themselves at the microscopic level generally.

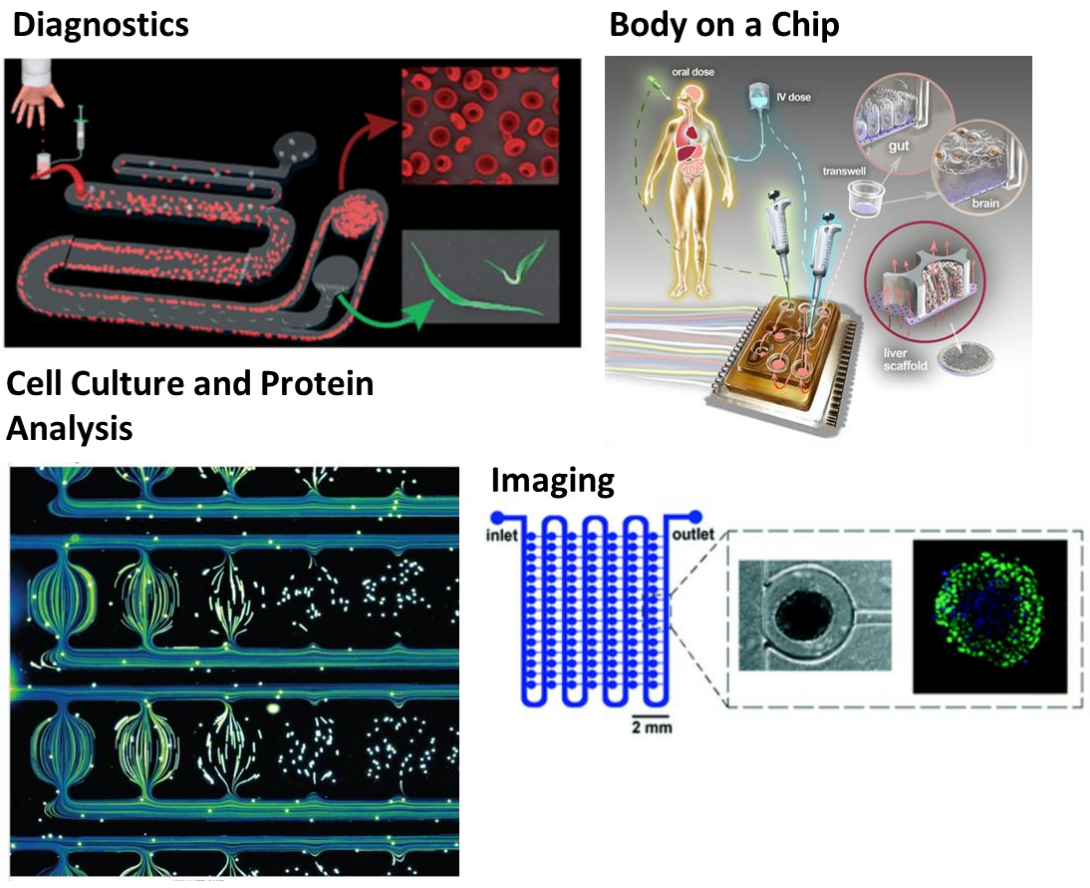


**Figure 2.1** Graphical example of common microfluidic applications tool. Diagnostics taken from [15]; body on a chip taken from [16]; advanced cell culture and protein analysis taken from [17] ; imaging taken from [18]

On the contrary, microchannels exhibit laminar flow, in which streamlines remain parallel. This flow regime enhances and facilitates the control of fluid handling, manipulation and mixing. The reason why laminar flows are dominant inside microchannels can be explained by considering the Reynolds number. The Reynolds number, Re, is a dimensionless number that Osborne Reynolds firstly determined by dynamic similarity using the Buckingham theorem after experimental studies on flow conditions in pipes. Re is the ratio between the inertial forces and viscous forces acting on a fluid. It is directly proportional to the fluid density, $\rho$, and velocity, $v$, and to the characteristic linear dimension or hydraulic diameter, $d$; it is inversely proportional to the fluid viscosity, $\mu$ (Equation 1).

$$Eq\ 1:\ Re = \frac{F_i}{F_\mu} = \frac{\rho v d}{\mu}$$

The value of the Reynolds number helps to discriminate if a system is in a laminar or turbulent flow regime. If Re falls under a value below 2000, the system under examination will be in a laminar regime, while if above 4000 under a turbulent regime. By looking at the definition of Re, it is apparent that in the case of microfluidic where channel size is in the micrometre range, Re will generally falls in a value below 2000, specially, when water is the fluid being handle inside the device (density=1 kg/m3; viscosity= 1cPoise); hence a laminar regime [19].

Microfluidic devices reduce reagent consumption and can integrate and automate multiple assays enabling high throughput screenings. Started in the late 1960s with works on gas chromatography and ink jet nozzle printers, microfluidic nowadays represents a powerful technological tool for point-of-care diagnostics, sample preparation, cell culture and protein analysis and to mimic human physiological environments for drug testing. Today, Microfluidic is also referred to as lab-on-a-chip or micrototal analysis systems (μTAS). The introduction of μTAS and lab-on-a-chip devices relies in the early 1990s, thanks to the work published by Andreas Manz et al., about the miniaturized capillary electrophpresis-based chemical analysis system on a chip [20]. For the first time the combination of classical analytical techniques and photolithographically defined microstructures was reported with dramatically reduced reagent consumption and faster separation. Silicon and glass have been the dominant substrate materials for the microfabrication of microfluidic devices. This is primarily driven by the fact that

microfabrication methods were well established by the semiconductor and electronics industry, and surface properties and derivation methods were well characterized and developed by the chromatography industry among others. Several material properties of glass make it a very attractive material for use in microfluidic systems; however, the cost of producing systems in glass is driving commercial producers to seek other materials. In 1998 Whitesides et co-workers published the first paper regarding the rapid prototyping of microfluidic structure in Polydimethylsiloxane, PDMS, a technique known as soft-lithography [21]. This pioneering work changed completely the way to manufacture microfluidic devices enabling faster translations between labs. In comparison to the fabrication of glass devices that involves a series of operations (e.g. substrates cleaning, lithography pattern and bonding) where each of them are often a time-consuming and expensive process, requiring several days, the method proposed from Whitesides at al., requires 24h from design to test (not including mask design and production). Soft lithography is summarised in figure 3. Briefly, the design of the microfluidic structure is converted into a mask by a high-resolution printer. A photoresist is deposited onto a silicon wafer though spin-coating and then exposed to UV light through the prepared photomask. The non cross-linked region is removed with a developer reagent, and the negative mould is prepared. Although PDMS in conjunction with soft lithography is the most common microfluidic substrate in use in academic laboratories thanks to its reasonable cost, ease of implementation and rapid fabrication method, PDMS has for some applications many disadvantages that will be discussed in chapter 6. Furthermore, PDMS moulding is still a process difficult to fully automate and not readily translatable into commercialisation.

## 2.2 Rapid Prototyping of thermoplastic Microfluidic devices

Over the past decades, many more materials have been used to manufacture microfluidic devices. A broad range of different plastics, as well as hydrogels, and paper were introduced in the field of microfluidics and POC to fulfil and satisfy the requirements of the final application. A survey based on a sample of selected microfluidic companies (shown in figure 2), modified by [22], reveals that 59 % of the commercially available devices are made of plastics (mainly thermoplastics), 12 % of glass, 12 % of papers, 6 % of elastomers and 6 % of epoxy resins [22]. The same trend is not followed at the research scale. By looking at the number of publications on Scopus using the keyword microfluidic and limiting the research to paper-based microfluidic, polymer microfluidic, PDMS microfluidic and glass microfluidic, one can observe that in Academia, 55 % in PDMS,

12 % in silicon and glass , 20 % is made of thermoplastic materials (12 % PMMA, 3 % COC and 5 % PC), and 13 % in paper.


**Figure 2.2** Sample of microfluidic companies and main material used.

Generally, silicon and glass are preferred for nanoparticle preparations, on-chip reactions, or when the use of aggressive solvent is required; Hydrogels are for bio-cellular applications, thermoplastics and thermosets are common for DNA analysis, protein assay and biological application in generals, while elastomers are preferred for cell cultures, screening and biochemical assays.

In table 2.1 are summarised the common materials used in microfluidic, their fabrication method, applications, advantages and disadvantages.

***Table 1 Materials for the fabrication of microfluidic device***

| *Material* | *Fabrication method* | *Applications* | *Advantages* | *Disadvantages* | *References* |
|---|---|---|---|---|---|
| Silicon and glass | Standard photolithography and soft lithography. Laser ablation | On-chips reactions; Droplet; Solvent extractions; In situ fabrication | Thermal conductivity; Stable electro-osmotic mobility; Resistance to organic solvent | High cost of fabrication; Dangerous chemicals involved; In situ fabrication | [23], [24] |

| | | | | | |
|---|---|---|---|---|---|
| Hydrogels (e.g. PEG, alginate, collagen etc) | Direct writing method; generation of channel and channel sealing | 3D cell cultures | Biocompatibility | Lower resolution in microfabrication; Incompatibility with organic solvent | [25][26] |
| Thermoplastics (e.g. PMMA, PC, PS, PET, PVC, ABS, PLA) | Thermomolding; Fusion deposition modelling; Laser cutting and bonding. | DNA Analysis; Protein assays | Resistance to alcohols; Low cost; rapid prototyping | Incompatibility with most of all organic solvent | [27] [28] [29][30] |
| Elastomers | Cast | Cell culture; Cell screening; Biochemical assay | Easy and low cost of microfabrication; High elasticity; Gas permeable; | Incompatibility with organic solvents; absortion of hydrophobic and small molecules | [31] |
| Paper | Photolithography | Biological, pregnancy test | Low cost | 2D microfluidic device | [32][33] |
| Hybrids | Combination of different material | | Integration of functionalities | High cost of fabrication | [34] |

**Table 2.1.** classes of materials for the fabrication of microfluidic device.

With respects to glass, silicon and PDMS, thermoplastic materials represent a cheaper solution for the fabrication of microfluidic device and can bring several benefit in terms of reduced cost and simplified manufacturing procedures, particularly when compared to glass and silicon [30], [35]. With respect to paper microfluidic for which only lateral flow assays are performed, thermoplastics enable to perform a broader range of assays. An additional benefit of thermoplastics which is extremely attractive, is the wide range of available plastic materials which allows the manufacturer to choose materials' properties suitable for the specific application. In addition to that, polymers possess several advantages over other materials. They are obtainable at low cost (few pounds per Kg), require relatively simple processing techniques and exhibit accurate repeatability in mass-production.

Furthermore, in recent years different rapid prototyping techniques have been developed and optimized for the production of thermoplastic microfluidic devices. This includes a technique developed in our laboratory, which enables the prototyping of a microfluidic device from design to test in less than 15 minutes [29]. There are different methods available to microstructure thermoplastic materials for rapid prototyping microfluidic devices. These methods can be categorized into replication and direct fabrication methods. The replication methods involve the preparation of a mould and can be summarised into imprinting, hot embossing and solvent casting. While the direct

fabrication methods can be divided as well into two subcategories: subtractive manufacturing methods such as mechanical machining, plasma etching, x-ray lithography and laser ablation and additive manufacturing methods e.g. 3D printing.

### *2.2.1 Replication Methods*

Replication methods involve the fabrication of a master mould. This can be carried out via photolithography as explained in the fabrication of PDMS microfluidic devices. The use of photolithography enables to manufacture highly precise moulds, with features down to the submicron scale. However, it requires highly skilled personnel, access to clean room facilities and the preparation of one single mould with 2D features can cost approximatively 514.00 $ (including the price of the technician salary, silicon wafer, high-resolution photomask, and clean room fees) [36]. If submicron features are not specifically required, a CNC milling machine can be employed to manufacture the mould [37]. In this latter case, the mould can be fabricated on a variety of material from steel to Teflon, with an approximately manufacturing cost of £ 1-20/per mould [37]. Once the mould is prepared, this can be readily used as a negative mould to cast the polymer via solvent casting, where the polymer is firstly dissolved in a solvent or via compression moulding. Another approach is to prepare a positive mould where a thermoset is cast on it and then used as negative mould. For example, Fiorini et al. [38], proposed this replication method to fabricate polyester and PMMA microfluidic devices. In the case of the polyester microfluidic device, this was cast into the prepared PDMS mould from the silicon master (fig. 2.4 A) adopting an *in situ* polymerization approach. Basically, the monomers of the polymer that needs to be polymerized are placed in the mould with an initiator and a catalyst and a polymerization reaction activated my mixing and heating.

For the preparation of the PMMA microfluidic device, the same group adopted a hot embossing approach (fig. 2.4B).

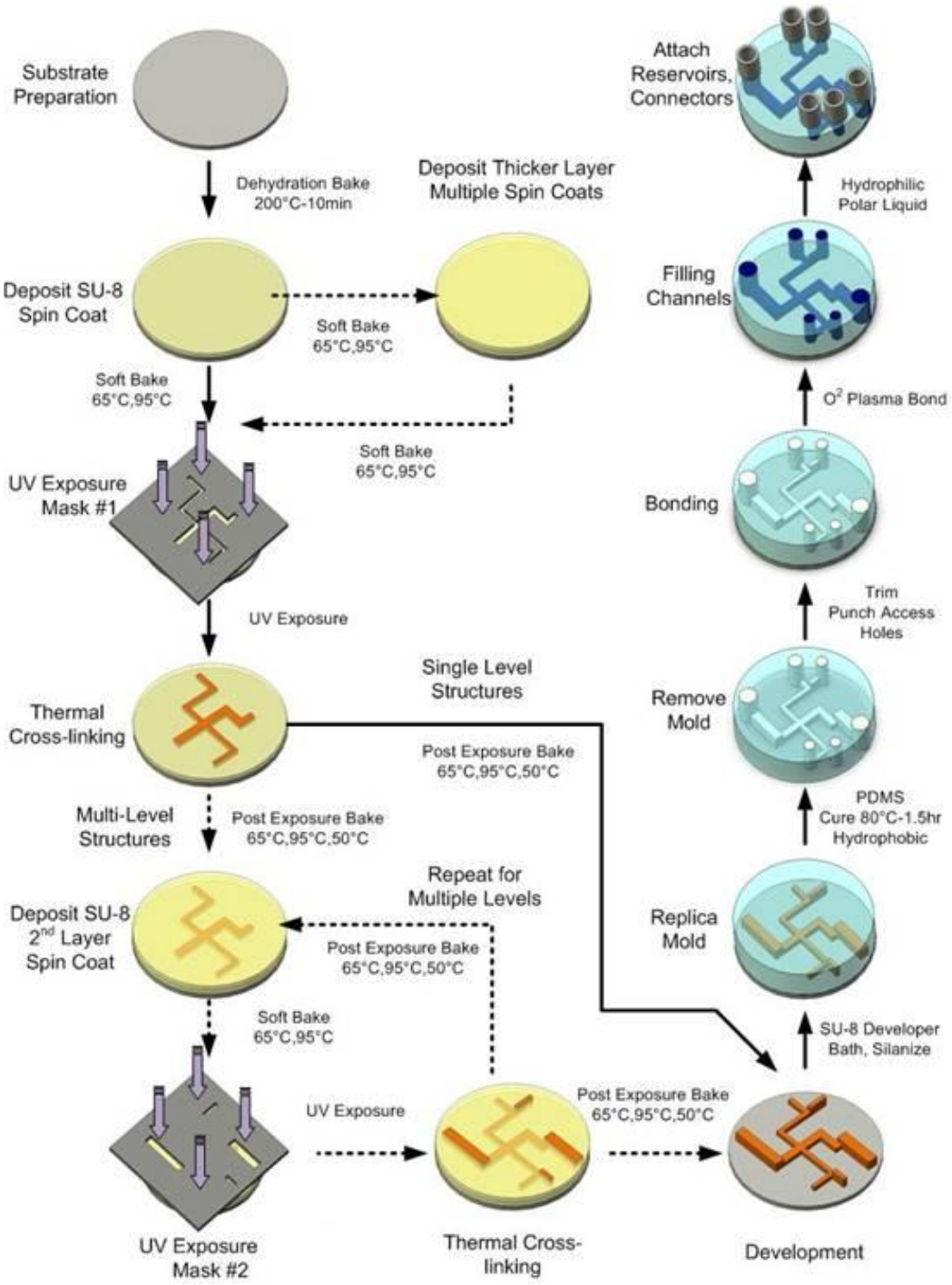


**Figure 2.3** Schematization process of soft lithography- from mould preparation to the test of the final PDMS microfluidic device. (taken from Glawdel, T., "Design, Evaluation, and Characterization of Electrokinetically Pumped Microfluidic Chips for Cell Culture Applications," M.A.Sc. Thesis, University of Waterloo, 2008.)

Hot embossing is a microstructuring process that allows to precisely transfer features from the mould to the polymer, by pressing the two part together [39]. The polymer is

heated up to temperature higher than its glass transition temperature, $T_g$. Once the polymer starts softening, pressure of the order of a few MPa is applied, and the polymer begins to take the shape of the mould. The shaped polymer is cooled down to a temperature below the glass transition temperature, and the pressure applied is decreased. Once at room temperature, the part is demoulded (Figure 2.4A and 2.4B).

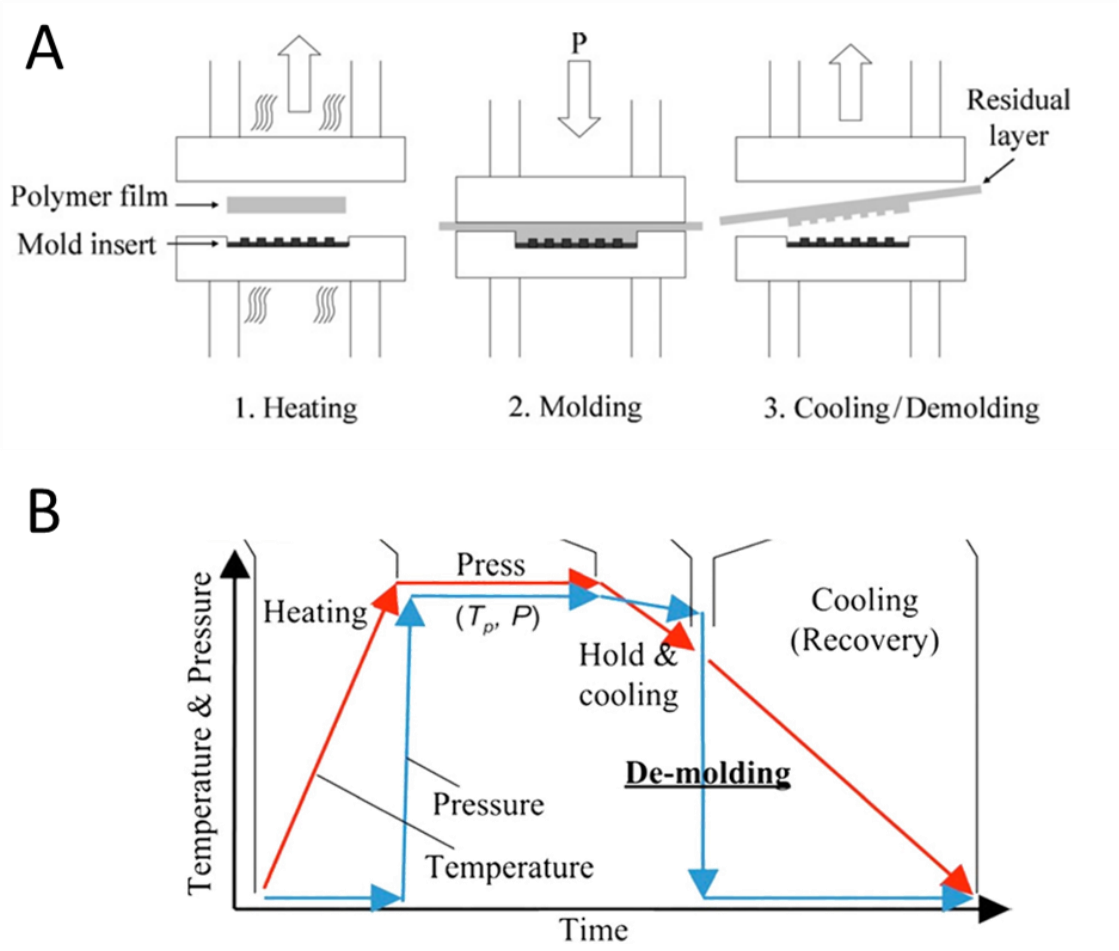


**Figure 2.4** Hot Embossing: A) schematic representation of the 3 steps involved in the hot embossing procedure (modified from [40]); B) temperature and pressure profile involved during the 3 steps of hot embossing (modified from [39])

The replication methods are cost effective, and usually applied in industry. In research settings, when different cycles of designing and testing are necessary, this method can rapidly become expensive and time consuming because of the price and the time to fabricate the mould, theoretically reducing the number of the manufactured part from 5000 down to 1000 per month, not considering the case when the mould is prepared via

casting PDMS, where the number of the possible prepared devices goes down to 150 per month [41].

### *2.2.2 Direct Fabrication methods*

Direct fabrication methods allows the preparation of up to 2000 pieces a month [41] and can be subcategorised into subtractive manufacturing and additive manufacturing. In general, subtractive manufacturing is a top-down manufacturing approach involving the removal of material from a starting block (workpiece). The related technologies that can be employed to microstructure microfluidic devices using a subtractive fabrication method approach are cutter plotter, CNC milling and laser ablation. Micropatterning using a cutter plotter is also known as xurography [42]. This technology involves the use of a razor blade to microstructure microfluidic channels. Usually, it is applied to pattern microchannel that are cut through double adhesive films and then enclosed between glass slides or thermoplastic materials [43]. The minimal reliable channel resolution achievable with this technology for complicated geometry is 300 µm [44]. Computer numerical control (CNC) milling is a machining process that makes use of a rotary cutter to remove material from the workpiece. Different parameters can be changed in order to obtain a

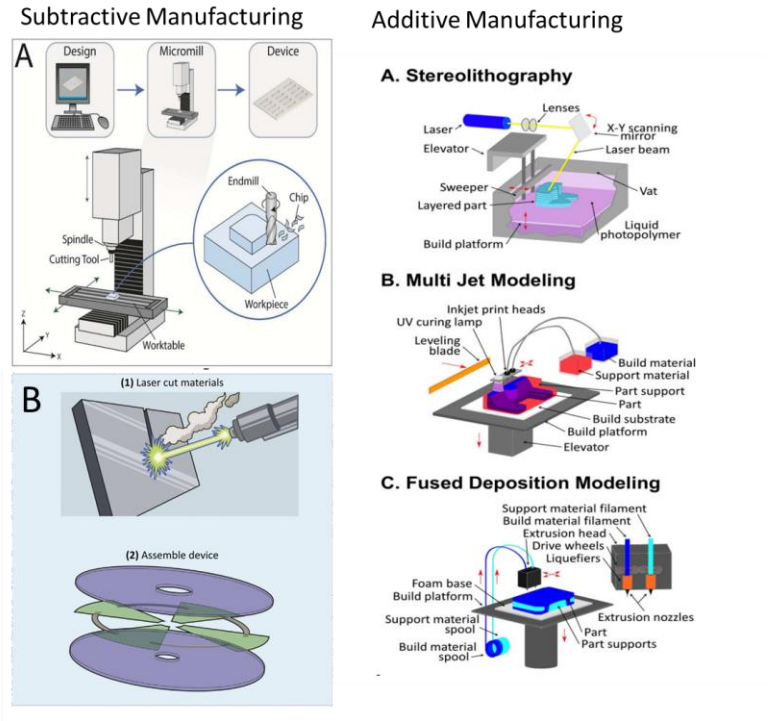


**Figure 2.5** On the left schematic representation of subtractive manufacturing approach: A) representation of the basic components of a CNC milling machine (modified from [37]); B) schematic representation of the step to manufacture microfluidic device, microstructuring the substrate material using a laser (modified from [45]). On the right schematic representation of 3D printers used in additive manufacturing. A)

stereolithography 3D printer; B) Multi jet or Poly Jet 3D printer; C) Fusion Filament Fabrication or Fusion deposition modelling 3D printer (taken from [46])

better accuracy and precision such as the translational speed of the stage where the working piece is, the spindle speed and feed rate, related to the power, and the kind of endmill used to remove the material by cutting along the chosen axes. One of the most undesired featured that can be observed using a CNC milling machining of thermoplastic are a high surface roughness and thermal induced damages to the material due to the heat generated by the friction of the rotary endmill in contact with the material. The surface roughness resolution is proportional to the feed rate and can vary between 0.4 -2 µm, while the precision of the minimum cutting tolerance can vary from 3 to 25µm and it is strictly related to the type of CNC milling machine. Usually high-end CNC milling (Typically with capital expenditure circa $15,000) have an accuracy of 25 µm [37], [41], [47]. Laser ablation makes use of lasers to remove material via fusion and/or vaporization cutting from a starting workpiece. Laser ablation technology will be explained in detail in chapter 5.

Additive manufacturing also known as 3D printing is used as a rapid prototyping method, both for thermoplastic materials and thermosets. Its attractiveness for the manufacturing and microfluidic community is twofold. First, it allows to obtain 3D monolithic structures in an unprecedented way, secondly it allows a trial and error approach for the fabrication of a design. Once a CAD design is prepared, 3D printing technologies do not require handling procedures, but can be started immediately. There are four main different 3D printing technologies that have been successfully used for the production of microfluidic devices: Inject 3D Printers (I3DP), Stereolithography (STL), 2 Photon Polymerization (2PP) and Fusion Deposition Modelling (FDM). The I3DP operates generating small droplets, powder based or photopolymer based, that are placed with high accuracy according to the sliced 3D model in layer by layer, where it each step cross sections of the final design is formed. When the inkjet material is powder based, an adhesive polymer solution is added at each step by the nozzle to bond the powder together and to from the first layer, the powder in excess is removed. Then another powder layer is added and the successive cross section bonded with other adhesive polymer solution. This process is repeated until all the slices of the final part are printed. The powder size is usually in the order of 50 to 100µm. In the case of the photopolymer ink, this is places drop by drop and the first slice of the model is photopolymerized by UV light. Different photopolymers can

be placed per each layer to form support and build material or to have a multimaterial printed part. The resolution of the printer in the z direction is limited to 200 μm. The 2PP allows to achieve printing resolution of tens of nanometers and it can be applied to the same materials currently employed for lithographic applications. It makes use of a femtosecond laser with a wavelength in the near infrared to selectively and precisely photo polymerize only in the confined area where the material is triggered by the laser pulse. This highly precise 3D printing technology have been employed mostly for the production of mould for microfluidic fabrication. One of its biggest limitation to directly print microfluidic devices is the printing time. In fact, as reported by Sugioka et al., to print a 1 $mm^3$ volume microfluidic structure several days are required [48]. STL 3D printer makes use as well of lasers and photopolymers. The photopolymer resin is usually placed on a tank. STL printers are available into two different configurations, free-surface or bat configuration. In the free-surface configuration the resin is polymerized always at its topmost region. In this case the build platform is always immersed in the resin tank. When a layer is polymerized the build platform is moved in the z direction downwards to expose another layer of resin to the surface. In the bat configuration, the resin is polymerized against the bottom of the resin tank and the build platform is suspended in air. Basically the build platform during the printing of each layer is immersed inside the resin tank, the laser hits the 2D cross section as per the sliced design to polymerize the resin then the build platform goes back in the original suspended position. This process is repeated until the final model is printed. In this last configuration the model results to be printed upside-down. The FFF 3D printing technology is maybe the most famous among all the others. Basically a thermoplastic material is extruded throughout a nozzle on a build platform following a coded path to print at each step the 2D cross section of the sliced 3D model. Despite very promising results, 3D printing technologies still have some challenges namely (i) printing time, (ii) multi-material manufacturing, (iii) assembly, (iv) print fidelity. Furthermore, post treatment are often required to overcome the difficulty in removing supporting material [49]. It is maybe to early now to truly appreciate the 3D printing technology to directly print microfluidic devices that have at least same characteristics in terms of transparency and channel dimension than other conventional materials employed in subtractive manufacturing. On the other hand 3D printing represents a faster and cost effective valid alternative for the fabrication of negative mould for replication methods [46].

## 2.3 The need for a sustainable solution

In 2013 the microfluidic market was estimated to $1.6 billion with a projection to be almost $4 billion in 2018 [50]. Microfluidic technologies were introduced with the promise to revolutionise the field of biological analyses and chemical syntheses, because it allowed the automation of laboratory equipment and in vitro diagnostic devices. The field that is benefiting the most from microfluidic technologies, is gene sequencing and point-of-care diagnostics [51]. Point-of-care diagnostics microfluidic will enable to perform diagnostic test and provide analyses capabilities that do not require specifically designed laboratory processing capabilities and can provide practical and marketable devices to address major clinical problems specially in developing world [52]. On the other hand, the use of disposable products in healthcare facilities and hospitals continues to increase [53]. The choice of disposable items is due to considerations on safety convenience, reduced risk of cross contamination and cost. In 1992, A study conducted on the medical waste of the Emmanuel Hospital Health Centre in Portland, Oregon (a 385 bed teaching hospital) shown that 939 tonnes of medical waste were produced annually, and the 85% of them was from disposable, single-use medical equipment [54]. Nowadays the waste produced by hospital and healthcare facilities in USA is estimated to be about 6 tonnes per day [55]. On a larger scale, over 300 million of metric tons of plastic waste are produced in the world annually, and the 50% of these plastics is from disposable items [10]. It can be therefore anticipated that new upcoming microfluidic technologies will add more volume of plastic waste. This additional waste could bear an increased financial burden for communities, linked the control of pollution emission. Anecdotal evidence shows that medical waste, including contaminated plastics, is, in the most extreme situations, disposed of in open fires or thrown on the road side [53], or combined with municipal waste [8]. Furthermore, there is documented evidence that incinerators, when available, are often rudimentary or poorly maintained and sometimes inadequately manned [56], [57].

Embedding sustainability and safety considerations at an early stage is key to reduce the impact that future technologies will have on the environment. In addition, it will help to reduce greenhouse gas emissions, dependence from fossil resources and support achievement of a net zero $CO_2$ emission by 2050, which is essential to deliver on post-Paris (COP 21) climate commitments [58]. The rationale behind material choice for the manufacturing of a new microfluidic device has always been driven by physical and chemical properties and prototyping technologies. It should not be surprising that

petrochemical derived polymers are currently favoured for research and development of microfluidic for point-of-care diagnostics in lab-on-chip format by both academic laboratories and industries. It is clear now that there is a clear need to address the amount of plastic waste and the way products are disposed of. This can be done by adopting a Design-For-Sustainability (DFS) approach. Design-for-sustainability is a branch of design for X, a set of engineer design principles that aim to manufacture successful commercial products [59]. In particular DFS aims to achieve zero-carbon emissions and minimal non-renewable resource use by choosing appropriate technology, materials and production processes at the design stage [60].

Thus, the full life cycle analysis of the final product needs to be undertaken at the design stage. Despite the importance and the relevance of the topic, to date, there are only few studies that have taken into consideration a sustainability approach for the next generation of microfluidic devices. For example, recycled and bio-based polymers have been proposed to manufacture microfluidic devices. So far very little attention has been given to recyclable material such as Poly ethylene terephthalate (PET). While paper microfluidics have been investigated widely in the past decade, the biodegradability of cellulose has never been underlined, or further investigated in microfluidic publications.

In the next sections, the state of the art of the material employed to manufacture environmentally sustainable microfluidic devices will be described. They will be categorized into: recyclable, and biodegradable substrate materials, in function of the different end-of-life scenarios that they can undergo.

### *2.3.1 Recycled substrate materials*

Recycling is a process that converts waste materials into new materials or energy. The introduction of recycling for the production of microfluidic devices can lead to a reduction of waste in healthcare, laboratory and industry, as well lower greenhouse gas emissions. In a laboratory setting, when a microfluidic device cannot be reused, this can be decontaminated and then mechanical recycled to manufacture and test another device. In this way, both the demand for new raw materials, and waste are decreased. Hence, the energy usage, air pollution and water pollution are reduced. In the same way, the adoption of chemically recycled material instead of pristine raw material will help to reduce the demand for material extraction and consequently the reduction of environmental pollution. Thermoplastic materials can be recycled adopting four different technologies.

The first one is the reuse of material following a washing step, which is not suitable for single-use items. The second one is mechanical recycling, the third one is chemical recycling and the last one is pyrolysis and energy recovery. A limited number of research studies have shown the possibility to use mechanically recycled PMMA for the production of optical fibre sensors [61] and microfluidic devices [62]. For instance, Wan et al. showed the possibility to thermo-mechanical recycle PMMA up to 4 iterations without losing optical properties and biocompatibility (Figure 2.6) [62]. Despite optimum results, these recycling processes require specific facilities, such as an extruder or an expensive heated press. In the case of single use medical devices, a sterilization step should be included prior to mechanical recycle the device. We have tested commercially available chemically recycled PMMA (Re-PMMA) as a novel PMMA substrate for microfluidic medical components [63].

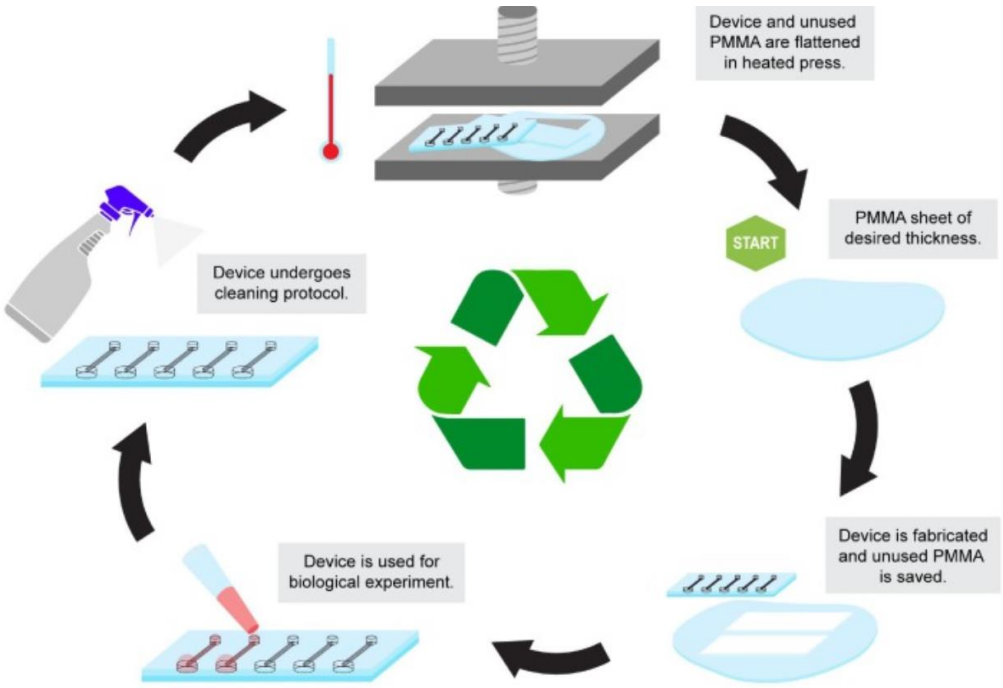


**Figure 2.6** Schematic diagram representing the protocol to mechanically recycle PMMA for the production of environmental friendly microfluidic device in a laboratory setting (taken from [64])

We proved that Re-PMMA perform as good as pristine PMMA in terms of microstructuring and bonding strength. Thus, petrochemical derived PMMA can be directly replaced by Re-PMMA in the production of microfluidic devices without any

optimization of the manufacturing protocol. This finding and an explanation of the chemical recycling process are shown in chapter 4.

Another thermoplastic polymer, largely employed and for which there is already a recycling stream route is PET. PET is the same polymer used in the plastic bottles industry. Differently from PMMA, PET is not largely used in the production of microfluidic devices but a few examples have been demonstrated in literature. A latter example is from Jackson et al., that used PET to fabricate semi-automated DNA extraction on a centrifugal device using mixing via an external magnetic field [65], [66]. The reason why PET is still not largely adopted by microfluidic researchers and manufacturers might be due to the fact that it is not easily available in sheets format. In fact, fabrication technologies of microfluidic devices from hard plastic employed both in academia and industry rely on CNC milling and Laser cutting, which require a sheet format substrate. Even though promising results have been shown, and the possibility to embrace a net zero $CO_2$ emission by adopting recycled thermoplastics, this route is still economically not convenient at the moment.

### *2.3.2 Bio-derived substrate material for the production of environmentally sustainable microfluidic devices*

The choice of a core material made of bio-derived products strongly decreases the potential environmental footprint associated to the raw material extraction, as well as could bring to several end-of-life scenarios with more environmentally sustainable possibilities. A small number of research groups have attempted to use bio-derived material for microfluidic production. Wallarabe and co-workers, chose Shellac, a thermoplastic polymer from natural origin, secreted from the female lac bug Kerria lacca, in order to reduce the environmental impact at the production, usage and end-of-life stage of microfluidic POC devices (Figure 2.7 A). Shellac has been used for the manufacturing of high volume consumables before the 1950s. For example, Shellac was first employed to produce phonograph before being replaced by PVC (Polyvinyl chloride) in 1948. Nowadays, Shellac is used as coating material for drug release, as food additive and as a dielectric layer to produce environmental-friendly transistors. One of the main advantage of this bio-derived resin is its low glass transition temperature, Tg. Shellac has a Tg of around 42°C, enabling the possibility of shaping it at lower temperature with respect to

other non-bio-derived polymers. Shellac could enable, for example, energy efficient hot-embossing. However, due to its brittle nature, in order to produce point of care devices in a green fashion, Wallrabe et al. had to dispense the shellac/ethanol solution onto paper to supply the system the proper mechanical properties to be suitable for a hot embossing process to imprint microfluidic structures on the shellac substrate (figure 2.7 A.i). Finally, the authors successfully showed the possibility to easy prototype and manufacture a POC device choosing carefully the primary resources and the fabrication methods to use only materials from renewable resources and for low-energy consumption, around 18 kWh/Kg, (Figure 2.7A.ii). Despite promising results, a limitation of this proposed green fabrication methods is that only 2D microfluidic structures can be prototyped and the integration of different components, such as electrodes or membranes can result difficult and cost expensive. Additionally, the need to use paper to provide functional support can limit the number of suitable microfluidic applications. For instance, all the application in which fluorescence analysis needs to be undertaken are hindered, because of the high autofluorescence of paper. Pursuing the same goal, Kokini and co [67] proposed Zein, a polyamine protein found in maize as a new sustainable substrate material for microfluidic applications.

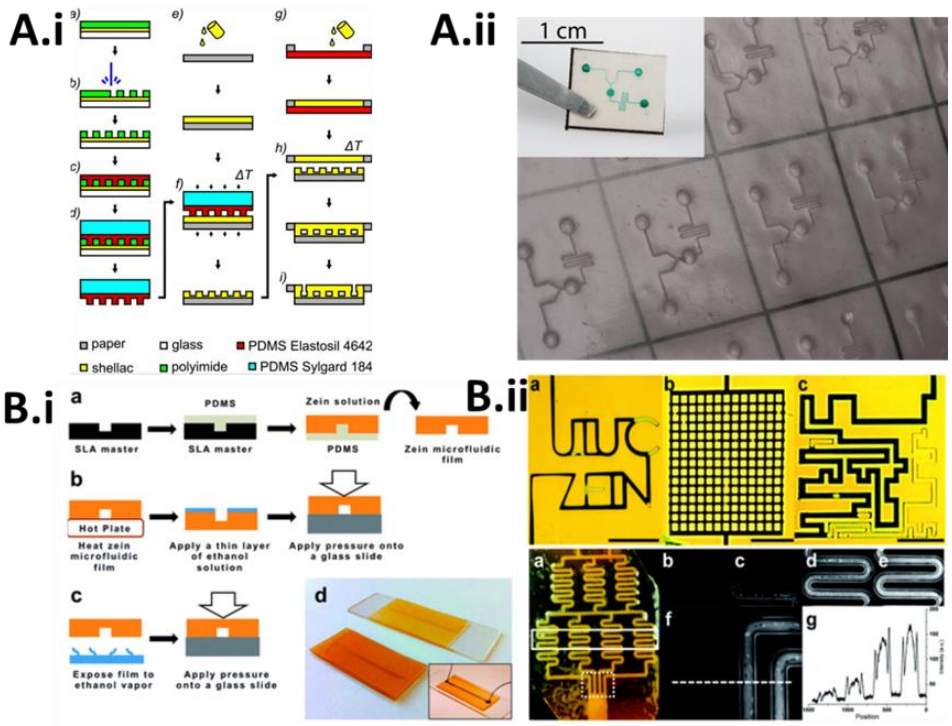


**Figure 2.7** A) Microfluidic device made of Shellac and paper. A.i) Schematization of the replica moulding protocol to manufacture the Shellac device: A.ii) Picture of the device with insert a device made of shellac and paper filled with blue food dye. (Taken from [68])**;** as can be observed from the picture, Shellac has a

good transparency but the presence of the paper can hinder its applicability in applications where low autofluorescence is needed B) Microfluidic gradient generator made of Zein corn protein. B.i) Schematization of the replica moulding protocol to manufacture the Zein device; B.ii) picture of the device (taken from [67]) showing a good transparency.

The work of Kokini et al emphasized the need of environmentally sustainable microfluidic devices especially when a great number of samples and/or trials are required. Zein is chemically composed of high amount of amino acids and it is currently used in the food industry to coat candy, nuts, fruits and pills as well as used in food packaging and in adhesives [69]. The authors relied on Zein for its excellent manufacturability in film shapes, with the possibility to tune end engineer the final substrate properties by changing the processing parameters. They successfully demonstrated the possibility to manufacture via solvent casting several complex microfluidic structures and proved good bonding strength to different substrates without any leakage (Figure 2.7 B.i-ii). Although, when in contact with water, due to protein precipitation Kokini et al. observed a lack in the transparency, with the Zein substrate becoming more opaque, leading the authors to bond the microstructured Zein substrate to glass. While transparency is not an issue for most devices placed in the market (especially for POC applications), transparency can become an issue when optical detection is needed, either to check the final design (optical quality control) and for analytical purposes (for example cell sorting and imaging).

Cellulose is a material already largely used in hospital, chemical industry, chemistry labs and in microfluidics. Cellulose is a water-insoluble homopolymer of glucose that is synthesized from plants and from some bacterials [70]. Cellulose is one of the most abudant biomaterials on the earth, it is low cost and easy to manufacture. Cellulose is used as substrate material for paper-based microfluidic applications. Those applications make use of lateral flow assays to detect pathogens and biomarkers utilising labelled antibodyes to capture and detect biomolecules through colotimetric readout. In these assays, the fluid is transported via capillary action, without the requirement for fluid handling equipment [71]. The fabrication methods of paper based microfluidic devices involve wax patterning, inject printing, photolithography, plotting and laser treatment [72]. Microwire electrodes can be incorporated to provide highly sensitive and selective virus detection via electrochemical impedence spectroscopy. Although, paper-based microfluidic is a highly environemntally sustainable and powerful technology, the use of lateral flow assays is limited and does not cover all microfluidic applications.

Advances in 3D printing technologies in the last five years, have permitted to reach a scale compatible with microfluidic features. A few examples of microfluidic chips have been demonstrated recently, with a focus on the use of a FDM 3D printer. Polylactic acid (PLA) is a material derived from starch and most commonly used in combination with FDM. One of the first examples was given by Morgan et al., in 2016. The authors tuned carefully the print-speed, nozzle temperature, build plate temperature and the fill density to show as proof of concept a droplet device for the encapsulation of live stem cells [73]. Another example was given by Tothill et al., who manufactured a 3D printed device for glucose assay [74]. Despite very promising results, the fabrication of PLA microfluidic device via FDM still have some limitation such as printing time, resolution, surface finish and post treatment required. Moreover, a good transparency has not been achieved yet. With this respect, research has been carried out in order to overcome the transparency issue. For instance, Gaal et al., used a glass slide as a window to have optical access to the 3D printed microfluidic channel, showing as proof of concept a microfluidic e-tongue capable of distinguish basic tastes [75]. Instead of incorporating a glass slide window, Bressan et al., show the possibility to directly print on a transparent PMMA slide to allow visualization. They have shown the possibility to produce silver and gold nanoparticle with tuneable dimension from 5 to 34 nm [76], [77]. Another example is given by Romanov et al., that to print high pressure and heat-resistant transparent microfluidic devices. They tested both a PLA and a nylon filament, to choose then PLA as a substrate material, because of its low autofluorescence, showing as a proof of concept a DNA melting device [78].

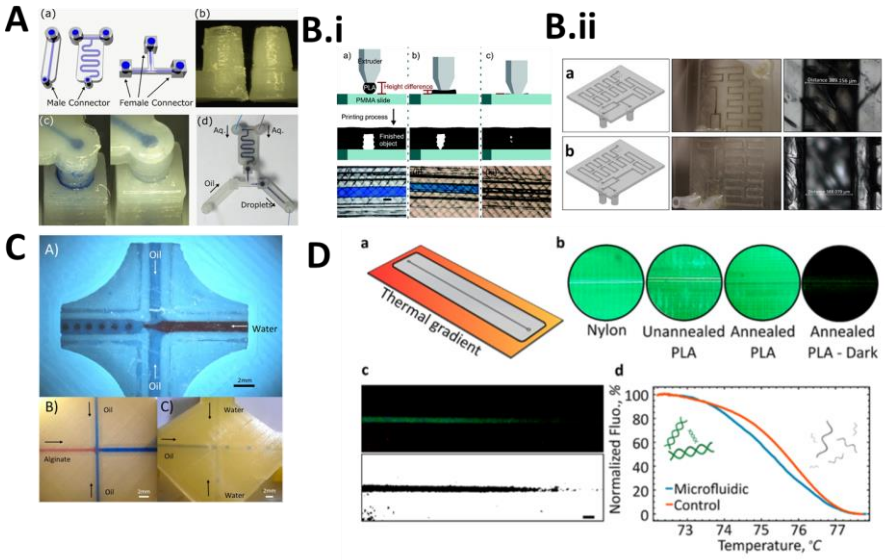

**Figure 2.8** 3D printed PLA microfluidic structure.A) droplet device (taken from [79]); B.i) schematic representation of 3D printing PLA microfluidic structure on a slide of PMMA, B.ii) CAD of the final device and picture of the channel to show transparency (taken from [74]); C) Droplet PLA 3D printed microfluidic device with an optical glass window integrated (top), droplet device without optical window (bottom) (taken from [28]); D) 3D printed microfluidic device for DNA melting analysis (taken from [78] )

While none of the authors mentioned the environmental credentials of PLA, these examples show the possibility to prototype environmentally sustainable microfluidic devices from a bio-derived, biodegradable material. 3D printing is an emerging technology in microfluidics, which still has limitations in terms of resolution, post-printing time and surface finish. Furthermore, the prototyped structures via FDM have not similar features to the one of a mass produced device via injection moulding.

By contrast, a layer-by-layer lamination approach allows flexibility in the design, is user friendly, low-cost, does not require the need of post treatment and can be applied to an almost unlimited number of materials [80], [81] . It also enables surface and local treatments, and integration of various complex elements, such as membranes or electrodes. In this respect, my own work has shown the possibility to $CO_2$ laser microstructure PLA to rapid prototype microfluidic devices in few minutes (Figure 9). The prepared devices have shown better performance with respect to qPCR inhibition in comparison to PMMA, good transparency without the need of integrating optical windows, better biocompatibility then other typical thermoplastic material employed for microfluidic cell culture or organ on a chip, and no absorption or adsorption of small molecules, and the possibility to integrate graphene water ink printed electrodes to perform electrochemical analysis [82], [83]. This work is presented in detail in this thesis in Chapters 5 and 6.

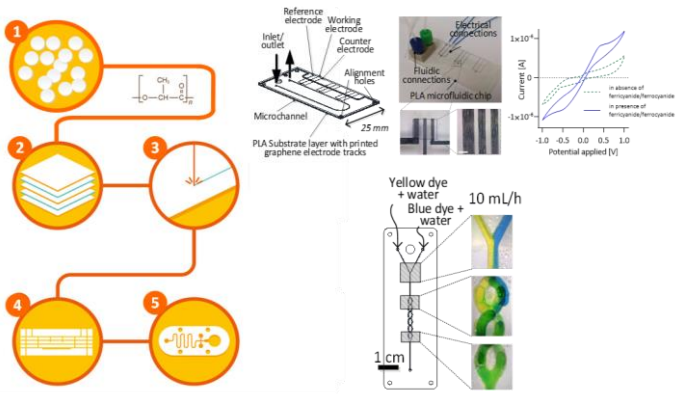


**Figure 2.9** schematic representation of the layer-by-layer laser based fabrication technique of environmentally sustainable microfluidic devices (on the left), schematization and a picture of a REDOX device (top right) and of a microfluidic mixer (bottom right). (modified from [82])

#### *2.3.2.1 Bio-derived non-biodegradable thermoplastic materials*

It is important to note that, more and more research is being carried out, both in academia and industry, on the synthesis of bioderived monomers such as isosorbide, in view to replace petrochemical derived monomers in the production of common thermoplastic materials such as: polycarbonate, poly methyl methacrylate, poly ethylene, or polyurethanes [68]. This material research will lead to the production of bioengineered material with tailored properties that can be used for the production of environmentally sustainable microfluidic devices. Here a note on the fact that these materials won't be biodegradable.

## 2.4 Conclusions

Material choice is a crucial part of the design process of microfluidic devices. Until now, researchers and engineers have focused on performance in terms of prototyping, mass-manufacturability, mechanical or chemical properties, but not sustainability. With the advent of point-of-care polymeric-based single-use devices, sustainability is a key aspect that needs to be addressed. A few solutions for the prototyping of sustainable microfluidic devices have been demonstrated, but they are not fully effective yet because they fail to meet requirements in terms of resolution and transparency, and they are not amenable to high volume production. For instance, in the case of Shellac and Zein for which a replication method based on mould preparation via photolithography has been shown, good resolution in terms of channel cross section and channel size has been demonstrated. However, both Shellac and Zein does not have a good transparency. This can be a drawback for applications where good optical properties are needed. On the other hand, the demonstrations made with sustainable transparent hard plastics, such as RePMMA and PLA, that are based on a layer-by-layer approach, rely on laser microstructuring technologies, for which the channel cross section is triangular or trapezoidal and the resolution is above 100 μm. Their manufacturability is not limited to laser microstructuring or to a layer-by-layer approach. Replication method can be adopted and good resolution and high reproducibility achieved. Although laser microstructuring gives restriction in terms of resolution and channel cross section, it is a fast and mask-free prototyping method, that can enable a faster and larger translation from conventional plastic to sustainable ones. It is important to underline that precise reproducible highly spatially resolved microfluidic geometries are influenced by the microstructuring technology adopted and not by the material properties itself. The material properties, such

as viscosity, flow rate, molecular weight and thermal properties will influence possible shrinkage and aspect ratio achievable.

In table 2.2 are summarized the material proposed so far for the production of environmentally sustainable microfluidic devices. The adoption of recycled or bioderived materials in the microfluidic field will form strong foundations to pursue the reduction of $CO_2$ emission and plastic pollution in the field. It is important to underline as well that the material choice cannot be decoupled from consideration and actions on how the used material is manufactured and disposed of. While point-of-care microfluidic or diagnostic biomedical devices used in hospital settings or at the research scale, are currently incinerated. However, if autoclaving is effective as decontamination method, recyclable material could then be separated and collected for chemical recycle, and biodegradable material could be composted. In the latter case, further studies will need to be undertaken to assess the complete biodegradation to avoid leaching of potential harmful compounds. These new approaches to hospital waste management would require new considerations in waste management workflow, training as well as policy and legal matters.

| | material | prototyping | transparency | demonstration | cost | end-of-life |
|---|---|---|---|---|---|---|
| Recyclable | PET | Layer by layer | Very good | DNA isolation | very low | CR, MR, I, L |
| | RePMMA | Layer by layer | Very good | Cell culture | high | CR, MR, I, L |
| Bio-derived | BioPET | Layer by layer | Very good | N.A. | low | CR, MR, I, L |
| | BioPC | Layer by layer | Very good | N.A. | low | CR, MR, I, L |
| | BioPMMA | Layer by layer | Very good | N.A. | high | CR, MR, I, L |
| Bio-derived And Biodegradable | Shellac | Replication method | medium | Microfluidic structures | low | C, I, L, |
| | Zein | Replication method | medium | Gradient generator | high | C, I, L, |
| | cellulose | Wax printing | N.A. | | very low | C, I, L, |
| | PLA | 3D printing, Layer-by-layer Replication method | good | Droplet, mixing, DNA melting, cell culture, protein analysis | low | C, CR, MR, I, L |

**Table 2.2.** Possible and demonstrated environmentally sustainable material for the production of microfluidic devices. CR=chemically recycled; MR=mechanically recycled; I= incineration; L= landfill; C= compostable. The table is not comprehensive of all the possible material that can be used for the production of microfluidic but take into account only key material that have been demonstrated or can be easily implemented at the research setting or in the mass market.

# Chapter 3: SOLVENT ASSISTED BONDING OF PMMA BASED MICROFLUIDIC DEVICES: CHOOSING THE RIGHT MATERIAL

## 3.1 Introduction

This chapter describes a practical guide to follow when embarking in the Poly methyl methacrylate, PMMA, choice when a safe and cost effective ultra-fast solvent assisted bonding method is chosen. The chosen bonding protocol developed by Liga et al. 2016 [29], enables to prototype in less than 15 minutes from design to test up to 19 layers of complex microfluidic devices.

Among all of the thermoplastic materials, hard plastics, used for the production of microfluidic devices at the research scale, PMMA is one of the most used [27]. PMMA is transparent, has good mechanical properties, it is slightly hydrophilic and it is commercially available worldwide in sheets format of different thickness sizes (< 0.2 mm up to 25 mm) [84], [85]. PMMA is a popular choice because of its known optimal workability in conjunction with prototyping methods to produce complex microstructures, e.g. CNC milling, laser cutting, laser engraving, and hot embossing. Furthermore, PMMA can be mass processed via injection moulding, thus enabling a faster transition from the research scale to the market.

PMMA is manufactured by a number of different companies with brand names, such as Perspex, Plexiglass, Clarex, Clear Glass, Clear Acrylic. Although they have the same basic polymeric structure, their molecular weight could be significantly different if they are processed in different ways, such as casted or extruded. Extruded PMMA sheets require to start from a grade of PMMA pellets/beads with a lower molecular weight with respect to the cast one, due to the processing technology that requires a material with a lower viscosity. They might be different as well from a macroscopic point of view. Casted PMMA will show higher optical properties than extruded one because it is casted between two glass plates which transfer on the final sheet a higher surface finish. Extruded PMMA will have better tolerance in terms of thickness but with final heterogenous properties. Furthermore, additives may be used to add UV resistance and/or anti flammable properties.

The research community has developed, tuned and optimized several bonding methods for the production of PMMA based microfluidic devices. Fusion, thermal, surface activated, direct and indirect, lamination reversible bonding methods have been developed. All of this bonding protocols have advantages and disadvantages, but they cover most of the required final properties needed by the chosen microfluidic application [86]–[98]. Might it be the case that each developed prototyping method and protocol to produce microfluidic devices in PMMA is not universally applicable, if the starting material is different?

### *3.1.1 Solvent Assisted Bonding of PMMA: Choosing the right solvent*

Solvent assisted bonding is one of the most preferred direct bonding methodologies to prototype microfluidic devices in hard plastics [97], [99], [100]. With respect to thermal bonding it requires lower temperature and has, in general, lower channel deformations. With respect to surface activated or chemical bonding methodologies, such as Plasma or UV bonding, it does not require expensive apparatus and it can be applied in low resource settings lab [99].

This method can be carried out applying the solvent in its liquid or in its vapour phase. A solvent is that chemical that can interact with another material (solute), where in the binary system solvent-solute the attraction forces between the solvent and the solute are bigger than the one of each component of the system with itself. The eligibility criteria to select the proper solvent and its applicability in a liquid or in a vapour phase can be carried out taking into account the solubility parameter of the polymer and the solvent of choice[90], [101]. The solubility parameter also known as Hildebrandt parameter (δ) is defined as the square root of the cohesive energy density for each molecular system. It has the dimension of the square root of a pressure $(\text{MPa})^{0.5}$. The cohesive energy ($C$), defined in equation (1) is the difference between the latent heat of vaporization ($H^0$) and the mechanical work resulting from the evaporation. The last one was approximated by Hildebrandt as to the product of the gas constant ($R$) and the absolute temperature ($T$), divided by the molar volume of the solvent ($v$).

$$1)\ C = \frac{H^0 - RT}{v}$$

If a chemical and a polymer have similar solubility parameter numbers, it is more likely that the first one is a good solvent for the second one

For example, PMMA has a solubility parameter of 20.1 $(MPa)^{0.5}$ [102], while Methylene dichloride, Chloroform, Isopropanol, Ethanol and Water of 19.8, 18.7, 23.4, 26.0 and 47.9 $(MPa)^{0.5}$ respectively [102], (Table 1).

| Material | PMMA | Methylene dichloride | Chloroform | Isopropanol | Ethanol | Water |
|---|---|---|---|---|---|---|
| Solubility parameter δ $(Mpa)^{0.5}$ | 20.1 | 19.8 | 18.7 | 23.5 | 26.0 | 47.9 |

**Table 3.1 solubility parameter of PMMA, methylene dichloride, chloroform, isopropanol, ethanol and water**

The solubility parameters of PMMA and water are substantially different, so PMMA does not dissolve in water. While, PMMA readily dissolves at room temperature in methylene dichloride and chloroform, for which the solubility parameters are very similar to the one of PMMA. In this case, the solvent assisted bonding using methylene dichloride or chloroform can be carried out at room temperature. However, because of the strong compatibility between PMMA and methylene dichloride and between PMMA and chloroform, the solvent should be applied in its vapour phase in order to confine the action of the solvent only at the surface and to better control the process, avoiding channel deformation during bonding. The bonding protocol can be then optimized by tuning the exposure time of the solvent in the vapour phase and the pressure. In the case of the solute/solvent systems of PMMA/Isopropanol and PMMA/Ethanol, the solubility parameters are slightly different. In fact, PMMA does not dissolve at room temperature either in Isopropanol or in Ethanol. The solubility parameter of liquids changes with temperature. In particular, an increase in temperature results in a decrease of the solubility parameter [90]. Hence for the case of isopropanol and ethanol that do not act as solvents at room temperature, a temperature increase will drop their solubility parameter and they will act as a solvent for PMMA. In this case, the bonding method can be carried out with the solvent in a liquid phase and the bonding protocol can be optimized by tuning temperature, pressure and time. With respect to all the beforehand mentioned solvents, the use of ethanol and or isopropanol has a number of advantages including the fact that they are innocuous, less aggressive and in low volume they do not require to be handled

in a fume hood, as non-toxic and extremely cheap (~$ 5/L). Our group has therefore chosen Ethanol as our standard way of bonding microfluidic devices [29].

### *3.1.2 Ethanol-PMMA bonding mechanism*

Ethanol is an external plasticizer to PMMA. It acts by changing the thermal and mechanical properties of the material and lowering its glass transition temperature, Tg and by increasing the elongation at break and the impact strength.

When the solvent hits the polymer, a mechanism of absorption/adsorption takes place. The sorption of the solvent molecules into the surface leads to a swell of the polymer at its topmost region, increasing the free volume in the polymeric structure and thus decreasing its Tg. In the case of the couple PMMA-Ethanol, the Tg is decreased at temperatures lower than ambient temperature (11°C), enabling the self-diffusion of the polymeric chains.

The bonding mechanism taking place is not only thermodynamically driven but it is kinetic as well. Due to ethanol volatility and the difference in the solubility parameter between ethanol and PMMA, the process needs to be carried out at temperature higher than room temperature.

In the method developed by Liga et al, 2016, 10 µl/cm$^2$ of solvent are spread between the layers of PMMA to be bonded. Thanks to the flatness of the layers and to the compatibility between the solvent and the polymer, a liquid thin film spreads very fast between the part to be bonded together.

Then the prepared sandwich is placed in a hot press at 70 °C, for 2 minutes, with the layers kept in contact applying a pressure of 1.57 MPa. Under these conditions, the ethanol can act as a solvent and the diffusion of the polymer chains between the two layers starts with consequently bonding formation[1].

### *3.1.3 Solvent Assisted Bonding of PMMA: Choosing the right material*

In order to prove the wide applicability of their developed protocol, Liga et al., 2016, tested their bonding method using PMMA sheets manufactured from different suppliers and with different processing technologies such as casting and extrusion, including Clarex

[1] Fun fact: the bonding properties of ethanol with respect to PMMA have been exploited for a while. In the second half of the 20$^{th}$ century, theoretical and applied research have been carried out to study the use of Ethanol as self-healing agents to heal cracks in PMMA samples [205] .

® cast, Perspex® cast, Perspex® extruded and Oroglas ® cast. They did not notice differences in the bonding strength between the casted and extruded Perspex® PMMA, with same bonding strengths value as Clarex®, about 300 N. While, the bonding strength in the Oroglas ® bonded samples was found to be half that of other materials.

While it would have been reasonable to expect differences in the bonding strength or bonding quality of the extruded samples, the lower bonding strength of the cast Oroglas® came as a surprise. Looking at the physical, thermal and mechanical properties provided by in the manufacturertechnical datasheets (table 2) no noticeable differences are stated but for the water absorption (%). As can be seen from table 3.2 Oroglas® should has a higher water absorption compared to Perspex (Clarex data was not available). Water absorbed by polymer is considered to be present in the free volume and can act as a moisture changing the macroscopical properties when attached to the macromolecules with a hydrogen bond. The presence of the absorbed water can decrease the mechanical moduli and the Tg.. This higher water absorption would suggest a higher mobility of the polymer chains and thus the Oroglass bonding strength should be increased which is not in concordance with experimental evidences in Liga 2016.

Following this PMMA manufacturers were contacted to request their full physical and chemical characterisation but none replied. I was therefore tasked to investigate the reason for the difference in bonding strength in order to provide guidelines to researchers using PMMA for the fabrication of microfluidic prototypes. The results of this investigation were detailed in the article “Ultra-Fast-Prototyping of PMMA Structures for Micro-Engineering Applications: Choosing the Right Material” published in Advances in Manufacturing Technology XXXI , Volume 6, Series Advances in Transdisciplinary Engineering, pages 181-186. This publication is co-authored by myself (AO), Gioacchino Conoscenti (GC), Antonio Liga (AL), Valerio Brucato (VB), Marc P.Y. Desmulliez (MD), Nicola Howarth (NH), Vincenzo La Carrubba (VLC) and Maïwenn Kersaudy-Kerhoas (MKK). Myself and MKK gave substantial contribution to experimental conception and design, and analysis of the results. I conducted all the experiments but the Differential scanning calorimetry (DSC). GC performed the DSC experiments. I wrote the article. AL, VB, MD, NH and VLC proof read the article and contributed to the analysis of the results.

| Properties | Clarex ® | Perspex® cast | Perspex® Extruded | Oroglas® |
|---|---|---|---|---|
| Relative density | 1.19 | 1.19 | 1.2 | 1.19 |
| Water absorption [%] | - | 0.2 | 0.2 | 1.9 |
| T.S. at Yeld [MPa] | 75 | 75 | 75 | 85 |
| Elogational at breack [%] | 5 | 4 | 4 | 6 |
| Hardness [MScale] | - | 102 | 101 | - |
| Flexural Modulus | - | 3210 | 3030 | - |
| Coefficient of thermal expansion [mm/m C] | 0.07 | 0.077 | 0.078 | 0.065 |
| Light transmission [%] | - | 92 | 92 | 80 |
| Refractive index | 1.49 | 1.49 | 1.49 | |
| Softening temperature | - | 110 | 105 | 107 |

**Table 3.2** Properties of PMMA manufactured from different brands

## 3.2 Ultra-Fast-Prototyping of PMMA Structures for Micro-Engineering Applications: Choosing the Right Material

CO2 laser micromachining is a widely employed micro-manufacturing technique for the production and rapid-prototyping of microstructures. Poly(methyl methacrylate) (PMMA), due to its optical properties and mass-manufacturing compatibility, is often the material of choice for laser machining of microfluidic devices to be used for clinical, environmental and educational purposes [29], [45], [103]–[107]. Additionally, it has been utilised for diffraction gratings [108] and optical waveguides [109]. To address the need for fast design cycles, we have recently developed an ultrafast prototyping technique to manufacture multi-layer PMMA micro-devices [29]. Using this safe, rapid and cost-effective technique, we have shown that it is possible to manufacture, in less than 15 minutes from design to test, multi-layer structures (up to 19 layers), withstanding pressures of at least 6.2 MPa (with mean of 8 MPa, highest reported to date) and with minimal channel deformation (<5%). Our technique has the potential to accelerate translational research, particularly in the microfluidic field. This ultrafast prototyping technique was applied to PMMA from various sources. Although our technique was found to be broadly applicable to PMMA from a variety of manufacturers, it raised several

questions about the typical physico-chemical characteristics of PMMA that a standard user should consider when selecting material for laser-induced ablation and solvent-assisted bonding.

The manufacturability of PMMA devices using lasers has been well researched, particularly involving the employment of CO2 lasers [91], [107], [110], [111]. Surprisingly though, the range of physico-chemical PMMA characteristics has been largely ignored and its effect on laser-matter interactions typically under-reported, with many publications focusing on a single source of PMMA. One investigation examined the effects of laser power and processing speed on the depth, width and surface profiles of micro-channels formed with PMMAs of different molecular weights [112]. However, the PMMA sheets used were custom-made from pellets and did not correspond to commercially available products. Although bulge and pore formation were observed, with poorer laser cut qualities for higher molecular weights reported, no consideration was provided to the influence of physico-chemical factors on kerf taper angle or bonding of PMMA layers. Therefore, in order to address this issue, four types of PMMA have been sourced and their properties determined.

This has enabled their roles in the different bonding strengths and laser-cut qualities, produced in the context of our ultra-fast prototyping technique (machining and bonding), to be evaluated.

## 3.3 Materials and methods

### *3.3.1 PMMA material*

PMMA sheets of 2.0 mm thicknesses were acquired from Weatherall Ltd (UK) (Clarex® cast), Easter Road Plastics Ltd, (UK) (Oroglas® cast) and Engineering and Design Plastics Ltd (UK) (Perspex® cast and extruded).

### *3.3.2 Laser set-up*

For laser micromachining, the CO2 commercial laser cutter Epilog Mini 18, 30 W from Epilog was used. The laser speed can be adjusted from 0 to 100%, where 100% corresponds to actual speed of 85 mm/s. The laser power can be adjusted from 0 to 100% corresponding to actual power of 0 to 30 W. The software CorelDraw (Corel Corporation, Canada) was used to transfer drawings to the laser cutter.

### *3.3.3 PMMA bonding*

We have described the PMMA bonding procedure in [29], In this procedure, absolute Ethanol (%w > 99.95%w, Sigma-Aldrich, UK) was used as a solvent. A custom-made

heating plate maintained the layers at the correct temperature during bonding. As a source of pressure, we used a Bonny Doon Classic 20-Ton Manual Press (Rio Grande, USA). After laser cutting the desired shapes using a CO2 laser cutter (Epilog Mini 18, Epilog, USA) PMMA layers were cleaned with clean-room tissue and ethanol to remove dust. 10 µl/cm2 of ethanol were then spread between each layer before bonding.

### *3.3.4 Shear stress analysis*

The shear stress testing has been described in details in [29]. Standard tensile test equipment (Instron 3367, Instron, UK) was used with an elongation speed of 0.05 mm/s and recorded the highest load to date before sample break. The two sides of T-bones specimens were laser cut from 2.0 mm thick sheets and then bonded together. The various commercial samples were tested at the optimum parameters 70°C, 5 tons at the ram for 120 seconds as described in [29]. Between 6 and 12 specimens were used for each set of parameters, so as to ensure reproducibility of results.

### *3.3.5 Gel permeation chromatography (GPC)*

A GPC Shimadzu was used with a PLgel MIXED-D column (300 x 7.5 mm, particle size 5 µm) to determine the weight molecular weight (Mw) and the PDI (polydispersity index) of the different PMMA samples.

### *3.3.6 Water and Ethanol absorption*

PMMA samples of each brands have been laser cut to manufacture 8 $mm^3$ cubes. Three cubes per each brands have been cut, weighted and singularly placed in a 5mL tube containing water or ethanol and left in overnight. After 12 hours, cubes weight was recovered and the solution uptake calculated as $(W_{wet}-W_{dry})/W_{dry}$ x 100.

Where $W_{wet}$ is the weight of the wet sample after 12 hours incubation in water or ethanol and $W_{dry}$ the weight of the sample before being soaked overnight.

### *3.3.7 FT-IR Spectroscopy Attenuated Total Reflectance (ATR-FTIR)*

ATR-FTIR, analysis was carried out collecting 200 scans in the range of 4000-400 cm-1, with a resolution of 4 cm-1 using a Nicolet Is5 spectrophotometer

### *3.3.8 Differential Scanning Calorimetry (DSC)*

A DSC131 evo (Setaram Instrumentation, France) was used to measure thermal properties of the 4 sets of PMMA. 14 mg of each sample were placed in a 30 µl aluminum

pan and heated at a rate of 10°C/min from 30 to 250°C after a preconditioning at 30°C for 10 mins and following a stabilizing at 250°C for 10 mins was used to characterize the materials. All tests were carried out in triplicates.

### *3.3.9 Kef width, kerf depth and kerf taper angle*

Kerf width and kerf depth measurements were carried out cutting 1 cm slits in 2 mm thickness PMMA sheets from each supplier. Laser power, speed and frequency were chosen as input parameters in order to find the minimal features achievable in terms of kerf width, and the optimum parameters to completely cut through the sheet.

Cross section of the cut was evaluated by measuring the kerf taper angle as previously defined in [113]. All the measurements were conducted via image analysis from photographs acquired with a Dino-Lite Premier digital microscope. For each measurement, at least 3 readings were taken to check the regularity of the cut.

## 3.4 Results and Discussion

### *3.4.1 Variations in bonding strength*

PMMA sheets are mainly produced using two methods: casting or extrusion. While extrusion produces PMMA sheets with better thickness tolerances, cast PMMA exhibits higher thermal stability and better optical properties. Shear stress tests have been carried out in order to assess how production methods affect the bonding strength. Interestingly, both cast and extruded Perspex® PMMA performed similarly to Clarex® PMMA where shear stress results gave nearly overlapping bonding strengths (Figure 1). Unexpectedly, Oroglas® cast PMMA exhibits half the bonding strength with respect to the other samples.

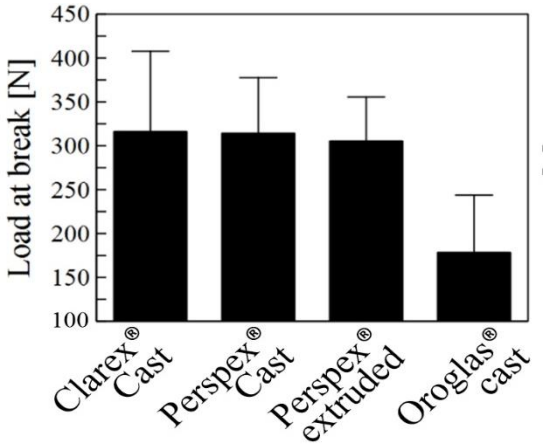


***Figure 3.1. Bonding strength of various brands and types of PMMA. Error bars show the standard deviation.***

### *3.4.2 Determination of PMMA physico-chemical characteristics and discussion about their influence on bonding strength*

The previous results suggested that the applicability of our bonding method did not depend on the manufacturing process. According to the material data sheet reported by the suppliers the four samples should perform similarly, nevertheless no thorough characterisation with respect to molecular weight is provided by the manufacturer.

We first hypothesized that a difference in molecular weight ($M_w$) could explain the different bonding strength obtained [29]. However, a GPC analysis revealed that while all cast samples, including Oroglas®, had comparable $M_w$ (Figure 2), only the Perspex® extruded sample has a significantly lower $M_w$.

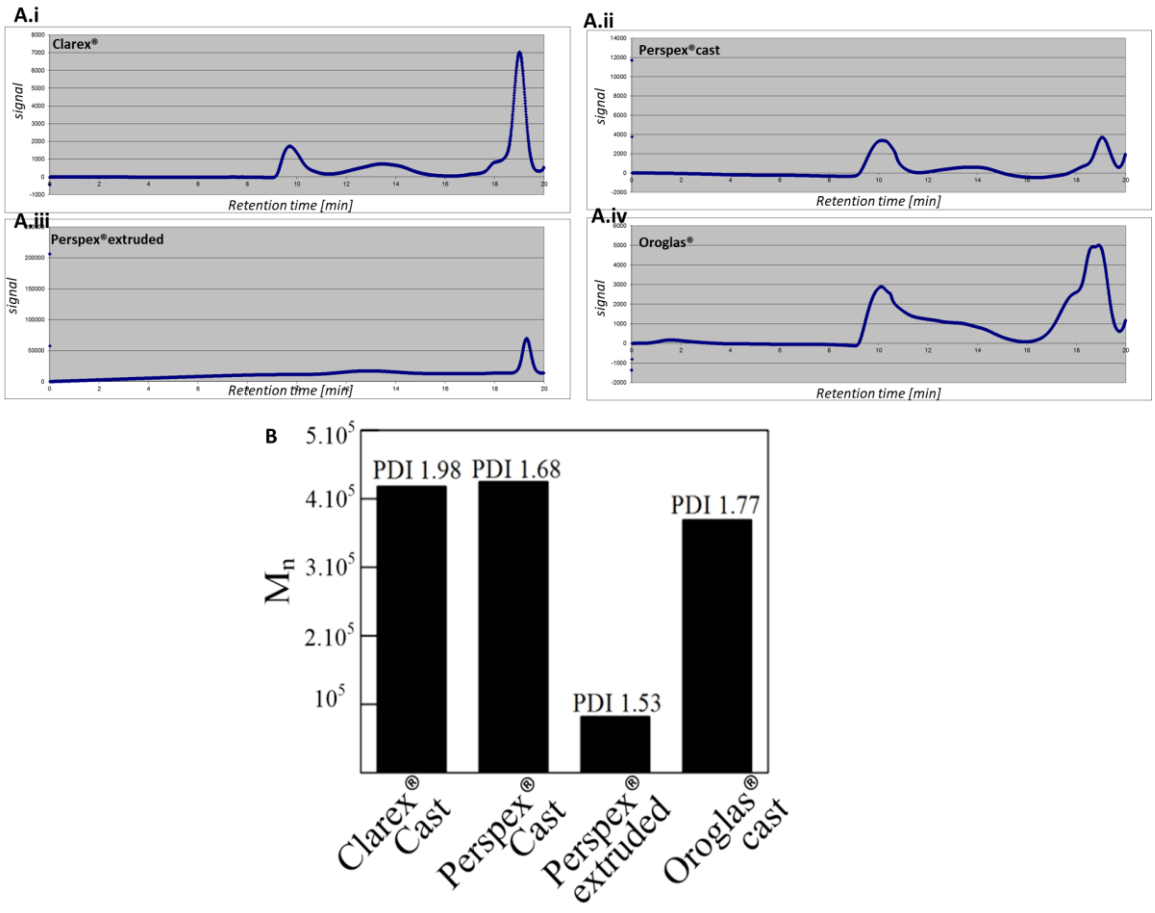


**Figure 3.2**. Molecular weight of the different brands of PMMA. A) GPC Chromatogramme of A.i) Clarex ® cast; A.ii) Perspex ® cast; A.iii) Perspex ® extruded; A.iv) Oroglas ®. B) Number average molecular weight and Polydispersity index of the tested samples.

We also found that all four PMMA samples had comparable water swelling ratios of the order of 2%. These findings imply that molecular weight cannot solely account for the observed differences in bonding strength.

The second hypothesis aimed at checking the surface chemistry of the sheets from the different brands. An ATR-FTIR analysis could help to determine whether the PMMA sheets have been undergone under surface treatments that could have potentially hindered the bonding efficiency.

No differences in the surface chemistry have been noticed in the spectra of the examined samples in the fingerprint region (500-2000 $cm^{-1}$) as well as in the single bond stretching region (2500-4000 $cm^{-1}$), where usually functional groups are detected (Figure 3)

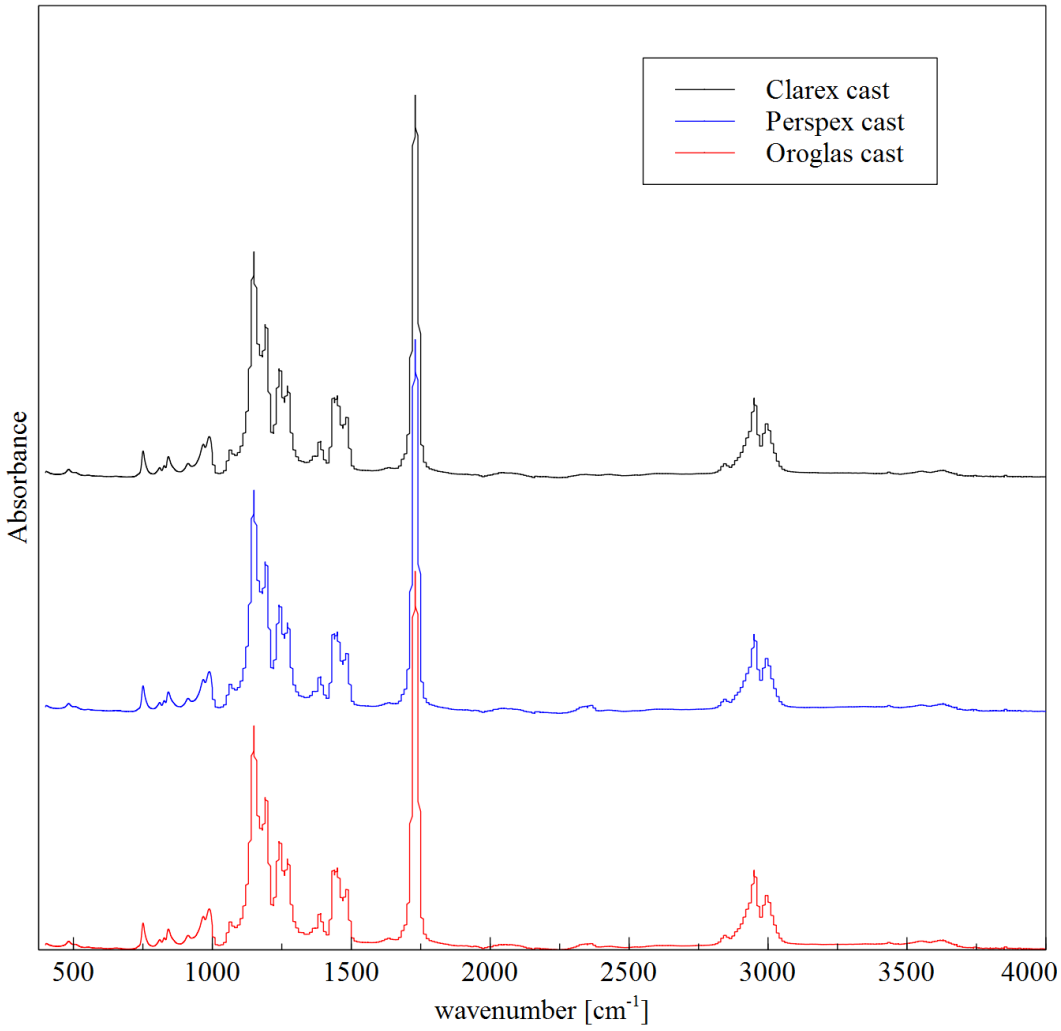


**Figure 3.3**. ATR-FTIR spectra of the Clarex® cast (black curve), Perspex® cast (blue curve) and Oroglas® cast (red curve).

As last hypothesis was that the bonding strength difference could be attributed to a difference in thermal properties such as the glass transition temperature, $T_g$. A DSC analysis demonstrated that all four PMMAs have a $T_g$ between 115ºC and 120ºC, as shown in Figure 4, however both Clarex® and Oroglas® showed an additional phase transition with features similar to a glass transition at 170ºC. While for Clarex® the associated energy to this second glass transition is 2.3 J/g and it is comparable to its first transition phase; for the Oroglas® the energy is 7.8 J/g, almost 4 times the Clarex® one and 3 times bigger than its first transition phase. It is likely that the difference of thermal response might justify the difference observed in bonding strength, although further investigations are needed to establish the nature of these possible additives or impurities.

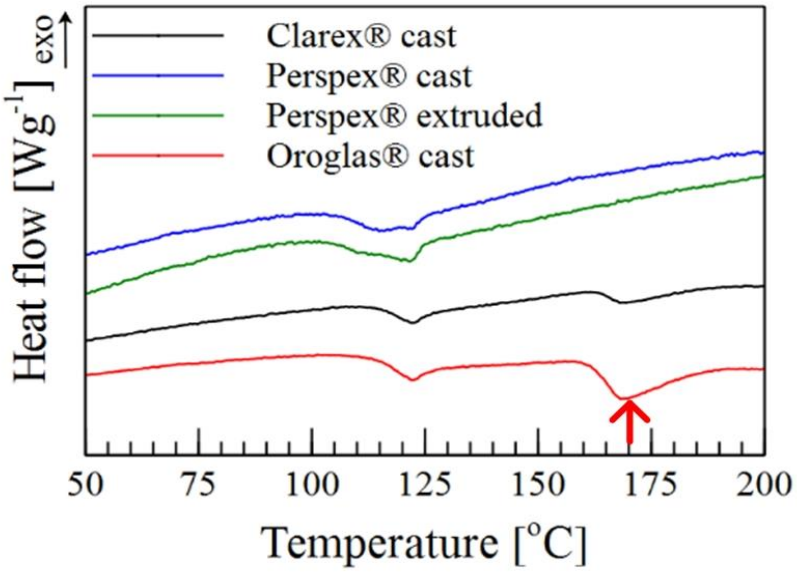


**Figure 3.4**. DSC thermogramme of Calrex® cast (black curve). Perspex® cast (blue curve); Perspex® extruded (green curve) and Oroglas® cast (red curve). The red arrow points out the second transition temperature strongly exhibited by Oroglas® samples.

### *3.4.3 Investigation on laser-cut quality and channel topology*

We have investigated the effects of laser power and speed on kerf width for the 4 PMMA samples from different manufacturers as shown in Figure 5.

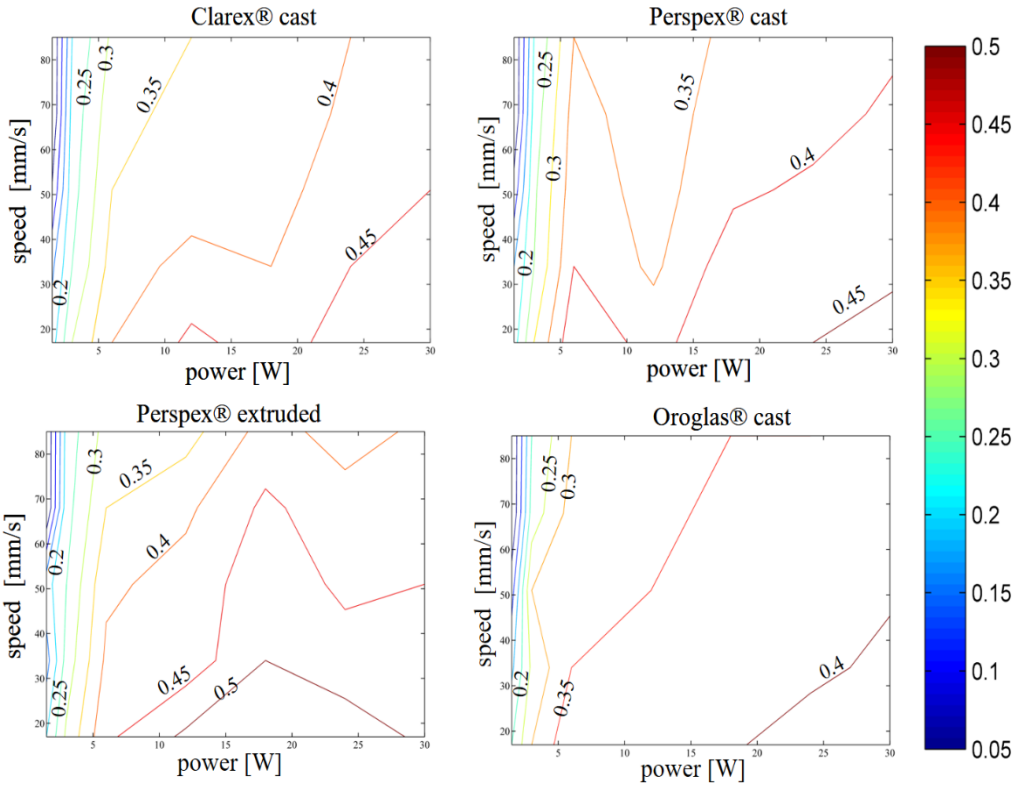


**Fig. 3.5** Kerf width (mm) as a function of the laser power and speed for PMMA from four sources.

Generally and as expected, an increase in laser power led to an increase in kerf width. All cast samples showed the same behaviour in terms of kerf width and depth, while extruded PMMA samples showed the formation of recast layers and larger kerf widths. A minimum kerf width of 56 µm was achieved by using a laser power of 6 W and a speed of 51 mm/s on Clarex® and Perspex® cast.

At the maximum laser power of 30 W with a speed of 17 mm/s, the kerf depth was found to be about 2 mm, whereas for the maximum speed, using the minimum laser power (6 W), the kerf depth was determined to be 150 µm for all types of PMMA samples. The extruded PMMA yielded the smallest kerf taper angle (Figure 3A) at the expense of a recast layer of about 50 µm (black arrows, Figure 3B). Several cracks and the tendency to arch and deform during laser cutting due to the relaxation of stress induced during manufacturing, were noticed. In contrast, none of the cast samples appeared to form recast layers.

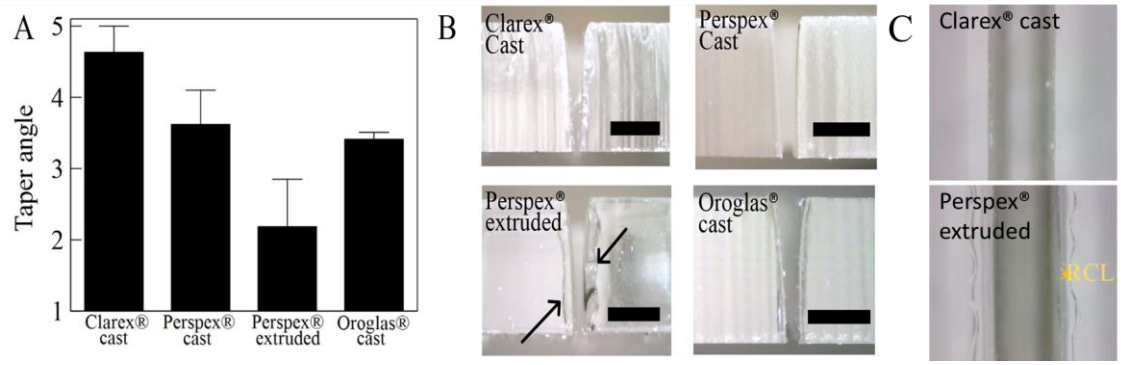


**Fig. 3.6** (A) Kerf taper angle of the different PMMAs. (B) Cross sections of PMMA samples (scale bar is 500 um). Black arrows point out the recast layer C) Top view of a laser cut on Clarex® cast PMMA (top) and Perspex® extruded PMMA bottom, recast layer highlighted in yellow

## 3.5 Conclusions

This chapter reports a method I developed to assess and predict the material compatibility with respect to the solvent assisted bonding method previously developed in my group. The deep understanding of the bonding mechanism is of fundamental relevance in order to translate the knowledge developed in bonding other commons thermoplastic materials for the production of microfluidic devices to more environmentally sustainable substrate solutions, such as chemically recycled PMMA and PLA. Firstly, I have described the use of the Hildebrandt parameters as a tool to help to select the appropriate solvent when adopting a solvent assisted bonding method and their applicability in a vapour or liquid phase. For sake of clarity it is important to note that the Hildebrandt parameters represent an extremely simplified descriptors of complex systems such as polymer/solvent. For these systems, the Hansen parameters (that are not discussed in here as their argumentation goes far behind the objective of this thesis) represent better descriptors. Secondly, the ultra-fast ethanol assisted bonding method developed in my group has been described and its applicability to different brands of PMMA is illustrated. Finally, a comparison of the $CO_2$ laser cut quality between the different brand of PMMAs has been carried out, showing that extruded PMMA with respect to cast PMMA shows the formation of a recast layer while laser cutting. This feature can potentially hinder the quality of the bonding. Thus, it is envisaged to choose cast PMMA when the substrate material is microstructured via $CO_2$ laser cutting. With respect to the bonding efficiency, in terms of bonding strength, after testing several hypotheses to check the influence of the molecular weight, and surface characteristics of the different grades on the bonding quality, I find out, while checking the thermal properties of the different grades via differential scanning calorimetry, that the bonding strength was affected by the presence of contaminants. As the solvent assisted bonding method is thermodynamically regulated,

I have proved that carrying out a DSC analysis can help to predict if a further optimization of the bonding parameters, in terms of temperature, pressure and time, need to be undertaken.

# Chapter 4: RECYCLED PMMA: A GREEN PERSPECTIVE

## 4.1 Introduction

In this chapter chemically recycled PMMA (Re-PMMA), is introduced as suitable material to manufacture environmentally sustainable microfluidic devices, embracing a Design for Sustainability (DfS) approach. As discussed in the state of the art, there is an increased awareness of plastic pollution worldwide. Increased environmental regulations and calls for governmental actions have led to greater sustainability and disposability considerations at the design stage, together with manufacturability, functionality and cost. So far, only a few research groups have focused on sustainability consideration in the design production of microfluidic devices. Sadly, none of the proposed sustainable alternative, previously explained in chapter 2, have been largely embraced so far. This chapter briefly describes different DfS approaches, and gives an overview of the different recycling scenarios of thermoplastics, focussing on the chemical recycling process of PMMA. The main part of this chapter is based on a paper published in Advances in Manufacturing Technology XXXII in September 2018 and provide a practical guide to researchers when selecting Re-PMMA material for a more sustainable approach to micro-engineering and microfluidic rapid-prototyping in conjunction with the solvent assisted bonding method reported in chapter 3.

### *4.1.1 Design for sustainability*

In order to address the need of sustainability, engineers can adopt and embrace tools provided by DfS approaches. DfS is a design philosophy with the basic objectives of achieving sustainability by considering a number of principles for sustainability at the design stage, rather than retrospectively after production. According to Clark et al., DfS provides different methodologies to make sustainable improvements to products by adopting elements of life cycle analysis [114]. On a product innovation level there are different approaches that can be embraced to enhance the sustainability of a product, e.g. ‘Green Design’, ‘Eco design’, ‘Emotionally durable design’, ‘design for sustainable behaviour’, ‘Cradle-to-Cradle’ design, ‘Biomimicry’ design and ‘Design for the base of the pyramide’ [115]. All the beforehand mentioned approaches differ in function of the goal to be addressed. For instance, the main focus of the Green Design and Eco Design approach is to lower the environmental impact. The first one by following the waste hierarchy of reduce-reuse-recycle, while the latter one by considering the whole life cycle analysis of the product from raw material extraction to final disposal, considering all the

possible end-of-life scenarios, including the reduce-reuse-recycle approach. The other mentioned approaches focus on lowering the environmental impact considering the social perspective of the product, for example the 'Emotionally durable design' focuses in extending the lifespan of a product by extending the emotional attachment between the user and the product itself. 'Design for sustainable behaviour' has the goal to make end-users adopt a sustainable behaviour in terms of energy consumption. On the other hand, 'cradle-to-cradle' and 'biomimicry' design have their focus back on the material and on the design, respectively. The first one aims at using specifically only materials and energy from renewable resources that can become nutrient at their end of life. The latter one aims at taking inspiration by material functionality and conformation to design new product or redesign existing one. Due to the disposable nature of single-use microfluidic device products, 'Green design' and 'Eco design' are the more suitable approaches to address the need of sustainability, without imposing limitation in the design and increasing the cost. In particular, Eco Design relies on analysing the life cycle of a product. The product life cycle starts with the extraction, processing and supply of the raw materials and energy needed for the product. It then covers the production of the product, its distribution, use (and possibly reuse and recycling), and its ultimate disposal. Environmental impacts of all kinds occur in different phases of the product life cycle and should be accounted for in an integrated way.

The DfS approach can be applied to medical microcomponents, taking into account to:

i. minimise non-renewable energy consumption;
ii. use environmentally preferable materials;
iii. protect and conserve water;
iv. minimise waste,
v. lengthen the product shelf-life,

In the following work, we have focused on the (ii) and (iv) points of the DfS approach: 'Use environmentally preferable materials' and 'Minimise Waste'. We have proposed replacing pristine PMMA, used in the previous chapter (chapter 3), by chemically recycled PMMA. The goal of this chapter is to prove equivalence in laser workability and bonding strength between the two materials.

## 4.2 Recycling of thermoplastics

Traditionally, Polyethylene therephthalate (PET), Polyethylene (PE), Polyvinyl chloride (PVC), Polypropylene (PP), Polystyrene (PS) and Polycarbonate (PC) are thermoplastic materials for which the recycling system is largely employed or recommended, because they represent the most predominant plastics in the market, especially in the packaging sector [116]. PMMA is an highly functional plastic and often used for LCD monitors, waveguides, optical fibres and microfluidic cartridges [85], but its recycling have lagged behind other thermoplastics for different reasons [117]. For instance, the no single-use nature of the item made of PMMA. Recycling systems can allow to reduce the volume waste of PMMA microfluidic devices and as well provide new PMMA material non-directly petrochemical derived, reducing the raw material extraction.

In general, recycling of thermoplastics can be carried out via mechanical recycling, chemical recycling or via energy recovery though incineration [118]. Mechanical recycling is the most widely adopted technology for recycling plastics. This can be carried out either post-industrial processing or post costumer use [119]. The main steps of the mechanical recycling involve, collection, sorting, washing, shredding and polymer reprocessing, usually via melting and remoulding. The mechanical recycling process is most effective when applied in post-industrial processing settings. In this case, scraps of the materials are immediately collected after the polymer processing. For example, scrap materials are produced from the sprue and runners (passage through the liquid material is introduced into the mould and from one part to another one) at each cycle of injection moulding. These scrap materials can be reprocessed as they can be blended with virgin material to produce fallout products or other functional parts. The recycled end-item does not require a sorting or cleaning process and the chemical composition and properties are known. On the other hand, the post customer use mechanical recycling is more challenging and has some limitations. Collection, sorting and washing are fundamental steps. In fact, polymer blends (mixture of two or more different polymers) have usually lower mechanical and thermal properties with respect of the properties of the single polymer composing the mixture. To overcome this issue often additives in the form of compatibilizing agents are added [118], [120], [121]. The sorting process is more often the most expensive and add different steps to the recycling process [116]. Nevertheless, if sorting is not carried out, the mechanical recycling cannot be adopted because in the mixture of polymer waste, there can be thermo-sensitive plastics that will go under

thermomechanical degradation during the recycling process. Or, in most cases, polymers of different colours end up all together creating additional challenges [118].

Chemical recycling is a recycling process that involves the depolymerisation of the polymer waste into its monomers components that can then be re-polymerized [116], [119]. In this case the final recycled product has the same properties of the virgin polymer. In addition, this process reduce the amount of raw material needed and the volume of waste produced. There are different chemical recycling processes and they can be categorized into, Chemolysis, Pyrolisys, Fluid catalytic cracking, Hydrocracking, KDV process and gasification[119], [122]. Fluid catalytic cracking, Hydrocracking, KDV and gasification are used to have more narrow outcome products and for the production of liquid fuel and biomass, while Chemolysis and Pyrolisys for monomer recycling. In particular, chemolysis can be carried out via hydrolysis, amminolysis and glycolysis and it is a process suited for all the polymer that are synthesized via polycondensation of ring-opening polymerization. The gold example is PET, for which this recycling process was firstly developed [123]. On the other hand, pyrolysis is a chemical recycling process that is suitable for plastic waste feeds difficult to depolymerize such as PMMA [124]. We opted to choose and test chemically recycled PMMA, because it is commercially available from different suppliers, thus it is readily accessible to embrace an environmental friendly approach to prototype single use microfluidic devices.

## 4.3 Rapid Prototyping for micro-engineering and microfluidic applications: Recycled PMMA, a sustainable substrate material

Poly(methyl methacrylate), (PMMA), is a thermoplastic material widely used for producing optical fibres, and a wide range of other consumables [85], [117]. Since the late 90s, thanks to its low cost, good workability both at the prototyping scale and at the mass manufacturing scale, PMMA has been used as substrate material for microfluidic applications. Some microfluidic applications on PMMA substrate include the analysis of amino and nucleic acids, peptides and proteins [125]. Given that an increasing number of these biomedical microfluidic devices are produced in single-use, disposable, format, a design for sustainability (DFS) approach when designing new microfluidic devices is desirable. Briefly, a DFS approach considers the full life cycle of the final device. Starting from the raw material extraction, the DFS includes an analysis of transportation, transformation of the raw material into intermediate material, the manufacturing process both at the prototyping scale and at the mass manufacturing one, the use of the device and its possible end of life scenarios. We have recently developed a safe and cost effective rapid prototyping method for the assembly of complex 3D microfluidic devices in PMMA [29]. This method involves the use of a CO2 laser cutter to shape the micro-channels in PMMA layers that are then bonded together using a 2 min ethanol assisted bonding method, enabling fast production cycles (15 min from design to test) (Fig 1A).

Taking a DFS approach, recycled PMMA (Re-PMMA) is proposed as a novel substrate material for microfluidic medical components. Thermoplastic materials can be recycled with different technologies including mechanical recycling, or chemical recycling. Mechanically recycled PMMA has been used for the production of optical fibre sensors [

[61], [126] and microfluidic devices [64]. Despite optimum results in terms of final optical qualities, in the case of single use medical devices, a sterilization step should be included prior to mechanical recycle the device. On the other hand, Re-PMMA from chemical recycling is commercially available from different brands. In chemical recycling the used thermoplastic is depolymerized through a heating process to break the macromolecular chains. After a distillation process all the impurities are separated to obtain recycled methyl methacrylate monomer with a purity up to the 99.8%, that are polymerized to obtain Re-PMMA with the same optical, mechanical and thermal properties of the pristine PMMA, (pPMMA). In this article, chemical and physical

characterisation tests are carried out to validate the suitability of Re-PMMA for microfluidic rapid–prototyping in comparison to pPMMA.

The results of this chapter have been published in Advances in Manufacturing Technology XXXII, Volume 8, Series Advances in transdisciplinary Engineering, pages 107-112 in September 2018. The article is co-authored by myself, Nicola Howarth (NH), Vincenzo La Carrubba (VLC) and Maïwenn Kersaudy-Kerhoas (MKK). I and MKK gave substantial contribution to experimental conception and design, and analysis of the results. I conducted all the experiments. NH and VLC proof read the article and contributed to the analysis of the results.

## 4.4 Materials and Method

### *4.4.1 PMMA material*

Re-PMMA sheets of 3 mm thickness were purchased from Cut Plastic Sheeting UK (100% recycled Clear Greencast Acrylic Sheet). pPMMA were purchased from Weatherall Ltd (UK) (Clarex® cast) from Easter Road Plastic LTD (Oroglass® cast) and from Engineering and Design Plastic LTD (UK) (Perspex®)

### *4.4.2 DSC Analysis*

A DSC 2010 (TA Instruments) was used to measure thermal properties of Re-PMMA and p-PMMA (Clarex®, Oroglas® and Perspex®) in order to reveal the presence of impurities. 14 mg of each sample were placed in a 30 µl aluminum pan and heated at a rate of 10°C/min from 30 to 250°C. All tests were carried out in triplicates.

### *4.4.3 Laser set-up*

A commercial CO2 laser cutter Epilog Mini 18 (30 W) from Epilog was used. The laser speed can be adjusted from 0 to 100%, where 100% corresponds to actual speed of 85 mm/s. The laser power can be adjusted from 0 to 100% corresponding to actual power of 30 W. The software CorelDraw (Corel Corporation, Canada) was used to transfer drawings to the laser cutter.

### *4.4.4 Re-PMMA Bonding*

To bond together the different PMMA layers, absolute Ethanol (%w > 99.95%w, Sigma-Aldrich, UK) was used as a solvent. A custom-made heating plate maintained the layers

at the correct temperature during bonding. As a source of pressure, we used a Bonny Doon Classic 20-Ton Manual Press (Rio Grande, USA). After laser cutting the desired shapes using a CO2 laser cutter (Epilog Mini 18, Epilog, USA) PMMA layers were cleaned with clean-room tissue and ethanol to remove dust. 10 µl/cm2 of ethanol were then spread between each layer before bonding at 70°C, 5 tons at the ram (corresponding to 15 bar) and for 2 minutes.

### *4.4.5 Shear stress analysis*

The shear stress testing has been described in details in [29]. Briefly, standard tensile test equipment (Instron 3367, Instron) was used with an elongation speed of 0.02 mm/s and recorded the highest load to date before sample break. The two sides of the dumbbell specimens were laser cut from 3.0 mm thick sheets and then bonded together according to section 1.4. Six specimens were used for each set of parameters to ensure reproducibility of results. Statistical analysis was carried out with a Student's t-test.

### *4.4.6 Burst test and Maximum Flow rate analysis*

In order to assess the quality of the bonding method on the Re-PMMA and the ability to effectively seal the channel, burst test analysis were carried out. Chips with a 300 µm wide channel leading to a dead-end were manufactured sandwiching two 3 mm layers, one of which served also for the fluidic connection. A syringe pump (Alladin, WPI), was used to actuate flow of a (5mg/mL) fluorescein solution within the specimens at 2 mL/min. As there is no way out, the air enclosed within the channel is gradually forced in a smaller volume and its pressure increases. Pressure changes were monitored with a pressure sensor (uPS 1800-T116, Labsmith). The same set-up was used in open-end chips, changing gradually the flow rate (from 5 to 300 mL/hr) to characterise the maximum flow rate allowed within the channel.

### *4.4.7 Kerf width and kerf depth characterization*

Kerf width and kerf depth measurements were carried out cutting 1 cm slits in 2 mm thickness PMMA sheets from each supplier. Laser power, speed and frequency were chosen as input parameters to find the minimal features achievable in terms of kerf width, and the optimum parameters to completely cut through the sheet. All the measurements were conducted via image analysis on ImageJ (version 1.51r) from photographs acquired with a Dino-Lite Edge digital microscope (AM4115T-GFBW, DinoLite, Taiwan). For each measurement, at least 3 readings were taken.

## 4.5 Results

### *4.5.1 DSC analysis*

Differential Scanning Calorimetry is a powerful tool enabling the understanding of material thermal behaviour in terms of crystallization, melting and glass transitions. PMMA, as an amorphous polymer, does not have any crystallization phase. The resulting DSC thermograms should theoretically show only one glass transition phase and a melting region. If a thermoplastic polymer shows more than one glass transition phase, this phenomenon could be due or because of the composite nature of the polymer itself or because it is under nanoconfinements [127]. As shown in chapter 3 and in the related publication [128], I have shown using DSC that the presence of impurities inside the material can affect the bonding strength. In figure 1 the thermogram of Re-PMMA does not shown any additional phase transition, Similarly Perspex cast do not show any secondary peaks. On the contrary, both pPMMA Clarex cast and Oroglass show a secondary Tg. The associated energy to this additional phase transition in Oroglas® is 7.8 J/g, 3 times bigger than its first transition phase and four times larger than Clarex second peak and was previously associated with lower bonding strength as shown in Figure 1 [128]. These results show that Re-PMMA can be adopted in conjunction with our bonding protocol.

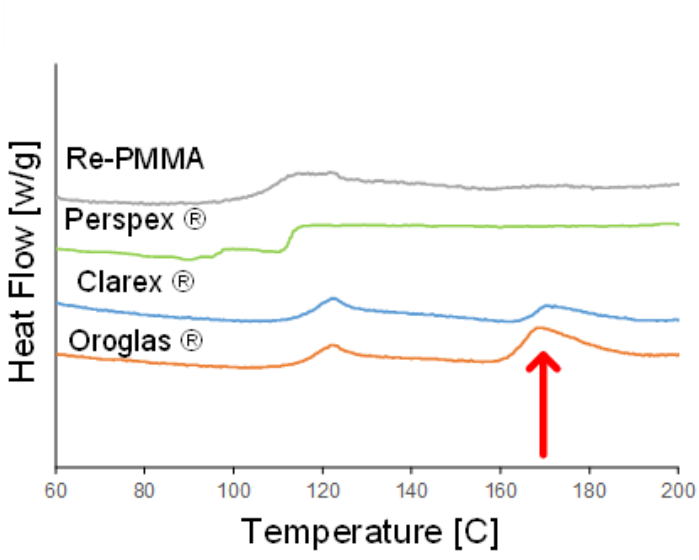


**Figure 4.1.** Thermograms of the Re-PMMA, Perspex®, Clarex® and Oroglas®, the red arrow points out the second glass transition for the oroglas®. As can be notices Re-PMMA has only one glass transition temperature.

### *4.5.2 Bonding strength*

Accordingly to the DSC results, Re-PMMA bonding strength is as comparable to the bonding strength previously reported for Clarex and Perspex materials (Figure 2 E) [128], During the shear stress tests not all the specimens were achieving delamination and some of them were arriving at break before the beginning of the delamination process (Figure 2 F).

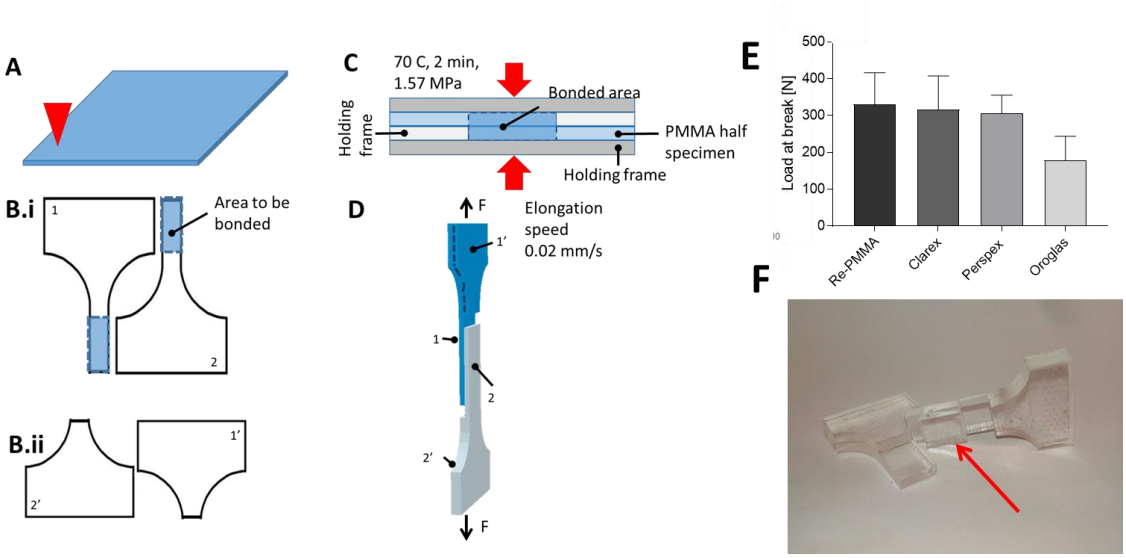


**Figure 4.2**. Sample preparation for the shear test. A) Laser cutting half T-bone specimen. B) Schematic of the design used to perform the shear test; B.i) design of the 2 half of the T-bone specimen. Highlighted in blue area to be bonded; B.ii) additional part to be cut and taped to the specimen to enable sample alignment and distribution of stress in the wanted area. C) Cross section overview of PMMA rapid-prototyping technique described. In grey and light grey holding frame, in light blue the 2 half T-bone specimen, and in dark blue the bonded area. D) schematic of the final sample to be tested with an elongation speed of 0.02 mm/s. E) Maximum bonding strength of Re-PMMA, Clarex®, Perspex® and Oroglas®. F) Photograph of the broken specimen (Re-PMMA). The black arrow points where the material break, showing the other part of the specimen still bonded.

### *4.5.3 Burst test and Maximum flow rate*

To determine the failure modes of our Re-PMMA prototyping technique, we determined the critical pressure and the maximum flow rate at which the microfluidic devices started leaking or delaminating. No delamination phenomena were noticed in all the devices tested. The maximum operative pressure was recorded to be about 528 kPa, no leaking from the connectors or delamination were observed, but a back pressure was noticed at the syringe pump and recorded from the set-up used as a pressure drop, as reported in fig.

3B.i. This underlining the robustness of the bonding method. The maximum operative flow rate recorded was 300 mL/hr (fig. 3B.ii); above this, leaking of the fluorescein solution was observed from the microfluidic connectors.

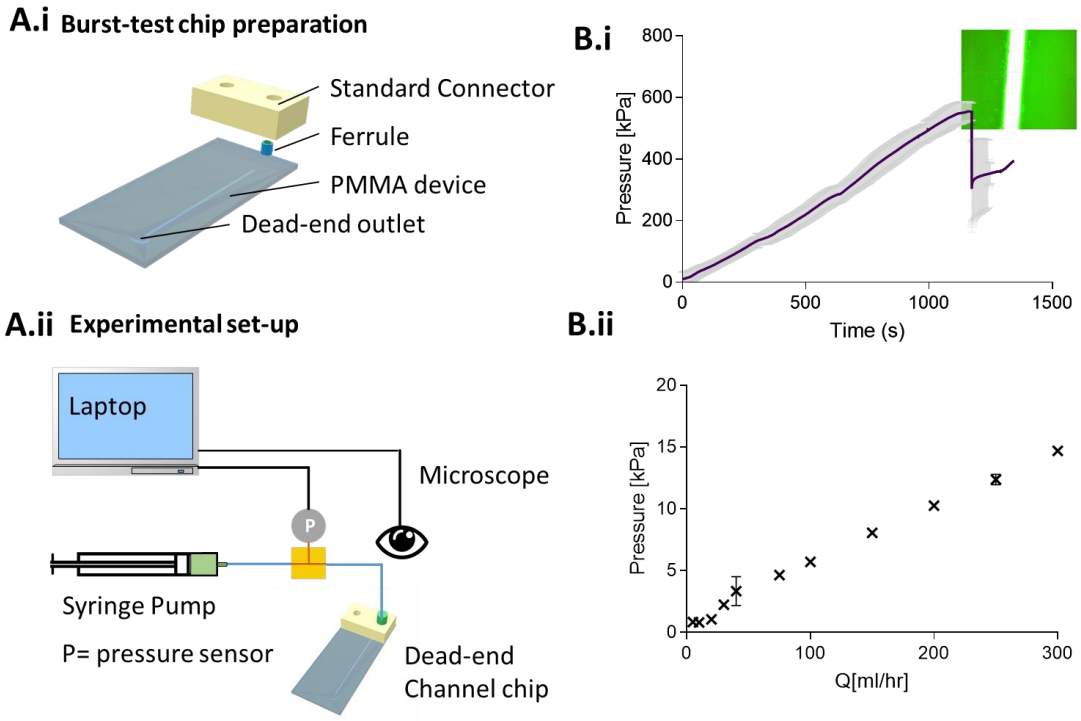


**Figure 4.3**. A) Experimental set-up; B.i) Burst test in close channels (width 250 µm). Maximum pressure difference in function of flow rate. Deviation is shown in grey; in insert, picture of the channel at the time of the test failure due to the backpressure of the syringe pump. No leakage is noticed. B.ii) Open channel tests. Input flow rate in function of pressure. 300mL/h was the pump maximum flow rate. For some points the error bar is shorter than the symbol.

### *4.5.4 Laser cut characterization*

We have investigated the influence of the CO2 laser power and speed to the kerf width and depth. In general, a lower speed allows results in a larger kerf width. On the other hand, at higher speed, deposited energy is reduced, resulting in a smaller kerf width. On the contrary, higher power result in larger and deeper cut with respect to a lower power. The smallest feature achievable was recorded to be 100 µm of kerf width and depth, using a laser power of 3 W and a speed of 85 mm/s (the maximum operative speed) using a 1.5" lens and focused onto the material surface.

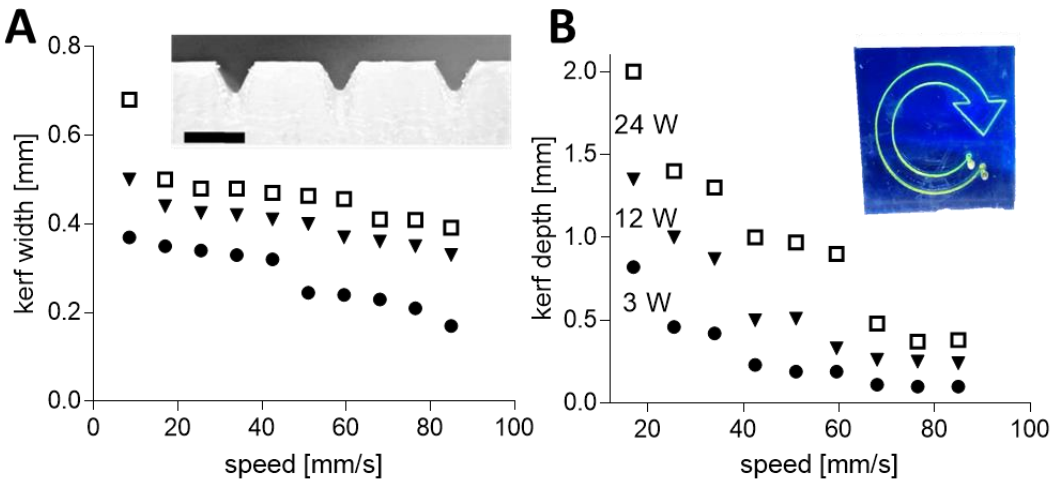


**Figure 4.4**. (A) Influence of laser power and speed on the kerf width. In insert a cross section picture of a channel engraved with a power of 12 W and a speed of 15 mm/s. scale bar is 500 µm (B) kerf depth. In insert a microfluidic chip made of recycled PMMA filled with fluorescein salt solution.

## 4.6 Conclusions

The purpose of the current study was to validate the use of a commercially available chemically recycled PMMA in conjunction with a rapid prototyping technique to manufacture microfluidic devices sustainably. A DSC analysis did not show the presence of impurities inside the material, suggesting the suitability of Greencast™ PMMA material with our bonding protocol, without optimisation of the bonding protocol. Several other manufacturers of chemically recycled PMMA were contacted for samples but none supplied material. Although it can be anticipated that other chemically recycled material may also be suitable for prototyping microfluidic devices, a DSC analysis is recommended before embarking in manufacturing. At the time of writing, Greencast™ is more expensive than pPMMA, however, it is a more environmentally sustainable approach when embarking in the production of microfluidic devices for research, teaching and public engagement activities

The choice of RePMMA resulted successful in order to prototype sustainable microfluidic devices, embracing a DfS approach. Differential scanning calorimetry analysis shown the compatibility of RePMMA in conjunction with our safe and cost effective bonding protocol. Furthermore, RePMMA does not show recast layer formation. Bonding strength, burst test and maximum flow rate are order of magnitude bigger than the one needed for common microfluidic applications. However, it needs to be underlined that

Re-PMMA and in general recycled polymers are, at the moment, more expensive than virgin polymers. For the specific case, at the time of writing, RePMMA is 22% more expensive than pristine PMMA (£39,26 against £32.12 for a 3 mm thick sheet (100x100cm) of Re-PMMA and pPMMA, respectively. Additionally, it can be anticipated that the choice of rapid prototyping PMMA in conjunction with a laser based layer-by-layer approach has some drawbacks, named as adsorption of small molecules and qPCR inhibition. However, the choice of Re-PMMA represents the more imminent environmentally sustainable approach that can be undertaken when rapid prototyping microfluidic devices for research, teaching and public engagement activities. With respect with the *in situ* mechanical recycled PMMA for microfluidic applications reported by Young's group, and mentioned in chapter 2, the choice of chemically recycled PMMA does not change the daily routine of the research. It can be envisaged and suggested that the adoption of the two approaches (starting the mechanical recycling iteration with Re-PMMA) with a specific control of the way on which the material is disposed of will help minimize the volume waste and the request of new raw material). Despite promising results and effective applicability of Re-PMMA as substrate material for microfluidic applications, still it has limited end of life scenarios if compared to biodegradable material (both petrochemical or bioderived). In the next chapters, we will focus on biodegradable material as new substrate material for the production of environmentally sustainable microfluidic devices.

# Chapter 5: MICROSTRUCTURING POLYLACTIC ACID VIA LASER ABLATION FOR THE FABRICATION OF ENVIRONMENTALLY SUSTAINABLE MICROFLUIDIC DEVICES

## 5.1 Introduction

Polymeric materials are cost-effective, easy to manufacture, light in weight, and have tuneable properties. They are the material of choice for the production of disposable, single-use, biomedical devices [5]. Syringes are, for instance, the perfect example on how the use of plastics, radically and positively changed public health and help eradicate the risk of cross-contamination. However, as already dwelled upon in the previous chapters, there is the urgent need to take into consideration the sustainability of disposable biomedical product. The vast majority of medical plastics are derived from non-renewable, fossil-based, sources [2], [6], [8], [53], [129]–[131]. The use of recycled plastics, as for example the use of recycled PMMA, represents a suitable sustainable solution, but the need of specific infrastructure and the logistics required to collect and recover, and the cost involved in recycling PMMA (as opposed to other thermoplastics material such as HDPE and PET (bottles), for which it is already existing a recycling stream) makes it challenging. Regrettably, recycling is not an economically advantageous option, and up to the 30-50% of plastic waste cannot be recycled. Bioplastics, which are polymers derived from organic biomass sources, represent a more suitable solution in this sense [132]–[134], and especially thanks to the broad range of end-of-life scenarios that they offer.

This chapter describes the rationale behind the choice of Polylactic acid for the sustainable production of microfluidic devices in conjunction with a low impact micromanufacturing technique such as laser ablation.

## 5.2 Polylactic acid

An alternative to petrochemical-derived polymers, is Poly-lactic acid (PLA), a common biodegradable thermoplastic that is produced from starch. Polylactic acid (PLA) or Poly(2-hydroxypropanoate) accordingly with the IUPAC nomenclature is an aliphatic alpha polyester. It was firstly discovered by Carothers et al, in 1932 while conducting a study on polycondensation processes of different monomers, including lactade [135].

They were able to polymerize a low molecular weight PLA (3000 Da). Only a few years later, in 1935, the first patent, claiming a process to synthesize a polymer from lactide via ring opening polymerization, came out [136]. This patent enabled to produce for the first time high molecular weight PLA, that could be cast into strong film or spun into fibers. At the time, the biodegradability of the material was not a requirement, so the success of PLA in the medical field had to wait until the 1966, when it was firstly proposed as material in biomedicine as resorbable surgical implant [137]. Due to high cost and low availability, PLA applications have been restricted until the early 1990s when the bioplastics industry changed direction dramatically and moved towards more durable bioplastic [138], [139]. In that period, Cargill Corporation developed its own method to highly produce lactide and PLA in a continuous process, leading then to the creation of Nature Work, one of the largestcompany producing PLA resins for different applications, from clothing to food packaging [140].

The number of journal articles on PLA has grown exponentially in the 2007-2012 period and covers a wide range of fields as reported in Fig.

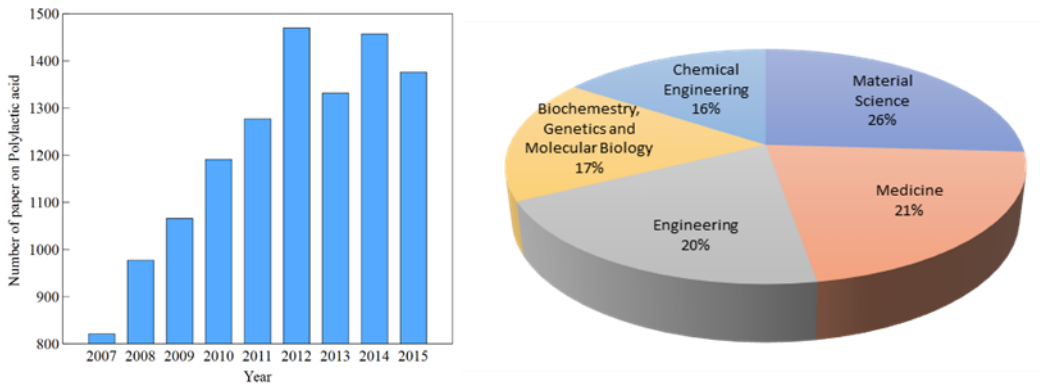


Figure 4.2 (LEFT) Number of article, review, conference paper, book chapter and editorial about Polylactic acid during the last 9 year; (RIGHT) area regarding Polylactic acid. Source: Scopus. Keywords used: Polylactic acid, Poly(lactic acid), PLA, Polylactide

As a polyester, PLA can be processed by a wide range of method, just as petroleum-derived materials. Injection molding, extrusion, hot embossing, solvent casting, film blowing have been used to machine PLA [141]. In the field of additive manufacturing, PLA gained more and more attention after the popularity of the fusion filament deposition 3d printing started, due to its elasticity, low melting point, low odour and viscosity. Apart

from medical grade PLA, PLA is a relatively cheap material, at £ 7 per Kg of pellets, making it highly competitive in the pellets polymer market. PLA has been used from several years now in the food industry, for example as biodegradable lid for coffee cups. More recently, PLA has appeared in the scientific consumable market, with Sigma Aldrich proposing biodegradable plastic stirrer made of PLA.

With respect to the other bio-derived materials proposed for the production of environmentally sustainable microfluidic devices seen in chapter 2, the translation to the mass market of PLA does not represent a drawback. In fact, PLA is already used in the electronics industry, food packaging, and in the biotechnology field. For example, Fujitsu is now producing keyboards keys and computer cases made of PLA, while Sony is using PLA to manufacture cases of different electronics and the first CD entirely made of PLA was proved and placed in the mass market by Sanyo [142].Beyond the beforehand mentioned good manufacturing properties of PLA and the fact that it is derived from renewable resources, PLA brings different end-of-life scenarios. For instance, it can be reused, recycled, composted, incinerated and go to landfill. Regarding recycling, this can be carried out via chemical recycling, where PLA is hydrolysed at high temperature to have a high yield recover of lactide and then repolymerized to obtain high molecular weight PLA; and mechanical recycled, where PLA, after collection, sorting, cleaning and grinding, is remelted and reprocessed. PLA can be composted via industrial composting facilities or with home composting piles if heated up to 45°C, which can represent the most appropriate solution to get rid of POC microfluidic devices made of PLA after a decontamination process, specially, in low-resource settings hospitals. Another possibility as end of life scenario of PLA is the energy recovery via incineration because it has a calorific power very close to the one of cellulose materials. Furthermore the combustion of waste PLA is significantly lower than those associated with combustion of other plastics, with low or non- detectable emission factors [143]. The less desirable end of life scenario for PLA is landfilling.

In order to develop our ultra-fast prototyping technique with PLA we need to investigate the laser machining of PLA sheets, which has never been explored in depth. Prior to explore the laser-matter interaction a brief overview of different lasers for microfabrication will be given, analysing more in depth $CO_2$ lasers.

## 5.3 Laser Ablation

Laser ablation is a commonly used manufacturing technique to microstructure materials for the fabrication of microfluidic devices. With respect to other subtractive microstructuring techniques that do not require a mould, such as CNC milling and digital craft cutter, it is a faster and cleaner process that requires less post-processing [37][41]. Furthermore, laser ablation is considered a green technology [126]. After the discovery of the ruby laser in 1960 [144], [145] that lead to the first practical example of laser ablation, several others laser have been developed and employed to microstructure and to induce topological changes to a material. In 1997 the first example of laser ablation for the production of polymer microfluidic devices was demonstrated[27]. Nowadays several lasers are available to microstructure polymeric materials, covering a broad range of wavelengths going from the deep UV to the far IR. In function of the laser chosen and the related wavelength, different phenomena can take place during the ablation process. For instance, UV lasers lead to mostly athermal processes, that rely on material removal from photon absorption. In general, when the laser hits the material, the absorption of photons leads to transfer bound electrons to a more energetic state, with a consequently inter and intra-molecular energy conversion to heat and bond scission. When a critical number of bonds are broken an explosive vaporization of the substrate where the laser is focused on will take place. The exact mechanism of polymeric material removal under UV laser irradiation is not fully explained yet, but both photochemical and photothermal phenomena have been observed experimentally [27].

When it comes to polymer microstructuring via laser ablation, Excimer lasers can represent the ideal tool for a precise micromachining. The ablation process generated by excimer lasers is predominantly driven by photochemical degradation. The UV radiation energy fed by excimer lasers is equal or larger than the bond-dissociation energy of chemical groups typically present in a polymeric structure. This “cold” ablation process enables to produce microstructures without generating thermal deformation and recast layers in the material. Thus obtaining a clean and clear cut. In order to maximize the photon absorptions by the sample the laser wavelength should be chosen carefully.

Ultrashort pulses lasers such as femtosecond and picosecond lasers are lasers that emit pulses with a duration of femto (10-15 s) and pico (10-12) seconds respectively. Those kind of lasers allow to obtain a cold ablation process [146]. Basically, the material undergoes through a multi-photon absorption with a high peak intensity. In this case the material can be machined even if it is transparent to the laser wavelength [147].

Even if the lasers listed so far allow to micromachine polymeric materials (down to

channel width of 10 µm) with high precision and avoiding thermal deformation, those apparatuses are expensive and requires highly trained personnel. On the other hand, $CO_2$ lasers are cheaper, more available, and come in an automated "plotter" format amenable to microstructuring.

#### *5.3.1.1 $CO_2$ Laser micromachining*

In 2015, the global market for $CO_2$ lasers was estimated to be $ 9.17-11.7 billion, expecting $ 16.0 billion in 2020 [148]. 40,000 $CO_2$ laser cutting machines are installed worldwide [149]. Although $CO_2$ laser cutter was invented as a technology to process metals, it is a popular process applied to non-metallic materials as well, e.g. glass, woods, thermoplastics, thermosets and elastomers [150].

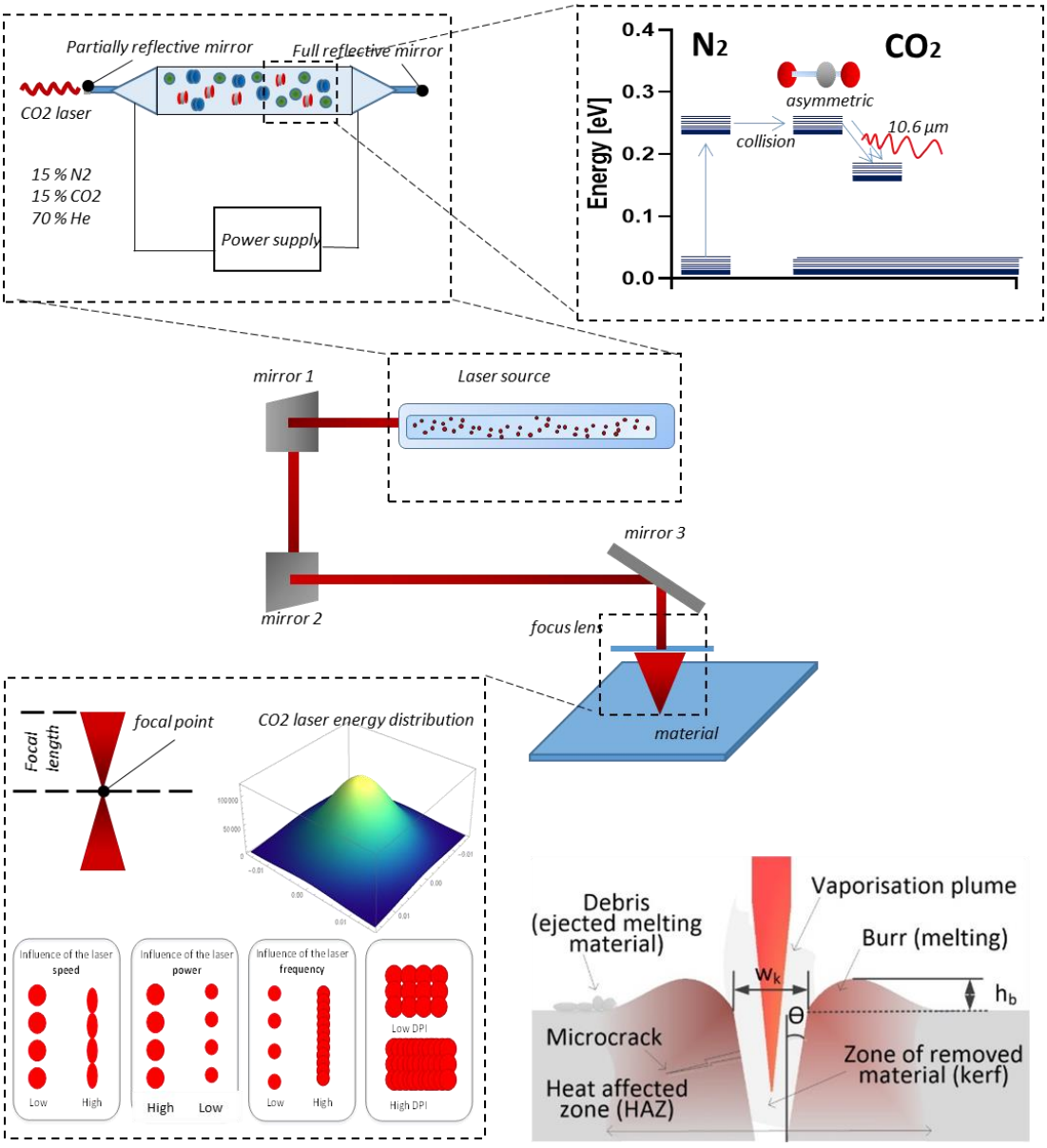


Figure 5.10 Schematic representation of $CO_2$ laser cutting: in the centre schematic representation of a typical $CO_2$ laser cutter (not in scale); on the top left corner, schematic representation of the laser source tube; on the top right corner schematic representation of the energy level of $N_2$ and $CO_2$ after and before

excitation. On the bottom left corner, schematic representation of the influence of the laser speed, power, frequency and dpi of a typical commercial laser cutter on the shape of ablated spot; on the bottom right corner schematization of the Laser cutting process. w k represents the kerf width and h b the burr height.

Generally, a $CO_2$ laser cutter is composed by a $CO_2$ laser tube, a series of mirrors and a focus lens positioned on an arm that can move in the x and y direction. The light is generated inside the laser tube, that contains a mixture of gas composed by 15% of carbon dioxide, 15 % of nitrogen and 70 % of helium. The tube is connected to a power supply that generates a high voltage electricity that pass through the tube. The gas molecules are then excited to a higher state and while returning to their medium state they will emit a photon. Nitrogen can hold an excited state for a longer period of time without emitting photons. The excited nitrogen will then collide with the $CO_2$ molecules. This will bring a portion of the $CO_2$ molecules in an excited state that will exhibit an asymmetric stretch. At the same time, the collision with the helium atoms will help emptying population from the lowest electronic states of the $CO_2$, allowing the population inversion. Consequently, photons with 10.6 μm wavelength will be emitted when the $CO_2$ molecule will decay to the medium state. At the two extremities of the laser tube there are 2 mirrors that form a laser cavity, so that the emitted laser radiation can circulate through the tube and the emission will get amplified. One of these mirrors, the output coupler, is partially reflective in order to allow the emitted radiation to escape. The laser is then guided the surface of the material through the mirror system and the focal lens.

During laser cutting the tightly focused beam generated by the laser, is applied on the material surface that undergoes a localised melting (known as fusion cut) or vaporization process [151]. The main process taking place during laser cutting of thermoplastics is fusion cut, with the exception of PMMA that is cut via vaporization [152]. During cutting the heat generated by the laser can diffuse through the material altering its microstructure and properties. This area, called Heat Affected Zone (HAZ), is strictly related to the thermal properties of the material (e.g. thermal diffusivity) its thickness and to the laser power, speed and frequency. On the other hand, the presence and form of a recast layer close to the cut is dependent on the beam energy, gas pressure and exact laser cutting mechanism taking place [153]. The height of the recast layer is defined as burr (Figure 5.1).

Different methodologies have been developed to evaluate how polymeric materials react to laser cutter machining. The HAZ dimensions, recast layer, surface roughness,

dimensional precision, kerf quality and mechanical properties after laser cutting can help to discriminate if a material has a good workability or not [151]. Caiazzo et al., 2005, reported a study on the laser cutter quality on three different thermoplastic polymers polyethylene (PE), polypropylene (PP) and polycarbonate (PC) with different thickness, analysing the heat affected zone and surface roughness after laser cut. Considering the quality of the cut edges, faces and the presence of re-solidified molten material the authors concluded that the PC "workability" is high, due to a smaller HAZ, absence of recast zone a good quality if cut edges, PP is medium-high and PE lower. In a different study on polymethylmethacrylate (PMMA), PC and PP, Davim, Barricas et al., 2008, reported the PMMA $CO_2$ laser cutter workability as very high. Similarly, the behaviour of laser-cut PMMA was investigated from different authors [154], [155] in order to find best process parameters to reduce HAZ, burr and surface roughness. The laser workability difference between different polymer arises from their difference in molecular structure, Thermal properties like the latent heat of vaporisation, melting enthalpy, laser beam absorptivity, specific heat and whether they are amorphous (PMMA, PC) or semi-crystalline (PP, PE, PLA), all affect the workability.
In table 5.1 are reported the most common thermoplastic materials investigated in the $CO_2$ laser cutter machining. While in table 3 is shown the qualitatively dependence of the kerf quality from the input
parameters of the laser cutter and from the thermal properties of the materials.

***Table 1***

| | Materials | Input parameter | Output parameters | | | | | | References |
|---|---|---|---|---|---|---|---|---|---|
| | | | HAZ [um] | Burr [um] | Ra [um] | Kw | Kd | Ka | |
| Amorphous | PMMA | 200-1400W | 120-220 | 100-250 | 7-10 | 0.4 - 1.5 | - | - | [150] [156] [157][158][154] |
| | PS | 120-500 W | 400-600 | 600-800 | 6-9 | - | - | - | [159] |
| | PC | 500 W | 210-370 | 90-300 | 2.01 | 297 - 370 | - | - | [152][156][157][158] |
| | HDPE | 200-1400W | 319-622 | - | 1.07 | 319 - 629 | - | - | [152] |
| | LDPE | 120W | 450-700 | 100-250 | 1-2.5 | - | - | - | [159] |
| | PP | 200-1400W | 250-400 | NA | 0.6-1 | 326 - 534 | - | - | [152][156][157][158] |
| Semi-crystalline | PLLA | 25 W | 80-110 | - | - | 70-80 | 70-100 | 15-30 | [160][161] |
| | PLGA | 25 W | 80-100 | - | - | 70-160 | 70-160 | 15-75 | [161] |

Table 5.1 Common thermoplastic materials used in $CO_2$ laser machining. The output parameters reported are the heat affected zone (HAZ), Burr, surface roughness ($R_a$), kerf width ($K_w$), kerf depth ($K_d$) and kerf taper angle ($K_a$).

$CO_2$ laser micromachining is a widely employed micro-manufacturing technique for the production and rapid-prototyping of microstructures. Poly(methyl methacrylate) (PMMA), due to its optical properties and mass-manufacturing compatibility, is often the material of choice for laser machining of microfluidic devices to be used for clinical, environmental and educational purposes [45]–[48].

| | *Laser cutter input parameters* | | | *Material properties* | | |
|---|---|---|---|---|---|---|
| | *Laser Power* | *Cutting Velocity* | *Frequency* | *absorptivity* | *Latent heat of vaporisation or of melting* | *Vaporisation or Melting temperature* |
| ***HAZ*** | ↑↑ | ↓ | ↑ | ↑↑ | | |
| ***Burr*** | ↑ | ↓ | ↑ | | | ↑↑ |
| ***Kerf width*** | ↑ | ↓ | | ↑ | ↓ | |
| ***Kerf depth*** | ↑ | ↓↓ | ↑ | ↑↑ | ↓ | ↓ |

Table 5.2 Qualitative dependence of the kerf quality parameters with respect to an increment of the processing ones. e.g. if the laser power increases the heat affected zone increases

### *5.3.2 Laser Ablation of Polylactic acid*

Over the past decade, most research has investigated the use of different lasers to change the topology of PLA to enhance cell adhesion on construct for tissue engineering, and as a tool to manufacture polymeric resorbable stents. As outcomes laser induced changes in the surface chemistry and in the mechanical properties have been studied to better understand the laser ablation mechanism on PLA and as well whether if lasers are suitable tools to microstructure and manufacture PLA. For instance, Garskaite et al., used a Yb:kGW femtosecond laser with a maximum power of 20 mW and a maximum speed of 1 mm/s to produce micro and nanostructure on a composite scaffold of PLA as matrix and carbonated hydroxyapatite as filler. Their goal was to selectively expose to the microstructured surface the crystals of carbonated hydroxyapatite to enhance cell adhesion [162]. A more focused study on the material response under laser radiation is the one conducted by Stepak et al. The authors used a 248 nm KrF excimer laser to manufacture bioresorbable stent [163]. Because of the energy provided by the laser is higher than the bond dissociation energy of methyl and hydroxyl groups in the backbone and end groups of the polymer, they investigated the possible degradation effect induced by the laser. The mechanism of the degradation under UV radiation in polymers usually

lead to an autocatalyitic photodegradation, with a dramatic decrease of the final mechanical properties [164]. The study showed that the use of KrF laser induces a photodegradation within the entire volume of the ablated film, with presence of a recast layer [163]. Another study that investigated PLA response under laser radiation is the one conducted by Jia et. al [165]. Differently from the previous analysed study, Jia and co-workers used a femtosecond laser with a wavelength of 1040 nm, using a laser power of 0.8 W and a cutting speed of 0.04 mm/s. Even though femtosecond lasers enable to induce a cold ablation process, the authors observed the presence of a recast layer, reported as surface swelling. In order to overcome this unwanted feature, they analysed the ablation process under water. In this last case, they noticed the absence of laser damage, but the presence of cavities in the ablated region, coming from the gas release during the ablation. A further study was conducted by Ortiz et al., where a picosecond laser was used, and the effect of the crystallinity degree of PLA on the ablation quality was investigated [166]. The authors reported a combination of photochemical and photothermal degradation, with the latter having a major role in the ablation process. As in the previous studies analysed, presence of cavities was noticed in the irradiated surface, with a pore diameter from 500 nm to 1 μm. The authors concluded that picosecond laser is a promising technique to microstructure PLA [166]. Rodrigues at al., 2016, using a $CO_2$ laser cutter to obtain PLA porous scaffold from a pre-fabricated 3D printed bar, shown that the laser cutter does not influence strongly material properties and the final sample presented the desired structure. While, Stepak et al., 2014, with the aim of fabricate biodegradable stent in PLA and Poly lactic-co-glycolic acid (PLGA) with a $CO_2$ laser cutter, reported the formation of a heat-affected zone and the re-solidification of molten material on cut edges, because the cutting process is linked to vaporization and melt shearing, and investigated processing parameters, e.g. laser power and cutting velocity, to obtain the minimum HAZ and dimensional stability. They concluded that it could be possible by choosing the right parameters to produce Polylactic-based biodegradable stent using $CO_2$ laser cutting. Further research into laser interactions with PLA material will be of interest to the material science community in particular for tissue regeneration whereby PLA scaffolds could be nanostructured for specific effects, creating a vascular network or 3D printed PLA scaffold could be marked as precise location in a post-processing mode, uniting subtractive and additive manufacturing capabilities to achieve desired shapes.

The study presented in the next session will focus on the optimization of $CO_2$ laser cut quality of polylactic acid sheets with different crystallinity degree in order to reduce recast layer formation. Unlike to previously conducted study, where focus has been made on the ablation of film of PLA, our study aims to cut through 2 mm thick sheets. Furthermore, even though previously research has been conduct on the fabrication of PLA microfluidic devices (either 3D printed or via casting), no focus has been put on the sustainability aspect of the material.

## 5.4 Laser ablation of polylactic acid sheets for the rapid prototyping of sustainable, single-use, disposable single components

This paper, published in ACS Sustainable Chemistry and Engineering (IF 6.97) in February 2018, is co-authored by myself (AO), Ieva Keraite (IK), Antonio Liga (AL), Gioacchino Conoscenti (GC), Stuart Coles (SC), Holger Schulze (HS), Till T. Bachmann (TB), Khaled Parvez (KP), Cinzia Casiraghi (CC), Nicola Howarth (NH), Vincenzo La Carrubba (VLC) and Maïwenn Kersaudy-Kerhoas (MKK). Myself and MKK gave substantial contribution to experimental conception and design, and analysis of the results. I performed all experiments but the electrode printing, electrochemical measurements, and biological measurements and contributed to the analysis of the results. I.K. performed all biological experiments and contributed to the analysis of the results. A.L. contributed to the analysis of the results. G.C. contributed to the material characterizations. S.C. contributed to the literature on lifecycle analysis of PLA. H.S. performed the electrochemical measurement. T.B. contributed to the reagents and materials and the analysis of the electrochemical measurement results. K.P. printed the electrodes. C.C. contributed to the reagents and materials and the conception and analysis of the electrode printing results. The manuscript was written by myself, N.H., and M.K.K. in close consultation with all authors.

ACS Sustainable Chemistry & Engineering

Research Article

pubs.acs.org/journal/ascecg

# Laser Ablation of Poly(lactic acid) Sheets for the Rapid Prototyping of Sustainable, Single-Use, Disposable Medical Microcomponents

Alfredo E. Ongaro,[†,‡,§] Ieva Keraite,[†,‡] Antonio Liga,[†,‡] Gioacchino Conoscenti,[§] Stuart Coles,[∥] Holger Schulze,[‡] Till T. Bachmann,[‡] Khaled Parvez,[⊥] Cinzia Casiraghi,[⊥] Nicola Howarth,[†] Vincenzo La Carubba,[§,#] and Maïwenn Kersaudy-Kerhoas*[,†,‡]

[†]Institute of Biological Chemistry, Biophysics and Bioengineering, School of Engineering and Physical Science, Heriot-Watt University, Edinburgh EH14 4AS, United Kingdom

[‡]Division of Infection and Pathway Medicine, Edinburgh Medical School, College of Medicine and Veterinary Medicine, The University of Edinburgh, Edinburgh EH164SB, United Kingdom

[§]Department of Civil, Environmental, Aerospace and Materials Engineering (DICAM), University of Palermo, Viale delle Scienze building 6, 90128 Palermo, Italy

[∥]Sustainable Materials and Manufacturing Group, WMG, University of Warwick, Coventry CV4 7AL, United Kingdom

[⊥]School of Chemistry, University of Manchester, Manchester M13 9PL, United Kingdom

[#]ATeN Center − CHAB, Università di Palermo, Viale delle Scienze building 18, 90128 Palermo, Italy

*Supporting Information*

**ABSTRACT:** The employment of single-use, disposable medical equipment has increased the amount of medical waste produced and the advent of point-of-care diagnostics in lab-on-chip format is likely to add further volume. Current materials used for the manufacture of these devices are derived from petroleum sources and are, therefore, unsustainable. In addition, disposal of these plastics necessitates combustion to reduce infection risk, which has, depending on material composition, an undesirable environmental impact. To address these issues, we have developed a general approach for the rapid prototyping of single-use point-of-care cartridges prepared from poly(lactic acid), a sustainable material which can be milled and laser-cut as well as molded for translation to mass-market products. Here, the laser workability of poly(lactic acid) sheets is reported together with examples of microfluidic components. Furthermore, the low molecular adsorption in laser-ablated poly(lactic acid) channels and the compatibility of poly(lactic acid) for common on-chip bioassays, such as polymerase chain reaction (PCR), are demonstrated. This innovative prototyping technique can be easily translated to high volume manufacturing and presents exciting opportunities for future sustainable microfluidic laboratories as well as potential for sustainable disposable single-use microcomponents for clinical applications.

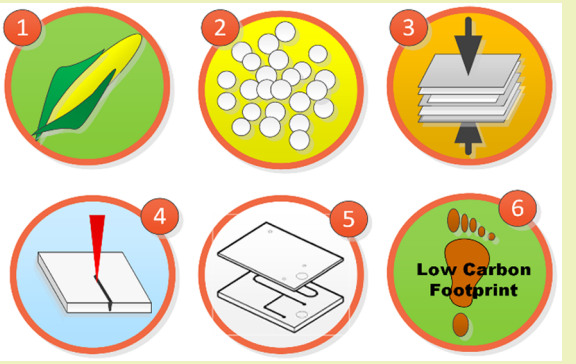


**KEYWORDS:** *Poly(lactic acid), Poly(methyl methacrylate), $CO_2$ laser cut, Sacrificial layer assisted manufacturing, kerf, Point of care, Micromachining, Microfluidic, Layer by layer, Rapid prototyping*

## INTRODUCTION

The demand for point-of-care testing is increasing at a fast pace, and the majority of these new tests are likely to be carried out in disposable plastic chips in order to eliminate the possibility of cross-contamination and alleviate the need for time-consuming sterilization. However, despite this clear trend[1] and the fact that plastic waste has become a global challenge,[2] there are only a limited number of reports in the literature focusing on the full life cycle of products used in the point-of-care environment.[3] Nearly all commercially available plastic chips or cartridges are made from petroleum-derived materials; these include predominantly poly(methyl methacrylate) (PMMA), cyclo-olefin copolymer (COC), polycarbonate (PC), and polystyrene (PS). These nondegradable polymers are currently favored for the production of microfluidic devices by both academic laboratories and industry and mirror the traditional plastic medical waste routes. Similarly, there is not enough debate about the amount of waste that disposable point-of-care devices will generate or how to deal with this type of waste, whether in a hospital or in a resource-poor setting. It has been shown that inadequately controlled incineration procedures and waste streams lead to the release of significant

Received: November 21, 2017
Revised: February 16, 2018
Published: February 16, 2018





DOI: 10.1021/acssuschemeng.7b04348
ACS Sustainable Chem. Eng. XXXX, XXX, XXX−XXX

quantities of pollutants.[2,4] Furthermore, anecdotal evidence gathered in Asia, Africa, and South America indicated that incinerators may not always operate properly or be manned by competent personal.[5−7] Thus, the additional waste generated by the increased consumption of disposable medical items may exacerbate these problems for such communities. Replacement of nondegradable polymers with biodegradable alternatives from nonfossil resources could be one solution to the growing concern around the increased production of pollutants from medical plastic waste.[11] A material of interest in this regard is poly(lactic acid) (PLA), a common biodegradable thermoplastic produced from the naturally occurring compound lactic acid, which itself is prepared from the simultaneous saccharification and fermentation of starch. With good biocompatibility credentials and approval by the US Food and Drug Administration (FDA) for use in humans, PLA has attracted much attention recently being utilized in tissue engineering, medical implants, surgical sutures, packages, fibers, and textiles[8] as well as being identified as a potential alternative material for the production of disposable biomedical items. The latter application is further supported by the finding that the impact of waste PLA combustion is significantly lower than that of other plastics.[12] Analogous to the petroleum-derived materials, PLA can be processed to high volume by extrusion or injection molding.

Having selected a material for the production of sustainable single-use medical microcomponents, we turned our attention to developing a method that would allow the rapid prototyping of devices. Rapid-prototyping methods have had enormous impact on manufacturing by allowing rapid iterations between design and testing of new product ideas.[13,14]

Recent advances in additive manufacturing resolution have permitted prototyping features at a microscale. PLA, thanks to its low elasticity and low melting point, has become a material of choice for additive manufacturing techniques such as fused deposition modeling[15] (FDM, or commonly referred as 3D printing). A few examples involving the 3D printing of PLA microfluidic chips have been reported.[16] However, 3D printing still poses some challenges, which prevent this technique being used routinely for the production of these devices, namely, printing time, complexity of multimaterial manufacturing, artifact assembly, print fidelity, often necessary postprinting treatments, difficulty in removing supporting material, and limited printer resolution (down to 300−500 $\mu$m is achievable for minimal features).[17,18] On the other hand, a layer-by-layer approach enables flexibility in the design, does not require postmanufacturing treatment, and can be applied to an unlimited number of materials.[19,20] It also allows for surface and local treatments and for electrode and membrane integration for the production of hybrid microfluidic devices. Furthermore, advances in multilayer rapid-prototyping techniques have permitted the manufacturing of complex microfluidic devices in less than 15 min from design to test.[21] This method involves laser cutting individual layers followed by multilayer bonding using a solvent assisted method.

Here, we propose a design for sustainability (DFS) approach[22] for the production of environmentally friendly medical microcomponents (Figure 1A). In this scheme, PLA is transformed from biomass into pellets. These pellets are transformed into sheets, which are used in a rapid-prototyping technique until a final design is put into production, and the device is then manufactured via injection molding, for example. The disposable medical microcomponents may be used in clinical settings, in home settings, or in the field (ambulance, mobile laboratories). Devices in contact with clinical samples such as blood, urine, or sweat are incinerated. In this scheme, several steps are well established. The harvesting of biomass for transformation of raw product into pellets is already commercially viable. Similarly, the high-volume production of PLA components is well controlled. The missing step for researchers and engineers is the ability to rapidly prototype microscale devices prior to production.

We here report the development of a simple and affordable layer-by-layer laser-based technique to engineer complex single-use microfluidic chips from PLA (Figure 1B). No solvent or harsh conditions are employed, and the technique only necessitates the use of low capital investment equipment. We

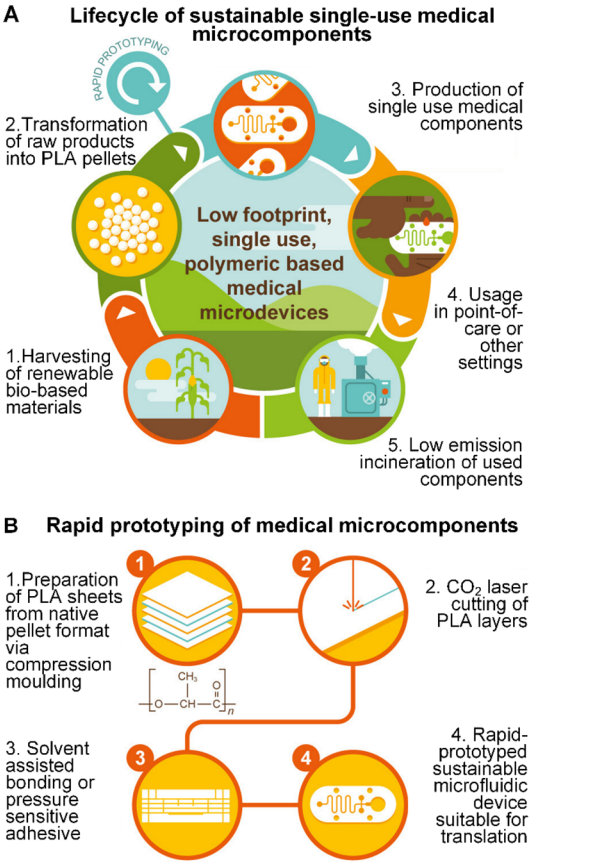


**Figure 1.** (A) Conceptual lifecycle for poly(lactic acid) (PLA) based single-use medical microcomponents such as microfluidic chips. From the lower left illustration clockwise: PLA monomers are produced via fermentation of corn or sugar taken from starch plants. The amount of equivalent $CO_2$ per kg of PLA Ingeo for corn production is about 0.25 kg $CO_2$ equiv/kg; the transformation from the raw product into PLA pellets is 1.038 $kCO_2$ equiv/kg PLA naturework Ingeo. The production of the microfluidic device from the pellets, usage of the microfluidic component in point-of-care or other settings, and incineration as possible end-of-life scenario of the PLA microfluidic device. Other possible scenarios as a function of the application of the device are mechanical recycling (0.6 kg $CO_2$ equiv/kg), industrial composting (1.5 kg $CO_2$ equiv/kg), anaerobic digestion (1 kg $CO_2$ equiv/kg), direct fuel substitution in and industrial facility (0.1 kg $CO_2$ equiv/kg), and incineration with heat recovery (1 kg $CO_2$ equiv/kg),[8−10] resulting in at least half lower impact on climate change with respect to other thermoplastic materials from nonrenewable resources. (B) Rapid prototyping scheme for the production of PLA based devices. In inset, chemical structure of PLA.


DOI: 10.1021/acssuschemeng.7b04348
ACS Sustainable Chem. Eng. XXXX, XXX, XXX−XXX

demonstrate good PLA workability in conjunction with $CO_2$ laser cutting and engraving, using a sacrificial layer assisted manufacturing method (SLAM). Following the observation of very low surface roughness, the potential benefits offered by integrated PLA-derived fluidic devices are presented through an investigation into molecular retention. Finally, complex microfluidic networks have been produced to show the potential of this technique for the rapid-prototyping of microengineered components for biomedical uses, in particular for point-of-care diagnostics.

## MATERIALS AND EXPERIMENTAL METHODS

**PMMA and PLA Material.** PMMA was obtained in 2 mm sheets (Clarex, Nitto Jushi Kogyo Co. Ltd., JP supplied by Weatherall Ltd., UK). Poly(lactic acid) (PLA Ingeo Biopolymer 3100HP) was supplied in pellet form by Nature Works LLC (Minnetonka, MN).

**Poly(lactic acid) Sheet Preparation.** To investigate the influence of the laser cut quality with respect to the physicochemical characteristics of PLA, four sets of PLA sheets were prepared via compression molding. Unlike PMMA, which is available in sheets of different thickness, PLA is only available in films or pellets. To make PLA sheets, PLA pellets were dried for 6 h at 80 °C, and then collected in a sandwich composed by a metal frame (with dimensions 11 cm width × 11 cm height, 2 mm thickness), two Teflon films (50 $\mu$m in thickness, DuPont Teflon), and two additional plates maintaining the assembly in place. Plates were preheated in a manual hydraulic heated press (by Carver, Inc.) to 210 °C, that is slightly above the melting point of the pellets (200 °C according to the supplier technical data sheet), and the sandwich with its frame was put between the heated plates. The stack containing the PLA pellet was maintained at 200 °C, under pressure with the following cycle: 4 min under 10 bar, 30 s under 50 bar, 30 s under 100 bar, and 30 s under 150 bar, so that a film with homogeneous thickness could be obtained. After this procedure, the heating system was switched off, and the plates were cooled down to room temperature through cooling water, circulating in a serpentine channel located within the plates. Then, the pressure was released, and the final sheet was unpacked. Four sets were prepared by changing the cooling rate with the aim to achieve various degrees of crystallinity (the temperature−time pressure−protocol is available in Supporting Information, section 1).

**Sheet Characterization by XRD.** The prepared PLA sheets were analyzed by X-ray diffraction (XRD) using a PANalytcal Empyrean with Cu K$\alpha$ radiation with a wavelength of $\lambda$ = 154 nm, to determine qualitatively and quantitatively the crystallinity degree. A $2\theta$ continuous scan type was used with a range from 5° to 80° to obtain the complete spectra of each sample.

**Sheet Characterization by DSC.** The quantitative determination of the crystallinity degree was carried out using a DSC131 evo (Setaram Instrumentation, France). Each sample was heated from 30 to 250 °C with a heating rate of 10 °C/min, after a precondition at 30 °C for 10 min. As previously reported by Naga et al.,[23] the crystallinity degree was estimated using the following eq 1:

$$X_c = \frac{(H_m - H_c)}{H_m^0} \times 100 \quad (1)$$

where $H_m$ and $H_c$ are, respectively, the melting enthalpy and the crystallization enthalpy, while $H_m^0$ is the theoretical melting enthalpy of a pure nondefective PLA crystal, 93 J/g.

**Laser Cutting, Imaging, and Dimensional Measurements.** In order to investigate the laser cut-quality and to provide a practical guide when choosing laser cut manufacturing on PLA, a $CO_2$ commercial laser cutter (Epilog Mini Helix) with a 2 in. lens (101.6 $\mu$m beam spot) was used to produce slits through the PMMA and PLA sheets. Laser power, speed and frequency were chosen as input parameters to determine PLA laser cutting behaviors in terms of heat affected zone (HAZ), kerf depth, width, and kerf taper angle. To evaluate cut accuracy, recast layer, kerf depth, and kerf width have been measured using a Dinolite microscope (Dino-Lite Premier2 AD7013MZT), while the determination of the heat affected zone was carried out using a polarized microscope (Olympus BX51). The determination of the kerf depth was carried out taking into account as input parameters laser power and speed, keeping the frequency (number of pulses that the laser fires per second) constant at 5000 Hz, since their influence on the kerf depth carries more weight than the frequency. All the measurements were rounded to the first decimal to provide a practical guide in the selection of the parameters to use cutting a thickness specific sheet. Scanning electron micrography (SEM) was used to understand the topology of the laser-cut microchannels. To determine the laser cutting parameters, the width of the molten layer was measured on photographs acquired from a Dino-Lite Premier digital microscope. Kerf depth and kerf width were measured via image analysis with ImageJ from photographs taken by Dino-lite. HAZ was measured via polarized microscopy (Olympus). To evaluate surface roughness average ($R_a$), squares of 4 mm by 4 mm were engraved on the surface of ultrahigh cooling rate (UHCR) and ultralow cooling rate (ULCR) PLA and PMMA and then analyzed with a white light interferometer (ZYGO) with 1 nm resolution in vertical direction. The $R_a$ quantitative determination was carried out using the software of the interferometer apparatus, Metro.Pro 8.2. To bind together the different PLA layers, a double sided adhesive tape (3 M tape 469 MP) was used, unless further specified.

**DNA Binding to PLA and PMMA.** To assess DNA binding to poly(lactic acid) (PLA) and poly(methyl methacrylate) (PMMA), Human Genomic DNA (Bioline) was diluted with water to 2 ng/$\mu$L and 20 ng/$\mu$L concentrations and incubated for 30 min with 8 $mm^3$ PLA and PMMA at room temperature. After incubation, DNA concentration of samples and controls was measured with Qubit and Nanodrop in triplicate. Real time quantitative PCR was performed using 2× Power SYBR Green PCR Master Mix (Thermo Fisher Scientific) to amplify 94 bp target with GAPDH primers (final concentration 200 nM): forward 5′-AGGTTTACATGTTCCAATATGATTCCA-3′ and reverse 5′-ATGGGATTTCCATTGATGACAAG-3′. The standard curve was created using a series of 5 serial dilutions of Human Genomic DNA, to assess the final concentration of the tested samples. Thermal cycling conditions involved a 10 min cycle at 95 °C followed by 40 cycles with 15 s at 95 °C and 60 s at 60 °C. Samples were amplified in duplicate using Mx3005P qPCR system (Agilent). Melting curve was performed as a control measure for nonspecific amplification.

**Chemical Leaching.** To investigate the leaching of chemicals from both PLA and the benchmark material PMMA, molecular grade water was incubated at room temperature in the presence of 8 $mm^3$ cubes of PLA and PMMA for 30 min, and then the UV−vis spectrum was analyzed using a microvolume spectrophotometer, Nanodrop instrument (ND-1000).

**PCR Inhibition.** To evaluate PCR inhibition, three different concentrations (2 ng/$\mu$L, 10 ng/$\mu$L, 20 ng/$\mu$L) of genomic DNA samples were mixed together with 2× Power SYBR Green PCR Master Mix, GAPDH primers (final concentration 200 nM), and molecular grade water and incubated with 8 $mm^3$ PLA and PMMA for 30 min on ice. A control without polymeric samples was prepared in the same way. The mixture was kept on ice to preserve the integrity of the polymerase contained in the PCR Master mix. After incubation, qPCR was performed with the same conditions as described previously. Melting curve analysis was done to check the quality of amplified product. Linear regression analysis was done in MxPro qPCR software ($R^2$ > 0.98).

**Electrode Printing.** The water-based biocompatible graphene ink was formulated from graphite via a previously published technique available in ref 24. The final concentration of the graphene ink used for the inkjet printing was 2.70 mg/mL A Dimatix DMP-2800 inkjet printer (Fujifilm Dimatix, Inc., Santa Clara, USA) was used to print electrodes on both PLA and PMMA substrates. Prior to printing, the substrates were cleaned with ethanol followed by drying under $N_2$ flow. The nozzle plate consists of a single row of 16 nozzles with a 23 $\mu$m diameter, spaced 254 $\mu$m apart, with typical drop size of 10 pL. The electrodes were printed onto the substrates at 40 °C with 35 mm


DOI: 10.1021/acssuschemeng.7b04348
ACS Sustainable Chem. Eng. XXXX, XXX, XXX−XXX

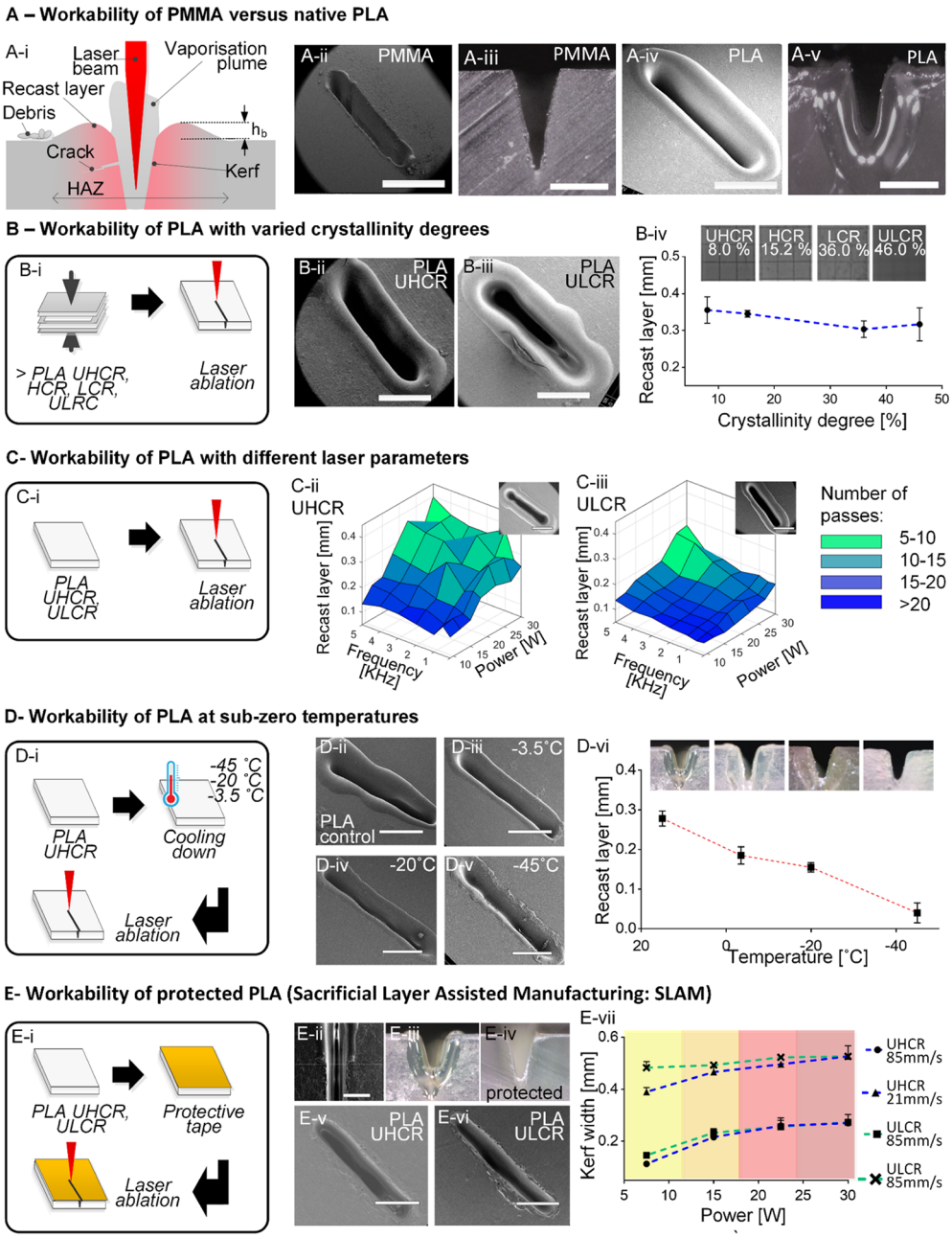


**Figure 2.** Laser workability of PLA. (A) Workability of PMMA versus native PLA: (A-i) Laser cutting process. $w_k$ represents the kerf width and $h_b$ the burr height. (A-ii) SEM picture of laser ablated PMMA (*S*, 85 mm/s; *P*,15 W; *F*, 5000 Hz), scale bar is 1 mm. (A-iii) Cross section of the PMMA kerf, scale bar 0.6 mm. (A-iv) SEM picture of laser ablated PLA (*S*, 85 mm/s; *P*, 15 W; *F*, 5000 Hz), scale bar is 1 mm. (A-v) Cross section of the PLA kerf, scale bar 0.6 mm. (B-i) Workability of PLA with varied crystallinity degree. (B-ii) SEM picture of laser ablated UHCR PLA (*S*, 85 mm/s; *P*, 15 W; *F*, 5000 Hz), scale bar is 0.8 mm. (B-iii) SEM picture of laser ablated ULCR PLA (*S*, 85 mm/s; *P*, 15 W; *F*, 5000 Hz), scale bar is 0.8 mm. (B-iv) Recast layer width as a function of the crystallinity degree of the produced PLA sheets; in inset, pictures of the prepared sheets. (C-i) Workability of PLA with different laser parameters. (C-ii) Recast layer width of UHCR sheet as a function of the laser power and frequency; in inset, SEM picture of the UHCR sheet (*S*, 85 mm/s; *P*, 15 W; *F*, 2500 Hz). (C-iii) Recast layer width of ULCR sheet as a function of the laser power and frequency; in inset, SEM picture of the ULCR sheet (*S*, 85 mm/s; *P*, 15 W; *F*, 2500 Hz). (D-i) Workability of PLA at subzero temperature. (D-ii) SEM picture of laser ablated UHCR at room temperature (*S*, 21.25 mm/s; *P*, 22.5 W; *F*, 5000 Hz), scale bar 0.8 mm. (D-iii) SEM picture of laser ablated UHCR at −3.5 °C (*S*, 21.25 mm/s; *P*, 22.5 W; *F*, 5000 Hz), scale bar 0.8 mm. (D-iv) SEM picture of laser ablated UHCR at −20 °C (*S*, 21.25 mm/s; *P*, 22.5 W; *F*, 5000 Hz), scale bar 0.8 mm. (D-v) SEM picture of laser ablated UHCR at −45 °C (*S*, 21.25 mm/s; *P*, 22.5 W; *F*, 5000 Hz), scale bar 0.8 mm. (D-vi) Recast layer width of UHCR sheet as a function of the starting working temperature; in inset, cross section picture of the samples cut with different starting temperature; (E) Workability of protected PLA. (E-ii) SEM picture of the laser kerf on protected and unprotected UHCR (*S*, 21.25 mm/s *P*, 22.5 W *F*, 5000 Hz), scale bar is 0.5 mm. (E-iii) Cross-section picture of the unprotected UHCR cut. (E-iv) Cross section picture of the protected cut. (E-v) SEM picture of laser ablated protected UHCR (*S*, 21.5 mm/s; *P*, 22.5 W; *F*, 5000 Hz), scale bar is 1 mm. (E-vi) SEM picture of laser ablated protected ULCR (*S*, 21.25 mm/s; *P*, 22.5 W; *F*, 5000 Hz), scale bar is 1 mm. (E-vii) Kerf width as a function of the laser power of UHCR and ULCR at fixed frequency (*F*, 5000 Hz) and two different speeds (*S*, 85 and 21.25 mm/s). The kerf depth, kd, associated is (from left to right) 1.6−0.5 mm (first zone), 0.9−0.3 mm (second zone), 0.6−0.15 mm (third zone), and 0.4−0.1 mm (fourth zone).



DOI: 10.1021/acssuschemeng.7b04348
ACS Sustainable Chem. Eng. XXXX, XXX, XXX−XXX

spacing between the drops. The number of printing passes for all the electrodes was 60.

**Electrode Testing.** The graphene electrodes printed on PLA and PMMA substrates and embedded in 1 mm wide and 0.8 mm high PLA microfluidic channels were electrochemically characterized with an Autolab PGSTAT 128N potentiostat (Metrohm Autolab, Herisau, Switzerland) controlled with Nova 2.1.2 software by recording cyclic voltammograms (CV) in the presence of 5 mM potassium ferricyanide and 5 mM potassium ferrocyanide in 0.1 M KCl solution and 0.1 M KCl solution as well as without potassium ferricyanide and potassium ferrocyanide (negative control) at 10 mV/s scan rate.

**Statistical Analysis.** All statistical tests were performed with the student's *t* test unless otherwise stated.

## RESULTS AND DISCUSSION

**PLA Laser Cutting Quality.** $CO_2$ laser cutting is an established material manufacturing technology, widely used due to its low cost and rapidity and good quality depending on the material. This technique has been applied to both metallic and nonmetallic materials, for example, glass, wood, thermoplastics, thermosets, and elastomers.[25−27] During cutting, the laser beam is focused onto the material surface, causing a localized melting or vaporization or both.[28] The heat generated by the laser diffuses through the material altering its microstructure and properties in an area named the heat affected zone (HAZ) (Figure 2A-i). The HAZ is strictly related to the thermal properties of the material (e.g., thermal diffusivity), its thickness, and the laser power, speed, and frequency. In addition, the presence of a recast layer (or burr) close to the cut depends on the beam energy, gas pressure, and exact laser cutting mechanism taking place.[29] Different methodologies have been developed to evaluate how a polymeric material's behavior interacts with laser machining. The HAZ dimensions, recast layer, surface roughness, dimensional precision, kerf quality, and mechanical properties after laser cutting can help to determine whether a material has good workability or not. The laser workability differences between different polymers arise from differences in their molecular structures, thermal properties (latent heat of vaporization, melting enthalpy, specific heat), laser beam absorptivity, and degree of crystallinity. In general, the cutting of thermoplastics is principally achieved by fusion cutting, except in the case of PMMA where the main process involved is vaporization.[30] PMMA is commonly used in conjunction with laser-based rapid-prototyping techniques due to its optical transparency and good $CO_2$ laser workability.[31,32] In contrast, it has been shown that $CO_2$ laser cutting of PLA occurs through a combination of melt shearing and vaporization.[33,34] We compared the workability of 2 mm thick PMMA (Figure 2A-ii,iii) and PLA sheets (Figure 2A-iv,v) and found that PLA has a reduced workability, as exemplified by the large recast layer in the PLA cut (about 90 $\mu$m high) as opposed to PMMA cut for the same laser parameters (frequency, power, speed), which has no recast layer. Furthermore, we observed thermal deformation of PLA due to the high energy of the laser and the lower thermal diffusivity under lower speed. This constrains the operator to using high speed at the cost of a higher number of passes to obtain a cut-through feature (data not shown).

**Investigating the Laser Workability of PLA with Different Degrees of Crystallinity.** The large recast layer produced in the laser-cut PLA sample makes this material impractical for use in the context of a layer-by-layer prototyping technique due to a reduced surface contact during the assembly. However, we hypothesized that the PLA polymer structure could be manipulated to reduce the HAZ and, in particular, the recast layer, so as to produce better cut quality, compatible with a layer-by-layer assembly developed in ref 21.

To investigate this hypothesis, four types of PLA sheets were produced with differing degrees of crystallinity using a compression molding technique: ultrahigh cooling rate (UHCR), high cooling rate (HCR), low cooling rate (LCR), and ultralow cooling rate (ULCR) (Supporting Information, section 1). The purpose was to investigate the influence of the cooling protocol on the overall morphology on the nanoscale (size of crystal lamellae) and on the mesoscale (size and amount of crystalline aggregates such as spherulites) (according to Continuous Cooling Transformation proposed for polymeric materials[35]) and, in turn, to study the behavior of these different PLA types when subjected to $CO_2$ laser cutting. During the phase transition from liquid to solid, a rapid cooling rate does not provide the time necessary for crystallites to form and, by freezing the polymer into a disordered structure, generates an amorphous status. As expected, we were able to tune the nanoscopic architecture and the molecular structure and obtain four materials with varying degrees of crystallinity as evidenced by XRD and DSC analysis (Supporting Information, section 1). Fast cooling rates (UHCR and HCR protocols) led to the formation of amorphous sheets while lower cooling rates (LCR and ULCR protocols) resulted in semicrystalline sheets. The degrees of crystallinity for the PLA sheets produced using the UHCR, HCR, LCR, and ULCR protocols were determined to be around 8%, 15%, 36%, and 46%, respectively. However, we found that the crystallinity degree of PLA did not influence the recast layer on 2 mm cuts made in material obtained with the UHCR, HCR, LCR, and ULCR protocols at the same frequency, speed, and power, respectively, 5000 Hz, 85 mm/s, and 15 W (Figure 2B). The UHCR protocol gave the best transparency (insets in Figure 2B-iv) and was preferentially used for the rest of the study, alongside the ULCR protocol for comparison.

**Influence of Laser Power on PLA Workability.** Since the crystallinity did not influence the recast layer height, we investigated if the laser power would have the effect desired (reduced recast layer), while the laser head speed was kept at the maximum value (85 mm/s). Although it was possible to reduce the width of the recast layer to 95 $\mu$m in cut-through samples, up to 25 beam passages were required (Figure 2C-ii,iii), hence reducing the practicality of the technique and its rapid-prototyping credentials.

**Investigating the Laser Workability of PLA at Different Temperatures.** As a different solution, we hypothesized that cooling the material prior to the cutting process could reduce the flow of melted material and therefore prevent or reduce the undesired recast layer (Figure 2D-i). We cooled 2 mm PLA sheets for 30 min at −3.5 °C, −20 °C, and −45 °C, respectively, on ice, in a freezer, and on dry ice, prior to cutting 2 mm long slits at set parameters (*S*, 21.25 mm/s, *P*, 22.5 W). Cooling the material from room temperature to −45 °C resulted in an 85% decrease in the size of the recast layer in conjunction with a decrease in the kerf width (Figure 2B, Supporting Information, section 2). Due to significant decrease in recast layer, a lower cutting speed (21.25 mm/s, enabling just two passes for cut-through) was used in this experiment. However, although this method proved successful (Figure 2D-iii,iv,v,vi), material deformations were still observed. Furthermore, the additional step involving storage of the material at


DOI: 10.1021/acssuschemeng.7b04348
ACS Sustainable Chem. Eng. XXXX, XXX, XXX−XXX

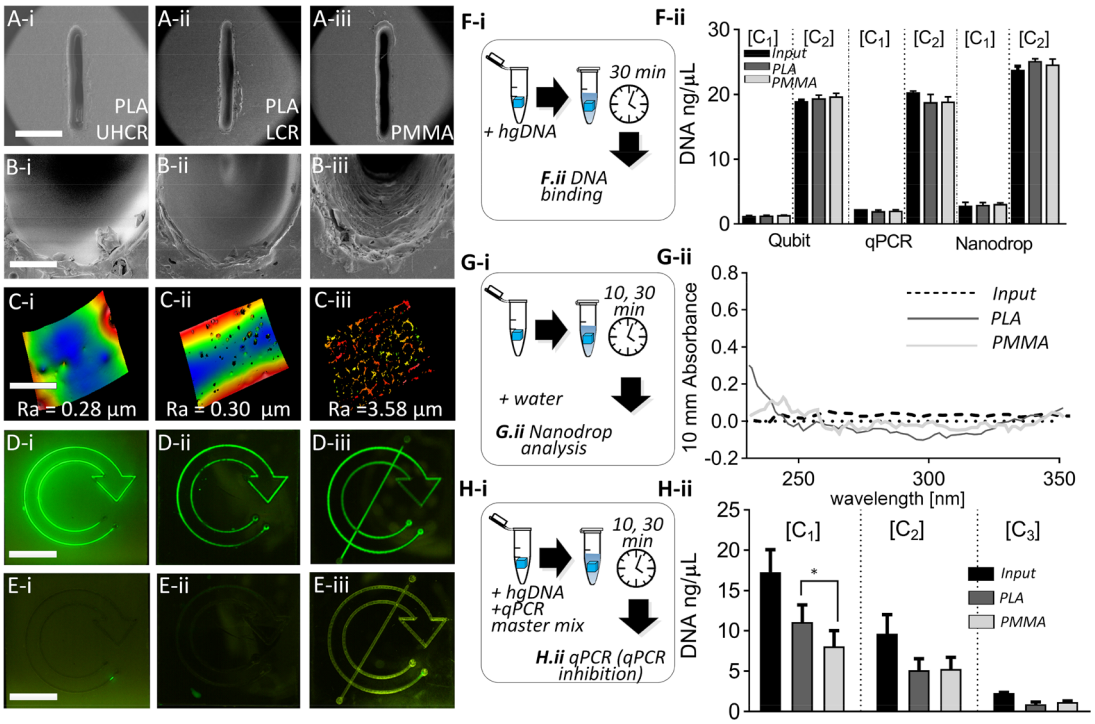


**Figure 3.** (A) SEM picture of top view of a slit cut with power 15 W, speed 42.5 mm/s, and frequency 5000 Hz on (A-i) protected UHCR PLA, (A-ii) protected ULCR PLA, and (A-iii) PMMA. Scale bar is 1 mm. As can be seen no substantial difference is present between the PLA samples and PMMA one. (B) SEM images of top view of channel ends: (B-i) UHCR PLA, (B-ii) ULCR PLA, and (B-iii) PMMA. Scale bars are 100 $\mu$m. Pore formation can be noticed in PMMA cut edge. (C) Surface roughness from interferometer analysis: (C-i) UHCR PLA, (C-ii) ULCR PLA, and (C-iii) PMMA. Scale bar is 0.50 $\mu$m. (D) Photographs acquired with a Dinolite fluorescent microscope on (D-i) ULCR PLA, (D-ii) UHCR PLA, and (D-iii) PMMA after injecting fluorescein inside the channel and (E-i–iii) washing the channel with DI water. (F-i) Protocol for DNA binding. (F-ii) Nonspecific DNA binding Qubit results, qPCR, and nanodrop results. (G-i) Protocol for leaching experiment. (G-ii) Leaching experiments results. (H-i) Protocol for qPCR inhibition. (H-ii) qPCR inhibition results.

−45 °C prior to prototyping limits the usefulness of this technique.

**Investigating the Laser Workability of PLA with a Protective Tape: Sacrificial Layer Assisted Manufacturing (SLAM).** A third solution was investigated and involved the application of adhesive tape as a sacrificial layer (Figure 2E-i), which was placed on the material prior to laser cutting.[36,37] It was hypothesized that the film would provide a thermal shield, spreading the heat out onto the whole surface thereby effectively decreasing the laser beam absorptivity of the system. A 100 $\mu$m thin paper tape was applied across the material and resulted in the complete absence of a recast layer (Figure 2D-ii), regardless of the chosen laser power, speed, and frequency. Pits, of approximately 20 $\mu$m diameter, were observed on the external edges of the slits (Supporting Information, section 3). We were not able to measure how deep were these pits; however they are reminiscent of nanopits reported in another publication.[38] The absence of recast layer was observed on PLA of various crystallinity degrees (Figure 2E-ii,iv,v,vi). Various tapes and thicknesses were tested. The thickness of the tape influences the final shape of the kerf (Supporting Information, section 3). Paper tape used for masking was found to be safer and easier to remove from PLA once cut than plastic tapes. This SLAM method, using a protective paper tape adhesive of 100 $\mu$m thickness, was used in the rest of this study.

**Influence of Laser Cutting Power and Speed on Kerf Width and Taper Angle with SLAM.** Measurements of kerf depth and width for cuts produced in protected, 2 mm PLA sheets (UHCR and ULCR) when using a range of laser speeds (21.25–85 mm/s) and powers (7.5–30 W) reveal that the laser cut features are not influenced by the degree of crystallinity of the PLA sheets (Figure 2E-vii and Supporting Information, section 4). At higher powers, deeper and larger cuts were observed. Similar effects were obtained by operating at lower speeds. The influence of speed on kerf depth is greater than that of power until the cutting velocity falls below 42.5 mm/s. This is probably due to power dispersion in the system.

**A Model to Describe the Effect of the Tape and Predict the Kerf Profile.** In order to predict the kerf profile as a function of ablation parameters (speed and power), a semiempirical model has been developed, derived from a mathematical model previously reported by Prakash and Kumar.[39,40] In their work, the prediction of kerf profile and depth in PMMA material was based on an energy balance that assumed that the energy provided by the laser was absorbed by the material sufficiently to raise the surface temperature and vaporize it. The only thermal process considered in this model was vaporization, while PLA is cut via a combination of vaporization and melt shearing. In the new model for PLA ablation, we modified the energy balance to consider that the heat provided to the material lead to melting and vaporization phenomena. The full developed model for the kerf profile is available in Supporting Information, section 5. The comparison between the kerf shape model prediction and the experimental results for four different laser speeds on UHCR PLA with and without the application of the sacrificial layer is shown in Supporting Information, section 5. The percentage error in the prediction of the maximum kerf depth for the developed model


DOI: 10.1021/acssuschemeng.7b04348
ACS Sustainable Chem. Eng. XXXX, XXX, XXX−XXX

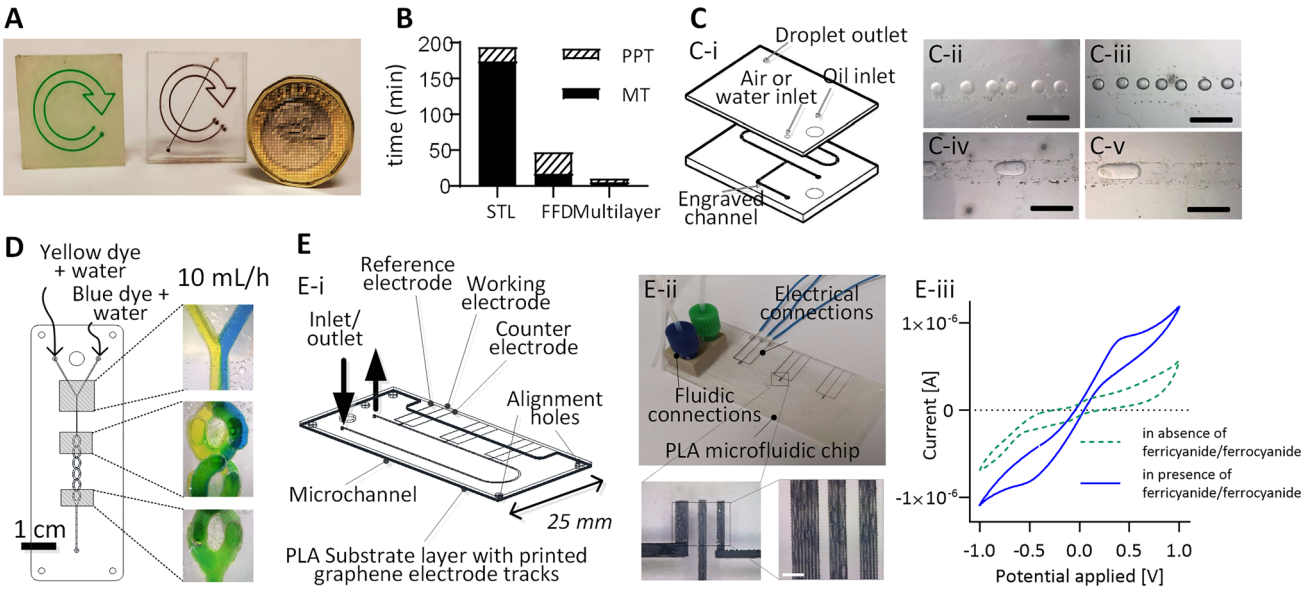


**Figure 4.** (A) Three layer microfluidic "recycle" sign: (left) ULCR PLA; (right) PMMA (B) Manufacturing time comparison between three different rapid prototyping techniques for the production of the microfluidic "recycle" sign. STL (stereolithography), FFD (fusion filament deposition), and multilayer (involving the $CO_2$ laser cutting of PLA sheets in a microstructured layer that are bonded together with a double-sided adhesive tape). (C) Two-layer microfluidic device for the production of water-in-oil and air-in-oil droplets. (C-i) Blow-up view of the chip design. (C-ii) Water in oil droplet, flow rate ratio 0.1; (C-iii) air in oil droplet, flow rate ratio 0.1; (C-iv) water in oil droplet, flow rate ratio 1; (C-v) air in oil droplet, flow rate ratio 1. Scale bar is 1 mm. (D) Five layer micromixer device. (E) Three layer hybrid microfluidic device: (E-i) schematic representation of the device; (E-ii) (top) photograph of the final prototype device, (bottom left) picture of the printed electrodes on PLA, (bottom right) particular of the water injection printed graphene electrodes. Scale bar is 0.2 mm. (E-iii) Electrochemical characterization of the hybrid device with a cyclic voltammetry (CV) at 10 mV/s scan rate. Blue straight line CV in the presence of ferricyanide/ferrocyanide, green dotted line in absence of ferricyanide/ferrocyanide.

is 5%. This model will allow future users to accurately predict cut profiles in PLA materials.

**Suitability of PLA for Biological Protocols.** The difference in surface roughness is a key feature of a laser-cut PLA microchannel versus a PMMA channel. We investigated the influence of the ULCR and HCR manufacturing protocols on the surface roughness and compared this to a PMMA standard sample. $CO_2$ laser cutting of PMMA leads to the formation of porous structures in the working zone due to the vaporization process taking place. In contrast, during the laser cutting of PLA, the melting process prevails over the vaporization one.[41,42] The outcome is that a smoother channel surface is achieved for PLA with respect to PMMA (Figure 3A,B). An interferometry analysis (Figure 3C) has shown that, when using the same protocol, the average $R_a$ of PMMA is on the order of 3 $\mu$m, while that for PLA is 0.3 $\mu$m (Figure 3). This order of magnitude difference in surface roughness between PMMA and PLA will undoubtedly create new opportunities in the use of PLA for the rapid prototyping and production of microfluidic devices, showing comparable features with mass manufacturing techniques. First, reduced wall roughness may enable better flow properties such as a higher critical Reynolds number for transition from laminar to turbulent flow and no local recirculation.[43] Second, the smoother channel surface will considerably decrease molecular adsorption as surface to volume ratios will be minimized. The nonspecific adsorption of molecules is a recurring concern for microfluidic designers and diverse solutions have been deployed in an attempt to overcome this problem.[44] Nonspecific adsorption can lead invariably to a loss of molecular markers or reduced assay performance. For example, the PCR inhibition noted when using some polymeric systems (e.g., silicon, PDMS, and PMMA) has been attributed to polymerase adsorption on the channel walls.[45] In order to compare the nonspecific molecular binding properties of PLA and PMMA laser cut channels, the microchannels in two equivalent microfluidic devices were filled with a solution of fluorescein (5 mg/mL), incubated for 30 min, and imaged (Figure 3D-i,ii,iii). Subsequently, the channels were flushed with 10 mL of deionized (DI) and reimaged (Figures 3E-i,ii,iii). Analysis of the fluorescent images showed that after washing, the PMMA channels had retained on average 18% of the initial fluorescein while the PLA channels had retained only 5%. This finding supports our expectation that the smoother channel surfaces obtained with PLA result in decreased molecular adsorption relative to PMMA and, therefore, demonstrates an additional advantage of sustainable PLA devices over PMMA systems.

Nonspecific DNA binding to bulk PLA material was also investigated and compared to PMMA. Cubes of 8 $mm^3$ of each material (PLA and PMMA) were incubated for 30 min in aqueous solutions containing two different concentrations of Human Genomic DNA (2 ng/$\mu$L and 20 ng/$\mu$L) (Figure 3F-i). The tested samples and the control concentrations of hgDNA were measured by Qubit fluorescence measurement and real-time quantitative PCR (qPCR) with a Nanodrop spectrophotometer as described in the Materials and Experimental Methods section. No significant unspecific binding was detected at either concentration in the presence of PMMA and PLA using both measurement methods (Figure 3F-ii).

Leaching of polymeric components from the bulk material is another issue in microfluidic systems. Although the mobility of low molecular weight oligomers in the whole polymer is known, few studies have looked into this potential problem in detail.[28] It has been suggested that this uncontrolled and


DOI: 10.1021/acssuschemeng.7b04348
ACS Sustainable Chem. Eng. XXXX, XXX, XXX−XXX

undesired leaching could lead to cytotoxicity, interference with cellular signaling pathways, or PCR inhibition.[46] To investigate differences in leaching between the benchmark material PMMA and PLA, molecular grade water was incubated at room temperature in the presence of 8 $mm^3$ cubes of PLA and PMMA for 30 min. The 260 and 280 nm wavelength absorbance of the water from each sample was then analyzed using a microvolume spectrophotometer, Nanodrop instrument, to assess the presence of leached molecules that could negatively interact in the quantification of nucleic acids[19,46] (Figure 3G-i,ii). The absorbance spectrum indicates that both PLA and PMMA are almost inert. (Figure 3G-ii). Finally, it has been suggested that qPCR inhibition by polymers might be induced by polymerase inhibition rather than nonspecific binding.[45,47] Here qPCR inhibition was evaluated by incubating the polymerase in the presence of PMMA or PLA materials. Solutions containing template hgDNA at three different concentrations, PCR master mix, and an 8 $mm^3$ cube of PMMA or PLA were incubated for 30 min at room temperature. PLA and PMMA materials were found to produce comparable inhibition at hgDNA concentrations of 2 ng/$\mu$L and 10 ng/$\mu$L (Figure 3H-i,ii). At higher concentrations of hgDNA (20 ng/ $\mu$L), PCR inhibition was higher ($p < 0.05$) when the polymerase was incubated with PMMA than PLA.

In conclusion, PLA has been found to be comparable or better than the commonly employed, nonsustainable material of PMMA in terms of roughness following laser-cutting, leaching, nonspecific binding and PCR inhibition.

**PLA-Based Multilayer Microfluidic Cartridges.** The ability to precisely laser-cut PLA sheets can be applied to the fabrication of multilayer disposable components, of varying complexities and functionalities, such as microfluidic chips. Examples of such components have been prepared using PLA and PMMA and feature 2 and 3 layers, respectively, as shown in Figure 4A. Each layer was cut from 2 mm sheets and manually assembled (see Materials and Experimental Methods section for details). The PLA device represents the first attempt to fabricate a multilayer device from this material using a laser-cut, laminated technique. The prototyping times for fabrication of the same design using three different techniques have been compared. The techniques investigated were our established multilayer technique and two additive manufacturing solutions, fused deposition modeling and stereolithography. The time to postprocess each part was included as it is a recognized challenge in the production of 3D printed microfluidic devices.[17,48] We found that our technique was at least 2 times faster than other 3D printing techniques (Figure 4B). Due to the transparency of the UHCR PLA sheet (Supporting Information, section 1), imaging of our prototypes, as required for several biomedical applications, is possible. On the contrary, when PLA is 3D printed via FFD, a multimaterial solution (e.g., glass observation window) had to be devised for imaging in microfluidic circuits.[16,48] Droplet production is another common microfluidic functionality. On-site microdroplet production in disposable, single-use devices is highly desirable, for example, for enhanced ultrasound imaging at the point of administration. Droplet production has been successfully integrated into PLA-derived microfluidic systems and tested at a range of flow rate ratios (Figure 4C). Mixing is also needed in most biochip protocols. This was achieved in the PLA device using a five-layer split and recombine mixer at 10 mL/h (Figure 4D).

Finally, to broaden the demonstration of possible functionalities on single-use point of care devices, low environmental impact water-based graphene inks[24] were used to produce electrodes directly on the surface of PLA samples and integrated into a device in the view to enable analytical functionalities such as sensing (Figure 4E-i,ii). These electrodes were integrated into a microfluidic channel. Cyclic voltammetry allows monitoring of redox behavior of chemical species. In particular, ferricyanide/ferrocyanide redox reaction is commonly used in electrochemistry to assess electrode functionality.[49] A solution containing 5 mM potassium ferricyanide and potassium ferrocyanide was introduced inside the channel, and redox currents were measured as described in the Materials and Experimental Methods section. The resulting voltammogram (blue, Figure 4E-iii) showed a clear potassium ferricyanide reduction and potassium ferrocyanide oxidation peak, while a negative control in the absence of potassium ferricyanide/ferrocyanide (green, Figure 4E-iii) showed no peaks, thereby confirming that the graphene electrodes on the PLA substrate function as expected and that no further modifications are necessary.

## OUTLOOK

We have developed a method enabling a complete, sustainable, and low-carbon footprint lifecycle for single-use, disposable medical microcomponents. Starting from a polymer material derived from renewable sources, PLA, sheets of material of various thicknesses and physicochemical properties were produced. The $CO_2$ laser workability was improved by using a sacrificial layer method (SLAM) to completely eradicate the recast layer normally present on the cut material. The laser-cut sheets were then assembled into multilayered components using double-sided adhesive tape. Using this rapid prototyping technique, complex devices were rapidly produced and tested. We have demonstrated the use of these multilayer components to form complex 5 layer microfluidic mixers and devices for microdroplet production. When the development of the device is completed, providing a good design for manufacture approach has been followed, a device could be mass-manufactured in the same material, PLA, with very limited design changes, using microinjection molding or other suitable techniques. PLA-based single-use medical microscale components have a low carbon footprint and additive-free PLA can be incinerated safely in rudimentary setting. We envisage that other techniques with sustainability credentials, such as paper microfluidics could be used in a noncompetitive way with polymeric material as each will have their own niche applications. The two materials might also be used together to benefit from a wider range of functionalities. Ultimately, the sustainability and, in particular, the ability to incinerate any material in a safe way will depend on the addition of additives to the raw material. In that regard, the control of biopolymer production and quality controls by regulators will be important in producing PLA material for truly sustainable and safe material for medical applications.

## ASSOCIATED CONTENT

### Supporting Information

The Supporting Information is available free of charge on the ACS Publications website at DOI: 10.1021/acssuschemeng.7b04348.



DOI: 10.1021/acssuschemeng.7b04348
ACS Sustainable Chem. Eng. XXXX, XXX, XXX−XXX

DSC and XRD analysis of the prepared PLA sheets, laser workability of PLA at different temperatures, investigation of the laser workability with protective tape of different thickness, influence of the crystallinity degree on the kerf depth and width on ablated protected PLA, mathematical model to predict kerf profile, and FTIR spectra of PLA and of the paper tape (PDF)

## AUTHOR INFORMATION


### Corresponding Author

*E-mail: m.kersaudy-kerhoas@hw.ac.uk.

### ORCID

Alfredo E. Ongaro: 0000-0003-3084-6798

Khaled Parvez: 0000-0003-2851-9907


### Author Contributions

A.O. performed all experiments except the electrode printing, electrochemical measurements, and biological measurements and contributed to the analysis of the results. I.K. performed all biological experiments and contributed to the analysis of the results. A.L. contributed to the analysis of the results. G.C. contributed to the material characterizations. S.C. contributed to the literature on lifecycle analysis of PLA. H.S. performed the electrochemical measurement. T.B. contributed to the reagents and materials and the analysis of the electrochemical measurement results. K.P. printed the electrodes. C.C. contributed to the reagents and materials and the conception and analysis of the electrode printing results. N.H., V.L.C., and M.K.K. conceived and designed the study and contributed to the analysis of the results. The manuscript was written by A.O., N.H., and M.K.K. in close consultation with all authors. All authors have given approval to the final version of the manuscript.

### Notes

The authors declare no competing financial interest.

## ACKNOWLEDGMENTS

A.O and A.L are funded by a James Watt scholarship. I.K. is funded by a Medical Research Scotland studentship. M.K.K. receives funding from the Royal Academy of Engineering, the Royal Society, and the Engineering and Physical Sciences Research Council, EP/R00398X/1. C.C. and K.P. acknowledge the Grand Challenge EPSRC grant EP/N010345/1. We thank Mark Leonard for assistance with the SEM imaging and Valeria Arrighi and Filipe Vilela for access to equipment.

## REFERENCES


(1) Point-of-Care Diagnostics Market by Products (Glucose, Cardiometabolic Monitoring, & Infectious Disease Testing Kits, Cardiac & Tumor Markers), End Users (Home, Hospitals, Ambulatory Care), Over-the- Counter & Prescription Based - Global Forecast to 2021. https://www.marketsandmarkets.com/Market-Reports/point-of-care-diagnostic-market-106829185.html. Report Code: MD 2702 (accessed July, 2016).

(2) Singh, P.; Sharma, V. P. Integrated Plastic Waste Management: Environmental and Improved Health Approaches. *Procedia Environ. Sci.* **2016**, *35*, 692−700.

(3) Unger, S. R.; Hottle, T. A.; Hobbs, S. R.; Thiel, C. L.; Campion, N.; Bilec, M. M.; Landis, A. E. Do single-use medical devices containing biopolymers reduce the environmental impacts of surgical procedures compared with their plastic equivalents ? *J. Health Serv. Res. Policy* **2017**, *22*, 218.

(4) Sullivan, J. B., Krieger, G. R. *Clinical Environmental Health and Toxic Exposures*, 2nd ed.; Lippincott Williams & Wilkins: Philadelphia, 2001.

(5) Awodele, O.; Adewoye, A. A.; Oparah, A. C. Assessment of medical waste management in seven hospitals in Lagos, Nigeria. *BMC Public Health* **2016**, *16*, 1−11.

(6) Yang, C.; Peijun, L.; Lupi, C.; Yangzhao, S.; Diandou, X.; Qian, F.; Shasha, F. Sustainable management measures for healthcare waste in China. *Waste Manage.* **2009**, *29*, 1996−2004.

(7) Da Silva, C. E.; Hoppe, A. E.; Ravanello, M. M.; Mello, N. Medical wastes management in the south of Brazil. *Waste Manage.* **2005**, *25*, 600−605.

(8) Castro-aguirre, E.; Iñiguez-franco, F.; Samsudin, H.; Fang, X.; Auras, R. Poly (lactic acid) — Mass production, processing, industrial applications, and end of life ☆. *Adv. Drug Delivery Rev.* **2016**, *107*, 333.

(9) Vink, E. T. H.; Rábago, K. R.; Glassner, D. A.; Gruber, P. R. Applications of life cycle assessment to NatureWorks polylactide (PLA) production. *Polym. Degrad. Stab.* **2003**, *80*, 403−419.

(10) Vink, E. T. H.; Glassner, D. a.; Kolstad, J. J.; Wooley, R. J.; O'Connor, R. P. ORIGINAL RESEARCH: The eco-profiles for current and near-future NatureWorks® polylactide (PLA) production. *Ind. Biotechnol.* **2007**, *3*, 58−81.

(11) North, E. J.; Halden, R. U. Plastics and environmental health: The road ahead. *Rev. Environ. Health* **2013**, *28*, 1−8.

(12) Chien, Y.-C.; Liang, C.; Liu, S.-H.; Yang, S.-H. Combustion kinetics and emission characteristics of polycyclic aromatic hydrocarbons from polylactic acid combustion. *J. Air Waste Manage. Assoc.* **2010**, *60*, 849−855.

(13) Rayna, T.; Striukova, L. From rapid prototyping to home fabrication: How 3D printing is changing business model innovation. *Technol. Forecast. Soc. Chang.* **2016**, *102*, 214−224.

(14) Jiang, R.; Kleer, R.; Piller, F. T. Predicting the future of additive manufacturing: A Delphi study on economic and societal implications of 3D printing for 2030. *Technol. Forecast. Soc. Chang.* **2017**, *117*, 84−97.

(15) Malinauskas, M.; Rekštytė, S.; Lukoševičius, L.; et al. 3D Microporous Scaffold Manufactured via Combination of Fused Filament Fabrication and Direct Laser Writing Ablation. *Micromachines* **2014**, *5*, 839−858.

(16) Morgan, A. J. L.; Hidalgo San Jose, L.; Jamieson, W. D.; et al. Simple and versatile 3D printed microfluidics using fused filament fabrication. *PLoS One* **2016**, *11*, e0152023.

(17) Waheed, S.; Cabot, J. M.; Macdonald, N. P.; et al. 3D printed microfluidic devices: enablers and barriers. *Lab Chip* **2016**, *16*, 1993−2013.

(18) Macdonald, N. P.; Cabot, J. M.; Smejkal, P.; Guijt, R. M.; Paull, B.; Breadmore, M. C.; et al. Comparing Micro fluidic Performance of Three-Dimensional (3D) Printing Platforms. *Anal. Chem.* **2017**, *89*, 3858−3866.

(19) Walsh, D. I.; Kong, D. S.; Murthy, S. K.; Carr, P. A. Enabling Microfluidics: from Clean Rooms to Makerspaces. *Trends Biotechnol.* **2017**, *35*, 383−392.

(20) Fu, L.; Ju, W.; Yang, R.; Wang, Y. Rapid prototyping of glass-based microfluidic chip utilizing two-pass defocused CO2 laser beam method. *Microfluid. Nanofluid.* **2013**, *14*, 479−487.

(21) Liga, A.; Morton, J. A. S.; Kersaudy-Kerhoas, M. Safe and cost-effective rapid-prototyping of multilayer PMMA microfluidic devices. *Microfluid. Nanofluid.* **2016**, *20*, 164.

(22) Arnette, A. N.; Brewer, B. L.; Choal, T. Design for sustainability (DFS): the intersection of supply chain and environment. *J. Cleaner Prod.* **2014**, *83*, 374−390.

(23) Naga, N.; Yoshida, Y.; Noguchi, K.; Murase, S. Crystallization of Amorphous Poly(Lactic Acid) Induced by Vapor of Acetone to Form High Crystallinity and Transparency Specimen. *Open J. Polym. Chem.* **2013**, *3*, 29−33.

(24) Mcmanus, D.; Vranic, S.; Withers, F.; et al. Water-based and biocompatible 2D crystal inks for all-inkjet-printed heterostructures. *Nat. Nanotechnol.* **2017**, *12*, 343−350.




DOI: 10.1021/acssuschemeng.7b04348
ACS Sustainable Chem. Eng. XXXX, XXX, XXX−XXX

(25) Zhou, B. H.; Mahdavian, S. M. Experimental and theoretical analyses of cutting nonmetallic materials by low power CO2-laser. *J. Mater. Process. Technol.* **2004**, *146*, 188−192.
(26) Davim, J. P.; Barricas, N.; Conceição, M.; Oliveira, C. Some experimental studies on CO2 laser cutting quality of polymeric materials. *J. Mater. Process. Technol.* **2008**, *198*, 99−104.
(27) Isiksacan, Z.; Guler, M. T.; Aydogdu, B.; Bilican, I.; Elbuken, C. Rapid fabrication of microfluidic PDMS devices from reusable PDMS molds using laser ablation. *J. Micromech. Microeng.* **2016**, *26*, 035008.
(28) Vasiga, D. A Review of Carbon Dioxide Laser on Polymers. *Internationl Journal of Engineering and Technology* **2015**, *4*, 874−877.
(29) Sun, S.; Brandt, M. Laser Beam Machining. *Nontraditional machining processes* **2013**, 35.
(30) Caiazzo, F.; Curcio, F.; Daurelio, G.; Minutolo, F. M. C. Laser cutting of different polymeric plastics (PE, PP and PC) by a CO 2 laser beam. *J. Mater. Process. Technol.* **2005**, *159*, 279−285.
(31) Klank, H.; Kutter, J. P.; Geschke, O. CO(2)-laser micromachining and back-end processing for rapid production of PMMA-based microfluidic systems. *Lab Chip* **2002**, *2*, 242−246.
(32) Hong, T.-F.; Ju, W.-J.; Wu, M.-C.; Tai, C.-H.; Tsai, C.-H.; Fu, L.-M. Rapid prototyping of PMMA microfluidic chips utilizing a CO2 laser. *Microfluid. Nanofluid.* **2010**, *9*, 1125−1133.
(33) Antończak, A. J.; Stępak, B.; Szustakiewicz, K.; et al. Effect of CO 2 laser micromachining on physicochemical properties of poly (L -lactide). *Proc. SPIE* **2014**, *9286*, 92860Z.
(34) Malinauskas, M.; Lukosevicius, L.; Butkus, S.; Paipulas, D. Femtosecond Pulse Light Filament-Assisted Microfabrication of Biodegradable Polylactic Acid (PLA) Material. *J. Laser Micro/Nanoeng.* **2015**, *10*, 222−228.
(35) Brucato, V.; Kiflie, Z.; La Carrubba, V.; Piccarolo, S. Continuous Cooling Transformation (CCT) as a Flexible Tool to Investigate Polymer Crystallization under Processing Conditions. *Adv. Polym. Technol.* **2009**, *28*, 86−119.
(36) Stępak, B.; Antończak, A. J.; Bartkowiak-Jowsa, M.; Filipiak, J.; Pezowicz, C.; Abramski, K. M. Fabrication of a polymer-based biodegradable stent using a CO2 laser. *Arch Civ Mech Eng.* **2014**, *14*, 317−326.
(37) Gu, L.; Yu, G.; Li, C. A fast and low-cost microfabrication approach for six types of thermoplastic substrates with reduced feature size and minimized bulges using sacrificial layer assisted laser engraving. *Anal. Chim. Acta* **2018**, *997*, 24−34.
(38) Viertel, T.; Pabst, L.; Olbrich, M.; et al. Generation of nanovoids inside polylactide using femtosecond laser radiation. *Appl. Phys. A: Mater. Sci. Process.* **2017**, *123*, 789.
(39) Prakash, S.; Kumar, S. Profile and depth prediction in single-pass and two-pass CO 2 laser microchanneling processes. *J. Micromech. Microeng.* **2015**, *25*, 035010.
(40) Prakash, S.; Kumar, S. Experimental and theoretical analysis of defocused CO $_2$ laser microchanneling on PMMA for enhanced surface finish. *J. Micromech. Microeng.* **2017**, *27*, 025003.
(41) Grabow, N.; Schlun, M.; Sternberg, K.; Hakansson, N.; Kramer, S.; Schmitz, K.-P. Mechanical properties of laser cut poly(L-lactide) micro-specimens: implications for stent design, manufacture, and sterilization. *J. Biomech. Eng.* **2005**, *127*, 25−31.
(42) Grabow, N.; Bunger, C.; Schultze, C.; et al. A biodegradable slotted tube stent based on poly(l-lactide) and poly(4-hydroxybutyrate) for rapid balloon-expansion. *Ann. Biomed. Eng.* **2007**, *35*, 2031−2038.
(43) Chen, Y.; Zhang, C.; Shi, M.; Peterson, G. P. Role of surface roughness characterized by fractal geometry on laminar flow in microchannels. *Phys. Rev. E Stat Nonlin Soft Matter Phys.* **2009**, *80*, 026301.
(44) Regehr, K. J.; Domenech, M.; Koepsel, J.; et al. Biological implications of polydimethylsiloxane-based microfluidic cell culture. *Lab Chip* **2009**, *9*, 2132−2139.
(45) Kodzius, R.; et al. Inhibitory effect of common microfluidic materials on PCR outcome. *Sens. Actuators, B* **2012**, *161*, 349−358.
(46) Kolari, K.; Satokari, R.; Kataja, K.; Stenman, J.; Hokkanen, A. *Sens. Actuators, B* **2008**, *128*, 442−449.
(47) Bhattacharjee, N.; Urrios, A.; Kang, S.; Folch. The Upcoming 3D-printing revolution in microfluidics. *Lab Chip* **2016**, *16*, 1720−1742.
(48) Gaal, G.; Mendes, M.; de Almeida, T. P.; et al. Simplified fabrication of integrated microfluidic devices using fusion deposition modeling 3d pinting. *Sens. Actuators, B* **2017**, *242*, 35−40.
(49) Obaje, E. A.; Cummins, G.; Schulze, H.; Mahmood, S.; Desmulliez, M. P. Y.; Bachmann, T. T. Carbon screen-printed electrodes on ceramic substrates for label-free molecular detection of antibiotic resistance. *Journal of interdisciplinary Neuromedicine* **2016**, *1*, 93−109.


DOI: 10.1021/acssuschemeng.7b04348
*ACS Sustainable Chem. Eng.* XXXX, XXX, XXX−XXX

# Laser ablation of polylactic acid sheets for the rapid prototyping of sustainable, single-use, disposable medical micro-components

## Supplementary Information

Alfredo E. Ongaro[1,2,3], Ieva Keraite [1,2], Antonio Liga[1,2], Gioachino Conoscenti[3], Stuart Coles[4], Holger Schulze[2], Till T. Bachmann[2],

Khaled Parvez[5], Cinzia Casiraghi[5], Nicola Howarth[1], Vincenzo La Carubba[3,6] & Maïwenn Kersaudy-Kerhoas[1,2]*

[1] *Institute of Biological Chemistry, Biophysics and Bioengineering, School of Engineering and Physical Science, Heriot-Watt University, Edinburgh EH14 4AS, United Kingdom*
[2] *Division of Infection and Pathway Medicine, Edinburgh Medical School, College of Medicine and Veterinary Medicine, The University of Edinburgh, Edinburgh EH164SB, United Kingdom*
[3] *Department of Civil, Environmental, Aerospace and Materials Engineering (DICAM), University of Palermo, Viale delle Scienze building 6, 90128 Palermo, Italy*
[4] *Sustainable Materials and Manufacturing Group, WMG, University of Warwick, Coventry, CV4 7AL, United Kingdom*
[5] *School of Chemistry, University of Manchester, Manchester M13 9PL, United Kingdom*
[6] *ATeN Center – CHAB, Università di Palermo, Viale delle Scienze building 18, 90128 Palermo, Italy*

*Corresponding author: m.kersaudy-kerhoas@hw.ac.uk

Totals- 11 pages, 9 figures, 2 tables

**1. Material characterization**

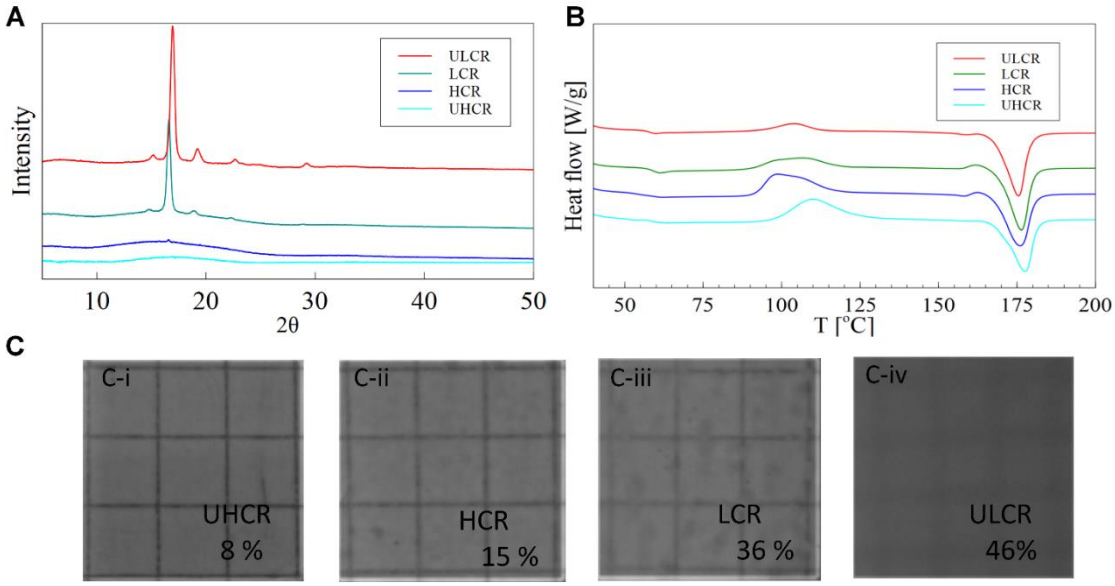


**Figure S1.** Characterisation of PLA sheet samples. (A) XRD data A. As expected lower cooling rates lead to more crystalline PLA structures as evidenced by the presence of peaks. The four protocols lead to four unique material with a decreasing range of crystallinity (B) The DSC data correlates the XRD data. (C) Photographs of PLA samples. The more crystalline PLA (LCR, ULCR) sheets are more opaque while the amorphous sheets (UHCR, HCR) as expected are more translucent. (C-i) Ultra high cooling rate sheet with a crystallinity degree of 8.011%; (C-ii) High cooling rate sheet ith a crystallinity degree of 15.21%; (C-iii) Low cooling rate sheet with a crystallinity degree of 36.01%; (C-iv) Ultra low cooling rate sheet with a crystallinity degree of 45.97%.

**Table S1** Comparison between PMMA and PLA weigth and price per sheet

| **Material** | **Weight of pellets per sheet (11x11x0.2 cm) or Weight of final sheet** | **Cost per sheet (11x11x0.2 cm)** |
|---|---|---|
| PLA | 33 gr | 0.42-0.61[2]USD |
| PMMA | 30 gr | 0.36 USD |

[2] 0.42 $ Price from Alibaba.com (1 TON minimum order); 0.61 price from Natureworks®

**2. Investigating the laser workability of PLA at different Temperature**

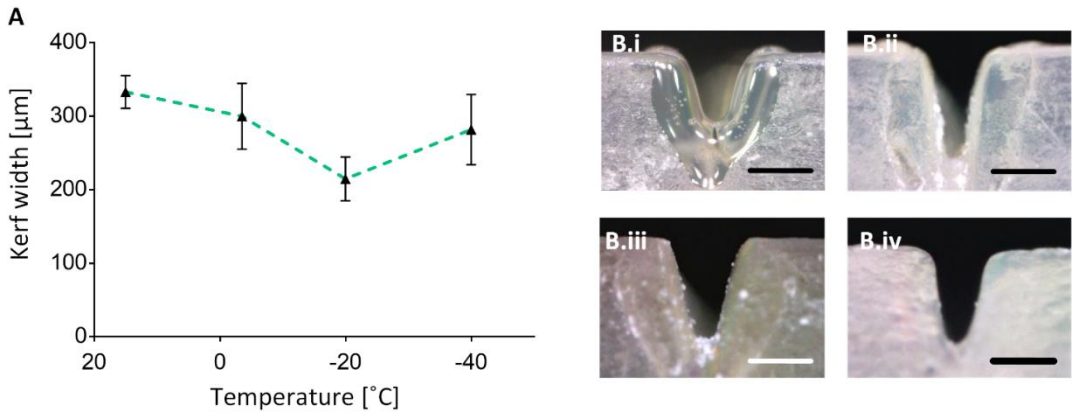


**Figure S2.** (A) Recast layer width [µm] in function of the different starting temperature; B.i) kerf cross section picture of UHCR cut at room temperature; B.ii) kerf cross section picture of UHCR cut at -3.5 ˚C; B.iii) kerf cross section picture of UHCR cut at -20 ˚C; B.iv) kerf cross section picture of UHCR cut at -45 ˚C. scale bar is 0.3 mm. Cut parameters: Power 15 W, Speed 42.5 mm/s and Frequency 5000 Hz.

**3. Investigating the laser workability with a protective tape**

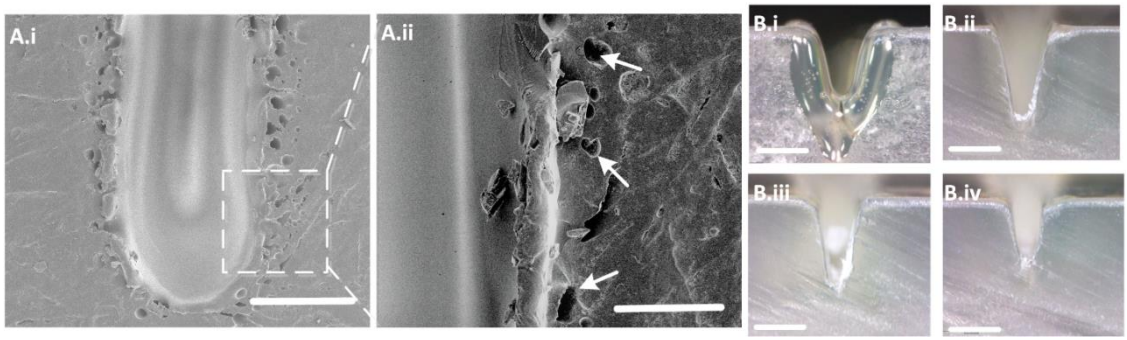


**Figure S3.** A.i) SEM picture of top view of a slit cut with a protective tape (Power 22.5 W, Speed 21.25 mm/s and Frequency 5000 Hz), scale bar is 0.2 mm; A.ii) Detail of the micropits found on the edges of the laser cut PLA scale bar is 0.1 mm B.i) kerf cross section picture of the ablated UHCR without the tape B.ii) kerf cross section picture of the ablated UHCR cut with paper tape as protective layer. Tape thickness 100 µm, kerf width 0.44 mm, kerf depth 0.52mm; B.iii) kerf cross section picture of the ablated UHCR with acrylic tape as protective layer. Tape thickness 165 µm, kerf width 0.36 mm, kerf depth 0.47mm; B.iv) kerf cross section picture of the ablated UHCR with paper tape as protective layer. Tape thickness 200 µm, kerf width 0.29 mm, kerf depth 0.31 mm. Scale bar is 0.3mm.

**4. Influence of crystallinity on the kerf depth and width of the recast layer on ablated protected PLA**

The amorphous and semi-crystalline sheets do not present statistical differences in the laser cut behaviour, using a tape covering. To a higher power a deeper and a larger cut are noticed as it is for a lower speed. A deeper kerf depth can be obtained when decreasing the speed, due to a longer laser interaction with the material, and consequently to a higher laser energy per surface unit. As can be observed in the kerf depth behaviour in function of the laser power and velocity, the influence of the speed on the kerf depth is higher

than the power influence until the cutting velocity is below 42.5 mm/s, probably due to some power dispersion in the system.

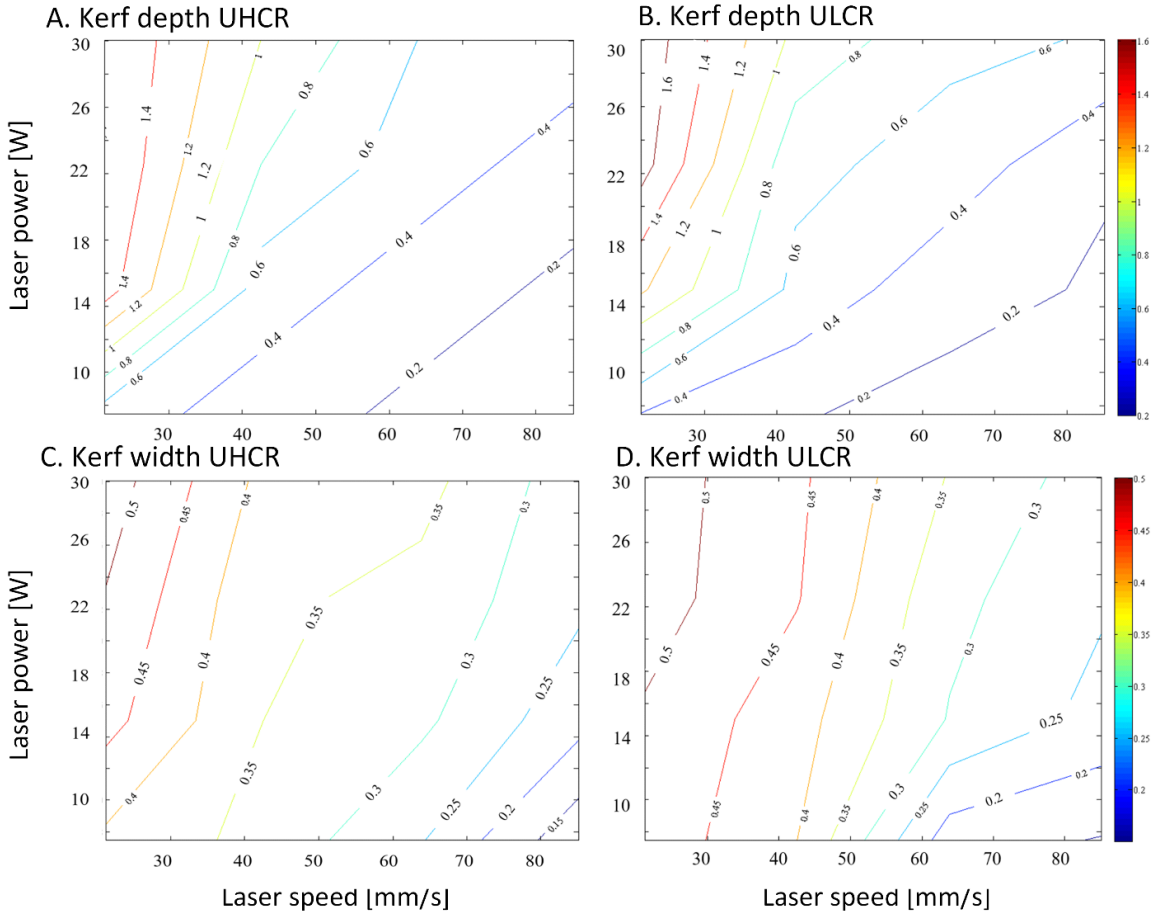


**Figure S4**. Kerf depth and width (mm) in function of the laser power and speed. (A) UHCR kerf depth; (B) ULCR kerf depth; (C) UHCR kerf width; (D) ULCR kerf width

## 5. A mathematical model to predict kerf profile

We developed a mathematical model able to predict the kerf profile in function of the physico-chemical material parameters and the machining parameters of the $CO_2$ laser in use (e.g. laser speed, power, laser wavelength, laser profile). Many studies have been conduct to predict the final features of a $CO_2$ laser cut in polymeric materials[1,2,3,4]. Empirical, semi-empirical and mathematical model and/or making use of finited element analysis simulation and artificial neural networks have been developed to predict the width of the heat affected zone (HAZ), kerf width, depth and taper angle[5,6] . While an empirical model can be useful to study the experimental evidence; a mathematical model will led to a systematic understanding of the phenomenon taking place, and the physico-chemical material characteristics to consider for producing microfeatures in a new material. Kumar et al [7,8] recently developed a mathematical model to predict the kerf profile after a single and/or multistep laser cut, and to predict the kerf width under defocusing beam condition on Polymethyl methacrylate (PMMA). Despite ignoring the local intensity distribution of laser, the local absorptivity and conduction loss, their model demonstrated and average error prediction in the kerf depth of only 6%.

Their model was based on an energy balance, and considers that the energy provided by the laser was absorbed by the material, and sufficient to raise the surface temperature and to vaporize it. The only thermal process taking place in their model was vaporization. While this is true for PMMA, where polymeric chains are broken via depropagation and because of the high volatility of its monomers MMA [2]; it is not the same for PLA, as for other common thermoplastics e.g. HDPE, LDPE, PC[4] .As previously study reports, PLA is cut via a combination of vaporization and melt shearing [4,5]. For this reason, and considering the presence of a substantial recast layer (Figure 2 A.iii, from the main text), the energy balance should consider that the absorbed energy is transformed in an increment of energy to melt and vaporize the material.

Eq. (1) $$\Delta E_{abs} = \Delta E_{melt} + \Delta E_{vap} + \Delta E_{crystallization}$$

Let's suppose that the laser beam focused on the top surface of the material moves in the x direction with a speed of $U_1$. The optical laser beam intensity can be written as follow:

Eq. (2) $$I_1 = I_{01} e^{\frac{-2(x^2+y^2)}{\omega^2}}$$

Where $I_{01}$ is the intensity of the laser at the beam centre corresponding to

Eq. (3) $$I_{01} = \frac{2P_1}{\pi\omega^2}$$

With $P_1$ as the average laser power and ω the laser beam spot radius.

Considering a finite element of the material with dimension $\Delta x \Delta y = A_1$, irradiated by the laser beam for a finite time $\Delta t = \Delta x / U_1$, the energy absorbed by the material will be:

Eq. (4) $$\Delta E_{abs} = \alpha I_{01} e^{\frac{-2(x^2+y^2)}{\omega^2}} \Delta A_1 \frac{\Delta x}{U_1}$$

Eq. (5) $$\Delta E_{abs} = \Delta E_{melt} + \Delta E_{vap}$$

Eq. (6) $$\Delta E_{melt} = \Delta m_1 [c_p(T_m - T_a) + H_m]$$

Eq. (7) $$\Delta E_{vap} = \Delta m_2 [c_p(T_v - T_a) + H_l]$$

Eq. (8) $$\Delta E_{cr} = \Delta m_3 [c_p(T_c - T_a) + H_c]$$

Where $\Delta m = \rho \Delta A_1 \Delta z$. We can assume that the difference in the change in mass and in depth, for the removed material during the different process taking place is neglectable. In this way $\Delta m_1 = \Delta m_2 = \Delta m_3$.

Solving equation (1) with respect to (4) and (5) one obtains:

Eq. (9) $$\alpha I_{01} e^{\frac{-2(x^2+y^2)}{\omega^2}} \Delta A_1 \frac{\Delta x}{U_1} = \rho \Delta A_1 \Delta z \{[c_p(T_c - T_a) + H_c][c_p(T_m - T_a) + H_m] + [c_p(T_v - T_{a'}) + H_l]\}$$

That solved with respect to Δz became:

Eq. (10) $$\Delta z = \frac{\alpha I_{01} e^{\frac{-2(x^2+y^2)}{\omega^2}}}{U1\rho} \Delta x$$

That for limiting case is:

Eq. (11) $$dz = \frac{\alpha I_{01} e^{\frac{-2(x^2+y^2)}{\omega^2}}}{U1\rho\{[c_p(T_c - T_a) + H_c] + [c_p(T_m - T_a) + H_m] + [c_p(T_v - T_{a'}) + H_l]\}} dx$$

Integrating (8)

Eq. (12) $\int_0^{z1} dz = \frac{1}{U1\rho\{[c_p(T_c-T_a)+H_c]+\Delta m_1[c_p(T_m-T_a)+H_m]+\Delta m_1[c_p(T_v-T_{a'})+H_l]\}} \int_{-\infty}^{+\infty} \alpha I_{01} e^{\frac{-2(x^2+y^2)}{\omega^2}} dx$

And considering $Z = Z_{max} e^{\frac{-2y^2}{w^2}}$, where $Z_{max}$ is the maximum depth of the cut at the centre of the beam (9) became:

Eq. (13) $Zmax = \frac{\alpha}{\rho\{[(T_c-T_a)+H_c]+\Delta m_1[c_p(T_m-T_a)+H_m]+\Delta m_1[c_p(T_v-T_{a'})+H_l\}} \sqrt{\frac{2}{\pi\omega^2}} . \frac{P}{U}$

To compare the model with the experimental results, an input power of 30 W and a frequency of 5 kHz were chosen, while the speed was varied from 0 to 100% in 10% increments (8.5, 17, 25.5, 34, 42.5, 51, 59.5, 68, 76.5 and 85 mm/s). The kerf depth was measured in triplicate for each point and plotted in function of the inverse of the speed, to have a linear correlation since it stands in inverse proportion to the laser speed.

The model and experimental data were plotted. They both show a linear trend with the same slope (Figure S5). The model is shifted by a constant C=X with regards to the experimental data.

Surprisingly, as can be seen in figure S5, the proposed model underestimates the kerf depth. It was reasonable to expect an overestimation of the kerf depth because the model does not take into account energy loss in the experimental system.

A possible explanation to this relies on the choice of the laser beam absorptivity value, $\alpha$. $\alpha$ has been experimentally determined as per section 6, taking the absorptivity value for a wavelength of 10.6 μm, corresponding to a wavenumber of 940 $cm^{-1}$. However, Commercial $CO_2$ lasers, as the one used, can lasing wavelength that fluctuate at around 10.6 μm, so the absorptivity value could change terribly.

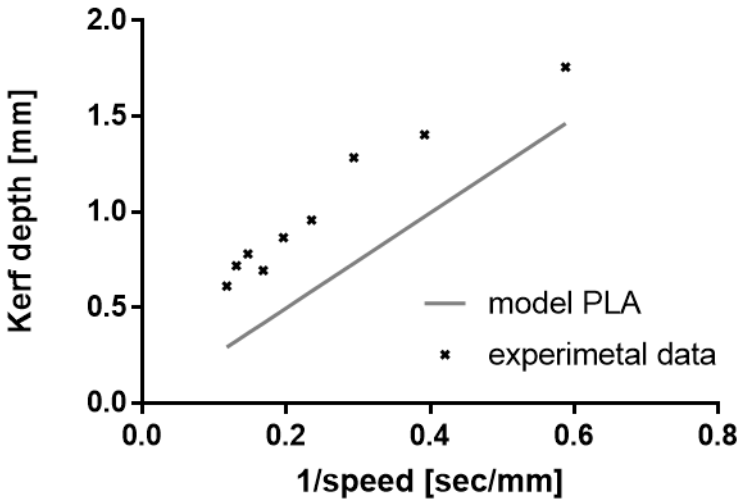


**Figure S5**: experimental and model-predicted kerf depth plot in function of the inverse of the speed

However, to obtain a complete overlap of the model with the fitting curve, the coefficient to be add to the maximum kerf depth prediction is $C=Z_0$, were $Z_0$ is the maximum kerf depth for a laser power of 30W and a laser speed of 85 mm/s (the maximum speed) (Figure S6)

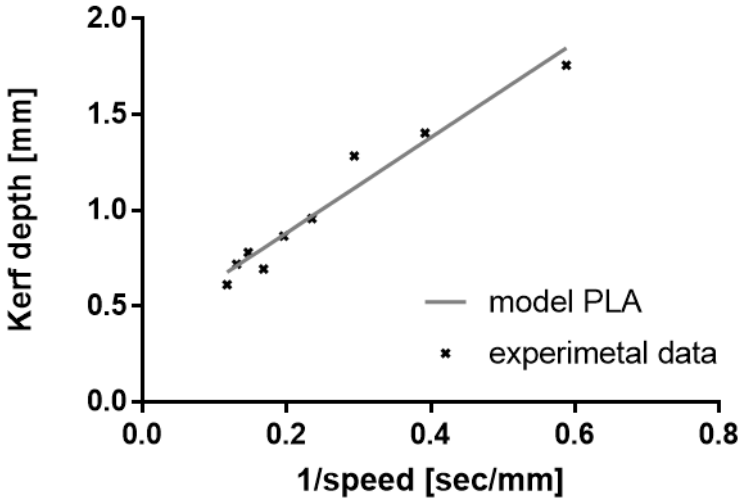


**Figure S6**: experimental and calibrated model-predicted kerf depth plot in function of the inverse of the speed

The same rationale was applied to developed a similar model for the system with the tape. The absorptivity of the tape and PLA materials (section 5), were included and weighed in function of their thickness. The same coefficient C was added to this model which produced a very good fit for both the model.

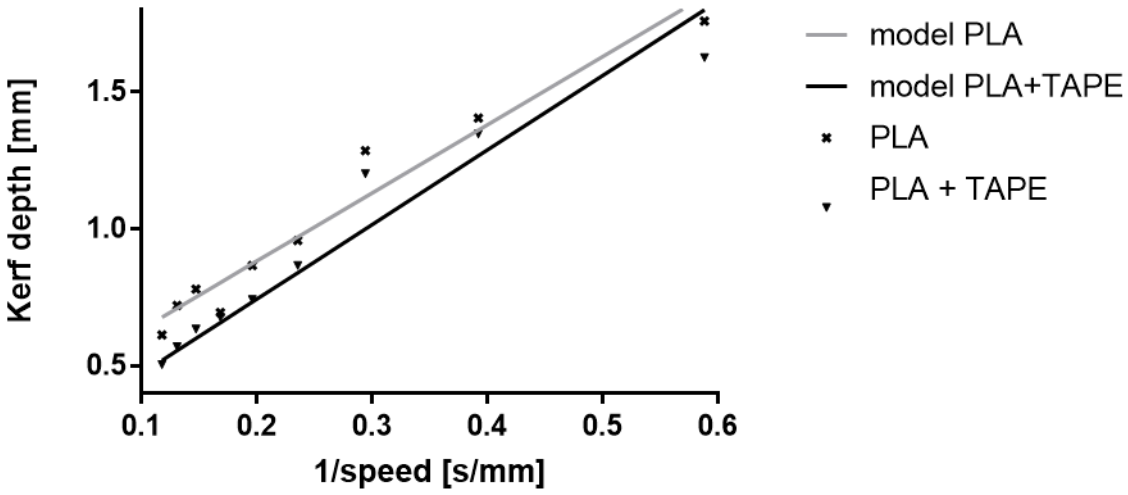


**Figure S7**: experimental and calibrated model-predicted kerf depth plot in function of the inverse of the speed, for the cut with and without the sacrificial layer.

While the kerf profile can be derived from the so determined $Z_{max}$, as follow:

Eq. (14) $$Z = Z_{max} e^{\frac{-2y^2}{w^2}}$$

| | |
|---|---|
| Kerf depth | $Zmax = \frac{\alpha}{\rho[\{(T_c - T_a) + H_c] + \Delta m_1[c_p(T_m - T_a) + H_m] + \Delta m_1[c_p(T_v - T_{a'}) + H_l\}} \sqrt{\frac{2}{pigrecow\text{^}2}} . \frac{P}{U}$ |
| Kerf profile | $Z = Z_{max} e^{\frac{-2y^2}{w^2}}$ |

**Table S2** kerf depth and kerf profile equation

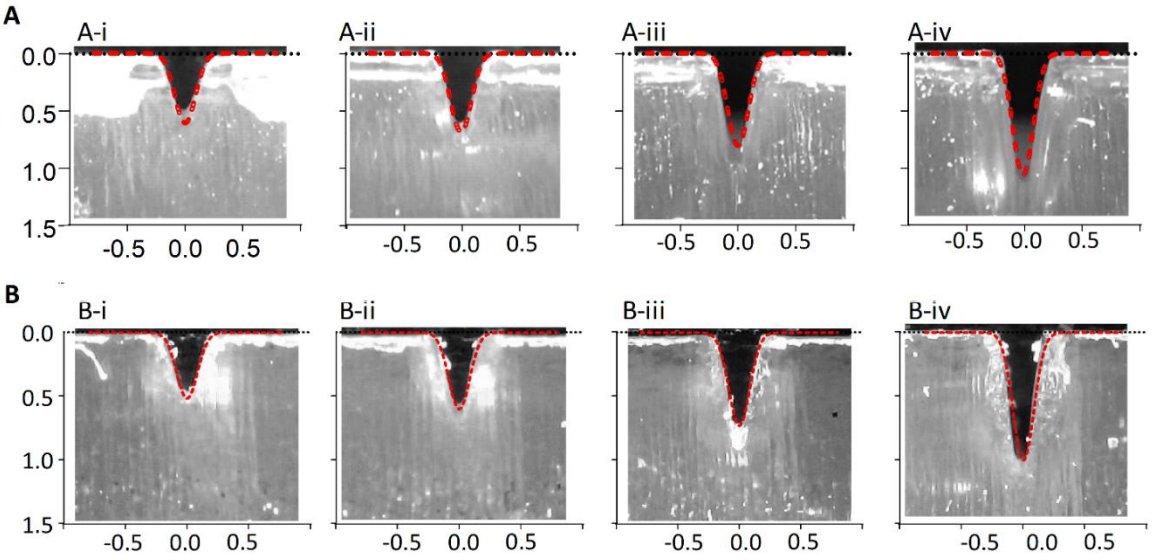


**Figure S8** Actual and predicted kerf profile for a cut without (A) and with sacrificial layer (B) for a fixed laser power of 30 W. (A.i) s= 85 mm/s ;(A.ii) s= 68 mm/s;(A.iii) s= 51mm/s;(A.iv) s= 34 mm/s ;(B.i) s= 85 mm/s; (B.ii) s= 68 mm/s; (B.iii) s= 51 mm/s; (B.iv) s= 34 mm/s.

### 6. laser beam absorptivity determination

The laser beam absorptivity of both PLA and the tape was determined using a FTIR spectrophotometer (Thermo scientific, NICOLET iS5 FT-IR spectrophotometer) measuring the absorptivity at the specific $CO_2$ laser wavelength 10.6 μm, corresponding to a wavenumber of 940 $cm^{-1}$.

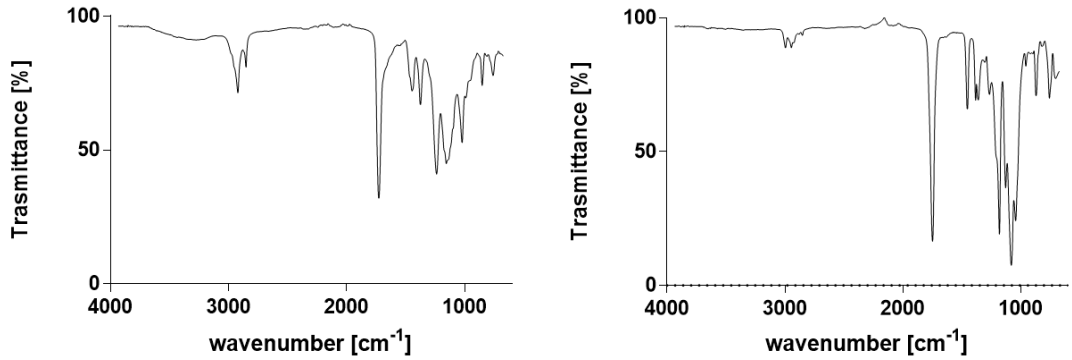


**Figure S9**: FTIR spectra of the tape (on the left) and of UHCR PLA (on the right)

**References**


1. Zhou, B. H. & Mahdavian, S. M. Experimental and theoretical analyses of cutting nonmetallic materials by low power CO2-laser. *J. Mater. Process. Technol.* **146,** 188–192 (2004).

2. Snakenborg, D., Klank, H. & Kutter, J. P. Microstructure fabrication with a CO2 laser system. *J. Micromechanics Microengineering* **14,** 182–189 (2004).

3. Choudhury, I. a. & Shirley, S. Laser cutting of polymeric materials: An experimental investigation. *Opt. Laser Technol.* **42,** 503–508 (2010).

4. Davim, J. P., Barricas, N., Conceição, M. & Oliveira, C. Some experimental studies on CO2 laser cutting quality of polymeric materials. *J. Mater. Process. Technol.* **198,** 99–104 (2008).

5. Savu, I. D., Savu, S. V. & Sirbu, N. A. Heat affected zones in polymer laser marking. *J. Therm. Anal. Calorim.* **115,** 1427–1437 (2014).

6. Dowden, J. *Springer Series in Materials Science 119 The Theory of Laser Materials Processing*.

7. Kumar, S. P. and S. Profile and depth prediction in single-pass and two-pass CO 2 laser microchanneling processes. *J. Micromechanics Microengineering* **25,** 35010 (2015).

8. Prakash, S. & Kumar, S. Experimental and theoretical analysis of defocused $CO_2$ laser microchanneling on PMMA for enhanced surface finish. *J. Micromechanics Microengineering* **27,** 25003 (2017).

9. Stępak, B. D., Antończak, A. J., Kozioł, P. E., Szustakiewicz, K. & Abramski, K. M. Laser micromachining and modification of bioabsorbable polymers. *Proc. SPIE - Int. Soc. Opt. Eng.* **8968,** 896809 (2014).

10. Grabow, N. *et al.* Mechanical properties of laser cut poly(L-lactide) micro-specimens: implications for stent design, manufacture, and sterilization. *J. Biomech. Eng.* **127,** 25–31 (2005).

## 5.5 Conclusion

In this chapter I showed that Polylactic acid is an ideal material for the production of environmentally sustainable, single-use, microfluidic devices in conjunction with laser ablation. Polylactic acid shows a good workability with $CO_2$ laser cutting and has a good potential for the manufacturing of sustainable multilayer chips for biomedical applications. Interesting features of PLA laser-cut channels have been observed; for example, the presence of a recast zone and high deformation were observed at the beginning of this study, potentially hindering the use of PLA sheets in rapid-prototyping of multi-layer microfluidic devices. I have found that the use of a covering tape as a sacrificial layer to decrease the laser beam absorptivity of the material and the heat diffusion is a solution to the earlier issue. The melting cutting process still remain the main phenomena taking place during laser cutting and characterizes the quality of the surface of the cut zone. With this respect PLA wall and channel are one order of magnitude smoother, compared to PMMA. This feature makes laser cut PLA channels superior to PMMA, with respect to adsorption of small hydrophilic molecules such as fluorescein salt and to qPCR inhibition.

This sustainable manufacturing technique presents exciting opportunities for the development of more sustainable microfluidic devices in the future as well as opening up the potential for sustainable, disposable, single-use micro-components for clinical applications.

# Chapter 6: POLYLACTIC ACID A SUSTAINABLE, BIOCOMPATIBLE, TRANSPARENT SUBSTRATE MATERIAL FOR ORGAN-ON-CHIP, AND MICROFLUIDIC APPLICATION

## 6.1 Introduction

In this chapter Polylactic acid, PLA, a high biocompatible polymer, extensively employed as material to produce scaffold for tissue engineering, or as drug encapsulation carrier for drug delivery applications [167]–[170], it is introduced as suitable substrate material for microfluidic cell culture and organ-on-chip, OOC, applications.

This chapter briefly describes the substrate material properties that need to be taken into account when considering interaction with cells and tissues. The evolution of the material requirements employed for cell and tissue culture is described and the current challenges are analysed. The main part of this chapter is based on a preprint paper published in biorxiv in July 2019 and assess the suitability of PLA with respect to microfluidic cell culture and OOC applications. The relevant material properties of PLA are explored and compared to the one of PDMS, the current gold standard material, and to the one of other thermoplastic polymers used to produce OOC devices.

## 6.2 The evolution of Substrate Materials for Cell and Tissue Culture: from the flasks to organ on chip

The origin of cell and tissue culture starts in 1907 [171]. Professor Ross Harrison as part of his research was growing tissue in test tubes to study the development of frog nerve fibrosis [172]. Test tubes are finger like length tubes open at the top and closed at the bottom made of glass. At the time, glass, thanks to its high availability and inertness, was the material of choice both in chemistry and in biology laboratories and in the healthcare sector. Another method, that gave the birth to cell culture as we know it today is due to Professor Harrison. Herrison developed the so called hanging drop technique. In the hanging drop technique, slices of tissues are embedded in plasma on the reverse side of a glass cover slip. Professor Carrel and Burrows in 1940 further developed this technique to study cells. They were collecting the cells migrating from the drop into glass plates. To

Carrel recognition is due the invention of the first tissue culture flasks made out of glass and called D-flask.

It is only that in 1930, that thanks to a collaboration between Carrel and Charles Lindbergh, Pyrex glass was introduced and adopted as flask material for tissue culture [172]. Pyrex glass is a borosilicate glass with low thermal expansion properties, it is resistant to high heat and can be autoclaved for sterilization. In 1950 the first 2D monolayer cell culture was carried out on flask and dishes. The hypothesis that collagen serves as a kind of solid substrate and support for cells in the organism lead Erhmann and Gey in 1956 to successfully report the first collagen "coating" to enhance cell attachment and growth on Pyrex of cells that previous studies showed poor growth capacity, e.g. kidney, cartilage and embryonic fibroblast cells [173]. In the same period, the need for disposable substrates for cell and tissue culture was taking hold. In fact, glass culture vessels required time-consuming and careful cleaning procedures to avoid detergent, and solvent residues interfered with other cell culture experiments and processes [171]. Researcher started to test different plastic materials (e.g. Polystyrene and polyvinyl chloride) to find a suitable disposable material for flasks and dishes. In the same period the first 96 well plate was developed [174]–[176]. In the 1960s, polystyrene, PS, became the substitute to glass thanks to its transparency, manufacturability, ease of moulding and sterilization [177]. However, it was immediately recognised that the chemistry of PS, for some applications, was representing a drawback. In fact, the phenyl groups in the polymer structure do not provide anchoring point to the cells. In 1966 a wet-chemistry approach to modify PS surface chemistry by sulfonating the surface was introduced to increase the surface wettability. With the proposed method, serum proteins were facilitated to be absorbed by the charged surface and they were providing a better environment for the culture of vertebrate cells [178]. More research and more methods, including oxidation plasma treatment, have been proposed, leading to the PS flasks, petri dishes and well plates now in use.

If on one hand 2D cell and tissue culture have led to exceptional discoveries, for example vaccines, on the other hand they do not represent and mimic the complex environment hosting the cells. To this respect, tissue engineering, microfluidic cell culture and organ-on-chip are multidisciplinary field of science that aim to provide a better and suitable model to mimic the *in vivo* microenvironment that host the cells. The aim of tissue engineering is not directly to provide a better model to study cells but to replace biological

tissue [179]. To do so, it makes use of scaffold to host the cells, that can grow and differentiate to the desired tissue or organ to be replaced. Scaffold are usually made of bioresorbable materials that can degrade in physiologically condition after new tissue or organ formation. Several materials have been engineered to address the goal of tissue engineering, such as polylactic acid and its copolymer, polyethylene glycol and its copolymer, alginate, hydrogels and so on. Different from tissue engineering, microfluidic has provided a powerful tool for single cell analysis, for example for mechanical characterization of cells, or to culture cells for drug testing. Organ-on-chip (OOC), brings together tissue engineering and microfluidic to provide advanced microphysiological systems for cell and tissue culture. An OOC device scales down to the minimal physiological function and organ function. The material of choice to manufacture OOC devices is PDMS. PDMS is biocompatible, transparent, has a good oxygen permeability, it is easy to manufacture at the research scale and it has predictable molecular binding. The use of PDMS has enabled, thanks to its stiffness, to the possibility to add mechanical stimuli at the device.

### *6.2.1 PDMS drawbacks*

For certain applications, PDMS poses some challenges, namely channel deformation, evaporation, leaching of uncured monomer, hydrophobic recovery and absorption of small hydrophobic molevules. The absorption of Hydrophobic compounds via diffusion through the bulk of PDMS, is maybe the biggest drawback of the material. Because of low interchain forces and low intermolecular interactions governed mainly by London dispersion forces [180], PDMS is flexible and highly permeable and it has a porous supremolecular network. If on one hand, permeability plays a key role for microfluidic cell culture and OOC applications enabling the right supply of $O_2$ and $CO_2$, on the other hand it leads to absorption of small (< 500 Da) hydrophobic molecules and permeation of compounds [181]. For instance, Regehr et al., have shown that PDMS absorbs and release Estrogen in a dose and extraction dependent manner, without reaching an absorption saturation point [182]. Another example was demonstrated by Toeple et al. The authors showed that Nile Red a small hydrophobic fluorescent molecule diffuses from the solution inside the bulk of PDMS [181]. The absorption and sequestering of hydrophobic compounds from the media or from the solution is particularly detrimental when studying drug response and effects, reducing the available drug dose and toxic threshold. With this respect several research has been carried out in order to solve this drawback. Waters et al., analysed the effect of plasma surface treatments on the

absorption of pharmaceutical compounds, such as acetyl salicylic acid, Salicylic acid and others in order to avoid their permeation inside PDMS [183]. They found that regardless of plasma exposure time, hydrophobic compounds were still absorbed by PDMS. Meer et al., tested two different lipid-based coatings to prevent the absorption of verapamil, bepridil, Bay K 8644 and nifedipine, four drugs that can affect the heart [184]. They showed a reduction in drug absorption of about 80%. In order to better understand and predict the absorption of small molecules, Wang et al, tested different pharmaceutical compounds and provided a quantitative correlation between the partition coefficient of the compounds and absorption into PDMS [185]. The partition coefficient is defined as the ratio of concentration of a compound in octane (nonpolar phase) and in water (polar phase), and it is usually an exponential number. It is common to express the partition coefficient as its logarithm, logP [186], [187]. Wang et al., shown that molecules with a logP < 2.66 exhibit an absorption lower than 10%, while molecules with higher logP are highly absorbed and sequestered by PDMS. Furthermore, they showed that if PDMS is coated with $TiO_2$ or glass, the absorption is reduced [185]. A recent study conducted by Auner et al., measured the binding kinetics of 19 compounds relevant for toxicologist study and established a method to use the experimentally derived kinetic parameters to model the absorption inside PDMS based microfluidic devices. They provided a criterion to predict which compounds are likely to be absorbed in PDMS and thus difficult to interpret effects on cells [188]. Despite useful informations, a drawback of their study is that they tested untreated PDMS, while usually PDMS is functionalized to enhance the hydrophilicity, especially for cell culture applications. Furthermore, they did not take into account the molecular weight of tested compounds. All the methods developed to prevent the non-specific adsorption and absorption of molecules into PDMS via coating or via surface modification methods such as passivation of the elastomer surface with bovine serum albumin or detergent, or covalent attachment of PEG prior surface oxidation, only successfully stop adsorption, and have a weak temporaney effect in stopping the absorption of compounds [189]. In this respect, Quake and co-workers successfully developed a method to modify PDMS. The method relies on a sol-gel treatment of PDMS to fill the polymer matrix with silica nanoparticle. In this way, the transparency, gas permeability and biocompatibility are preserved and the absorption of hydrophobic compound stopped [189]. Another drawback due to the high permeability of PDMS is induced changes in osmolality, because of the evaporation of water through the bulk of PDMS [190]. Osmolality is defined as the total number of solute per one Kilogram of water of solution [191]. It is important during cell culture that the media osmolality is

constant, for instance mammalian gametes and embryos culture requires an osmolality of 265-285 mmol/kg [192]. Heo et al., reported that mammalian cells are particularly sensitive to osmolality shift and their behaviour is critically affected. They conducted a study in order to model and predict osmolality shift through PDMS with different thicknesses and provided a method to remedy this issue. Parylene coated PDMS prevents water vapour evaporation and thus prevents changes in the osmolality. Other methods reported to avoid evaporation during static cell culture on chip are placement of water or medium filled reservoirs, or submerging the chip in water, or by using PCR tape [193]. Another possible problem with PDMS, that researchers took care of, is the hydrophobic recovery effect. After plasma or UV ozone treatment to increase the hydrophilicity of PDMS, free siloxanes in the polymer network migrate from the bulk of the material to the surface; thus, the surface properties of PDMS return into their native state one week after the treatment [194]. In order to avoid changes in the surface properties, the functionalised device can be stored at sub-zero temperature, or channels can be filled with DI water.

The flexibility and the stiffness of PDMS can lead to flow induced channel deformation [193]. This phenomenon can affect application where a precise control of the shear stress is needed, especially while culturing monolayer endothelial cells [195], [196]. In order to prevent channel deformation, PDMS stiffness can be increased by curing it for a longer time at higher temperature with more curing agent. It needs to be underlined that flow induced channel deformation and flexibility have been the material characteristics that have allowed to produce devices for mechanobiology and the first organ on a chip device [197], [198]. Flexibility has been used to produce stretching to mimic physiological breathing movements and as well to supply mechanical stimuli to the cells [197].

The biggest limiting factor of PDMS is that mass manufacturing of PDMS microfluidic devices it is difficult to fully automate on a large scale [199]. Recently, Hiltunen et al., reported the first roll-to-roll (R2R) thermal imprinting method to fabricate integrated PDMS–paper microfluidics enabling tens of thousands of replicates to be produced per hour [200]. The method proposed can enable to fastener the translation process from the lab bench to the mass market. However, the manufacturing industry at the moment still prefers methods such as hot embossing or injection moulding, not translatable to PDMS [190]. There is the need, then, to translate the design of the proof of concept microfluidic device made of PDMS to a design compatible with injection moulding and/or hot

embossing of a thermoplastic material [201]. Nevertheless, this translation brings several challenges, and different factors need to be taken into account in order to guarantee the functionality of the final mass manufactured device. Transparency, autofluorescence, biocompatibility, water vapour permeability, oxygen transport and possible absorption of small compounds are some of the material properties that need to be considered in order to provide to end-users with consistent devices. Thanks to the demonstrated high biocompatibility of PLA, in the next section the study I conducted to assess the material suitability as substrate material for microfluidic cell culture and organ on a chip application will be presented. Evidence of PLA suitability for advanced microfluidic 3D cell culture have been shown previously [202]. Despite promising results, no characterization and assessment of transparency, autofluorescence, absorption/adsorption of small molecules and comparison with other thermoplastic have been carried out, thus resulting in a stand-alone study. The study I have conducted is focused on assessing material suitability for cell culture and to provide useful information to end-user and to industry as well. Furthermore, it embraces and underlines the environmentally sustainable aspect of our choice.

## 6.3 Polylactic acid a sustainable, biocompatible, transparent material for Organ-on-a-chip and microfluidic applications

This paper, in preprint on biorxiv from June 2019, and published on Analytical Chemistry, ACS, in April 2020, is co-authored by myself (AO), Davide Di Giuseppe (DG), Ali Kermanizadeh (AK), Allende Miguelez Crespo(AC), Arianna Mencatti (AM), Lina Ghibelli (LG), Vanessa Mancini (VM), Krystian L. Wlodarczyk (KW), Duncan P. Hand (DH), Eugenio Martinelli (EM), Vicki Stone (VS), Nicola Howarth (NH), Vincenzo La Carrubba (VLC), Virginia Pensabene (VP) and Maïwenn Kersaudy-Kerhoas (MKK). Myself, MKK and VP gave substantial contribution to experimental conception and design, and analysis of the results. I performed all experiments but the cell culture and tracking experiments. I manufactured all the devices tested and developed the method to permanently functionalize the surface of PLA, as well as the bonding method. I performed numerical simulation of the oxygen permeability. DG, AM and LG performed the tracking experiment and EM helped with the analysis of the results. AK performed the A549 and C3A cell culture and AM the Huvecs cell culture experiment. KW performed the femtosecond laser microstructure and characterization and DH helped to analyse the results. NH and VLC helped with the analysis and discussion of the results. The manuscript was written by myself and M.K.K. in close consultation with all authors.

analytical chemistry

pubs.acs.org/ac Article

# Polylactic is a Sustainable, Low Absorption, Low Autofluorescence Alternative to Other Plastics for Microfluidic and Organ-on-Chip Applications

Alfredo E. Ongaro, Davide Di Giuseppe, Ali Kermanizadeh, Allende Miguelez Crespo, Arianna Mencattini, Lina Ghibelli, Vanessa Mancini, Krystian L. Wlodarczyk, Duncan P. Hand, Eugenio Martinelli, Vicki Stone, Nicola Howarth, Vincenzo La Carrubba, Virginia Pensabene, and Maïwenn Kersaudy-Kerhoas*

Cite This: https://dx.doi.org/10.1021/acs.analchem.0c00651 Read Online

ACCESS | Metrics & More | Article Recommendations | Supporting Information

**ABSTRACT:** Organ-on-chip (OOC) devices are miniaturized devices replacing animal models in drug discovery and toxicology studies. The majority of OOC devices are made from polydimethylsiloxane (PDMS), an elastomer widely used in microfluidic prototyping, but posing a number of challenges to experimentalists, including leaching of uncured oligomers and uncontrolled absorption of small compounds. Here we assess the suitability of polylactic acid (PLA) as a replacement material to PDMS for microfluidic cell culture and OOC applications. We changed the wettability of PLA substrates and demonstrated the functionalization method to be stable over a time period of at least 9 months. We successfully culture human cells on PLA substrates and devices, without coating. We demonstrated that PLA does not absorb small molecules, is transparent (92% transparency), and has low autofluorescence. As a proof of concept of its manufacturability, biocompatibility, and transparency, we performed a cell tracking experiment of prostate cancer cells in a PLA device for advanced cell culture.

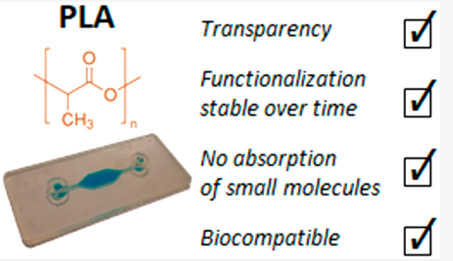


Organ-On-Chip (OOC) is the convergence of two emerging research areas, microfluidics and tissue engineering, meeting the requirements for more physiologically accurate human tissues. OOC devices provide advanced models for cell and tissue culture, accelerating and facilitating the understanding of human biology, toxicology, disease progression, and prognosis, while overcoming important ethical, financial, and interspecies variances related to animal experimentations.[1]

Since the birth of the first OOC device in 2007,[2] complex functionalities have been added to devices, leading to the so-called body-on-a-chip or human-on-a-chip fields. The translation from the research to the market was relatively fast. To date, at least 28 companies are proposing body- and tissue-on-a chip devices.[3] The material of choice in most organ-on-chip platforms has been poly(dimethylsiloxane) (PDMS), a thermo-curable elastomer. The majority of companies present in the OOC market (57%) sells PDMS products (Supporting Information, SI). Although PDMS is biocompatible, transparent, gas permeable, flexible, and relatively easy to manufacture at small scale, some issues have been encountered by consumers while using PDMS devices for certain applications. These problems include channel deformation, high evaporation, leaching of uncured oligomers, absorption of hydrophobic compounds, and unstable surface treatment which can lead to inconsistent and unpredictable results with respect to some biological outcomes.[4] While some of these issues have been overcome (e.g., via Soxhlet extraction in ethanol, or other organic solvent, to remove un-cross-linked oligomers[5]), PDMS molding still remains a difficult process to fully automate[6] and significantly slows down the translation from the research to the mass market production.

The need for alternative materials to PDMS is such a concern for the industry, that the US Small Business Innovation Research, SBIR, has recently funded studies to find non-PDMS alternatives, providing specific requirements to be addressed, e.g., transparency, biocompatibility, no absorption, and manufacturability.

Poly methyl methacrylate (PMMA), polycarbonate (PC), cyclic olefin polymers and copolymers (COP and COC, respectively), and polystyrene (PS) are some common materials proposed from different suppliers as scalable alternatives. These thermoplastic materials present the

Received: February 13, 2020
Accepted: April 1, 2020
Published: April 1, 2020





https://dx.doi.org/10.1021/acs.analchem.0c00651
Anal. Chem. XXXX, XXX, XXX−XXX

advantage of being relatively inexpensive, and could translate easily to the mass market. However, these materials do not always exhibit good biocompatibility and are fossil-based, and therefore unsustainable.

In a recent study, we explored the mechanical properties of polylactic acid (PLA), a biocompatible thermoplastic material derived from renewable resources as an environmentally friendly substrate material for the production of environmentally sustainable, single-use microfluidic devices, adopting a design for sustainability approach.[7] PLA has been widely studied in the context of tissue engineering, and approved by the FDA as a drug carrier. Evidence of PLA suitability for advanced microfluidic 3D cell culture have been shown previously.[8] Additionally, PLA is compatible with high volume production such as microinjection molding. PLA is also easily workable and compatible with rapid-prototyping. For example, a number of researchers have manufactured PLA-based devices using 3D-printing. 3D-printed PLA structures are often nontransparent and demand postprocessing. However, PLA can be formed into sheets, machined by laser cutting or milling, integrated to other structures such as electrodes or membranes, and assembled into complex microfluidic devices.[7]

Despite the increasing use of PLA in the field of microfluidics, no characterization and assessment of transparency, autofluorescence, absorption of small molecules, and comparison with other thermoplastic have been carried out on PLA. Here we provide evidence that PLA is a suitable replacement to other polymers in organ-on-a-chip applications, readily translated to the mass market. We investigate surface properties, biocompatibility, absorption of hydrophobic and hydrophilic small compounds (<900 Da), and optical properties of PLA in comparison to PDMS and with other reference polymers such as PS. Finally, we provide an example of cell-tracking through a PLA-based microfluidic device.

## METHODS

**Materials.** Polylactic acid (Natureworks 2003D) was purchased from Naturework in pellet format. PMMA Clarex was purchased from Weatherall, Ltd., in a 1 mm sheet form. PDMS Sylgard 184 was purchased from Dow Corning, while COC (Topas) and PC (RS components) were acquired in 1 mm sheets. All the reagents used were purchased from Sigma-Aldrich, unless specified in the text.

**PLA Functionalization.** The functionalization process was an alkaline surface hydrolysis. NaOH was dissolved in DI water to prepare 0.01, 0.1, 0.5, and 1 M solution concentrations. The pristine PLA, pPLA, sample was dipped inside the solution and kept in for specified amount of time (0, 10, 30, 60, 120 s). Then the sample was washed with water and dried with compressed air. To measure the effect of the functionalization time, and solution concentration, the contact angle of the samples was measured using a custom-made static contact angle apparatus.[9] The images acquired via a Dinolite digital microscope (Dino-Lite Premier2 AD7013MZT) were analyzed using the image analysis freeware ImageJ (plugin contactj). Each measurement was carried out 6 times. To assess the chemical changes at the surface an attenuated total reflection, ATR-FTIR analysis was carried out collecting 200 scans in the range of 4000−400 cm-1, with a resolution of 4 $cm^{-1}$ using a Nicolet Is5 spectrophotometer. The effect of the surface functionalization on the surface were studied using a white light interferometer (Zygo) with 1 nm resolution in vertical direction. The Roughness (Ra) quantitative determination was carried out using Metro.Pro 8.2. For morphology analysis SEM (Quanta FEG 650 SEM) images were acquired in high vacuum mode.

**PLA Biocompatibility.** Biocompatibility of PLA was tested by culturing human hepatoblastoma C3A cell line, A549 cells, and human umbilical vein endothelial cells (HUVECs). We compared the biocompatibility of PLA with other common thermoplastic material used for microfluidic cell culture and with PDMS. Cell survival in a PLA cell culture microfluidic device was tested with HUVECs and compared with respect to a PDMS device. Details regarding the cell culture and staining process can be found in SI S3.

**Finite Element Analysis.** Finite element analysis was conducted using FEATool MultiphysicsTM version 1.10 (Matlab) to determine the oxygen concentration level inside the microfluidic cell culture chamber. A simplified 2D model of the PLA microfluidic device was designed. The oxygen diffusion coefficient of $2.5 \times 10^{-12}$, $3.5 \times 10^{-9}$, $4 \times 10^{-9}$, and $2.14 \times 10^{-5}$ $m^2/s$ was used for PLA, PDMS, water, and air, respectively, taken from previously published studies.[10,11] Details regarding the numerical simulations can be found in SI S3

**Microfluidic Device Preparation.** To manufacture the PLA organ-on-chip devices, first PLA sheets were manufactured using a manual hydraulic heated press as per the method described in ref 7. Then each layer was cut using a $CO_2$ laser cutter (Epilog Mini Elix 30W) using SLAM approach, which consists of applying a thin tape (100 $\mu$m) on the material prior to laser-cutting (ref 7). The use of a commercial $CO_2$ laser enables the formation of channels with 200 $\mu$m minimum size, however, other types of laser could deliver smaller channel widths. Some examples are discussed in Figure S4. The layers were cleaned by sonication in pure ethanol. The cleaned layers were functionalized by dipping them in a 1 M NaOH solution for 60 s, then cleaning them with water, 2-propanol, and compressed air. The surfaces were then chemically activated under UV exposure (254 nm) for 45 s. Layers were bonded together placing them in a sandwich composed of two glass slides, and kept them in contact at 50 °C for 10 min. Once the assembly has cooled down to room temperature, it is disassembled, and the device is ready to be tested.

**Small Molecules Absorption.** To assess the bioinertness of the material, the prinstine PLA (*p*PLA) was compared with functionalized PLA (*f*PLA), and with PDMS. To test the absorption of hydrophobic compound Nile Red was dissolved in EtOH 99% to obtain a solution concentration of 1 $\mu$M. To test the absorption of hydrophilic compounds fluorescein salt was dissolved in DI water (1uM). A fluorescent microscope (AM4115T-GFBW) was used to take the fluorescent images and the image analysis via ImageJ. Details of the manufacturing protocol can be found in SI S5.

**PLA Optical Properties.** The transparency of the materials was tested by analyzing the transmittance of the light through the samples in the visible region using a UV−vis spectrophotometer (Shimadzu UV-2550). The autofluorescence of the plastic materials of interest was measured using a Leica SP8 3X STED laser scanning microscope equipped with two Internal Spectral Detector Channels (PMT). More details of the protocol used to measure material autofluorescence can be found in SI S6.

**Cell Imaging and Tracking on a PLA Device.** A small-scale inverted microscope suitable to work in high humidity environments (incubators) with factory standard optics,


https://dx.doi.org/10.1021/acs.analchem.0c00651
Anal. Chem. XXXX, XXX, XXX−XXX

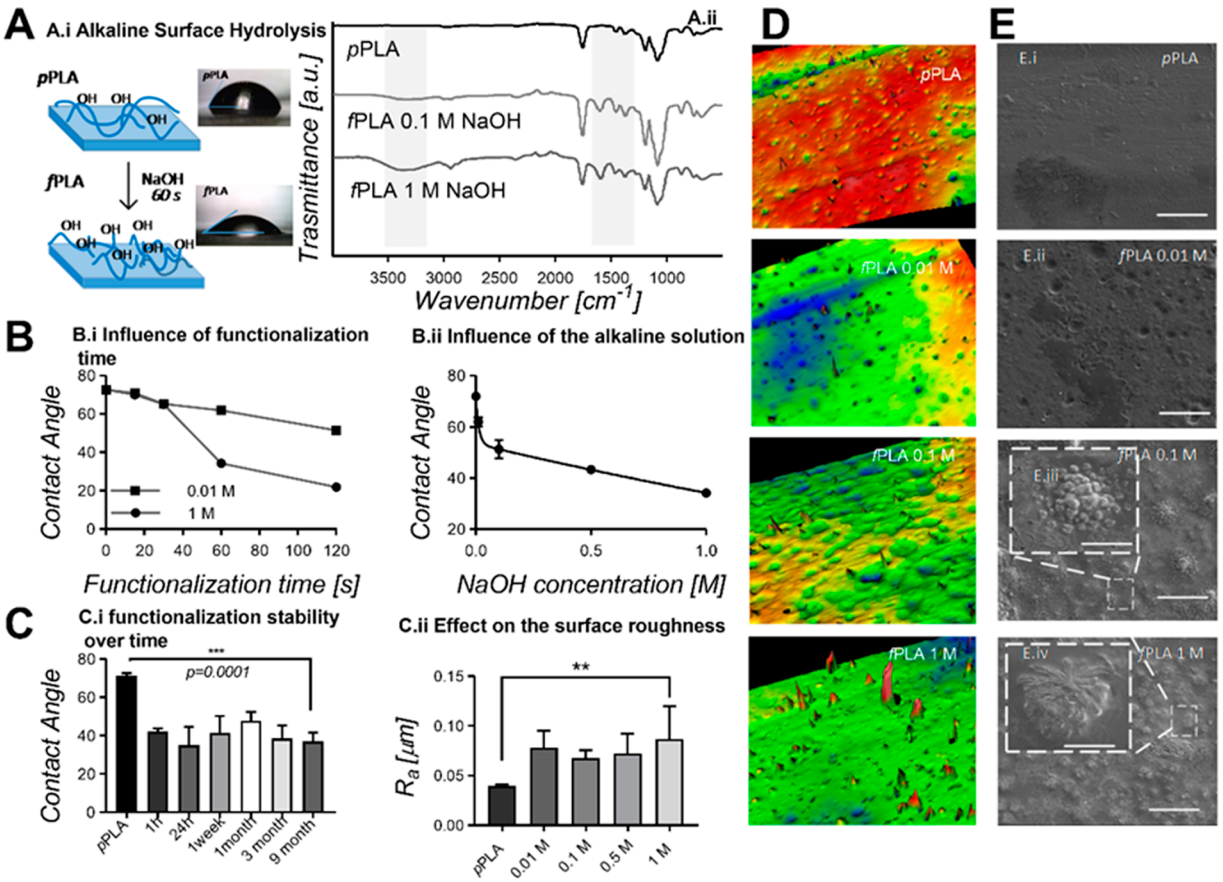


**Figure 1.** Tuning the surface properties of PLA. (A.i) Functionalization mechanism via Alkaline Surface Hydrolysis and photographs of a DI water drop on the pristine PLA substrate (top) and on the functionalized PLA substrate (bottom). (A.ii) FTIR spectrum of pristine PLA (black curve), functionalized PLA using a concentration of 0.1 M of NaOH solution (light gray curve), and a concentration of 1 M of NaOH (gray curve). The gray areas underline the areas where a change in the spectrum is observed due to the functionalization. The first one (from left to right) at 3200 $cm^{-1}$ is indicative of the formation of hydroxyl groups, the second one highlights a stretching of the C−C groups indicative of a partial hydrolysis of the treated surface. (B.i) Influence of the functionalization time on the final contact angle for two different solution concentration, 0.01 M (box) and 1 M (circle). The two connecting lines are just to guide the eye. For all the points the error bars are shorter than the height of the symbol. (B.ii) Influence of the NaOH concentration on the final contact angle after 60 s of functionalization. The experimental results are fitted with a two-phase exponential decay function. For some points the error bar is shorter than the high of the symbol. (C.i) Stability of the functionalization method adopted over nine months. (C.ii) Effect of the solution concentration on the final surface roughness of the functionalized substrate after 60 s functionalization. (D) Interferometer pictures of the unfunctionalized and funcionalized PLA surfaces with different solution concentration after 60 s functionalization time. Interestingly, a pillar formation structure is noticed with an increase of the pillar density with respect to the solution concentration. While an increase of surface roughness is visible on SEM imaging, the pillar formation is partly damaged by the conductive gold layer. (E) SEM pictures of the unfunctionalized and functionalized PLA surfaces with different solution concentration after 60 s functionalization time. Atomic force microscopy imaging of pristine and functionalized PLA was also used to confirm the pillar formation. Data shown in Figure S2.

custom aluminum structure, and fully sealed electronics was used to perform cell tracking. The video sequence is then processed by a proprietary software (Cell-Hunter) elsewhere validated in cancer immune interaction and block replication in prostate cancer cells.[12] For the sake of comparing the kinematic characteristics of cells involved in the competing experiments, we extracted standard descriptors such as average speed, curvature, and angular speed, along with the coefficient of diffusion. The distribution of such descriptors was computed over all the tracks extracted. Details of the cell imaging and tracking experiment can be found in SI S7.

## RESULTS

**PLA Functionalization.** An OOC device provides support for tissue attachment and organization to simulate organ-level physiology. The first interaction between the cells and the device happens at the material surface. The requirements for a suitable substrate material for healthy cell environment and tissue adhesion, are wettability, surface roughness, and chemical composition.[13,14] PLA is a hydrophobic polymer, which is a limiting factor for cell attachment. To address this, surface treatments are required to increase the substrate wettability.[15,16] The most widely utilized and preferred surface modification methods rely on oxygen plasma and UV-ozone treatments.[17] However, several studies have reported the nonpermanent nature of those functionalization methods, leading to the short-term recovery of the hydrophobic property.[18] Such a phenomenon is particularly exhibited by PDMS, with a drastic increase of the contact angle 1 week after the treatment.[18] To overcome the hydrophobic recovery issue, PDMS devices need to be used just straight after the functionalization process, which further limits their industrial applications. The contact angle value gives a quantitatively measure of the hydrophilic or hydrophobic nature of a surface. In particular, a material is hydrophilic if it has a contact angle


https://dx.doi.org/10.1021/acs.analchem.0c00651
Anal. Chem. XXXX, XXX, XXX−XXX

below 90°, and hydrophobic if the contact angle is above 90°. Our PLA sheet manufacturing protocol produces a slightly hydrophilic surface with a weak wettability. The measured contact angle is about 77°−80°(Figure 1A), while the desired contact angle for cell culture applications is 45° ± 4° (appropriate contact angle to avoid electrostatic interactions with hydrophilic molecules[18]). In order to permanently modify the surface properties of *p*PLA, a wet-chemistry approach was adopted (Figure 1A). Using this functionalization process, the final contact angle can be tuned by changing the functionalization time and the solution concentration (Figure 1B). This functionalization protocol is stable over time, with no evidence of a hydrophobic recovery effect, even 9 months after the functionalization, at room temperature storage (Figure 1C.i). In accordance with previous results reported by Tham et al.,[19] this method acts on hydrolyzing and eroding the material surface, inducing a visible change in the surface roughness (Figure 1C.ii−E). In conclusion, the proposed functionalization protocol produces the desired contact angle for cell culture. The resulting formation of the −COOH and of −OH groups at the surface can be readily used for further conjugation of surface modifying species.[16,19]

**PLA Biocompatibility.** Biocompatibility in OOC devices can be defined as the absence of toxic effects to the cells or tissue interacting with the material, as well as evidence of optimal growth of the cultured cells or tissues. PLA has been widely used in medicine and its biocompatibility has been well established by a number of studies, typically demonstrating the lack of low inflammation after implantation and compatibility with surrounding tissue.[20−22] In this study, we specifically aimed at comparing the biocompatibility of pristine PLA (*p*PLA) versus functionalized PLA (*f*PLA), as well as against PS (control material), and PDMS. In SI S3, detailed materials and methods are given, as well as a comparison with other common thermoplastic materials. Cell proliferation and cell death of two cell lines, human hepatocellular carcinoma cells (C3A) and adenocarcinomic human alveolar basal epithelial cells (A549) were examined. At 48 h of cell culture of the C3A cells, only the substrates made of *p*PLA, *f*PLA, and *f*PDMS performed comparably with the control (albeit the differences with other polymers were small, Figure S3), and at 7 day time point *p*PLA and *f*PLA showed a decrease in cell death of 6% and 10% respectively, with respect to the control (Figure 2 A.i). For the A549 cells at 48 h of culture almost all the substrates performed comparably well with the PS control with no significant statistical differences in cell death, while at 7 days all polymers caused the same percentage of cell death as compared to control with the exception of PLA that demonstrated a decrease in cell death (Figure S3). Cell proliferation data are shown in Figure S4.

We also independently investigated the PLA biocompatibility with primary cells, which have a finite life span and a limited expansion capacity, compared to cancer cell lines. We cultured freshly isolated human umbilical vein endothelial cells (HUVECs) for 7 days on the same substrates Both *p*PLA and *f*PLA performed as the control PS (no statistical difference). Pristine PDMS (pPDMS) did not allow cell adhesion due to the intrinsic hydrophobic properties of the material (Figure 2A.ii). Overall, the toxicity data of cancer and primary cells indicates that PLA is a suitable material for cell culture. Translating from a PS substrate to a PLA substrate was found to be marginally better for A549 and C3A cells, and similar for HUVECs.

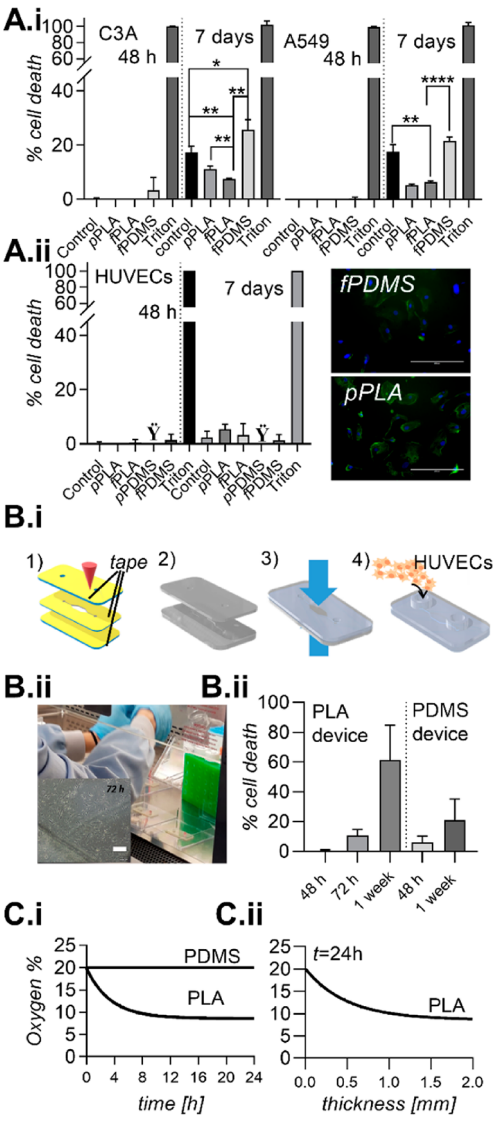


**Figure 2.** (A) Assessing the material biocompatibility off-chip. Percentage of cell death of C3A, A549 (A.i) and HUVEC cells (A.ii) at 48 h and 7 days time points. For detailed methods, see S4. The positive control (noted Control) is uncoated PS wells. 0.1% Triton X-100 (Sigma, U.K.) (Triton) is a negative control, in uncoated PS cells, and provides 100% cell death comparison. HUVEC cells did not adhere on the pristine PDMS (Noted with a symbol: *). In the inset of A.ii, DAPI-actin staining of HUVECs at the 7 day time point on fPDMS and PLA (scale bar is 200 $\mu$m). (B) Cell culture on-chip. (B.i) Schematization of the protocol to manufacture the microfluidic device for culturing HUVECs: (1) $CO_2$ laser cutting the three layers using the SLAM approach; (2) cleaning and functionalizing the layers; (3) UV bonding the layers; and (4) device ready to be sterilized and used. (B.ii) Photograph showing the cells being loaded inside the device. In the insert, bright-field microscope photograph of healthy HUVECs cells with good confluence after 72 h culture, scale bar is 200 $\mu$m. (B.iii) Comparison of HUVECs cell death in the PLA and in the PDMS device. (C) 2D Numerical simulation of oxygen level inside the microfluidic culture chamber. (C.i) Simulated oxygen levels in function of culture time inside the PDMS and PLA microfluidic device. The oxygen level in the PLA level quickly reduces to 10% after a few hours. (C.ii) Simulated oxygen levels in the function of different thicknesses of PLA device sealing layer at 24 h. A thickness of 0.250 mm would enable oxygen levels to be within 5% of the atmospheric level after 24 h.


https://dx.doi.org/10.1021/acs.analchem.0c00651
Anal. Chem. XXXX, XXX, XXX−XXX

To further evaluate the biocompatibility of *f*PLA and its suitability as a substrate material for microfluidic cell culture and OOC application, a 3 layer microfluidic device consisting of a single cell culture rectangular chamber was fabricated as per the Methods section (Figure 2B.i). Primary HUVECs were cultured for 1 week to evaluate the morphology and proliferation. The material transparency and absence of autofluorescence enabled us to easily evaluate cell viability using the ReadyProbes kit (as shown in the inset of Figure 2B.ii), and the cells easily adhered onto the PLA microfluidic walls without the need for an adhesive protein coating. They formed a confluent layer after 3 days in culture, maintaining their natural morphology. We compared the performance of the PLA device with an identical single chamber PDMS device (Figure 2B.iii). No statistically significant differences were noticed in the culture of the cells between the two different substrate materials, up to 72 h. At 1 week time point, a significant increase in cell death was noticed inside the PLA device. This is likely to be related to the lower oxygen permeability of PLA with respect to PDMS, static condition of the culture (media changed every 24 h), and the increasing oxygen demand due to cell proliferation.[23] In order to evaluate the oxygen concentration inside the PLA cell culture chamber and compare it to a PDMS chamber, we used FEATool Multiphysics, a Matlab toolbox, to create a 2D model. A time-dependent condition was imposed, and the oxygen concentration was simulated over 24 h with a time step of 1 h, assuming an oxygen consumption rate of the cells of $0.37 \times 10^{-4}$ mol/s[24] (Figure 2C.i). We carried out different simulations by changing the thickness of the top sealing layer and plotted the oxygen concentration level at 24 h time point inside the microfluidic chamber in function of the thickness of the layer (Figure 2C.ii). The results from the numerical simulation suggest that using a 0.1 mm top sealing layer allows an oxygen level at 24 h comparable to a PDMS device. Alternatively, continuous perfusion of media may be used. Further studies taking oxygen permeability and design variable into account will be undertaken.

**Absorption of Small Molecules on PLA Substrates.** Several reports have shown that, unless treated, PDMS can absorb small hydrophobic compounds such as steroids and hormones.[25−29] This behavior can be explained by the porous and hydrophobic nature of its polymeric network. This phenomenon can be a major drawback in bioassays, in particular drug testing assays where drugs engineered for rapid delivery are typically smaller than 500 Da and diffuse uncontrollably inside the microfluidic device.[26,27] Several methodologies have been proposed to overcome this issue; however, they result in delays in prototyping or manufacturing time. Alternatively, PLA, as a thermoplastic material, should not show any absorption behavior. In this study, the absorption of both hydrophilic and hydrophobic compounds was assessed in laser-cut *p*PLA and *f*PLA and PDMS channels. To test the absorption of hydrophobic compounds, Nile Red, a small hydrophobic fluorophore (318.37 Da), was selected as a representative molecule, while fluorescein salt (376.27 Da) was selected to test the absorption of a typical hydrophilic compound. The devices have been designed and manufactured with a channel cross-section of 0.8 $mm^2$ (Figure 3A). A fluorescence image of each empty channel was taken with a microscope to create the null absorption reference point (Figure 3B.i). To create the maximum absorption reference point, the channel was filled with the fluorescent solution

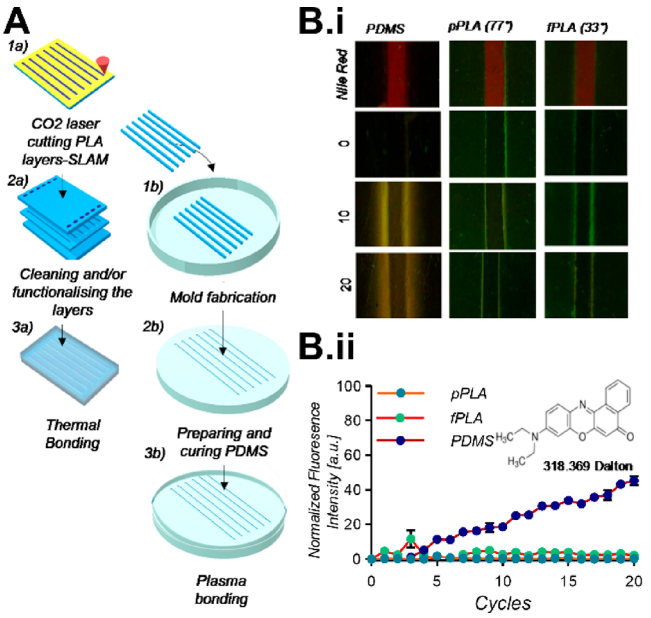


**Figure 3.** Investigation into the absorption of small molecules in PLA substrates. (A) PLA and PDMS prototyping protocol. (1a) SLAM method is used to cut a channel of 1 mm width and access holes from a 1 mm PLA sheet for channel and top layers, respectively. (2a) Top, bottom, and channel layers are cleaned and functionalized. (3a) The layers are bonded together. (1b) The cut PLA parallelepipeds from (1a) are used as a negative mold to fabricate the PDMS device to have the same channel cross-section for the different devices. (2b) The PDMS is mixed and placed in the mold and cured. (3b) Plasma bonding of the PDMS device. (B) Absorption of hydrophobic compounds. (B.i) Top view of the channel for (from left to right) PDMS, pristine PLA, and functionalized PLA. From the top to the bottom picture of the channel filled with a solution of Nile Red in ethanol (1 $\mu$M), representing one of the reference point; then picture of the empty channel, representing the 0 reference point, and picture of the channel at the $10^{th}$ and $20^{th}$ cycle. (B.ii) Normalized fluorescence intensity, measured at the center of the channel, plotted in function of the cycle number. In insert molecular structure and molecular weight of Nile Red.

(Figure 3Bi). The solution was incubated inside the channel for 60 s and then aspirated out of the channel from the outlet. Each channel was then cleaned with deionized water if loaded with Nile Red or with ethanol if loaded with fluorescein salt solution. A picture was taken after the cleaning cycle, and the fluorescence intensity measured with the imaging software ImageJ and normalized with respect to reference points. The rinsing−cleaning−imaging cycle was repeated 20 times (Figure 3B), and the normalized fluorescence intensity was plotted against the number of cycles (Figure 3B.ii). This experiment showed that PLA does not absorb hydrophobic or hydrophilic compounds, even when functionalized, while PDMS predictably absorbs small hydrophobic compounds (reaching 50% of absorption after 20 cycles), making PLA a superior material in this respect. In a preliminary study (data not shown), a hydrophilic but cationic dye, Rhodamine 6G, showed strong absorption in PDMS, and little or no absorption in PLA.

**Optical Properties of PLA: Transparency and Autofluorescence.** In order to study the organ functionality and biological responses at the cellular and molecular level, the optical properties of an organ-on-chip system substrate material, are of fundamental importance and relevance.[12] It is well established that PDMS, PMMA, PC, COP, and COC


https://dx.doi.org/10.1021/acs.analchem.0c00651
Anal. Chem. XXXX, XXX, XXX−XXX

have good or excellent optical properties and transparency. Furthermore, they have a low fluorescence background or autofluorescence, when irradiated near the UV wavelength, a desirable feature for fluorescent imaging.[30] The optical properties of PLA have been investigated and reported previously,[31] however, very little is known about PLA autofluorescence properties. Here the transparency and autofluorescence of PLA substrate was investigated, analyzing possible changes due to functionalization (*p*PLA versus *f*PLA) in comparison with PDMS, PMMA, PC, and COC substrates. We observed no difference between *p*PLA and *f*PLA with regard to transparency as transmittance of the light in the visible region (Figure 4A). *f*PLA showed 92% of transparency,

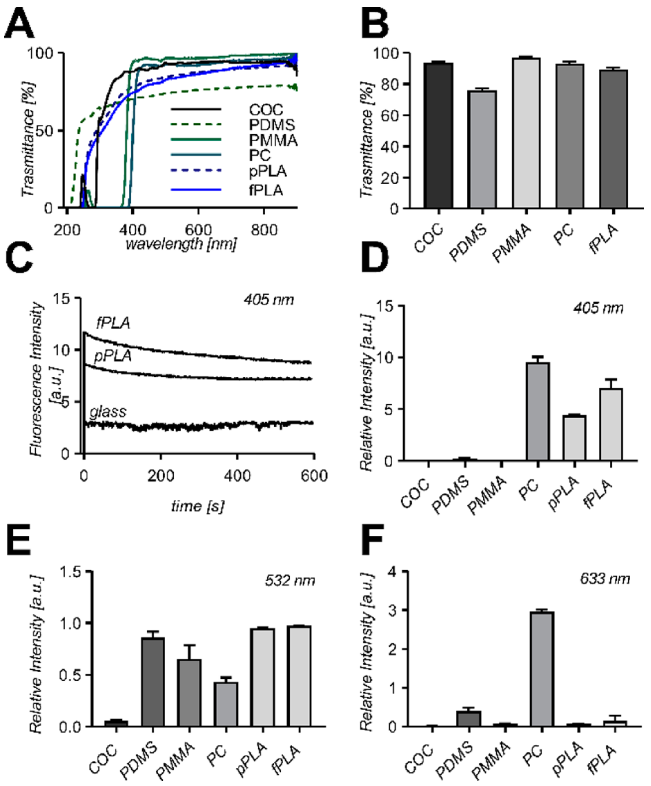


**Figure 4.** Investigation into PLA optical properties: (A) UV−vis spectrum of PLA (functionalized: fPLA and pristine PLA: pPLA) and different COC, PDMS, PMMA, and PC materials; (B) Comparison of light transmittance in the visible region of fPLA compared to COC, PDMS, PMMA, and PC substrate materials. (C) Fluorescence decay profile under 600 s continuum illumination of functionalized PLA, pristine PLA, and glass; autofluorescence intensity relative to glass of the different substrate materials after 60 s continuum illumination with 405 nm excitation (D), 532 nm excitation (E), and 633 nm excitation (F).

higher than PDMS, but lower with respect to the other materials tested. While PMMA showed the highest transparency (96%), followed by COC, PC, PLA, and PDMS (Figure 4 B). In OOC applications fluorescence imaging is often required over a period of time rather than instantly.[32] Hence, the analysis of the autofluorescence over time under illumination is highly beneficial. Therefore, next, the autofluorescence was measured over a period of 600 s (Figure 4C). *p*PLA and *f*PLA were analyzed and compared to glass, with data showing a gradual fluorescence decay for both. Contrary to the transparency behavior, a notable difference was noted between the pristine and the functionalized PLA, with *f*PLA showing a higher autofluorescence due to the increased presence of −OH groups in the functionalized sample. The use of material without defects such as bubbles or lamellae is of importance to the reduction of the background autofluorescence. Furthermore, the autofluorescence of *p*PLA and *f*PLA were measured and compared to COC, PC, PDMS, and PMMA with reference to glass. In these experiments, different wavelengths were tested, covering the range used in fluorescence microscopy. The fluorescence background was taken after 60 s illumination.[30] As expected, for all the materials tested, the autofluorescence decreased with increasing wavelengths. An exception to this was PC, which demonstrated a lower fluorescence background at 532 nm. PLA showed autofluorescence levels no higher than ∼1 times glass levels and comparable to the other tested materials (Figure 4D−F). Although the numerical fluorescence background measured for both pristine and functionalized PLA were higher than other materials, as shown in the Biocompatibility section (Figure 2), these results are not hindering PLA suitability for fluorescence imaging.

**Cell Tracking in a PLA Organ-On-Chip Device.** Organ-on-chip devices can be engineered to guide and spatially confine the cells. Recently, Biselli et al.[12] used an OOC device as a tool to study and quantitatively analyze the cancer-immune cell interactions via imaging analysis. The velocities, turning angle, and path of the moving cells were used as an indicator to study anticancer immune responses. Having demonstrated that the transparency of *f*PLA substrates is comparable to that of other common polymers used in microfluidics, we designed and manufactured an organ-on-chip device for cell tracking in a confined channel. A device composed of three layers was manufactured using a combination of hot embossing and Sacrificial Layer laser Assisted Method (SLAM) approaches from *f*PLA substrates[7] (Figure 5A). In this experiment, prostate adenocarcinoma PC-3 cells were cultured on the device, and a time lapse video was recorded as per material and method session in a $CO_2$ incubator at 37°C. A microphotograph of the region of interest was taken at 1 min intervals using a 4× magnification objective and videos analyzed with a custom written software as per material and method session. Kinematic descriptors such as speed, mean curvature, and angular speed were extracted and compared for a PS Petri dish, PLA disc, or inside a device. The kinematic descriptors between the PLA and the PS substrates were very similar despite slight difference of surface topology.[33] Additionally, the diffusion coefficient of individual cells was comparable on both substrates, thus demonstrating that cells on PS and PLA substrates have the same behavior (Figure 5B). However, the kinematic descriptors extracted from cell tracking in the PLA OOC device showed cell motility differences compared to the previous bare and open substrates (Figure 5C). Cell random walk was observed, but as expected, subdiffusivity was noted in the confined environment. This might be made worse due to the difference in the oxygen permeability of the material. The differences observed in cell motility could be overcome by providing a better surface topology, a protein coating in culture channels to improve cell adhesion, and reducing the thickness of the device or applying media flow for gas exchange.[34] In conclusion, the transparency of *f*PLA substrates allowed advanced cell tracking in the device, similarly to the control PS Petri dish, and we were able


https://dx.doi.org/10.1021/acs.analchem.0c00651
Anal. Chem. XXXX, XXX, XXX−XXX

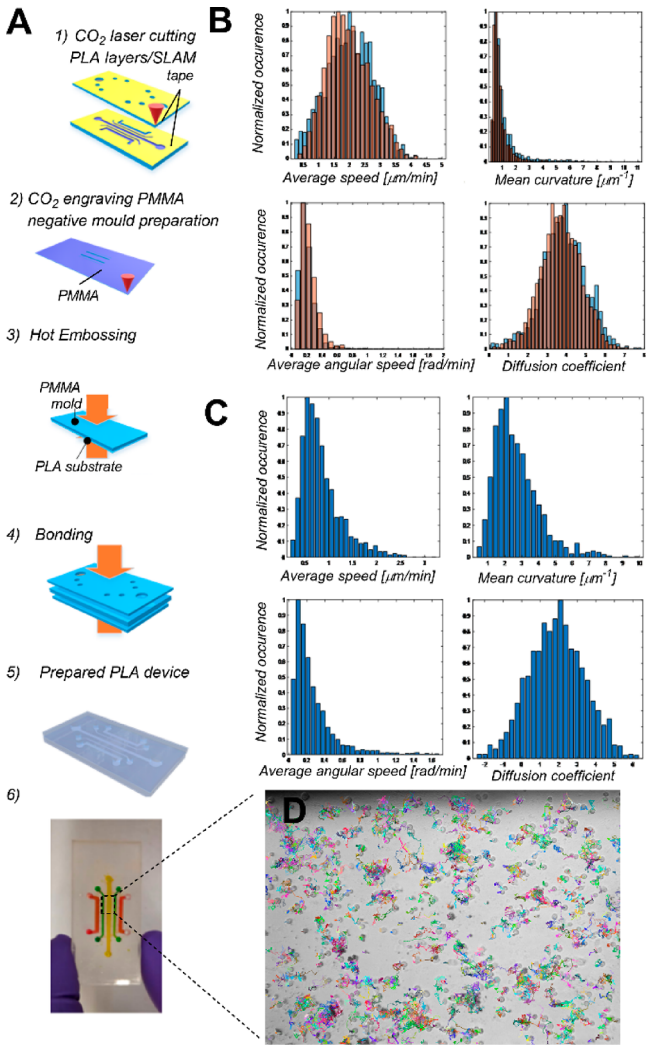


**Figure 5.** Demonstration of PLA suitability for cell tracking in organ-on-a-chip and microfluidic cell culture devices. (A) Schematization of the protocol to manufacture PLA organ-on-a-chip or microfluidic devices. (A-1) SLAM approach to create inlet and outlet holes in the top layer and to microstructure the channel on the middle layer. (A-2) Rastering a PMMA substrate to create a mold for the bottom layer with diffusion channels. (A-3) Hot embossing the structure from the PMMA mold to PLA, using a temperature of 70 °C and a pressure of 0.5 MPa for 15 min. (A-4) NaOH functionalization and UV activation of the surfaces with thermal bonding of the different layers. $T$ = 50 °C for 5 min. (A-5) The assembled device is cooled down while maintaining the layers in contact. (A-6) Photograph of the final device filled with red, green and yellow food dyes. (B) Statistics of the kinematic descriptors for PC-3 prostate cancer cells on a PLA open disk (blue bars) and on a PS well plate (orange bars). (C) Statistics of the Kinematic descriptors of the PC-3 prostate cancer cells on a PLA organ-on-chip device (image taken from the channel filled with yellow food dye). (D) Extracted PC-3 prostate cancer cell trajectories through the Cell-hunter software on a PLA device.

to observe a random cell confined walk in the PLA OOC device (Figure 5D).

## DISCUSSION

We performed a study to assess and fully characterize PLA suitability as a substrate material for microfluidic cell culture and organ-on-chip devices. We showed that PLA can offer many distinct advantages as a substrate for organ-on-chip applications over other polymers. First, we showed that PLA could be functionalized via a rapid (60 s) functionalization process using NaOH, reducing its native contact angle of about 70° to a contact angle of 40°, suitable for cell culture. We found this surface treatment to be stable over at least 9 months, which shows that commercial PLA devices treated in such a way would have excellent shelf life. Second, we showed that cells could be cultured on PLA surfaces, as easily as on conventional polystyrene (PS) Petri-dishes. Pristine and functionalized PLA performed better with regard to cell proliferation and cell toxicity compared to the majority of uncoated polymeric materials such as PMMA, PC, COC. Third, we demonstrated that PLA performed significantly better than PDMS with regard to the absorption of small molecules. Taking a hydrophilic representative molecule, Nile Red, of the same size as estrogen, a classic target compound in cell studies, we showed that PDMS absorbed 50% of the Nile Red after 20 load and wash cycles, while a similar PLA channel showed no absorption, whether or not it had been functionalized. Fourth, we showed that lab-made PLA substrates are highly transparent and present very little autofluorescence, enabling high quality imaging, which is demonstrated through a cell-tracking experiment in an organ-on-chip device. Fifth, advanced biological protocols such as random walk cell tracking were demonstrated in a PLA device. PLA is compatible with a range of complex integration, such as conducting electrodes, which we demonstrated in a previous publication (ref 7). While here we used a layer-by-layer approach to prototype organ-on-chip devices, PLA can also be formed, molded, and printed. PLA is a popular material for filament deposition modeling or 3D-printing, and 3D printed microfluidic devices have been demonstrated elsewhere.[35] However, these PLA 3D-printed devices currently lack the transparency necessary to enable high-resolution imaging and additional features are required to circumvent the lack of transparency. Here we showed that high PLA transparency can be achieved using molding and laser-cutting techniques, which apply to both prototyping and high-volume manufacturing.

Until now, other than ease of prototyping, one of the main reasons for choosing PDMS for OOC applications was its good oxygen permeability, with a diffusion coefficient of $3.5 \times 10^{-9}$ $m^2/s$. In our cell culture experiments, we found the PLA oxygen diffusion coefficient of $2.5 \times 10^{-12}$ $m^2/s$ to be a limiting factor. However, continuous media perfusion or thinner lids are expected to remove this limitation as shown by our simulation results. Additionally, the PLA lower oxygen diffusion coefficient enables the reduction and better control of water evaporation, and limit issues arising from osmolality differences induced by PDMS high oxygen diffusion coefficient.

The US Small Business Innovation Research, SBIR, has provided specific requirements for the assessment of novel material as a replacement of PDMS. With respect to these requirements, PLA fulfills 12 (eight demonstrated in this paper) out of 16 individual criteria (Table S2 for further discussion). This confirms PLA suitability as a next generation substrate material for advanced microfluidic cell culture and OOC applications.

## CONCLUSIONS

In summary, we have demonstrated the suitability of PLA as a new substrate material for organ-on-chip devices. Our approach is designed to address many disadvantages inherent


https://dx.doi.org/10.1021/acs.analchem.0c00651
Anal. Chem. XXXX, XXX, XXX−XXX

to a conventional PDMS microfabrication technique. In conjunction with its biocompatibility, inertness to small molecules, optical qualities, and PLA microfluidics will open opportunities to develop more sustainable solutions for organ-on-chip and microfluidic laboratories, in research or in industry. PLA represents a high-performing and more environmentally sustainable solution than other thermoplastic fossil-based materials proposed in the market. Ultimately, we envision that microfluidic device engineers will embrace a Design for Sustainability approach, and look into biopolymers, such as PLA, to develop sustainable single-use devices, for a wide range of applications, from organ-on-chip to point-of-care devices.

## ■ ASSOCIATED CONTENT

### Supporting Information

The Supporting Information is available free of charge at https://pubs.acs.org/doi/10.1021/acs.analchem.0c00651.

Additional details on materials employed in OOC companies; AFM images of pristine and functionalized PLA; details of biocompatibility experiments and cell death and proliferation on the different substrate employed in the study; production of microchannels with sub-100 $\mu$m width; details of small molecules absorption experiment; details of autofluorescence experiments and autofluorescence noise created by defects in the materials; details of cell tracking experiments; and comparison of PLA properties with SBIR criteria (PDF)

## ■ AUTHOR INFORMATION


### Corresponding Author

**Maïwenn Kersaudy-Kerhoas** − *Institute of Biological Chemistry, Biophysics and Bioengineering, School of Engineering and Physical Science, Heriot-Watt University, Edinburgh EH14 4AS, United Kingdom; Division of Infection and Pathway Medicine, Edinburgh Medical School, College of Medicine and Veterinary Medicine, The University of Edinburgh, Edinburgh EH164SB, United Kingdom;* orcid.org/0000-0002-8185-8230; Email: m.kersaudy-kerhoas@hw.ac.uk

### Authors

**Alfredo E. Ongaro** − *Institute of Biological Chemistry, Biophysics and Bioengineering, School of Engineering and Physical Science, Heriot-Watt University, Edinburgh EH14 4AS, United Kingdom; Division of Infection and Pathway Medicine, Edinburgh Medical School, College of Medicine and Veterinary Medicine, The University of Edinburgh, Edinburgh EH164SB, United Kingdom; Department of Engineering, Università degli Studi di Palermo, 90128 Palermo, Italy;* orcid.org/0000-0003-3084-6798

**Davide Di Giuseppe** − *Department of Electronic Engineering, University of Rome Tor Vergata, 00133 Rome, Italy*

**Ali Kermanizadeh** − *School of Medical Sciences, University of Bangor, LL57 2AS Bangor, United Kingdom*

**Allende Miguelez Crespo** − *Institute of Biological Chemistry, Biophysics and Bioengineering, School of Engineering and Physical Science, Heriot-Watt University, Edinburgh EH14 4AS, United Kingdom*

**Arianna Mencattini** − *Department of Electronic Engineering, University of Rome Tor Vergata, 00133 Rome, Italy*

**Lina Ghibelli** − *Department of Electronic Engineering, University of Rome Tor Vergata, 00133 Rome, Italy*

**Vanessa Mancini** − *School of Electronic and Electrical Engineering, Pollard Institute, University of Leeds, Leeds LS2 9JT, United Kingdom*

**Krystian L. Wlodarczyk** − *Institute of Photonics and Quantum Sciences, School of Engineering and Physical Science, Heriot-Watt University, Edinburgh EH14 4AS, United Kingdom*

**Duncan P. Hand** − *Institute of Photonics and Quantum Sciences, School of Engineering and Physical Science, Heriot-Watt University, Edinburgh EH14 4AS, United Kingdom*

**Eugenio Martinelli** − *Department of Electronic Engineering, University of Rome Tor Vergata, 00133 Rome, Italy*

**Vicki Stone** − *Institute of Biological Chemistry, Biophysics and Bioengineering, School of Engineering and Physical Science, Heriot-Watt University, Edinburgh EH14 4AS, United Kingdom*

**Nicola Howarth** − *Institute of Biological Chemistry, Biophysics and Bioengineering, School of Engineering and Physical Science, Heriot-Watt University, Edinburgh EH14 4AS, United Kingdom*

**Vincenzo La Carrubba** − *Department of Engineering and ATeN Center, Università degli Studi di Palermo, 90128 Palermo, Italy; INSTM, Palermo Research Unit, 90128 Palermo, Italy*

**Virginia Pensabene** − *School of Electronic and Electrical Engineering, Pollard Institute and School of Medicine, Leeds Institute of Medical Research, University of Leeds, Leeds LS2 9JT, United Kingdom;* orcid.org/0000-0002-3352-8202

Complete contact information is available at: https://pubs.acs.org/10.1021/acs.analchem.0c00651


### Author Contributions

A.O., N.H., V.L.C., V.P., and M.K.K., designed the research; A.O., A.M.C., D.V., A.K., D.D.G., A.M., L.G., K.W., V.M., and V.P. performed research; V.S. and D.H. contributed to reagents and analytic tools; A.O., A.K., D.D.G., N.H., E.M., V.P., and M.K.K. analyzed data; and A.O. and M.K.K. wrote the paper. All authors read and reviewed the paper. All authors have given approval to the final version of the manuscript.


### Funding

A.O. is funded by a James Watt scholarship. A.O., V.P., E.M., and M.K.K. acknowledge the Organ-On-A-Chip Technologies Network Sabbatical funding scheme. M.K.K. acknowledges funding from the Engineering and Physical Sciences Research Council, EP/R00398X/1. V.P. acknowledges the PROM project (Project number 748903), funded by H2020-MSCA-IF-2016 and the MRC Confidence in Confidence scheme.


### Notes

The authors declare no competing financial interest.

## ■ ACKNOWLEDGMENTS


We thank Professor Rory Duncan for access to the Edinburgh Super-Resolution Imaging Consortium (ESRIC) Facility.


## ■ REFERENCES


(1) Bhatia, S. N.; Ingber, D. E. *Nat. Biotechnol.* **2014**, *32* (8), 760−772.

(2) Zhang, B.; Korolj, A.; Lai, B. F. L.; Radisic, M. *Nat. Rev. Mater.* **2018**, *3*, 257−278.

(3) Zhang, B.; Radisic, M. *Lab Chip* **2017**, *17*, 2395−2420.

(4) Wang, Y.; Burghardt, T. P. *Anal. Biochem.* **2018**, *563*, 56−60.

(5) Li, S.; Gong, X.; Mc Nally, C. S.; Zeng, M.; Gaule, T.; Anduix-Canto, C.; Kulak, A. N.; Bawazer, L. A.; McPherson, M. J.; Meldrum, F. C. *RSC Adv.* **2016**, *6*, 25927−25933.
(6) Mohammed, M. I.; Haswell, S.; Gibson, I. *Procedia Technol.* **2015**, *20* (July), 54−59.
(7) Ongaro, A. E.; Keraite, I.; Liga, A.; Conoscenti, G.; Coles, S.; Schulze, H.; Bachmann, T. T.; Parvez, K.; Casiraghi, C.; Howarth, N.; et al. Laser Ablation of Polylactic Acid Sheets for the Rapid Prototyping of Sustainable, Single-Use, Disposable Medical Micro-Components. *ACS Sustainable Chem. Eng.***2018**, *6* (4)4899.
(8) Huang, J.-H.; Kim, J.; Ding, Y.; Jayaraman, A.; Ugaz, V. M. *PLoS One* **2013**, *8* (9), e73188.
(9) Lamour, G.; Hamraoui, A.; Buvailo, A.; Xing, Y.; Keuleyan, S.; Prakash, V.; Eftekhari-Bafrooei, A.; Borguet, E. *J. Chem. Educ.* **2010**, *87* (12), 1403−1407.
(10) Ochs, C. J.; Kasuya, J.; Pavesi, A.; Kamm, R. D. *Lab Chip* **2014**, *14* (3), 459−462.
(11) Drieskens, M.; Peeters, R.; Mullens, J.; Franco, D.; Lemstra, P. J.; Hristova-Bogaerds, D. G. *J. Polym. Sci., Part B: Polym. Phys.* **2009**, *47* (22), 2247−2258.
(12) Biselli, E.; Agliari, E.; Barra, A.; Bertani, F. R.; Gerardino, A.; De Ninno, A.; Mencattini, A.; Di Giuseppe, D.; Mattei, F.; Schiavoni, G.; et al. *Sci. Rep.* **2017**, *7*, 1−12.
(13) Danis P, D.; Ian S, M.; Malika, A.; William, M. G. Effect of Surface Wettability of Osteosarcoma Cells on Plasma. *J. Biomater. Appl.* **2011**, *26*.
(14) Riveiro, A.; Macon, A. L. B.; del Val, J.; Comesana, R.; Pou, J. Laser Surface Texturing of Polymers for Biomedical Applications. *Front. Phys.* **2018**, *6* DOI: 10.3389/fphy.2018.00016.
(15) Ahadian, S.; Civitarese, R.; Bannerman, D.; Mohammadi, M. H.; Lu, R.; Wang, E.; Davenport-Huyer, L.; Lai, B.; Zhang, B.; Zhao, Y.; et al. Organ-On-A-Chip Platforms: A Convergence of Advanced Materials, Cells, and Microscale Technologies. *Adv. Healthcare Mater.* **2018**, *7* (2), 1700506.
(16) Pellegrino, L.; Cocchiola, R.; Francolini, I.; Lopreiato, M.; Piozzi, A.; Zanoni, R.; Scotto d'Abusco, A.; Martinelli, A. *Colloids Surf., B* **2017**, *158*, 643−649.
(17) Chu, P. K.; Chen, J. Y.; Wang, L. P.; Huang, N. *Mater. Sci. Eng., R* **2002**, *36*, 143−206.
(18) van Midwoud, P. M.; Janse, A.; Merema, M. T.; Groothuis, G. M. M.; Verpoorte, E. *Anal. Chem.* **2012**, *84*, 3938−3944.
(19) Tham, C. Y.; Abdul Hamid, Z. A.; Ahmad, Z.; Ismail, H. *Adv. Mater. Res. (Durnten-Zurich, Switz.)* **2014**, *970*, 324−327.
(20) Grigoriev, T. E.; Bukharova, T. B.; Vasilyev, A. V.; Leonov, G. E.; Zagoskin, Y. D.; Kuznetsova, V. S.; Gomzyak, V. I.; Salikhova, D. I.; Galitsyna, E. V.; Makhnach, O. V.; et al. *Bionanoscience* **2018**, *8*, 977−983.
(21) da Silva, D.; Kaduri, M.; Poley, M.; Adir, O.; Krinsky, N.; Shainsky-Roitman, J.; Schroeder, A. *Chem. Eng. J.* **2018**, *340*, 9−14.
(22) Ramot, Y.; Haim-zada, M.; Domb, A. J.; Nyska, A. *Adv. Drug Delivery Rev.* **2016**, *107*, 153−162.
(23) Wagner, B. A.; Venkataraman, S.; Buettner, G. R. *Free Radical Biol. Med.* **2011**, *51* (3), 700−712.
(24) Zirath, H.; Rothbauer, M.; Spitz, S.; Bachmann, B.; Jordan, C.; Müller, B.; Ehgartner, J.; Priglinger, E.; Mühleder, S.; Redl, H.; et al. *Front. Physiol.* **2018**, *9*, 1−12.
(25) van Meer, B.J.; de Vries, H.; Firth, K.S.A.; van Weerd, J.; Tertoolen, L.G.J.; Karperien, H.B.J.; Jonkheijm, P.; Denning, C.; IJzerman, A.P.; Mummery, C.L. *Biochem. Biophys. Res. Commun.* **2017**, *482* (2), 323−328.
(26) Regehr, K. J.; Domenech, M.; Koepsel, J. T.; Carver, K. C.; Ellison-Zelski, S. J.; Murphy, W. L.; Schuler, L. A.; Alarid, E. T.; Beebe, D. J. *Lab Chip* **2009**, *9* (15), 2132.
(27) Gomez-sjoberg, R.; Leyrat, A. A.; Houseman, B. T.; Shokat, K.; Quake, S. R. *Anal. Chem.* **2010**, *82* (21), 8954−8960.
(28) Wang, J. D.; Douville, N. J.; Takayama, S.; ElSayed, M. *Ann. Biomed. Eng.* **2012**, *40* (9), 1862−1873.
(29) Toepke, M. W.; Beebe, D. J. *Lab Chip* **2006**, *6* (c), 1484−1486.
(30) Piruska, A.; Nikcevic, I.; Lee, H.; Ahn, C.; Heineman, W. R.; Limbach, A.; Seliskar, C. J. *Lab Chip* **2005**, *5*, 1348−1354.
(31) Kobayashi, J.; Asahi, T.; Ichiki, M.; Oikawa, A.; Suzuki, H.; Watanabe, T.; Fukada, E.; Shikinami, Y. *J. Appl. Phys.* **1995**, *77* (7), 2957−2973.
(32) Lu, B.; Zheng, S.; Quach, Q.; Tai, Y. *Lab Chip* **2010**, *10*, 1826−1834.
(33) Baptista, D.; Teixeira, L.; van Blitterswijk, C.; Giselbrecht, S.; Truckenmuller, R. *Trends Biotechnol.* **2019**, *37* (8), 838−854.
(34) Al-Ani, A.; Toms, D.; Kondro, D.; Thundathil, J.; Yu, Y.; Ungrin, M. *PLoS One* **2018**, *13*, e0204269.
(35) Romanov, V.; Samuel, R.; Chaharlang, M.; Jafek, A. R.; Frost, A.; Gale, B. K. *Anal. Chem.* **2018**, *90*, 10450−10456.


https://dx.doi.org/10.1021/acs.analchem.0c00651
*Anal. Chem.* XXXX, XXX, XXX−XXX

# Supporting Information

# Polylactic is a sustainable, low absorption, low auto-fluorescence, alternative to other plastics for Microfluidic and Organ-On-Chip applications

## Supplementary Information

Alfredo E. Ongaro[1,2,3], Davide Di Giuseppe[4], Ali Kermanizadeh[5], Allende Miguelez Crespo[1], Arianna Mencattini[4], Lina Ghibelli[4], Vanessa Mancini[6], Krystian L. Wlodarczyk[7], Duncan P. Hand[7], Eugenio Martinelli[4], Vicki Stone[1], Nicola Howarth[1], Vincenzo La Carrubba[8,9], Virginia Pensabene[6,10], Maïwenn Kersaudy-Kerhoas*[,1,2]

[1]Institute of Biological Chemistry, Biophysics and Bioengineering, School of Engineering and Physical Science, Heriot-Watt University, Edinburgh EH14 4AS, United Kingdom,

[2]Division of Infection and Pathway Medicine, Edinburgh Medical School, College of Medicine and Veterinary Medicine, The University of Edinburgh, Edinburgh EH164SB, United Kingdom,

[3]Department of Engineering, Università degli Studi di Palermo, Viale delle Scienze building 5, 90128 Palermo, Italy,

[4]Department of Electronic Engineering, University of Rome Tor Vergata, Rome, Italy

[5]School of Medical Sciences, University of Bangor, Bangor, United Kingdom,

[6]School of Electronic and Electrical Engineering, Pollard Institute, University of Leeds, Woodhouse Lane, Leeds, LS2 9JT, United Kingdom.

[7]Institute of Photonics and Quantum Sciences, School of Engineering and Physical Science, Heriot-Watt University, Edinburgh EH14 4AS, United Kingdom,

[8]INSTM, Palermo Research Unit, Viale delle Scienze building 6, 90128 Palermo,

[9]ATeN Center, Università degli Studi di Palermo, Viale delle Scienze building 18, 90128 Palermo

[10]School of Medicine, Leeds Institute of Medical Research, University of Leeds, Woodhouse Lane, Leeds, LS2 9JT, United Kingdom.

*Corresponding author: m.kersaudy-kerhoas@hw.ac.uk

Totals- 11 pages, 7 figures, 2 tables

**SI content:** Additional details on materials employed in OOC companies; AFM images of pristine and functionalized PLA; Details of biocompatibility experiments, cell death and proliferation on the different substrate employed in the study; Details of the 2D numerical simulation of Oxygen levels;

Production of microchannels with sub-100 μm width; details of small molecules absorption experiment; details of autofluorescence experiments and autofluorescence noise created by defects in the materials; details of cell tracking experiments; Comparison of PLA properties with SBIR criteria.

## S1 Materials used in the mass production of Organ-on-a-chip devices.

The emerging companies have been taken from [1]

| Material | Company |
|---|---|
| PDMS | Tissuse,emulate,alveolix,Nortis,Aspect,Synvivo,4DBiodesygne,Aimbiotech, uorgano, EHT echnologies, Axosim, Xona, microbrainbt, ananda |
| PC | Hesperos, Nortis |
| PS | Hepregen, Organovo, Insphero, 3Dbiomatrix, Huret corporation, Axosim, EHT technologies |
| COC | Xona, Mimetas |
| Unspecified THERMOPLASTIC | Draper, CnBio, |
| SU8 | Aspect |
| SILICONE | Hesperos, |

**Table S1** List of materials used for the production of Organ on chip devices and associated companies

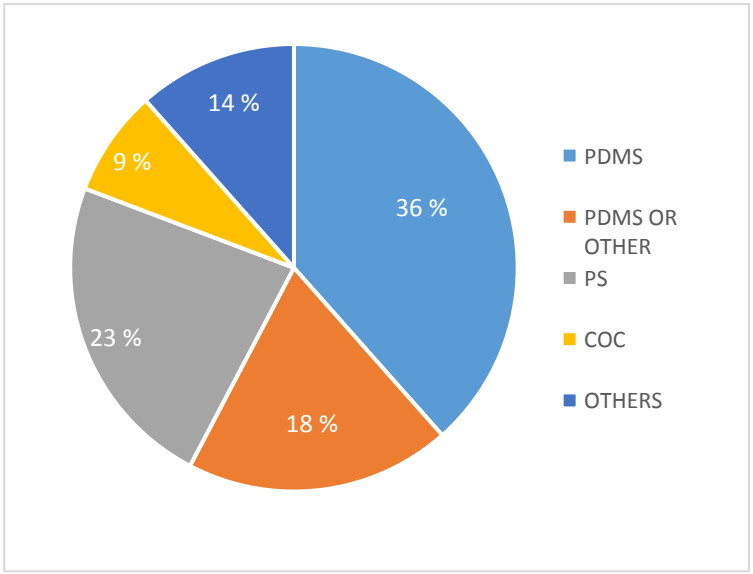


**Figure S1** Percentage of material employed for the production of Organ on chip devices

## S2. PLA functionalization

.

Atomic force Microscope Imaging of Pristine and Functionalized PLA was performed with Dimension FastScan Atomic Force Microscope (ScanAsyst, Bruker), operating in tapping mode with a triangular Silicon Nitride cantilever (FASTSCAN-A probe, Bruker) at resonant frequency of ≈1500 kHz. The scan field was 5x5 $\mu m^2$ and the amplitude of the height profile was recorded, with maximum peak values of 39.2 nm for the functionalized PLA (fPLA) corresponding to the rod formation already seen in the interferometry data, Figure 1.

**Figure S2 Atomic Force Microscope Imaging of Pristine and Functionalized PLA**

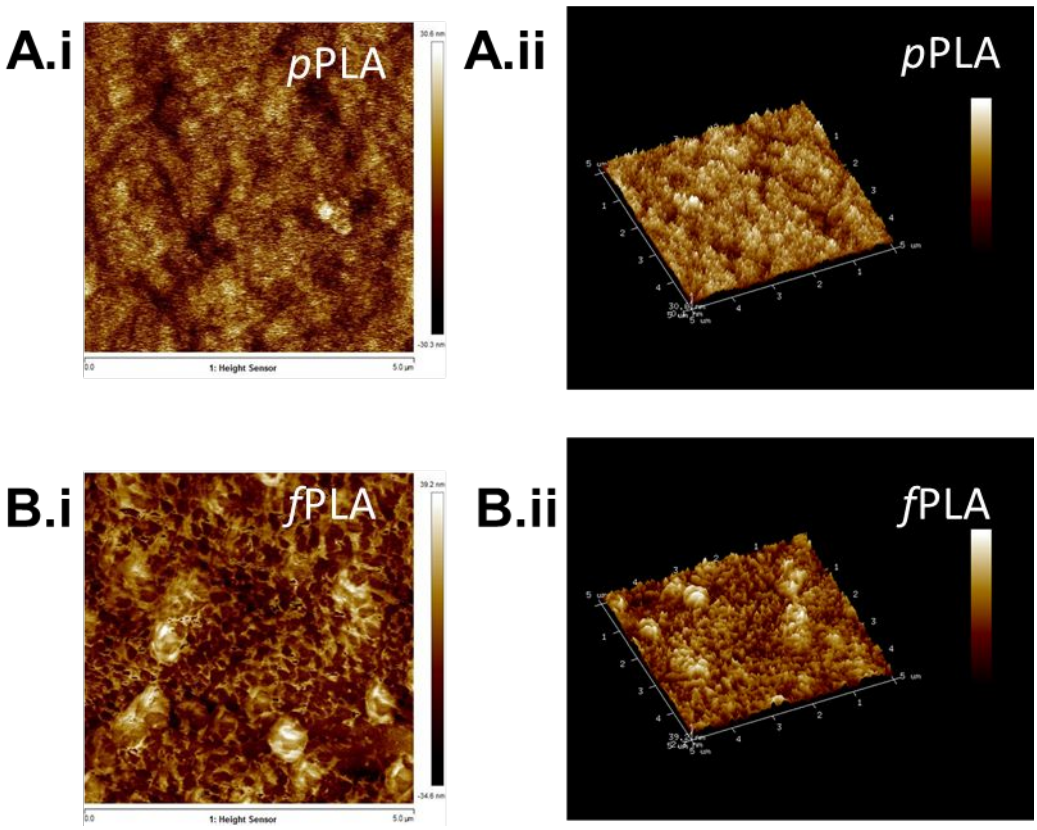


## S3. PLA Biocompatibility

### Materials and Method

### PLA biocompatibility experiments with C3A and A549 cells

The human hepatoblastoma C3A cell line was obtained from the American Type Culture Collection (ATCC, USA). The cells were maintained in Minimum Essential Medium Eagle (Gibco, UK) with 10% foetal bovine serum (FBS) (Gibco, UK), 2 mM L-glutamine, 100 U/ml penicillin/ streptomycin, 1 mM sodium pyruvate and 1% nonessential amino acids (all Sigma, UK) (termed complete medium), at 37°C and 5% CO2. The A549 cells were purchased from ATCC and maintained in RPMI (GIbco, uk) with 10% FBS, 100 IU/ml non-essential AA, 2 mM L glutamine and 100 U/ml Penicillin/Streptomycin.

For the biocompatibility experiments, both cell types were seeded in one 24-well plate at a cell density of 50,000 cells per well in 1 ml of complete medium. The medium was changed every 48 hrs up

to a period of 7 days. Subsequent to appropriate cell culture period (48 hrs or 7 days) the cell supernatants were collected and frozen at -80°C and later used for the adenylate kinase assay.

Cell death was evaluated through the loss of cell membrane integrity using a ToxiLight™ bioassay kit (Lonza, USA). Briefly, 20 µl of cell supernatant was transferred to a luminescence compatible plate before the addition of 80 µl of adenylate kinase (AK) detection buffer. The plates were incubated for 5 min at room temperature and luminescence quantified. These experiments included a positive control: polystyrene cell culture treated plastic and a negative control: 0.1% Triton X-100 (Sigma, UK).

Cell proliferation was evaluated using the alamar blue assay. The supernatant was removed from all well, and stored in a freezer -80ºC as described above. 1 ml of diluted alamar Blue reagent (Sigma, UK) (0.1 mg/ml) reagent was added to all (Sigma, UK). The plates were incubated at 37ºC for 90 minutes and fluorescence was measured at 544/590nm. These experiments included a positive control: polystyrene cell culture treated plastic and a negative control: 0.1% Triton X-100 (Sigma, UK).

These experiments are meant to investigate the biocompatibility of our in-house manufactured PLA for in-vitro use with no contact to living animals. For all in-vivo use, or for preparation of products to be in contact with the animal bodies, ISO 10993 guidelines should be followed.

**PLA material and device biocompatibility with HUVEC cells**

Devices were sterilized using EtOH, filled with culture medium and equilibrated in incubator (37 °C, 5% $CO_2$) for 3 h before cell loading. HUVECs P6 were cultured on flask in EGM™-2 Endothelial Cell Growth Medium-2 BulletKit ™ (Lonza). Cells were detached and loaded in PLA devices with seeding density 1 x106 cells/ml. Devices were placed in incubator (37 °C, 5% $CO_2$) to allow cells to adhere to the surface for 30 min. Then, 200 µl medium was added to inlet and outlet ports, and replaced every 24 h. To evaluate cell viability, a live dead assay (ReadyProbes® Cell Viability Imaging Kit (Blue/Green)) was used after 3 days and 7 days of culture.

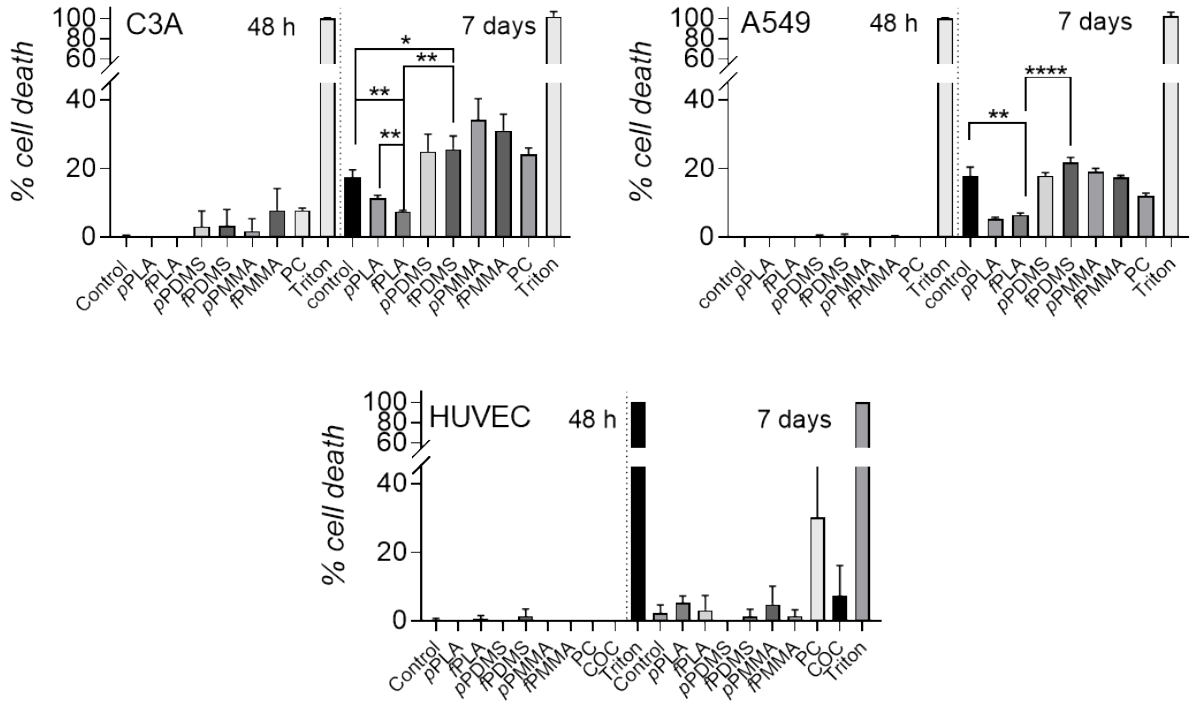


**Figure S3** Comparing PLA biocompatibility with common thermoplastic material used for advanced microfluidic cell culture and OOC applications. Cell death data for C3A, A549 and HUVECs on uncoated discs of fPLA,pPLA PDMS, fPDMS,

fPMMA, pPMMA, PC and COC. The positive control is an untreated PS well and the negative control is a untreated PS well with 0.1% Triton X-100.

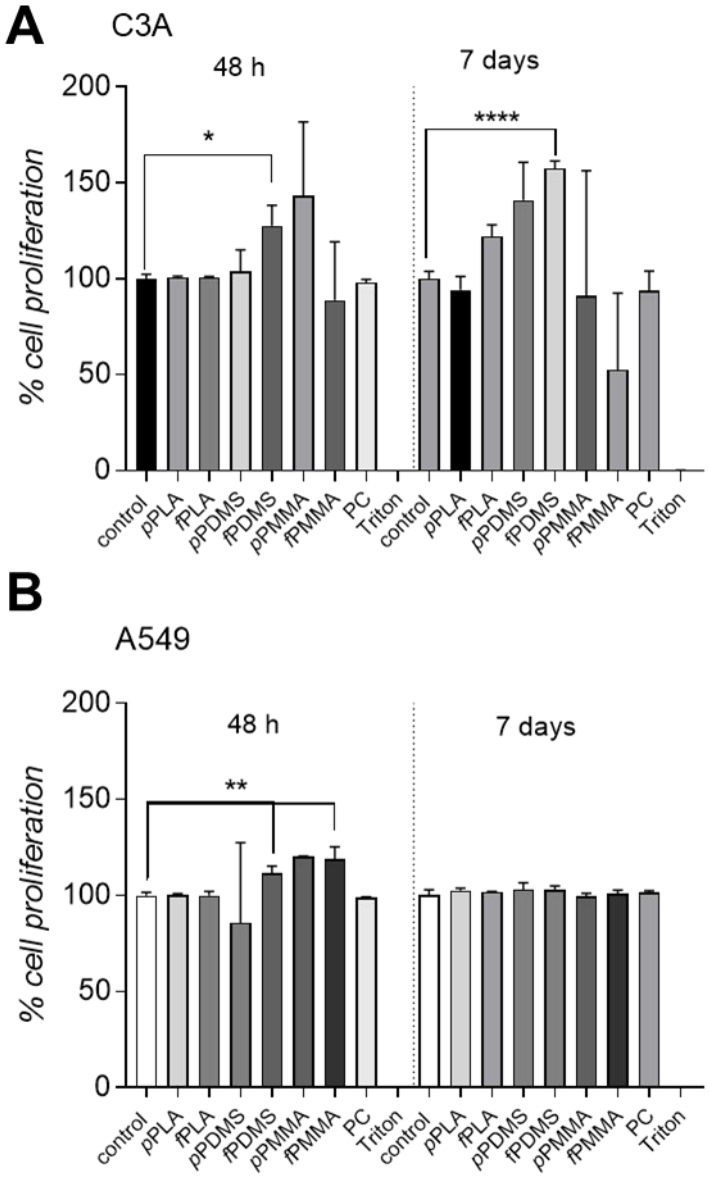


**Figure S4** Cell Proliferation data for C3A (A) and A549 (B) on uncoated discs of fPLA,pPLA PDMS, fPDMS, fPMMA, pPMMA, PC. The positive control is an untreated PS well and the negative control is an untreated PS well with 0.1% Triton X-100..

### Finite Element Analysis of the Oxygen level inside the microfluidic cell culture chamber

A simplified 2D model of the PLA microfluidic device was designed (75x3.6mm device, 25x0.8 mm cell culture chamber, with 2 mm inlet and outlet holes, 12x8mm reservoir placed on the top of the 2mm sealing layer). the Oxygen diffusion coefficient of 2.5x10-12, 3.5x10-9, 4x10-9 and 2.14x10-5 m2/s was used for PLA, PDMS, water and air respectively, taken from previously published studies [2,3]. We Imposed the starting concentration level of Oxygen inside the material device of 0%, and of 20% in water. To simulate the oxygen consumption rate, a consumption of oxygen of 0.37x104 mol/s was imposed on a rectangular region of (25x0.08mm) at the bottom part of the cell culture chamber.

## S4. Production of microchannels with sub-100 µm width.

A $CO_2$ laser cutter enables limited resolution and minimum channel width. In our experience, regardless of the Epilog $CO_2$ laser input parameters chosen (e.g. laser power, speed, frequency and focus), channel widths smaller than 100 µm are impossible to achieve with good reproducibility in PLA, or any other material. However, when channel widths with size between 20 – 100 µm are needed (e.g. for the production of perfusion barriers) picosecond lasers can be used. Here, as a proof of concept, a complex 2D structure has been generated on PLA using a picosecond laser micromachining system (Trumpf TruMicro 5x50) at Heriot-Watt University. The laser system enables the machining of various materials (including glass and transparent polymers) using a laser beam of the diameter smaller than 35µm (as measured at $1/e^2$ of its maximum intensity).

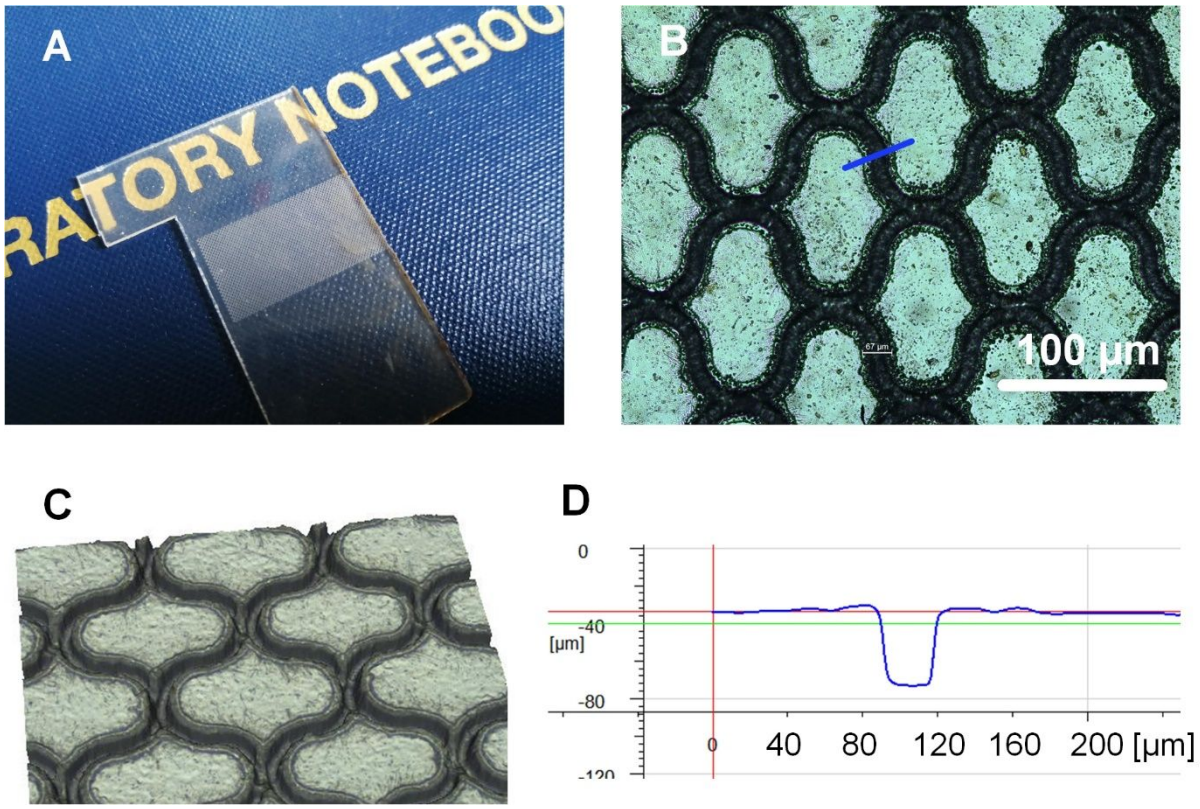


**Figure S5:** A) photograph of the PLA sample with sub-100 µm honeycomb structures. B) The honeycomb structure was generated using a 24 µm diameter laser spot of the wavelength of 515 nm. The pulse energy was 46.9 µJ, pulse repetition frequency was 40 kHz, whereas the laser beam scan speed was 80 mm/s. The laser system allows the generation of microchannels on PLA with different depths and reproducible widths below 100 µm. C) Alicona surface profile showing the honeycomb channel features with depths of 40 µm D) Example surface profile obtained on the Alicona profilometer. The cross-section represented here is indicated in blue on B) and is measured to be 40 x 67 µm.

## S5. Small molecules absorption

### Details of Materials and Method

To assess the bio-inertness of the material, pristine PLA was compared with functionalised PLA and with PDMS. To manufacture the device, specifically 6 channels of 1 mm width and 0.8 mm depth were cut through the PLA layers. The remaining cut pieces were used as negative mould to manufacture the PDMS device. The PLA device were then assembled as per chip preparation section. To manufacture the PDMS device, PDMS was mixed with the curing agent with a weight ratio of 1:10 and poured into a PS petri dish where the negative mould had been previously attached using a double sided adhesive tape (3M tape 469 MP). The PDMS was then left for 1h30 at room temperature prior to being placed for 1h at 80°C on a heated plate. In the same way a PDMS layer with input and output access holes were prepared. The two layers were then bonded together using an oxygen plasma treatment for 2 minutes (Diener electronic plasma surface technology). To test the absorption of hydrophobic compound Nile Red (Sigma Aldrich) was dissolved in EtOH 99% to obtain a solution concentration of 1 µM. To test the absorption of hydrophilic compounds fluorescein salt was dissolved in DI water (1uM). A fluorescent microscope (AM4115T-GFBW) was used to take the fluorescent images and the image analysis freeware ImageJ was used to analyse the fluorescence intensity. An advantage of this absorption experimental set-up is that it is fast and it does not require specific apparatus.

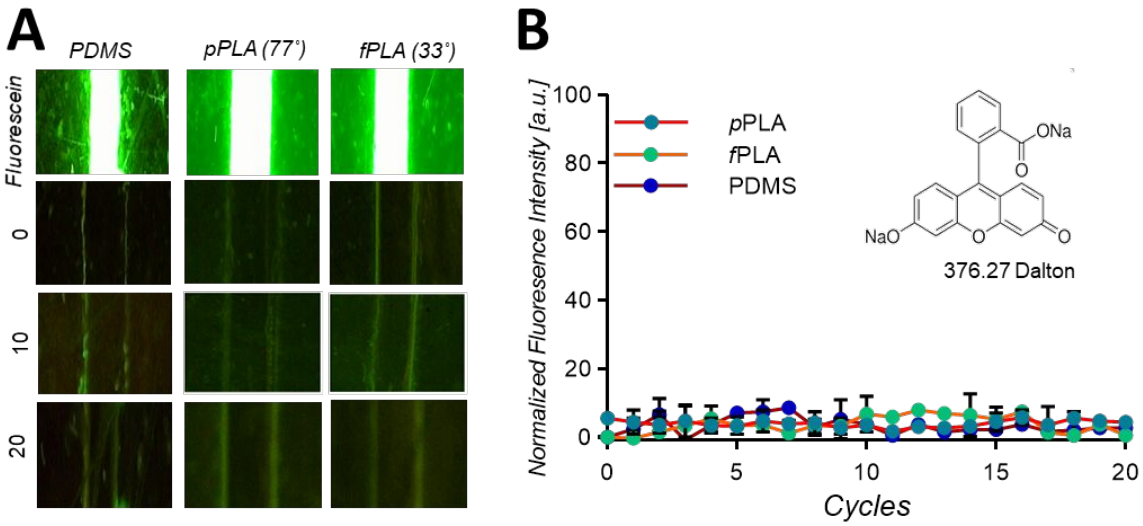


**Figure S6 Checking absorption of hydrophilic molecule**: A) Top view of the channel for (from left to right) PDMS, pristine PLA and functionalized PLA. From the top to the bottom picture of the channel filled with a solution of fluorescein salt in DI water (1µM), representing one of the reference point; then picture of the empty channel, representing the reference point, and picture of the channel at the 10th and 20th cycle. B.) Normalized fluorescence intensity, measured at the centre of the channel, plotted in function of the cycle number. In insert molecular structure and molecular weight of the fluorescein salt.

## S6. PLA Optical properties

The transparency of the materials was tested analysing the transmittance of the light in the visible region using a UV-VIS spectrophotometer (Shimadzu UV-2550). The autofluorescence of the plastic materials of interest was measured using a Leica SP8 3X STED laser scanning microscope equipped with two Internal Spectral Detector Channels (PMT). Current from the PMT was amplified and data was acquired using the software LAS X from Leica. Laser Kit WLL2 (supercontinuum white light laser [pulsed]), 200 excitation lines from 470-670 nm was used as light source. The fluorescence was filtered by suitable laser filters for 405 nm (emission filter 460/510 nm), 532 nm (emission filter 580/640 nm)

and 633 nm (emission filter 650/720 nm). Materials were wiped with ethanol preceding the imaging and were attached to a microscope slide before placing them on the microscope stage. The microscope objective (20x) was focused at the bottom surface of the samples and the objective was moved towards them. Auto-fluorescence imaging was done after 60 seconds illumination of each sample at each laser wavelength of interest (405, 532 and 633 nm excitation wavelengths). For each sample three unbleached sample spots were identified and selected for illumination. The analysis of the material auto-fluorescence long term recovery was done by illuminating and recording the samples for 10 min at both 405 nm (emission filter 460/510 nm) and 633 nm (emission filter 650/720 nm) wavelengths

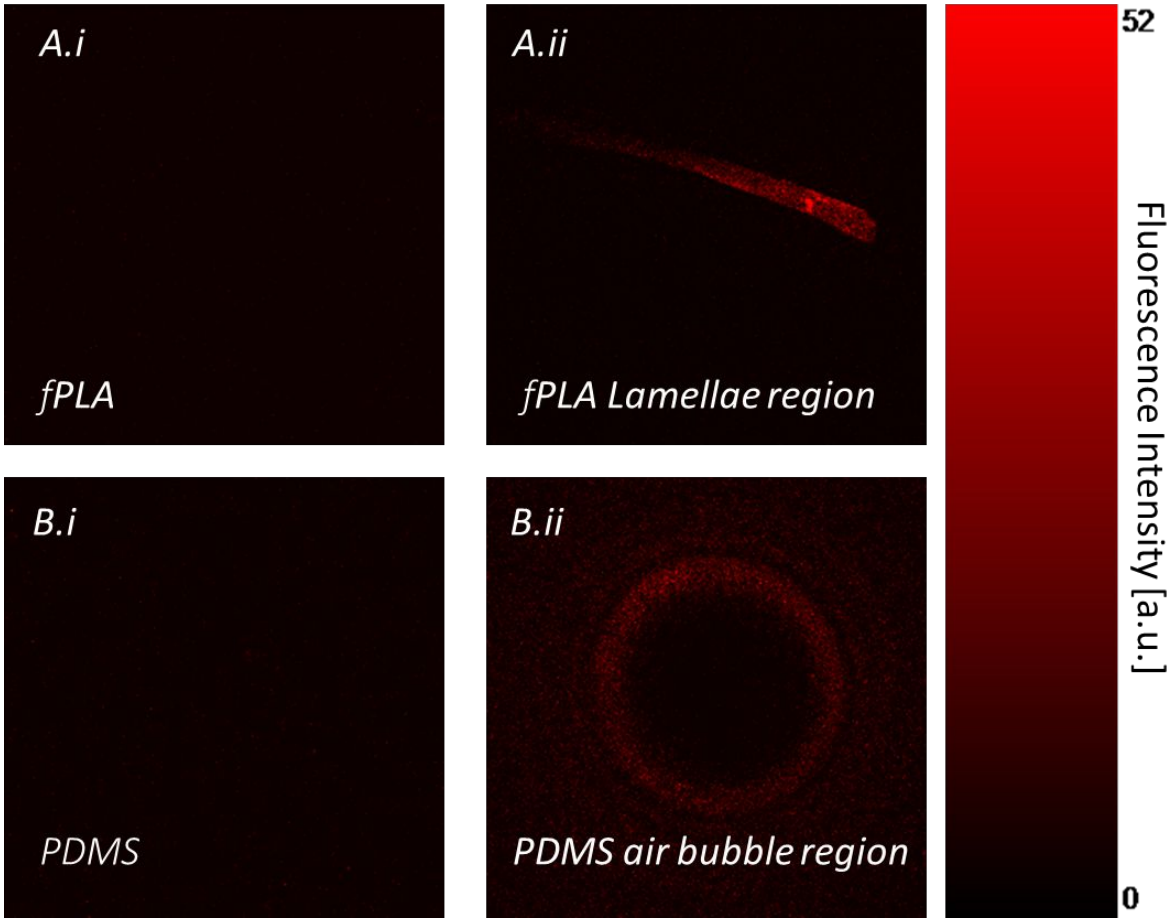


**Figure S7 PLA Optical properties**. Ai) Fluorescent background of well manufactured in 1 mm thick sample of fPLA. No background fluorescence is noticeable. A,ii) Fluorescent background of well manufactured in 1 mm thick sample of fPLA with a defect. An increased fluorescent background around a lamellae indicates a localized crystallisation. It is important that PLA pellets are not dried at temperature above 50°C (PLA glass transition temperature). Such defect indicates sub-optimal drying condition before sheet moulding B.ii) Fluorescent background of well manufactured in 1 mm thick sample of PDMS with some trapped bubble due to incorrect degassing process. An increased fluorescent background in visible around the bubble. The presence of an air bubble represents a discontinuity inside the bulk of the material which results in an increase auto-fluorescent background.

## S7. Cell imaging and tracking on a PLA device

Details of material and methods

**Cell Culture.** PC-3 prostate cancer cells were cultured at 37°C in a 5% CO2 humidified atmosphere in RMPI (10% fetal bovine serum, 100,000 units/litre penicillin, 50 mg/L streptomycin and 200mM glutamine). Cell seeding in PLA support (1st method). PC-3 cells were seeded on PLA lab-on-chip at a final concentration of 20.000 cells/80µL. Eve-ry hour new RPMI fresh medium was slowly added to pre-vent the channels from drying out completely. Cell seed-ing in PLA support (2nd method). PC-3 cells were seeded on PLA lab-on-chip at a final concentration of 20.000 cells/80µL. Tips containing 20µl of RMPI were positioned at the end of each microfluidic channel to allow replacing the medium every 24 hours (instead of 1 hour).

**Cell imaging.** A customized microscope has been de-signed for the scope: the prototype consists of a small-scale inverted microscope suitable to work in high humid-ity environments (incubators) with factory standard op-tics, custom aluminium structure and fully sealed elec-tronics. A custom firmware was implemented in Matlab2017a® environment in order to have full control on acquisition methods and light exposure. The microscope time setting used was one frame per minute for a total of 12hr. The captured images have a FOV of 1.2mm width by 1mm height with a spatial resolution of 0.33 µm/px.

**Cell tracking.** The video sequence is then processed by a proprietary software, Cell-Hunter elsewhere validated in cancer immune interaction 25,34 and block replication in prostate cancer cells 35. With the aim to speed up the cell localization process, images were downsampled at a spa-tial resolution of 0.66 µm/px. Typical dimension of cells involved allows us to avoid localization errors. The locali-zation step is implemented by the Circular Hough Trans-form (CHT) method, under the assumption of circular-shaped objects, that simultaneously allows one to locate cell nuclei in a given image providing an accurate estimate of individual cell radii. Cell occlusion and overlapping problems are solved through the geometrical mechanism behind. After cell nuclei are located, an improved proximi-ty tracking approach based on the Munkres' solution to the non-square Optimal Assignment (OA) problem is ap-plied. Track refining procedure related to the reliable as-sumption of low expected cell motility with respect to the very high frame rate achieved by the microscope allows to reduce false tracks and join small tracks in a whole.

**Cell track kinematic characterization**. For the sake of comparing the kinematic characteristics of cells involved in the competing experiments, we extracted standard de-scriptors such as average speed, curvature, and angular speed, along with the coefficient of diffusion 36. The dis-tribution of such descriptors computed over all the tracks extracted are shown in Fig. 5B and C.

## S8. Comparison with Criteria established by SBIR

The US Small Business Innovation Research, SBIR, has provided specific requirements for the assessment of novel material as replacement of PDMS (https://www.sbir.gov/sbirsearch/detail/1508473). With respect to these requirements, PLA fulfills 11 (eight demonstrated in this paper) out of 16 individual criteria (Table S2 for further discussion). The remaining four criteria could be demonstrated in further studies. This confirms PLA suitability as next generation substrate material for advanced microfluidic cell culture and OOC applications.

| *SBIR criteria* | *This work* | *Comment* |
|---|---|---|

| | | |
|---|---|---|
| Optical clarity – proven ability of material to allow penetration of light at wavelengths of ~400-700nm. | ✓ | 89.4% of transmitted light in the visible region. Low autofluorescence. |
| Defined gas permeability of oxygen and carbon dioxide | ☑ | Three order of magnitude lower than PDMS as reported in literature data[3] |
| Non-toxic and biocompatible to a wide variety of iPSC-derived cells and tissues (5-10 cell/tissue types tested). | ☑ | Not tested in this work, but previously assessed in literature[4,5] |
| Widely available/accessible, either whole or by material components. | ✓ | Multiple suppliers. Ingeo NatureWork, Total Corbion, Sigma Aldrich, Purac, Resomer. |
| Proven reliable and reproducible manufacturing properties. | ✓ | Injection Moulding, laser cutting, hot embossing |
| Easily manipulated without the need for extensive specialist equipment (above what PDMS requires). | ✓ | No clean room, functionalization via hydrolysis (no need of plasma treatment) |
| Proven ability for manufacture of microfluidic components e.g. channels, ports, etc. | ✓ | Layer by layer approach, moulding [6], injection moulding. |
| Proven lack of microfluidic channel cross-contamination at distances of <20μm for a variety of substances e.g. cell culture media, drugs, compounds, small molecules etc. | ✗ | N.A. |
| Reliable and predictable (variability <5%) molecular binding properties e.g. Log P, surface binding of plasma proteins etc. | ✓ | Unfunctionalized PLA can potentially bind Apo A1 lipoprotein [7] |
| Non-reactive with other standard materials used in MPS production e.g. glass, PDMS, poly(methyl methacrylate) (PMMA) etc. | ☑ | Not assessed in this work, proven in literature [8] |
| Proven success in culturing **at least** 5 types of viable, mature and functional iPSC-derived cell types and/or tissues; o Viability as shown by standard tissue-appropriate markers of cell health and survival e.g. lack of apoptotic markers; | ☑ | Not assessed in this work. iPSC derived neuronal stem cells [4], osteoblasts and osteoclasts[5], smooth muscle cells [9], hepatocytes [10] |
| Maturity as shown by presence of standard tissue-appropriate markers of mature phenotype or lack of differentiation markers; | ✗ | N.A. |
| Functionality as shown by presence of standard tissue-appropriate markers of cell functionality e.g. albumin secretion in hepatocytes; contractility in cardiomyocytes etc. | ✗ | N.A. |
| Employment of Quality Assurance manufacture standards to ensure the validity of analytical and quantitative measurements. | ✗ | N.A. |
| Proven success in fabrication and employment of the alternative material in a microfluidic setting. | ✓ | Rectangular single chamber, 5 chambers, 5 layers micromixer, droplet device, electrode device[11]. Vasculature network device [6]<br>Injection moulded fluidic 737 interaction |
| Proven success in replacement of PDMS in a microphysiological systems setting e.g. adaptation of existing MPS platforms with PDMS components replaced by the alternative material. | ✓ | Cell tracking experiment |

**Table S2. Criteria established by SBIR for the Development and production of an alternative material to PDMS. The sign ✓ indicates that the criteria is assessed in this work; ☑ not assessed in this work but assessed elsewhere; ✗ not assessed.**

## REFERENCES


(1) Zhang, B.; Radisic, M. Organ-on-a-Chip Devices Advance to Market. *Lab Chip* **2017**, *17*, 2395–2420. https://doi.org/10.1039/C6LC01554A.

(2) Christopher J. Ochs, Junichi Kasuya, Andrea Pavesi, R. D. K. Oxygen Levels in Thermoplastic Microfluidic Devices during Cell Culture. *Lab Chip* **2015**, *14* (3), 459–462.

https://doi.org/10.1039/c3lc51160j.Oxygen.

(3) Drieskens, M.; Peeters, R.; Mullens, J.; Franco, D.; Lemstra, P. J. Structure Versus Properties Relationship of Poly ( Lactic Acid ). I . Effect of Crystallinity on Barrier Properties. *Wiley Intersci.* **2009**, 2247–2258. https://doi.org/10.1002/polb.

(4) Lin, C.; Liu, C.; Zhang, L.; Huang, Z. H. I.; Zhao, P.; Chen, R.; Pang, M. A. O.; Chen, Z.; He, L.; Luo, C.; et al. Interaction of IPSC-Derived Neural Stem Cells on Poly ( L-Lactic Acid ) Nanofibrous Scaffolds for Possible Use in Neural Tissue Engineering. *Int. J. Mol. Med.* **2018**, *41*, 697–708. https://doi.org/10.3892/ijmm.2017.3299.

(5) Jeon, O. H.; Panicker, L. M.; Lu, Q.; Chae, J. J.; Feldman, R. A.; Elisseeff, J. H. Human IPSC-Derived Osteoblasts and Osteoclasts Together Promote Bone Regeneration in 3D Biomaterials. *Sci. Rep.* **2016**, No. February, 1–11. https://doi.org/10.1038/srep26761.

(6) Kim, J.; Huang, J.; Kim, J.; Ding, Y.; Jayaraman, A.; Ugaz, V. M. Embedding Synthetic Microvascular Networks in Poly ( Lactic Acid ) Substrates with Rounded Cross- Sections for Cell Culture …. Embedding Synthetic Microvascular Networks in Poly ( Lactic Acid ) Substrates with Rounded Cross- Sections for Cell Culture Ap. *PLoS One* **2013**, No. June 2014, 2–7. https://doi.org/10.1371/journal.pone.0073188.

(7) Stanislawski, L.; Nechaud, B. De; Christe, P. Plasma Protein Adsorption to Artificial Ligament Fibers. *J. Biomed. Mater.* **1995**, *29*, 315–323.

(8) Castro-aguirre, E.; Iñiguez-franco, F.; Samsudin, H.; Fang, X.; Auras, R. Poly ( Lactic Acid ) — Mass Production , Processing , Industrial Applications , and End of Life ☆. *Adv. Drug Deliv. Rev.* **2016**. https://doi.org/10.1016/j.addr.2016.03.010.

(9) Wang, Y.; Hu, J.; Jiao, J.; Liu, Z.; Zhou, Z.; Zhao, C.; Chang, L.; Chen, Y. E.; Ma, P. X.; Yang, B. Engineering Vascular Tissue with Functional Smooth Muscle Cells Derived from Human IPS Cells and Nanofibrous Scaffolds. *Biomaterials* **2014**, *35* (32), 8960–8969. https://doi.org/10.1016/j.biomaterials.2014.07.011.

(10) Carolina, N.; Thomas, E.; Brown, J.; Affairs, V. Functional Maturation of Induced Pluripotent Stem Cell Hepatocytes in Extracellular Matrix — A Comparative Analysis of Bioartificial Liver Microenvironments. *Stem Cells Transl. Med.* **2016**, *5*, 1257–1267.

(11) Ongaro, A. E.; Keraite, I.; Liga, A.; Conoscenti, G.; Coles, S.; Bachmann, T. T. T. T.; Parvez, K.; Casiraghi, C.; Howarth, N.; La, V.; et al. Laser Ablation of Polylactic Acid Sheets for the Rapid Prototyping of Sustainable , Single-Use , Disposable Medical Micro-Components. *ACS Sustain. Chem. Eng.* **2018**, *6* (4). https://doi.org/10.1021/acssuschemeng.7b04348.

## 6.4 Conclusions

Polylactic acid is here introduced as suitable candidate for the production of organ-on-a-chip and microfluidic cell culture devices both at the rapid prototyping scale as at the mass manufacturing one. PLA is a well-known material in the tissue engineering field, and it is approved from the food and drug administration for resorbable sutures and as a material in contact with food. In order to assess PLA suitability, surface and optical properties, biocompatibily, absorption and adsorption of small molecules have been characterized. A method to permanently change the surface wettability of PLA has been tuned adopting a wet-chemistry approach. The surface properties of the functionalized PLA substrates are stable over time and do not require particular storage condition. The biocompatibility of pristine and functionalized PLA have been tested and compared with polystyrene for cell culture, PMMA, COC, PC and pristine and functionalized PDMS with respect to two cancer cell lines and more sensitive Huvecs cells. The results show that there is not difference in cell viability between PLA and PS, enabling an easier transition for biologist moving from PS to PLA. The culture of Huvecs cells in a PLA cell culture microfluidic device have been tested and compared to the culture on a PDMS device. An increase in cell death has been noticed in PLA after one week of static cell culture. The difference in cell death between PLA and PDMS device is probably due to their difference in oxygen permeability. This hypothesis has been confirmed by a 2D numerical simulation of the oxygen concentration inside a PLA and a PDMS device. the results from the numerical simulation suggested that changing in the design, in particular in the thickness of the sealing layer, can help to guarantee the required oxygen concentration to the cells. The absorption and adsorption of small hydrophilic and hydrophobic molecules of PLA have been tested and compared to PDMS. $CO_2$ laser cut microchannels in both pristine and functionalized PLA do not absorb and adsorb small molecules. The optical properties of PLA have been characterized with respect to transmittance of the visible light and autofluorescence. The optical properties of PLA are as good as the one of other employed thermoplastic material in microfluidic and enable cell tracking in a microfluidic device.

The results reported in this chapter show that PLA is a suitable candidate for microfluidic cell culture and organ on a chip applications, showing better performance with respect to absorption and adsorption of small molecule and with respect of

biocompatibility than PDMS and other thermoplastic materials. Furthermore, PLA can be mass manufactured and it represents an environmentally sustainable alternative. Further studies will need to be undertaken to analyse the influence of PLA sealing layer thickness and oxygen permeability. A factor that this research does not take into account is the difference in the stiffness of the material, and no mechanical stimuli have been incorporated in the proposed design. With this respect, the piezoelectric properties of PLA can play a fundamental role in applying external mechanical stimuli to the cells and tissue cultured in the device or as an internal sensor [203], [204].

# Chapter 7: CONCLUSIONS AND FUTURE WORK

Microfluidic technologies are a powerful tool and they are revolutionizing the field of point-of-care diagnostics, cell culture and the pharmaceutical industry. It can be estimated that in the near future with a broad acceptance of microfluidic devices, this technology will flood the market. The increase demand of microfluidic as single-use device will require cheaper and more industrial embraced manufacturing technology than the one adopted at the research scale. It will also add more volume to the already saturated volume of plastic waste produced worldwide. This is the opportunity for material scientists to address this emerging technology and to embed sustainability considerations in the plastic industry at the design stage. Unfortunately, only a few research groups have focused on pursuing sustainability consideration at the design stage. Mass manufacturing material question and considerations are usually left later in the development of a new device. In this thesis I have adopt a design for sustainability approach to develop fast and green prototyping protocol to manufacture environmentally sustainable microfluidic devices and I have assessed the suitability of Re-PMMA and of PLA as new possible substrate materials.

In chapter 3 A method I developed to assess and predict the material compatibility with respect to a solvent assisted bonding method previously developed in my group is reported. In particular, in their previous research they observed that the protocol developed, enabling to bond in less than 15 minutes from design to test up to 19 layers of PMMA, was applicable without any further optimization to different grades of PMMA from different supplier, with the exception of one out of four tested. It is important when moving from one grade of material to another one to be able to predict if the bonding properties, e.g. bonding strength and burst test, are constant. After testing several hypotheses to check the influence of the molecular weight, and surface characteristics of the different grades on the bonding quality. I find out, while checking the thermal properties of the different grades via differential scanning calorimetry, that the bonding strength was affected by the presence of contaminants.

In chapter 4, I assessed the suitability of chemically recycled PMMA for the production of environmentally sustainable microfluidic devices in conjunction with laser based layer-by-layer manufacturing technique. DSC analysis revealed that absence of contaminants inside the material, thus the compatibility with the ethanol based solvent assisted bonding

method. I analysed the $CO_2$ laser interaction with Re-PMMA, and no recast layer was noticed. The choice of RePMMA resulted successful in order to prototype sustainable microfluidic devices, embracing a Green design approach, but at the time of writing RePMMA was more expensive than pristine PMMA, and as well available only at limited thicknesses.

Chapter 5 and 6 introduce PLA as new substrate material for the production of environmentally sustainable microfluidic devices for point-of-care, cell culture and organ on a chip applications. In chapter 5, first a method to fabricate PLA sheets with different crystallinity degree without the use of solvent is described. Then, a Sacrificial Layer Assisted Method, SLAM, I developed to microstructure PLA in conjunction with $CO_2$ laser cutting is reported. This method prevents burr formation during laser microstructuring, that hinder the bonding strength between layer of PLA when manufacturing microfluidic devices. As well as a protocol to fast check adsorption of small molecules on microfluidic walls, and to assess DNA binding a qPCR inhibition of materials. By comparing PLA with PMMA $CO_2$ laser microstructured channels, PLA showed smoother channel walls and consequently no adsorption of small hydrophilic molecule. PLA does not bind DNA and the inhibition of qPCR is lower than the one of PMMA. Furthermore, the water inject-printed graphene electrodes adhere better on the PLA surface than on the PMMA surface. In chapter 6, PLA properties with respect to organ-on-a-chip and microfluidic cell culture applications have been investigated. A method to permanently change the wettability of the material via a wet-chemistry approach is optimized and characterized. I proved that PLA does not absorb small hydrophobic molecules, and the biocompatibility is assessed and compared with other microfluidic materials. Optical transparency and autofluorescence of the material is investigated and compared with other thermoplastic materials and glass, showing that PLA has suitable optical properties for cell culture application. Finally, as proof of concept a cell tracking application inside a PLA device is proved.
The overall achievements of this thesis can be summarized as follow:

- A method to assess PMMA suitability, via differential scanning calorimetry, with respect to an ultra-fast, safe and cost-effective solvent assisted bonding protocol has been developed.

Although the developed method focuses on a very specific bonding protocol, the use of DSC may well have a bearing on assessing PMMA compatibility with other bonding

protocols developed by different research groups and to quickly and easily assess the presence of contaminants in the bulk of the material.

- Chemically Recycled-PMMA has been proven to be an environmentally sustainable candidate material for the fabrication of microfluidic devices. I have proven that the use of Re-PMMA can be immediately adopted by microfluidic manufacturers. The findings of this thesis suggests that all the available microstructuring and bonding methods used on PMMA can be translated to Re-PMMA without efficiency-loss.

The use of Re-PMMA as substrate material for the fabrication of microfluidic devices lays the groundwork for the adoption of circular economy principle in the microfluidic community.

- The use of polylactic acid for the fabrication of environmentally sustainable bio-derived microfluidic devices has been introduced. A method to $CO_2$ laser microstructure PLA has been developed. In particular, a Sacrificial Layer Assisted Method, SLAM, has been developed to overcome the recast layer formation. Two different bonding protocol have been tuned to efficiently manufacture PLA microfluidic devices. The two different methods can be adopted in mass manufacturing settings and rely on i) double sided pressure sensitive tape, indirect bonding, and ii) UV surface activation and thermal bonding, direct bonding. Different microfluidic designs e.g. split and recombine mixes, t-junction droplet device, cell culture rectangular chamber, recycle signs etc, have been manufactured in PLA to showcase the capability of the manufacturing protocol developed. A comprehensive characterization of the material properties with respect to microfluidic application has been undertaken. In particular, thermal properties, DNA binding, leaching of small molecules, absorption of small molecules, transparency, autofluorescence, biocompatibility and surface properties have been determined. A surface functionalization method based on alkaline surface hydrolysis has been developed to increase the material wettability. The proposed method shown a stability up to 9 months at room temperature storage condition.

  Low environmental impact water-based graphene electrodes have been successfully printed and integrated on a PLA device for electrochemical applications. A PLA microfluidic device for advanced cell culture and organ on a chip application have been produced and tested for advanced cell tracking studies.

The work on PLA has open up a robust discussion on the adoption of life cycle analysis and design for sustainability principles in the microfluidic community. As proof of this, Holger Becker, CTO of microfluidic ChipShop, one of the largest microfluidic companies in the world, has commented with respect to the work I have carried out during the PhD, that the microfluidic industry will have to contribute to the pressing environmental issue (Figure 7.1).

PLA is currently being applied for the fabrication of resorbable sutures, lid for coffee cups, stirrers, fridge interiors and can be potentially immediately employed for the fabrication of microfluidic devices. The adoption of PLA will not only bring new sustainability consideration but it will overcome some of the drawbacks that current materials have such as absorption and adsorption of small molecules. I envisage that PLA can replace the use of PDMS for advanced cell culture applications where the absorption of small molecules is unwanted.

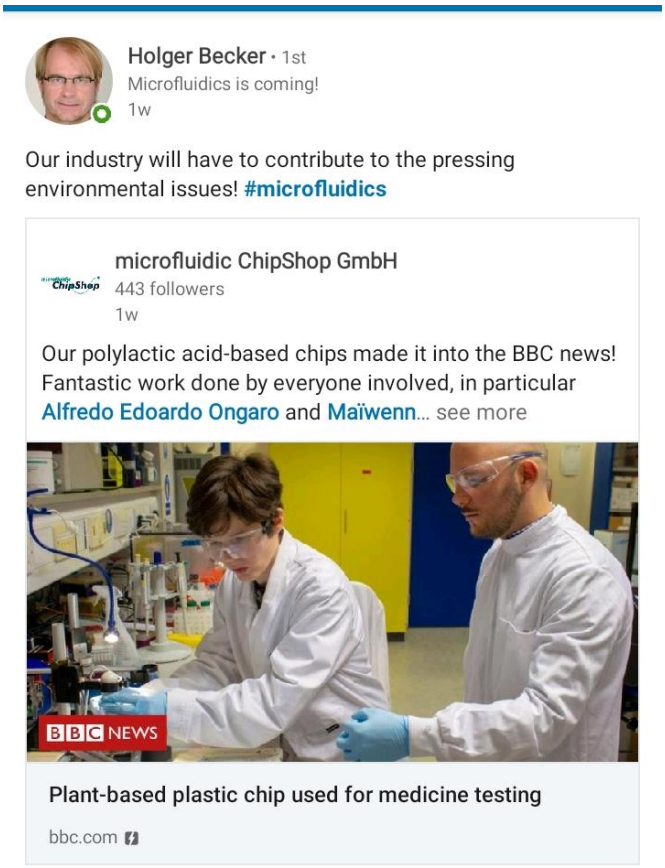


Figure 7.1 The comment of Holger Becker, CTO of microfluidic ChipShop, on the work about the use of PLA for microfluidic application.

- A microfluidic consortium between myself, Dr Maïwenn Kersaudy-Kerhoas, the University of Leeds in the person of Dr Virginia Pensabene and Francesco Colucci, the University of Roma Tor Vergata, represented by Prof Eugenio Martinelli, and two major European microfluidic manufacturers, Microfluidic

Chipshop and Micronit has been created with the goal to investigate in deep the mass manufacturabiliy of PLA for the production of devices for Organ on a chip applications.

The creation of the consortium has led to write a sabbatical funding project for the Organ on a chip Technologies Network for which the consortium has been awarded £ 10,627 (https://www.organonachip.org.uk/research/projects/1/next-generation-material-for-high-volume-production-of-sustainable-biocompatible-organ-on-chip-devices).

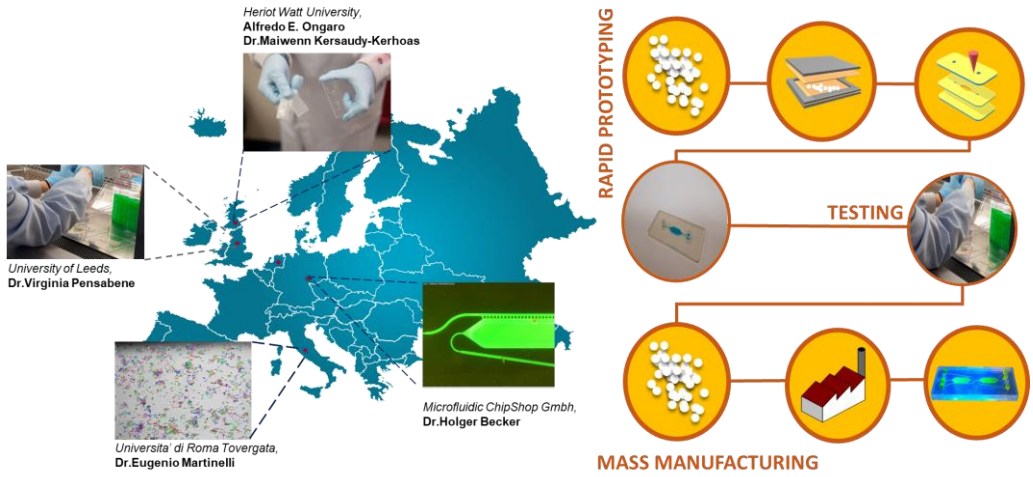


Figure 7.2

Furthermore, 300 injection moulded PLA devices for cell-cell interaction study from microfluidic ChipShop, 100 PLA slides to bond and seal the devices, and 300 injection moulded devices made of Durabio, a bioderived polycarbonate based material have been received.

## 7.1 Future work

The present study reported in this thesis provides one of the first comprehensive assessment of the use of PLA for microfluidic applications and the embracement of sustainability considerations for the material choice.

Future research will explore the use of the injection moulded microfluidic devices from ChipShop to develop a model of the gut-liver axis, mimicking enterohepatic circulation, using Caco-2 (gut) and HepaRG (liver) cell lines and assess their response to

paracetamol, compared with standard cell culture assays in collaboration with Prof Peter Hayes and Dr Katie Morgan from the Hepatology Lab at the University of Edinburgh. More in the specific, HepaRG and Caco2 cells will be cultured on microfluidic tissue culture plastic such as PLA, PS, PDSM to assess adherence and morphology. The assessment of cell viability morphology and functionality of the substrate materials will be compared with Corning plates as control. HepaRG and Caco2 cells will be separately cultured onto the microfluidic device to assess cell viability, morphology and functionality in a confined environment for a period of time of 12 days. Prior the culture a numerical simulation will be carried out to establish if the culture can be done in static or in a dynamic condition and to determine the optimum oxygen and $CO_2$ level that will be set in the incubator as schematically explained in figure 7.3.

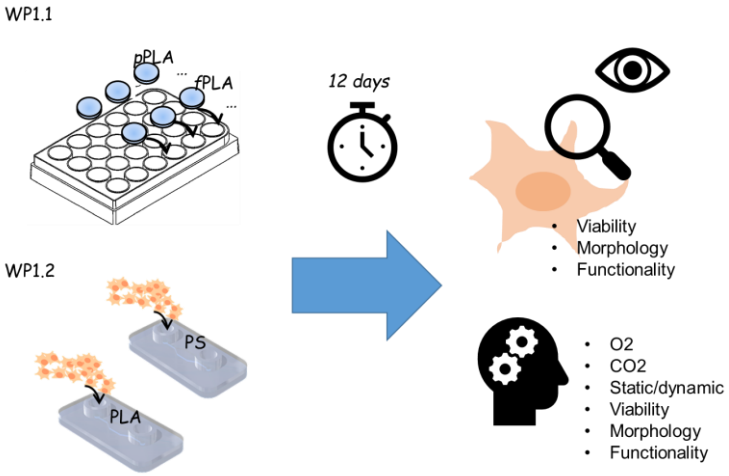


**Figure 7.3 schematic representation of the study to assess the device suitability for gut-liver co-culture study.**

Once optimisation of the culture protocol will be completed a trialith w 3 concentrations of paracetamol plus one control using the polylactic acid microfluidic system. 0, 5, 10 and 20mM paracetamol on Caco2->HepaRG->Caco2 (with 4mM representing a clinically safe dose) will be carried out.

Contemporary, coating efficiency of collagen and matrigel will be tested on pristine and functionalised PLA and the same biocompatibility study as per chapter 6 will be carried out.

In order to facilitate the implementation and dissemination of PLA use for the production of microfluidic devices for point-of-care, cell culture and organ-on-chip applications, further characterizations of the five bonding methods I developed during this 3 years of PhD (listed in table 7.1) and the publication of a bonding paper needs to be delivered.

| Bonding Method | Pros | Cons | Example | Bonding time | Ref. |
|---|---|---|---|---|---|
| **Indirect Bonding Double sided adhesive tape** | *User-friendly, no specific apparatus needed* | *Channel clogging, reduced transparency* |  | ~ 5 minutes | *ACS Sustainable Chem. Eng.*, **2018**, *6* (4), pp 4899–4908 |
| **Solvent assisted bonding** | *Room temperature bonding, easy to assemble multilayers* | *Loss in transparency and bulk mechanical properties, channel clogging* | | ~ 10 minutes (in function of the number of layers) | |
| **Thermal bonding** | *Easy to assemble multilayers, solvent-free* | *Possible channel deformation, physical bonding. Short operative working window* | 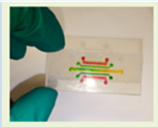 | ~ 30 minutes | MicroTAS 2018 |
| **Laser Absorption welding** | *Microstructuring and bonding with the same apparatus, short time required* | *No multilayers, loss in quality of surface roughness* | 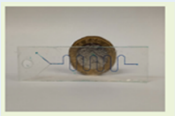 | ~ 5 minutes (in function of the bonding area) | MicroTAS 2018 |
| **UV assisted thermal bonding** | *Solvent-free, low pressure required, fast, good bonding strength* | *Alignment frame required, UV lamp and trained personnel required* |  | ~ 12 minutes | https://doi.org/10.1101/647347 |

**Table 7.1** schematization of the bonding method developed during the 3 years of PhD

# Bibliography


[1] S. Altin, A. Altin, B. Elevli, and O. Cerit, “Determination of hospital waste composition and disposal methods: A case study,” *Polish J. Environ. Stud.*, vol. 12, no. 2, pp. 251–255, 2003.

[2] E. S. Windfeld and M. S.-L. Brooks, “Medical waste management - A review.,” *J. Environ. Manage.*, vol. 163, pp. 98–108, 2015.

[3] S. Unger and A. Landis, “Assessing the environmental, human health, and economic impacts of reprocessed medical devices in a Phoenix hospital’s supply chain,” *J. Clean. Prod.*, vol. 112, pp. 1995–2003, 2016.

[4] W.-J. Lee, M.-C. Liow, P.-J. Tsai, and L.-T. Hsieh, “Emission of polycyclic aromatic hydrocarbons from medical waste incinerators,” *Atmos. Environ.*, vol. 36, no. 5, pp. 781–790, 2002.

[5] E. J. North and R. U. Halden, “Plastics and environmental health: The road ahead,” *Rev. Environ. Health*, vol. 28, no. 1, pp. 1–8, 2013.

[6] B. K. Lee, M. J. Ellenbecker, and R. Moure-Eraso, “Analyses of the recycling potential of medical plastic wastes,” *Waste Manag.*, vol. 22, no. 5, pp. 461–470, 2002.

[7] L. F. Diaz, L. L. Eggerth, S. Enkhtsetseg, and G. M. Savage, “Characteristics of healthcare wastes,” *Waste Manag.*, vol. 28, no. 7, pp. 1219–1226, 2008.

[8] V. Thakur and A. Ramesh, “Healthcare waste management research: A structured analysis and review (2005–2014).,” *Waste Manag. Res. J. Int. Solid Wastes Public Clean. Assoc. ISWA*, vol. 33, no. 10, p. 855, 2015.

[9] M. Tsakona, E. Anagnostopoulou, and E. Gidarakos, “Hospital waste management and toxicity evaluation: A case study,” *Waste Manag.*, vol. 27, no. 7, pp. 912–920, 2007.

[10] P. Singh and V. P. Sharma, “Integrated Plastic Waste Management: Environmental and Improved Health Approaches,” *Procedia Environ. Sci.*, vol. 35, pp. 692–700, 2016.

[11] M. Paraschiv, R. Kuncser, M. Tazerout, T. Prisecaru “New energy value chain through pyrolysis of hospital plastic waste.” , *Applied thermal engineering*, vol. 87, pp 424-433, 2015.

[12] K. Van De Velde and P. Kiekens, “Biopolymers: Overview of several properties and consequences on their applications,” *Polym. Test.*, vol. 21, no. 4, pp. 433–442, 2002.

[13] Y. Ikada and H. Tsuji, “Biodegradable polyesters for medical and ecological applications,” *Macromol. Rapid Commun.*, vol. 21, no. 3, pp. 117–132, 2000.

[14] G. M. Whitesides, “The origins and the future of microfluidics.,” *Nature*, vol. 442, no. 7101, pp. 368–73, 2006.

[15] J. O. Tegenfeldt, “Simplifying microfluidic separation devices towards field-detection of blood parasites,” *Anal. Methods*, vol. 8, no. 16, 2016.

[16] C. D. Edington *et al.*, “Interconnected Microphysiological Systems for Quantitative Biology and Pharmacology Studies,” *Sci. Rep.*, no. November 2017, pp. 1–18, 2018.

[17] C. Theo, H. Thubault, V. Valerie, B. Jean, and M. Théry, “Design of a 2D no-flow chamber to monitor hematopoietic stemm cellls,” *Lab Chip*, vol. 15, no. 1, 2015.

[18] H. Lu, “A microfluidic trap array longitudinal monitoring and multi-modal phenotypic analysis,” *Lab Chip*, pp. 3634–3642, 2017.

[19] N. Convery and N. Gadegaard, “30 years of microfluidics,” *Micro Nano Eng.*, vol. 2, no. January, pp. 76–91, 2019.

[20] A. Manz, E. Verpoorte, D. E. Raymond, C. S. Effenhauser, N. Burggraf, and H. M. Widmer, “u-TAS: Minitaturized total chemical analysis systems,” in *Micro Total Analyis systems*, 1995, pp. 5–27.

[21] D. C. Duffy, J. C. Mcdonald, O. J. A. Schueller, and G. M. Whitesides, “Rapid Prototyping of Microfluidic Systems in Poly ( dimethylsiloxane ),” *Anal. Chem.*, vol. 70, no. 23, pp. 4974–4984, 1998.

[22] F. Foret, P. Smejkal, and M. Macka, “Miniaturization and Microfluidics,” in *Liquid Chromatography: Fundamental and Instrumentations*, Elseies Inc., 2013, pp. 453–467.

[23] C. Iliescu, H. Taylor, M. Avram, J. Miao, and S. Franssila, “A practical guide for the fabrication of microfluidic devices using glass and silicon,” *Biomicrofluidics*, vol. 6, no. 1, pp. 16505–1650516, 2012.

[24] K. L. Wlodarczyk, D. P. Hand, and M. M. Maroto-valer, “Maskless , rapid manufacturing of glass microfluidic devices using a picosecond pulsed laser,” *Sci. Rep.*, vol. 9, pp. 1–13, 2019.

[25] M. Cabodi, N. W. Choi, J. P. Gleghorn, C. S. D. Lee, L. J. Bonassar, and A. D. Stroock, “A microfluidic biomaterial,” *J. Am. Chem. Soc.*, vol. 127, no. 40, pp. 13788–13789, 2005.

[26] J. O. C. Rosser I; Schlager, M; Purtscher, M; Jenner, F; and Ertl, P;, “Recent Advances of Biologically Inspired 3D Microfluidic Hydrogel Cell Culture Systems,” *HSOA J. Cell Biol. Cell Metab.*, vol. 2, no. 1, p. 5, 2015.

[27] H. Becker and L. E. Locascio, “Polymer microfluidic devices,” *Talanta*, vol. 56, no. 2, pp. 267–287, 2002.

[28] A. J. L. Morgan *et al.*, “Simple and versatile 3D printed microfluidics using fused filament fabrication,” *PLoS One*, vol. 11, no. 4, pp. 1–17, Apr. 2016.

[29] A. Liga, J. A. S. Morton, and M. Kersaudy-Kerhoas, “Safe and cost-effective rapid-prototyping of multilayer PMMA microfluidic devices,” *Microfluid. Nanofluidics*, vol. 20, no. 12, 2016.

[30] U. M. Attia, S. Marson, and J. R. Alcock, “Micro-injection moulding of polymer microfluidic devices,” *Microfluid. Nanofluidics*, vol. 7, no. 1, pp. 1–28, 2009.

[31] J. Friend and L. Yeo, “Fabrication of microfluidic devices using polydimethylsiloxane,” *Biomicrofluidics*, vol. 4, no. 2, pp. 1–5, 2010.

[32] Y. Xia, J. Si, and Z. Li, “Fabrication techniques for microfluidic paper-based analytical devices and their applications for biological testing: A review,” *Biosens. Bioelectron.*, vol. 77, pp. 774–789, 2016.

[33] X. Li, D. R. Ballerini, and W. Shen, “A perspective on paper-based microfluidics: Current status and future trends,” *Biomicrofluidics*, vol. 6, no. 1, pp. 12–14, 2012.

[34] S. T. Sanjay, M. Dou, J. Sun, and X. Li, “A paper/polymer hybrid microfluidic microplate for rapid quantitative detection of multiple disease biomarkers,” *Sci. Rep.*, vol. 6, 2016.

[35] K. Liu and Z. H. Fan, “Thermoplastic microfluidic devices and their applications in protein and DNA,” *Analyst*, vol. 136, pp. 1288–1297, 2011.

[36] A. K. Au, W. Lee, and A. Folch, “Mail-Order Microfluidics: Evaluation of Stereolithography for the Production of Microfluidic Devices,” *Lab Chip*, vol. 14, no. 7, pp. 1294–1301, 2014.

[37] D. J. Guckenberger, T. E. De Groot, A. M. D. Wan, D. J. Beebe, and E. W. K. Young, “Micromilling: A method for ultra-rapid prototyping of plastic microfluidic devices,” *Lancet*, vol. 15, no. 11, pp. 2364–2378, 2015.

[38] G. S. Fiorini, G. D. M. Jeffries, D. S. W. Lim, C. L. Kuyper, and D. T. Chiu, “Fabrication of thermoset polyester microfluidic devices and embossing masters using rapid prototyped polydimethylsiloxane molds.,” *Lab Chip*, vol. 3, no. 3, pp. 158–63, 2003.

[39] L. Peng, Y. Deng, P. Yi, and X. Lai, “Micro hot embossing of thermoplastic polymers : a review,” *J. Micromech. Microeng*, vol. 24, 2014.

[40] J. Giboz, T. Copponnex, and M. Patrice, “Microinjection molding of thermoplastic polymers : a review,” *Journal of Micromechanics and Microengineering*, vol.17, no 6, 2007.

[41] C. Tsao, “Polymer Microfluidics : Simple , Low-Cost Fabrication Process Bridging Academic Lab Research to Commercialized Production,” *micromachines*, vol. 7, no. 225, 2016.

[42] D. A. Bartholomeusz, R. W. Boutté, and J. D. Andrade, “Xurography : Rapid Prototyping of Microstructures Using a Cutting Plotter,” *J. microelectromechanical Syst.*, vol. 14, no. 6, pp. 1364–1374, 2005.

[43] V. Faustino, S. O. Catarino, R. Lima, and G. Minas, “Biomedical microfluidic devices by using low-cost fabrication techniques: A review,” *J. Biomech.*, vol. 49, pp. 2280–2292, 2016.

[44] M. Islam, R. Natu, and R. Martinez, “A study on the limits and advantages of using a desktop cutter plotter to fabricate microfluidic networks,” *Microfluid. Nanofluidics*, vol. 19, no. 4, pp. 973–985, 2015.

[45] D. I. Walsh, D. S. Kong, S. K. Murthy, and P. A. Carr, “Enabling Microfluidics: from Clean Rooms to Makerspaces,” *Trends Biotechnol.*, vol. 35, no. 5, pp. 383–392, 2017.

[46] N. Bhattacharjee, A. Urrios, S. Kang, and A. Folch, “The upcoming 3D-printing revolution in microfluidics,” *Lab Chip*, vol. 16, no. 10, pp. 1720–1742, 2016.

[47] A. Waldbaur, H. Rapp, K. Lange, “Processes, Let there be chip-towards rapid prototyping of

microfluidic devices: one-step manufacturing," *Anal. Methods*, vol. 3, no. 12, 2011.

[48] S. Koji and C. Ya, "Femtosecond laser three-dimensional micro- and nanofabrication," *Appl. Phys. Rev.*, vol. 041303, no. November 2014, 2014.

[49] S. Waheed *et al.*, "3D printed microfluidic devices: enablers and barriers," *Lab Chip*, vol. 16, no. 11, pp. 1993–2013, 2016.

[50] L. R. Volpatti and A. K. Yetisen, "Commercialization of microfluidic devices," *Trends Biotechnol.*, vol. 32, no. 7, pp. 347–350, 2014.

[51] S. R. Delaney and B. B. Suh-lailam, "Microfluidics : The Future of Testing ?," *Clin. Chem.*, vol. 2, p. 2018, 2018.

[52] E. K. Sackmann, A. L. Fulton, and D. J. Beebe, "The present and future role of microfluidics in biomedical research.," *Nature*, vol. 507, no. 7491, pp. 181–9, 2014.

[53] M. Ali, W. Wang, N. Chaudhry, and Y. Geng, "Hospital waste management in developing countries : A mini review," *Waste Manag. Res. J. Int. Solid Wastes Public Clean. Assoc. ISWA*, vol. 35, no. 6, pp. 581–592, 2017.

[54] D. J. Gilden, K. N. Scissors, and B. Reuler, "Disposable Products in the Hospital Waste Stream," *West. J. Med.*, pp. 2269–272, 1992.

[55] J. Morrow, "Reducing Waste in the Critical Care Setting," *Nurs Leadersh (Tor Ont)*. pp. 17–26, 2013.

[56] O. Awodele, A. A. Adewoye, and A. C. Oparah, "Assessment of medical waste management in seven hospitals in Lagos , Nigeria," *BMC Public Health*, pp. 1–11, 2016.

[57] C. Yang *et al.*, "Sustainable management measures for healthcare waste in China," *Waste Manag.*, vol. 29, no. 6, pp. 1996–2004, 2009.

[58] J. Bell *et al.*, "EU ambition to build the world's leading bioeconomy-uncertain times demand innovative and sustainable solutions," *N. Biotechnol.*, 2017.

[59] S. H. Kennet, "Introduction to engineering design," in *Engineering Design Priciples*, 1999, pp. 1–

15.

[60] J. H. Spangenberg, A. Fuad-luke, and K. Blincoe, “Design for Sustainability ( DfS ): the interface of sustainable production and consumption,” *J. Clean. Prod.*, vol. 18, no. 15, pp. 1485–1493, 2010.

[61] Rado *et al.*, “Polymethyl methacrylate ( PMMA ) recycling for the production of optical fiber sensor systems,” *Optics Express*, vol. 25, no. 24, pp. 71–80, 2017.

[62] A. M. D. Wan, D. Devadas, and E. W. K. Young, “Sensors and Actuators B : Chemical Recycled polymethylmethacrylate ( PMMA ) microfluidic devices,” *Sensors Actuators B. Chem.*, vol. 253, pp. 738–744, 2017.

[63] A. E. Ongaro, N. Howarth, V. La Carrubba, M. Kersaudy-Kerhoas, “Rapid Prototyping for Micro-Engineering and Microfluidic Applications: Recycled PMMA, a Sustainable Substrate Material,” *Adv. Transdiscipl. Eng.*, vol. 8, no. XXXII, pp. 107–112, 2018.

[64] A. M. D. Wan, D. Devadas, and E. W. K. Young, “Recycled Polymethylmethacrylate ( PMMA ) Microfluidic Devices,” *Sensors Actuators B. Chem.*, 2017.

[65] Z. Yin, Z. Yin, L. Sun, and M. Microfluidics, “Hot embossing / bonding of a poly ( ethylene terephthalate ) ( PET ) microfluidic chip,” *J. Micromech. Microeng*, 2008.

[66] K. R. Jackson *et al.*, “DNA purification using dynamic solid-phase extraction on a rotationally-driven polyethylene-terephthalate microdevice,” *Anal. Chim. Acta*, vol. 937, pp. 1–10, 2016.

[67] L. Jaupat and et al, “Green microfluidic devices made of corn protein,” *Lab Chip*, vol. 11, no. 20, 2011.

[68] R. Lausecker, V. Badilita, U. Gleißner, and U. Wallrabe, “Introducing natural thermoplastic shellac to microfluidics : A green fabrication method for point-of-care devices,” *Biomicrofluidics*, vol. 10, pp. 1–12, 2016.

[69] E. Corradini, P. S. Curti, A. B. Meniqueti, A. F. Martins, A. F. Rubira, and E. C. Muniz, “Recent advances in food-packing, pharmaceutical and biomedical applications of zein and zein-based materials,” *Int. J. Mol. Sci.*, vol. 15, no. 12, pp. 22438–22470, 2014.

[70] C. Brigham, *Biopolymers : Biodegradable Alternatives to Traditional Plastics*. Elsevier Inc.,

2018.

[71] C. Carrell *et al.*, “Beyond the lateral fl ow assay : A review of paper-based micro fl uidics,” *Microelectron. Eng.*, vol. 206, no. November 2018, pp. 45–54, 2019.

[72] Y. He, Y. Wu, J. Fu, and W. Wu, “Fabrication of paper-based microfluidic analysis devices: a review,” *RSC Adv.*, vol. 5, pp. 78109–78127, 2015.

[73] A. J. L. Morgan *et al.*, “Simple and versatile 3D printed microfluidics using fused filament fabrication,” *PLoS One*, vol. 11, no. 4, pp. 1–17, 2016.

[74] A. M. Tothill, M. Partridge, S. W. James, and R. P. Tatam, “Fabrication and optimisation of a fused filament 3D-printed microfluidic platform,” *J. Micromech. Microeng*, vol. 27, 2017.

[75] G. Gaal *et al.*, “Simplified fabrication of integrated microfluidic devices using fused deposition modeling 3D printing,” *Sensors Actuators B. Chem.*, vol. 242, pp. 35–40, 2017.

[76] L. P. Bressan *et al.*, “3D-printed microfluidic device for the synthesis of silver and gold nanoparticles,” *Microchem. J.*, vol. 146, no. January, pp. 1083–1089, 2019.

[77] L. P. Bressan, C. B. Adamo, R. F. Quero, D. P. De Jesus, and J. A. F. Silva, “A simple procedure to produce FDM-based 3D-printed microfluidic devices with an integrated PMMA optical window,” *Analytical Methods*, vol. 11, no. 8, 2019.

[78] V. Romanov, R. Samuel, M. Chaharlang, A. R. Jafek, A. Frost, and B. K. Gale, “FDM 3D Printing of High-Pressure, Heat-Resistant, Transparent Microfluidic Devices,” *Anal. Chem.*, vol. 90, pp. 10450–10456, 2018.

[79] S. Tsuda, H. Jaffery, D. Doran, and M. Hezwani, “Customizable 3D Printed ‘ Plug and Play ’ Millifluidic Devices for Programmable Fluidics,” *PLoS One*, pp. 1–13, 2015.

[80] M. I. Mohammed, M. Nazrul, H. Zainal, A. Kouzani, and I. Gibson, “Fabrication of microfluidic devices : improvement of surface quality of CO 2 laser machined poly ( methylmethacrylate ) polymer,” *J. Micromechanics Microengineering*, vol. 27, no. 015021, p. 12pp, 2017.

[81] K. G. Bruce, J. Alexander R, L. Christopher J, and B. L. Goenner, “A Review of Current Methods in Microfluidic Device Fabrication and Future Commercialization Prospects,” *Inventions*, vol. 3, no. 60, p. 25 pp, 2018.

[82] A. E. Ongaro *et al.*, “Laser ablation of polylactic acid sheets for the rapid prototyping of sustainable , single-use , disposable medical micro-components,” *ACS Sustain. Chem. Eng.*, vol. 6, no. 4, 2018.

[83] A. E. Ongaro *et al.*, “Polylactic is a Sustainable, Low Absorption, Low Autofluorescence Alternative to Other Plastics for Microfluidic and Organ-on-Chip Applications,”*Anal. Chem.* ASAP, 2020.

[84] M. Y. Kariduraganavar, A. A. Kittur, and R. R. Kamble, “Polymer Synthesis and Processing,” in *Natural and Synthetic Biomedical Polymers*, 1st ed., Elsevier Inc., 2014, pp. 1–31.

[85] U. Ali, K. J. B. A. Karim, and N. A. Buang, “A Review of the Properties and Applications of Poly (Methyl Methacrylate) (PMMA),” *Polym. Rev.*, vol. 55, no. 4, pp. 678–705, Oct. 2015.

[86] K. Liu, J. Xiang, Z. Ai, S. Zhang, Y. Fang, and T. Chen, “PMMA microfluidic chip fabrication using laser ablation and low temperature bonding with OCA film and LOCA,” *Microsyst. Technol.*, vol. 23, no. 6, pp. 1937–1942, 2017.

[87] A. Mathur, S. S. Roy, M. Tweedie, S. Mukhopadhyay, S. K. Mitra, and J. A. Mclaughlin, “Characterisation of PMMA microfluidic channels and devices fabricated by hot embossing and sealed by direct bonding,” *Curr. Appl. Phys.*, vol. 9, no. 6, pp. 1199–1202, 2009.

[88] Y. Gong, J. M. Park, and J. Lim, “An Interference-Assisted Thermal Bonding Method for the Fabrication of Thermoplastic Microfluidic Devices,” *Micromachines*, 2016.

[89] M. Laher and S. Hild, “A detailed micrometer scale investigation of the solvent bonding process", *RCS Adv*, vol. 4, 2013

[90] T. Tjeung, W. Lu, and F. De Rooij, “Thermally activated solvent bonding of polymers,” *Microsyst. Technol.*, no. 6, pp. 753–759, 2008.

[91] C. K. Chung, Y. C. Lin, and G. R. Huang, “Bulge formation and improvement of the polymer in CO2 laser micromachining,” *J. Micromechanics Microengineering*, vol. 15, no. 10, pp. 1878–1884, 2005.

[92] P. Chen and L. H. Duong, “Chemical Novel solvent bonding method for thermoplastic microfluidic chips,” *Sensors Actuators B. Chem.*, vol. 237, pp. 556–562, 2016.

[93] N. Ling, J. S. Lee, and N. Y. Lee, “Physical poly ( methylmethacrylate ) bonding coupled with selective microchannel hydrophobic coating for reliable sealing,” *Sensors Actuators A. Phys.*, vol. 265, pp. 168–173, 2017.

[94] F. Kotz, C. Richter, and B. E. Rapp, “‘ Liquid PMMA ’: Rapid Prototyping of Microfluidic Structures in Polymethylmethacrylate ( PMMA ) via direct lithography,” MicroTAS, pp. 1410–1412, 2015.

[95] X. Chen, T. Li, and Q. I. Gao, “A Novel method for rapid fabrication of PMMA microfluidic chip by laser cutting and sealing integration,” *Surface Review and Letters*, pp. 1–7, 2018.

[96] C. Liang, F. Meng, J. Li, and C. Liu, “Using CO 2 -laser bugle for ultrasonic bonding of thermoplastic micro fluidic devices,” *J. Mater. Process. Tech.*, vol. 252, no. April 2017, pp. 25–33, 2018.

[97] S. P. Ng, F. E. Wiria, and N. Tay, “Low Distortion Solvent Bonding of Microfluidic Chips,” *Procedia Eng.*, vol. 141, pp. 130–137, 2016.

[98] A. Bamshad, A. Nikfarjam, and H. Khaleghi, “A new simple and fast thermally-solvent assisted method to bond PMMA–PMMA in micro-fluidics devices,” *J. Micromechanics Microengineering*, vol. 26, no. 6, p. 065017, 2016.

[99] C. T. Æ. D. L. Devoe, “Bonding of thermoplastic polymer microfluidics”, *Microfluidics and nanofluidics*, pp. 1–16, 2009.

[100] A. E. Ongaro *et al.*, “Ultra-fast-prototyping of PMMA structures for micro-engineering applications: Choosing the right material,” in *Advances in Transdisciplinary Engineering*, 2017, vol. 6.

[101] B. John, “Solubility Parameters : Theory and Application,” *Am. Inst. Conserv.*, vol. 3, pp. 13–58, 1984.

[102] Ch. Wohlfarth, “Solubility parameter of poly(methyl Methacrylate),” in *Polymer Solutions*, Eds. Springer Berlin Heidelberg, 2010, pp. 1614–1614.

[103] L. Romoli, G. Tantussi, and G. Dini, “Experimental approach to the laser machining of PMMA substrates for the fabrication of microfluidic devices,” *Opt. Lasers Eng.*, vol. 49, no. 3, pp. 419–427, 2011.

[104] J. Jiang, J. Zhan, W. Yue, M. Yang, C. Yi, and C.-W. Li, “A single low-cost microfabrication approach for polymethylmethacrylate, polystyrene, polycarbonate and polysulfone based microdevices,” *RSC Adv.*, vol. 5, no. 45, pp. 36036–36043, 2015.

[105] M. I. Mohammed, E. Abraham, and M. P. Y. Desmulliez, “Rapid laser prototyping of valves for microfluidic autonomous systems,” *J. Micromechanics Microengineering*, vol. 23, no. 3, p. 035034, 2013.

[106] H. Bridle, J. Morton, P. Cameron, M. P. Y. Desmulliez, and M. Kersaudy-Kerhoas, “Design of problem-based learning activities in the field of microfluidics for 12- to 13-year-old participants???Small Plumbing!: empowering the next generation of microfluidic engineers,” *Microfluid. Nanofluidics*, vol. 20, no. 7, pp. 1–11, 2016.

[107] H. Klank, J. P. Kutter, and O. Geschke, “CO(2)-laser micromachining and back-end processing for rapid production of PMMA-based microfluidic systems.,” *Lab Chip*, vol. 2, no. 4, pp. 242–246, 2002.

[108] E. Tolstik *et al.*, “Non-local response in glass-like polymer storage materials based on poly (methylmethacrylate) with distributed phenanthrenequinone.,” *Opt. Express*, vol. 16, no. 15, pp. 11253–11258, 2008.

[109] H. Amid, R. Üter, and T. Hiel, “Characteristics and crosstalk of optical waveguides fabricated in polymethyl methacrylate polymer circuit board,” vol. 55, no. 32, 2016.

[110] S. P. and S. Kumar, “Profile and depth prediction in single-pass and two-pass CO 2 laser microchanneling processes,” *J. Micromechanics Microengineering*, vol. 25, no. 3, p. 35010, 2015.

[111] D. Snakenborg, H. Klank, and J. P. Kutter, “Microstructure fabrication with a CO2 laser system,” *J. Micromechanics Microengineering*, vol. 14, no. 2, pp. 182–189, 2004.

[112] N. C. Nayak, Y. C. Lam, C. Y. Yue, and A. T. Sinha, “CO 2 -laser micromachining of PMMA: the effect of polymer molecular weight,” *J. Micromechanics Microengineering*, vol. 18, no. 9, p. 095020, 2008.

[113] M. Madić, M. Radovanović, and M. Gostimirović, “Ann modeling of kerf transfer in Co2 laser cutting and optimization of cutting parameters using monte carlo method,” *Int. J. Ind. Eng. Comput.*, vol. 6, no. 1, pp. 33–42, 2015.

[114] G. Clark, J. Kosoris, L. N. Hong, and M. Crul, “Design for Sustainability: Current Trends in Sustainable Product Design and Development,” *Sustainability*, vol. 1, pp. 409–424, 2009.

[115] F. Ceschin and I. Gaziulusoy, “Evolution of design for sustainability: From product design to design for system innovations and transitions,” in *Design Studies*, vol. 47, Elsevier Ltd, 2016, pp. 118–163.

[116] S. M. Hong, E. Y. Chen, and G. Chem, “Chemically recyclable polymers: a circular economy approach to sustainability,” *Green Chem.*, vol. 19, no. 3692, 2017.

[117] Y. Kikuchi, M. Hirao, and T. Ookubo, “Design of recycling system for poly ( methyl methacrylate ) ( PMMA ). Part 1 : recycling scenario analysis,” *Int. J. Life Cycle Assess.*, vol. 19, pp. 120–129, 2014.

[118] J. M. Garcia and M. L. Robertson, “The future of plastics recycling,” *Science.*, vol. 358, no. 6365, 2017.

[119] K. Ragaert, L. Delva, and K. Van Geem, “Mechanical and chemical recycling of solid plastic waste,” *Waste Manag.*, 2017.

[120] J. Woo, L. Shanna, R. D. Aileen, Y. H. Saad, C. M. Seifert, and J. Lutz, “Using design strategies from microfluidic device patents to support idea generation,” *Microfluid. Nanofluidics*, vol. 0, no. 0, p. 0, 2018.

[121] L. A. Utracki, “Introduction to polymer blends,” in *Polymer Blends Handbook*, Netherlands: Kluwer Academic Publishers, 2003, pp. 1–122.

[122] I. A. Ignatyev, W. Thielemans, and B. Vander, “Recycling of Polymers : A Review,” *ChemSusChem*, vol. 7, pp. 1579–1593, 2014.

[123] D. S. Achilias and G. P. Karayannidis, “The Chemical Recycling of PET in the framework of sustainable development,” *Water, Air, & Soil Pollution: Focus* vol. 4, pp. 385–396, 2004.

[124] D. S. Achilias, “Chemical Recycling of Polymers . The Case of Poly ( methyl methacrylate ),” *Eurpean Polymer Journal*, vol. 43, pp. 271–276, 2006.

[125] Y. Chen, L. Zhang, and G. Chen, “Fabrication , modification , and application of poly ( methyl methacrylate ) microfluidic chips,” *Electrophoresis*, pp. 1801–1814, 2008.

[126] Y. Hsieh *et al.*, “Direct Micromachining of Microfluidic Channels on Biodegradable Materials Using Laser Ablation,” *Polymers (Basel).*, vol. 9, 2017.

[127] L. Li, D. Zhou, D. Huang, and G. Xue, “Double Glass Transition Temperatures of Poly(methyl methacrylate) Con fi ned in Alumina Nanotube Templates,” *Macromolecules*, vol. 47, no 1, pp 297-303, 2014.

[128] A. E. Ongaro, “Ultra-Fast-Prototyping of PMMA Structures for Micro-Engineering Applications : Choosing the Right Material,” in J Gao, M El Souri & S Keates (eds), *Advances in Manufacturing Technology XXXI - Proceedings of the 15th International Conference on Manufacturing Research*, pp. 181–186, 2017.

[129] C. E. Da Silva, A. E. Hoppe, M. M. Ravanello, and N. Mello, “Medical wastes management in the south of Brazil,” *Waste Management*, vol. 25, pp. 600–605, 2005.

[130] M. Makous, “Medical waste,” *Lancet*, vol. 359, no. 9316. p. 1528, 2002.

[131] D. C. J. Hutchins and S. M. White, “Coming round to recycling.,” *Bmj*, vol. 338, no. march, pp. 746–748, 2009.

[132] McKinsey & Co., “Rethinking the future of plastics,” *Sustain. Resour. Product.*, no. January, 2016.

[133] S. Thakur, C. Jyoti, S. Bjawna, V. ANkit, T. Sigitas, and T. vijay Kumar, “Sustainability of Bioplastics: Opportunities and Challenges,” *Curr. Opin. Green adn Sustain. Chem.*, 2018.

[134] H. Karan, C. Funk, M. Grabert, M. Oey, and B. Hankamer, “Green Bioplastics as Part of a Circular Bioeconomy,” *Trends Plant Sci.*, no. January, 2019.

[135] F. J. V. N. Wallace H. Carothers, G. L. Dorough, “Studies of polymerization and ring formation. X. the reversible polymerization of six-membered cyclic esters,” *Anal. Chem.*, vol. 52, pp. 761–772, 1932.

[136] Du Pont, “Polymeric Lactide Resin,” US1995970A, 1935.

[137] F. L. R. Kulkarni, K. Pani, C. Neuman, “Polylactic Acid for Surgical Implants,” *Arch Surg*, vol. 93, 1996.

[138] S. A. Miller, “Sustainable Polymers : Opportunities for the Next Decade,” *ACS Macro Lett.*, pp. 2–6, 2013.

[139] C. Washam, “Plastics go green,” *ChemMatters*, no. April, pp. 10–12, 2010.

[140] J. R. Dorgan, B. Braun, J. R. Wegner, and D. M. Knauss, “Poly ( lactic acids ): A Brief Review,” in *Degradable Polymers and Materials*, ACS Symposium Series, 2006, pp. 102–125.

[141] E. Castro-aguirre, F. Iñiguez-franco, H. Samsudin, X. Fang, and R. Auras, “Poly ( lactic acid ) — Mass production , processing , industrial applications , and end of life ☆,” *Adv. Drug Deliv. Rev.*, 2016.

[142] C. Manuela, P. MArtin, F. Marscheider-Weidemann, J. Schleich, H. Barbel, and A. Gerhard, “Techno-economic Feasibility of Large-scale Production of Bio-based Polymers in Europe,” *Tech. Rep. EUR 22103 EN*, 2005.

[143] Y.-C. Chien, C. Liang, S.-H. Liu, and S.-H. Yang, “Combustion kinetics and emission characteristics of polycyclic aromatic hydrocarbons from polylactic acid combustion.,” *J. Air Waste Manag. Assoc.*, vol. 60, no. 7, pp. 849–855, 2010.

[144] S. Ravi-kumar, B. Lies, X. Zhang, H. Lyu, and H. Qin, “Laser Ablation of Polymers : A Review.”

[145] J. Miller, “History , Scope , and the Future of Laser Ablation,” in *Laser Ablation*, vol. 28, no. 1896, 1994, pp. 1–10.

[146] C. G. K. Malek, “Laser processing for bio-microfluidics applications ( part I ),” *anal bioanal chem*, vol. 385, pp. 1351–1361, 2006.

[147] X. Liu, D. Du, and G. Mourou, “Laser Ablation and Micromachining with Ultrashort Laser Pulses,” *IEEE J. Quantum Electron.*, vol. 33, no. 10, pp. 1706–1716, 1997.

[148] A. J. Pinkerton, “Lasers in additive manufacturing,” *Opt. Laser Technol.*, vol. 78, pp. 25–32, 2016.

[149] M. R. Miloš Madi, “an Artificial Intelligence Approach for the Prediction of Surface Roughness in Co 2 Laser Cutting,” *J. Eng. Sci. Technol.*, vol. 7, no. 6, pp. 679–689, 2012.

[150] B. H. Zhou and S. M. Mahdavian, “Experimental and theoretical analyses of cutting nonmetallic materials by low power CO2-laser,” *J. Mater. Process. Technol.*, vol. 146, no. 2, pp. 188–192, 2004.

[151] D. Vasiga, “A Review of Carbon Dioxide Laser on Polymers,” *Int. J. Eng. Res. Technol.*, vol. 4, no. 03, pp. 874–877, 2015.

[152] F. Caiazzo, F. Curcio, G. Daurelio, and F. M. C. Minutolo, “Laser cutting of different polymeric plastics (PE, PP and PC) by a CO 2 laser beam,” *J. Mater. Process. Technol.*, vol. 159, no. 3, pp. 279–285, 2005.

[153] M. B. Shoujin Sun, “Laser Beam Machining,” in *Nontraditional Machining Processes: Research Advances*, 2013, pp. 35–96.

[154] A. Hossain, Y. Nukman, and A. M. Sifullah, “Effect of Process Parameter in Laser Cutting of PMMA Sheet and ANFIS Modelling for Online Control,” *MATEC Web Conf. ICMMR*, vol. 10003, 2016.

[155] I. a. Choudhury and S. Shirley, “Laser cutting of polymeric materials: An experimental investigation,” *Opt. Laser Technol.*, vol. 42, no. 3, pp. 503–508, 2010.

[156] J. P. Davim, N. Barricas, M. Conceição, and C. Oliveira, “Some experimental studies on CO2 laser cutting quality of polymeric materials,” *J. Mater. Process. Technol.*, vol. 198, no. 1–3, pp. 99–104, 2008.

[157] I. a. Choudhury and S. Shirley, “Laser cutting of polymeric materials: An experimental investigation,” *Opt. Laser Technol.*, vol. 42, no. 3, pp. 503–508, 2010.

[158] K.F: Tamrin, Y. Nukman, I.A.Choudhury, S.Shirley, “Multi objective optimization in precision laser cutting of different thermoplastics.”, *Optics and Lasers in Engineering*, vol. 67, pp. 57-65, 2015.

[159] A. Karimzad Ghavidel, M. Shabgard, and H. Biglari, “Microscopic and mechanical properties of semi-crystalline and amorphous polymeric parts produced by laser cutting,” *Journal of Applied Polymer Science*, vol. 133, no. 44. 2016.

[160] V. Matylitsky, F. Hendricks, and R. Patel, “Laser Micromachining of Bio-Absorbable Polymers: Impact of the Laser Process Parameters on the Machining Throughput and Quality,” *Spectra*

*Phys. Tech. Artic.*, vol. Paper M405.

[161] B. Stepal, A. J. Antonczak, M. Bartkowiak-Jwsa, J. Filipiak, C. Pezowicz, and K. M. Abramski, "fabrication of a polymer based biodegradable stent using a co2 laser," *Arch. Civ. Mech. Eng.*, vol. 14, pp. 317–326, 2014.

[162] E. Garskaite *et al.*, "Polylactic acid-nanocrystalline carbonated hydroxyapatite ( PLA-cHAP ) composite : preparation and surface topographical structuring with direct laser writing ( DLW )," pp. 1–30.

[163] P. Stępak, Bogusz D., arkadiusz J. Antonczak, Konrad Szustakiewicz, "Degradation of poly(L-lactide) under KrF excimer laser treatment," *Polym. Degrad. Stab.*, vol. 110, pp. 156–164, 2014.

[164] S.L. Fitton, R. N. Haward, "PHOTOCHEMICAL DEGRADATION OF THERMOPLASTICS," *Br. Polym. J.*, vol. 2, no. c, pp. 217–224, 1970.

[165] W. Jia *et al.*, "Effects of high-repetition-rate femtosecond laser micromachining on the physical and chemical properties of polylactide (PLA)," *Opt. Express*, vol. 23, no. 21, p. 26932, 2015.

[166] R. Ortiz, I. Quintana, J. Etxarri, A. Lejardi, and J. R. Sarasua, "Picosecond laser ablation of poly-L-lactide: Effect of crystallinity on the material response," *J. Appl. Phys.*, vol. 110, no. 9, 2011.

[167] A. J. R. Lasprilla, G. A. R. Martinez, B. H. Lunelli, A. L. Jardini, and R. M. Filho, "Poly-lactic acid synthesis for application in biomedical devices - A review," *Biotechnol. Adv.*, vol. 30, no. 1, pp. 321–328, 2012.

[168] X. I. Wang, G. Li, Y. Liu, W. Yu, and Q. Sun, "Biocompatibility of biological material polylactic acid with stem cells from human exfoliated deciduous teeth,"*Biomed Rep*, pp. 519–524, 2017.

[169] M. Kaduri, M. Poley, O. Adir, and N. Krinsky, "Biocompatibility , biodegradation and excretion of polylactic acid ( PLA ) in medical implants and theranostic systems," *Chem. Eng. J.*, vol. 340, no. January, pp. 9–14, 2018.

[170] M. S. Lopes, A. L. Jardini, and R. M. Filho, "Poly ( lactic acid ) production for tissue engineering applications," *Procedia Eng.*, vol. 42, no. August, pp. 1402–1413, 2012.

[171] B. J. A. Ryan, "Evolution of Cell Culture Surfaces," *BioFiles*, vol. 3.8, no. 21, pp. 6–9, 2008.

[172] M. W. Taylor, “A History of Cell Culture,” in *Viruses and Man: A History of Interactions*, Switzerland: Springer Internation publishing, 2014, pp. 41–52.

[173] R. L. Erhmann and G. O. Gey, “The Growth of Cells on a Transparent Gel of Reconstituted Rat-Tail collagen,” *J. Natl. cancer Inst.*, vol. 16, no. 6, 1956.

[174] S. L. Hood and G. Norris, “Dosimetry of Human Cell Cultures Irradiated at the Interface in Plastic and in Glass Dishes,” *Radiat. Res.*, vol. 14, no. 6, pp. 705–712, 1961.

[175] E. L. Nelson, “Disposable Culturing Device,” 3308039, US3308039A 1967.

[176] J. L. Melnick and E. M. Opton, “ASSAY OF POLIOMYELITIS NEUTRALIZING ANTIBODY IN DISPOSABLE PLASTIC PANELS *,” *Bull. World Health Organ.*, vol. 14, pp. 129–146, 1956.

[177] J. P. F. Max J. Lerman, Lembong Josephine, Shin Muramoto, Greg Gillen, “The Evolution of Polystyrene as a Cell Culture Material,” *Tissue Eng. Part B*, vol. 24, no. 5, pp. 359–372, 2018.

[178] H. Rubin, “Altering Bacteriological Plastic Petri Dishes for Tissue Culture Use,” *Public Health Rep.*, vol. 81, no. 9, pp. 843–844, 1966.

[179] M. E. Furth, A. Atala, W. F. Innovations, and N. Carolina, “Tissue Engineering : Future Perspectives,” in *Principles of Tissue Engineering*, Fourth Edi., Elsevier, 2014, pp. 83–123.

[180] P. Pdms and C. H. Sio, “Elastomers : Siloxane,” in *Encyclopedia of Materials Science and Technology*, 2001, p. 46.

[181] M. W. Toepke and D. J. Beebe, “PDMS absorption of small molecules and consequences in microfluidic applications,” *Lab Chip*, vol. 6, no. c, pp. 1484–1486, 2006.

[182] K. J. Regehr *et al.*, “Biological implications of polydimethylsiloxane-based microfluidic cell culture,” *Lab Chip*, vol. 9, no. 15, p. 2132, 2009.

[183] L. J. Waters, C. V Finch, A. K. M. M. H. Bhuiyan, K. Hemming, and C. Mitchell, “Effect of plasma surface treatment of poly ( dimethylsiloxane ) on the permeation of pharmaceutical compounds,” *J. Pharm. Anal.*, vol. 7, no. 5, pp. 338–342, 2017.

[184] B. J. Van Meer *et al.*, “Small molecule absorption by PDMS in the context of drug response bioassays,” *Biochem. Biophys. Res. Commun.*, vol. 482, no. 2, pp. 323–328, 2017.

[185] J. A. C. K. D. W. Ang, N. I. J. D. Ouville, S. H. T. Akayama, and M. O. E. L. S. Ayed, “Quantitative Analysis of Molecular Absorption into PDMS Microfluidic Channels,” *Ann. Biomed. Eng.*, vol. 40, no. 9, pp. 1862–1873, 2012.

[186] G. Johanson and K. Institutet, “Modeling of Disposition,” in *Comprehensive Toxicology*, 2010.

[187] J. Rice, “Partition Coefficients,” in *Organic Chemistry Concepts and Applications for Medical Chemistry*, Elsevier Inc., Ed. 2014, pp. 85–92.

[188] Al. W. Auner, K. M. Tasneem, D. A. Markiv, L. J. McCawley, and S. M. Huston, “Chemical-PDMS Binding Kinetics and Implications for Bioavailability in Microfluidic Devices,” *Lab Chip*, 2019.

[189] R. Gomez-sjoberg, A. A. Leyrat, B. T. Houseman, K. Shokat, and S. R. Quake, “Biocompatibility and Reduced Drug Absorption of Sol - Gel-Treated Poly ( dimethyl siloxane ) for Microfluidic Cell Culture Applications,” *Anal. Chem.*, vol. 82, no. 21, pp. 8954–8960, 2010.

[190] M. Rajendrani, “When PDMS isn’t the best,” *Anal. Chem.*, 2007.

[191] M. Rasouli, “Basic concepts and prctical equations on osmolality: Biochemical approach,” *Clin. Biochem.*, vol. 49, no. 12, 2016.

[192] Y. S. Heo *et al.*, “Characterization and Resolution of Evaporation-Mediated Osmolality Shifts That Constrain Microfluidic Cell Culture in Poly ( dimethylsiloxane ) Devices,” vol. 79, no. 3, pp. 1589–1597, 2007.

[193] D. B. Erwin Berthier, Edmond W.K. Young, “Engineers are from PDMS-land, Biologists are from Polystyrenia,” *Lab Chip*, vol. 12, no. 7, pp. 1224–1237, 2012.

[194] P. M. Van Midwoud, A. Janse, M. T. Merema, G. M. M. Groothuis, and E. Verpoorte, “Comparison of Biocompatibility and Adsorption Properties of Different Plastics for Advanced Micro fl uidic Cell and Tissue Culture Models,” *Anal. Chem.*, vol. 84, pp. 3938–3944, 2012.

[195] C. N. Baroud, “Microchannel deformations due to solvent-induced PDMS swelling †,” *Lab Chip*, 2010.

[196] T. Gervais, J. El-ali, and A. Gu, “Flow-induced deformation of shallow microfluidic channels,” pp. 500–507, 2006.

[197] H. Dongeun, M. Benjamin, M. Akiko, M.-Z. Martin, Y. H. Hong, and E. I. Donald, “Reconstituting Organ-Level Lung Functions on a Chip,” *Science (80-. ).*, vol. 328, 2010.

[198] V. A. Online, W. J. Polacheck, R. Li, and R. D. Kamm, “Microfluidic platforms for mechanobiology,” *Lab Chip*, vol. 13, no. 2252, pp. 2252–2267, 2013.

[199] S. Halldorsson, E. Lucumi, R. Gómez-sjöberg, and R. M. T. Fleming, “Advantages and challenges of micro fl uidic cell culture in polydimethylsiloxane devices,” *Biosens. Bioelectron.*, vol. 63, pp. 218–231, 2015.

[200] J. Hiitola-keinänen, S. Aikio, M. Harjanne, and M. Kurkinen, “Roll-to-roll fabrication of integrated PDMS-paper microfluidics for nucleic acid amplification †,” *Lab Chip*, vol. 18, no. 1552, pp. 1552–1559, 2018.

[201] T. Feature, “Putting microfluidics in other people ’ s hands,” *Nat. Methods*, vol. 15, no. 3, pp. 167–170, 2018.

[202] J. Huang, J. Kim, Y. Ding, A. Jayaraman, and V. M. Ugaz, “Embedding Synthetic Microvascular Networks in Poly ( Lactic Acid ) Substrates with Rounded Cross- Sections for Cell Culture Applications,” vol. 8, no. 9, pp. 55–58, 2013.

[203] M. Ando, S. Takeshima, Y. Ishiura, K. Ando, and O. Onishi, “Piezoelectric antibacterial fabric comprised of poly ( l-lactic acid ) yarn,” *Jpn. J. Appl. Phys.*, pp. 2–6, 2017.

[204] E. J. Curry *et al.*, “Biodegradable Piezoelectric Force Sensor,” *PNAS*, vol. 115, no. 5, 2018.

[205] P. Wang, S. Lee, and J. P. Harmon, “Ethanol-Induced Crack Healing in Poly ( methyl Methacrylate )*,” *J. Poly*, vol. 32, pp. 1217–1227, 1994.